PSDF

Technical Progress Report
Gasification Test Run TC11
April 7, 2003 - April 18, 2003

DE-FC21-90MC25140

Power Systems
Development Facility
Tel: (205) 670-5840
Fax: (205) 670-5843

TC11

http://psdf.southernco.com

POWER SYSTEMS DEVELOPMENT FACILITY TECHNICAL PROGRESS REPORT

GASIFICATION TEST RUN TC11

APRIL 7, 2003 – APRIL 18, 2003

DOE Cooperative Agreement Number
DE-FC21-90MC25140

Prepared by:
Southern Company Services, Inc.
Power Systems Development Facility
P.O. Box 1069
Wilsonville, AL 35186
Tel: 205-670-5840
Fax: 205-670-5843
http://psdf.southernco.com

April 2005

POWER SYSTEMS DEVELOPMENT FACILITY

DISCLAIMER

Available to the public from the National Technical Information Service, U.S. Department of Commerce, 5285 Port Royal Road, Springfield, VA 22161. Phone orders accepted at (703) 487-4650.

ABSTRACT

This report discusses Test Campaign TC11 of the Kellogg Brown & Root, Inc. (KBR) Transport Gasifier train with a Siemens Westinghouse Power Corporation (Siemens Westinghouse) particle filter system at the Power Systems Development Facility (PSDF) located in Wilsonville, Alabama. The Transport Gasifier is an advanced circulating fluidized-bed gasifier designed to operate as either a combustor or a gasifier in air- or oxygen-blown mode of operation using a particulate control device (PCD). Test run TC11 began on April 7, 2003, with startup of the main air compressor and the lighting of the gasifier start-up burner. The Transport Gasifier operated until April 18, 2003, when a gasifier upset forced the termination of the test run. Over the course of the entire test run, gasifier temperatures varied between 1,650 and 1,800°F at pressures from 160 to 200 psig during air-blown operations and around 135 psig during enriched-air operations. Due to a restriction in the oxygen-fed lower mixing zone (LMZ), the majority of the test run featured air-blown operations.

ACKNOWLEDGMENT

The authors wish to acknowledge the contributions and support provided by various project managers: Jim Longanbach (DOE), Neville Holt (EPRI), Nicola Salazar (KBR), Ben Wiant (Siemens Westinghouse). Also, the enterprising solutions to problems and the untiring endeavors of many personnel at the site are greatly appreciated. The project was sponsored by the U.S. Department of Energy National Energy Technology Laboratory under contract DE-FC21-90MC25140.

CONTENTS

TABLES

FIGURES

1.0 EXECUTIVE SUMMARY

1.1 SUMMARY

This report discusses Test Campaign TC11 of the Kellogg Brown & Root, Inc. (KBR) Transport Gasifier train with a Siemens Westinghouse Power Corporation (Siemens Westinghouse) particle filter system at the Power Systems Development Facility (PSDF) located in Wilsonville, Alabama. The Transport Gasifier is an advanced circulating fluidized-bed gasifier designed to operate as either a combustor or a gasifier in air- or oxygen-blown mode of operation using a particulate control device (PCD). Test run TC11 began on April 7, 2003, with the startup of the main air compressor and the lighting of the gasifier start-up burner. The Transport Gasifier operated until April 18, 2003, when a gasifier upset forced the termination of the test run. Over the course of the entire test run, gasifier temperatures varied between 1,650 and 1,800°F at pressures from 160 to 200 psig during air-blown operations and around 135 psig during enriched-air operations. Due to a restriction in the oxygen-fed lower mixing zone (LMZ), the majority of the test run featured air-blown operations.

TC11 was planned as a 250-hour test run to evaluate gasifier and PCD operations during a short term test using Falkirk lignite from North Dakota. The primary test objectives were:

- Operational stability – Characterize gasifier loop and PCD operations in both air- and oxygen-blown modes with short-term tests by varying coal-feed rate, oxygen/coal ratio, riser velocity, solids-circulation rate, system pressure, and oxygen distribution.
- Lignite operations – Evaluate the operation of the gasifier using lignite coal and study its effects on process performance, operational stability, and temperature profiles.
- Failsafe evaluation – Perform online tests of the PSDF-designed failsafe and the Pall fuse with hot g-ash injection to further characterize failsafe performance.

Secondary objectives included the following:

- Gasifier operations – Study the devolatilization and tar cracking effects from transient conditions during the transition from the start-up burner to coal feed. Evaluate the effect of process operations on heat release, heat transfer, and accelerated fuel particle heat-up rates. Study the effect of changes in gasifier conditions on transient temperature profiles, pressure balance, and synthesis gas composition.
- Process performance – Continue to evaluate effect of gasifier operating parameters such as steam/coal ratio, air distribution, solids-circulation rate, and gasifier temperature on CO/CO_2 ratio, carbon conversion, synthesis gas composition, synthesis gas lower heating value (LHV), sulfur and ammonia emissions, cold- and hot-gas efficiencies, tar cracking effects, transient temperature profiles, and the pressure balance.
- Fluidized-bed coal feeder commissioning – Commission and test the new coal feed system, and address the integration of the gasifier logic with the feeder logic.
- Ceramic ferrules – Continue to evaluate the performance of the ceramic ferrules in the syngas cooler.

- Particle size effects – Study the effect of particle size variations on standpipe operation including the effects of limestone and sand addition.
- Effect of moisture on the coal feed system – Study the effect of pulverized lignite moisture content on feed system operations.
- Back-pulse pressure measurements – Evaluate the effects of back-pulse pressure to optimize back-pulse parameters.

1.2 PSDF ACCOMPLISHMENTS

The PSDF has achieved over 4,985 hours of operation on coal feed and about 6,470 hours of solids circulation in combustion mode and 4,867 hours of solid circulation and 3,626 hours of coal feed in gasification mode of operation. The major accomplishments in TC11 are summarized below. For combustion-related accomplishments, see the technical progress report for the TC05 Test Campaign and for accomplishments in GCT1 through TC10 see the technical progress reports for the TC06, TC07, TC08, TC09 and TC10 Test Campaigns.

1.2.1 Transport Gasifier Train

The major accomplishments and observations in TC11 included the following:

Process

- The Transport Gasifier operated for 192 hours in TC11 using Falkirk lignite, accumulating over 167 hours in air-blown mode, 18 hours in oxygen-enriched air mode, and around 7 hours in oxygen-blown mode.
- As part of the characterization tests with lignite, the gasifier operated in a wide range of operating conditions in both air- and oxygen-blown modes. Temperatures ranged from 1,650 to 1,800°F in the mixing zone. Coal-feed rates ranged from 1,000 to 5,500 pph by weigh cell and the gasifier pressure in mixing zone ranged from 150 to 210 psig.
- Although the gasifier itself had no problems in gasifying the lignite, feeding the lignite into the gasifier proved to be difficult due to soft and hard lumps of coal forming in the grinding circuit. The coal mill circuit had difficulty in grinding the coal due to packing in the cooling screw on top of the storage silo, making gasifier conditions and syngas production unstable. In almost every case, the feeder unplugged easily, and coal feed normally resumed in less than 5 minutes. Feeding coke breeze maintained reactor temperatures during longer feeder trips.
- Due to the many coal feeder trips that occurred, the use of lignite at low feed rates was again tested as a start-up/restart fuel for the transport gasifier, instead of coke breeze. The coal successfully heated the gasifier from 1,100°F (the maximum temperature obtainable using the start-up burner in a reasonable time period) to 1,750°F without producing tar, provided that the unit was operated at a low coal-feed rate, producing about 1-percent carbon monoxide in the syngas.
- Even though the lignite proved difficult to feed, the gasifier ran better using lignite than with any other feedstock used to date. The lignite allowed high circulation rates and riser densities. Consequently, the temperature distribution in both the mixing zone and the riser was more uniform than in any previous test run, varying less than 10°F throughout the gasifier.
- Standpipe operations were much more stable in TC11 than in the previous few test runs. In general, solids inventory levels were much lower, possibly contributing to the smoother operations. In most cases, adjusting standpipe flows and lowering the solids inventory corrected standpipe problems. On the last day of operations, however, a bubble formed when workers were trying to use high-pressure nitrogen to clear a plugged pressure port in the gasifier during a period when the solids inventory was high.

The resulting upset may have contributed to the loss of circulation and the agglomeration that ended the test run. Additional standpipe nuclear density gauges should prove useful in determining the exact nature and location of standpipe problems.

- In the early portion of the run some unknown object restricted a portion of the lower mixing zone, causing pressures there to be much higher than the rest of the gasifier. The higher pressure prevented the oxygen system from delivering a sufficient flow rate to allow proper oxygen-blown operations. Eventually, (the day before the test run ended), the restriction became dislodged, resulting in higher oxygen flow rates for the oxygen-blown testing.
- Typical riser velocities ranged from 30 to 40 ft/s during oxygen-blown operations and between 40 and 60 ft/s during air-blown operations. The solids circulation rate was between 200,000 and 600,000 pph, assuming a slip factor of 2.
- The raw gas dry heating value reached 50 Btu/scf in air-blown mode and 80 Btu/scf in oxygen-blown mode, resulting in projected heating values for large-scale operations of up to 105 Btu/scf in air-blown mode and 215 Btu/scf in oxygen-blown mode. The heating values obtained from Falkirk lignite were lower than those obtained from PRB coal and Hiawatha bituminous coal at the same dilution factor. Despite the numerous coal feeder trips, the atmospheric syngas burner ran well burning the syngas generated from the lignite.
- The following table lists typical raw gas analysis data during air-blown, enriched-air, and oxygen-blown modes:

	CO Percent	H_2 Percent	CH_4 Percent	CO_2 Percent	H_2O Percent	N_2 Percent
Air-Blown	6.6	5.6	0.7	10	11.6	65.3
Enriched Air	4.6	6.5	0.5	10.8	18.1	59.3
Oxygen-Blown	10.7	10.1	1.6	13.3	18	46.1

- Based on the corresponding flow of coal, PCD solids, and synthesis gas, the carbon conversion averaged 97 percent, slightly higher than the carbon conversion seen when using PRB coal.
- Gasifier sulfur emissions were between 450 and 1,400 ppm. Without sorbent addition, the sulfur capture averaged 12.5 percent. Ammonia emissions averaged 500 ppm for air-blown operations and 1,250 ppm for oxygen-blown and enriched-air operations.
- The solids obtained from the standpipe sampling system had a mass mean particle diameter from 140 to 210 μ (increasing as TC11 progressed) and a carbon content typically below 1 percent. Solids obtained from the spent fines feeder possessed a mean particle diameter of under 20 μ and a carbon content of between 5 and 15 percent in air-blown and enhanced-air operation. Samples from the new loop seal sampling system

possessed carbon content values similar to those of the standpipe samples. The average mass mean diameter of the loop seal solids was around 140 μ.

- As in TC10, a large number of gasifier pressure taps became plugged during the run, resulting in the loss of some of the gasifier pressure differential pressure data. Although the plugged taps were not as numerous as in TC10, studies are continuing to examine the cause of the plugging pressure taps and develop further recommendations for avoiding plugged taps.
- A number of new automatic control systems operated for the first time in TC11. These systems included new aeration velocity controllers for the standpipe, loop seal, and gasifier J-leg as well as a new standpipe level control system to control the standpipe screw cooler and solids removal system. Each of these systems performed well and will be useful in automating the operations.
- The test run ended prematurely (2 days before planned shutdown) when excessively high standpipe levels (caused by a high coal-feed rate and insufficient standpipe solids removal system capacity) blocked the loop seal return leg, causing a loss of circulation. As a result, an agglomeration formed in the mixing zone just above and below the J-leg entry. The thermocouples did not detect a temperature excursion, and the mixing zone temperature was below 1,800°F.

Equipment

- During TC11, the atmospheric fluidized-bed combustor system operated only on fuel oil to provide superheated steam to the rest of the gasifier loop. Consequently, operations were smooth. The bed temperatures for most of the run were between 1,250 and 1,550°F.
- Most of the gas analyzers were online for the majority of the test run, presenting good gas composition data. The dry gas compositions added up to between 98 and 99.5 percent on a consistent basis.
- Even though the exit of the coal feeders plugged often while feeding lignite, the lock hoppers did not experience any difficulties in transferring the material from the atmospheric surge bin to the pressurized feed vessel. Also, the storage silos, transfer blow pots, low-pressure and high-pressure conveying lines, and surge bin did not experience any problems with soft and hard lumps in ground coal.
- During TC11, the original coal rotofeeder (FD0210), the new coal feeder (FD0200), and the coke breeze screw-type feeder each (FD0252) fed lignite to the gasifier. FD0210 proved to be the most practical, although it experienced many trips due to the exit plugging. Feed through the FD0200 feeder was erratic, although it did perform well during a brief period early in the run when it fed the dryer coal left in the system from the prerun offline feed tests. The FD0252 feeder plugged often at the exit mixer when the coal-feed rate was increased and it required a much larger amount of conveying nitrogen, diluting the syngas.
- The primary gas cooler performed well during TC11. The average flow rate through the cooler was 22,000 pph during air-blown operations and around 15,000 pph during oxygen-blown operations. The average inlet and outlet temperatures were 1,700 and 700°F, respectively.

- The solids removal systems performed fairly well. Instead of operating as a rotofeeder, the FD0530 g-ash feeder system operated as a blow pot without the star feeder in place. Ironically, the feed rate was much more stable than it has been using the star feeder. The standpipe screw cooler also operated well, but the associated transport system did not have sufficient capacity to control gasifier inventory at high coal feed rates.
- To prepare for the upcoming fuel cell test run, hot and cold gas cleanup tests were conducted with a slipstream of syngas. Hot gas cleanup tests were performed with mini-reactors containing commercial grade zinc oxide and activated alumina sorbents from Synetix. Cold gas cleanup tests were performed with impingers with various combinations of solutions. A thermal oxidizer was built to measure low levels of TRS accurately as SO_2 in the effluent stream. The tests show that the TRS can be reduced to below 100 ppb and ammonia and HCN to less than 1 ppm.
- The postrun inspections showed the gasifier and primary gas cooler to be in good order with no noticeable changes to the refractory inside.
- To evaluate the operational limits of the grinding circuit, tests to determine the rate of moisture evaporation, lignite ignition temperature tests at reduced oxygen levels, and an ASPEN simulation of the existing grinding circuit were initiated. Based on these results, the milling circuit will be operated during the outage to determine operational settings and required modifications to handle high moisture fuels.

1.2.2 PCD

The highlights of PCD operation for TC11 are listed below.

- The pressure drop in the PCD was controllable throughout TC11. During most of the coal run, the baseline differential pressure was about 45 to 55 inH_2O. During steady-state operations, the inlet temperature was about 725°F, and the face velocity was maintained at about 3 to 3.5 ft/min. Throughout periods of solids feed to the reactor, a 5-minute back-pulse cycle was used, as well as a back-pulse pressure of 320 psid on the top plenum and 600 psid on the bottom plenum. Filter surface thermocouple response during operations was normal, indicating no permanent buildup of char.
- The fines removal system operated fairly well during normal operations. To prevent the problem of overwhelming the solids removal system following reactor upsets, new control logic was tested during the run. This logic, which adjusts operating parameters appropriately in response to indications of high solids carryover, worked well and will continue to be used.
- Failsafe testing with hot char injection was performed with both the PSDF-designed failsafe device and the Pall fuse. Both devices showed good collection efficiencies, and they will be evaluated further in upcoming test runs.
- The PCD outlet loading measurements indicated good sealing of the filter vessel. All samples showed loading of less than 0.1 ppmw except for one sample taken at the beginning of the run which showed 0.27 ppmw loading.

- Inspections revealed neither char bridging nor filter failures. The seven Siemens Westinghouse inverted filter assemblies were not plugged.

2.0 INTRODUCTION

This report provides an account of the TC11 test campaign with the Kellogg Brown & Root, Inc. (KBR) Transport Gasifier and the Siemens Westinghouse Power Corporation (Siemens Westinghouse) filter vessel at the Power Systems Development Facility (PSDF) located in Wilsonville, Alabama, 40 miles southeast of Birmingham. The PSDF is sponsored by the U. S. Department of Energy (DOE) and is an engineering-scale demonstration of advanced coal-fired power systems. In addition to DOE, Southern Company Services, Inc., (SCS), Electric Power Research Institute (EPRI), and Peabody Energy are cofunders. Other cofunding participants supplying services, materials, or equipment currently include KBR, the Lignite Energy Council, and Siemens Westinghouse. SCS is responsible for constructing, commissioning, and operating the PSDF.

2.1 THE POWER SYSTEMS DEVELOPMENT FACILITY

SCS entered into an agreement with DOE/National Energy Technology Laboratory (NETL) for the design, construction, and operation of a hot gas clean-up test facility for pressurized gasification and combustion. The purpose of the PSDF is to provide a flexible test facility that can be used to develop advanced power system components and assess the integration and control issues of these advanced power systems. The facility also supports Vision 21 programs to eliminate environmental concerns associated with using fossil fuels for producing electricity, chemicals, and transportation fuels. The facility was designed as a resource for rigorous, long-term testing and performance assessment of hot stream clean-up devices and other components in an integrated environment.

The PSDF now consists of the following modules for systems and component testing:

- A Transport Reactor module.
- A hot gas clean-up module.
- A compressor/turbine module.

The Transport Reactor module includes KBR Transport Reactor technology for pressurized combustion and gasification to provide either an oxidizing or reducing gas for parametric testing of hot particulate control devices. The Transport Gasifier can be operated in either air or oxygen-blown mode. Oxygen-blown operations are primarily focused on testing and developing various Vision 21 programs to benefit gasification technologies in general. The hot gas clean-up filter system tested to date at the PSDF is the particulate control device (PCD) supplied by Siemens Westinghouse. The gas turbine is an Allison Model 501-KM gas turbine, which drives a synchronous generator through a speed reducing gearbox. The Model 501-KM engine was designed as a modification of the Allison Model 501-KB5 engine to provide operational flexibility. Design considerations include a large, close-coupled external combustor to burn a wide variety of fuels and a fuel delivery system that is much larger than the standard system.

2.2 TRANSPORT GASIFIER SYSTEM DESCRIPTION

The Transport Gasifier is an advanced circulating fluidized-bed reactor operating in air- or oxygen blown mode, using a hot gas clean-up filter technology (particulate control devices or PCDs) at a component size readily scaleable to commercial systems. The Transport Gasifier train is shown schematically in Figure 2.2-1. A tag list of all major equipment in the process train and associated balance-of-plant is provided in Tables 2.2-1 and -2.

The Transport Gasifier consists of a mixing zone, a riser, a disengager, a cyclone, a standpipe, a loop seal, and a J-leg. Steam and air or oxygen are mixed together and introduced in the lower mixing zone (LMZ) while the fuel, sorbent, and additional air and steam (if needed) are added in the upper mixing zone. The steam and air or oxygen along with the fuel, sorbent, and solids from the standpipe are mixed together in the upper mixing zone. The mixing zone located below the riser, has a slightly larger diameter than the riser. The gas and solids move up the riser together, make two turns and enter the disengager. The disengager removes larger particles by gravity separation. The gas and remaining solids then move to the cyclone, which removes most of the particles not collected by the disengager. The gas then exits the Transport Gasifier and goes to the primary gas cooler and the PCD for final particulate clean-up. The solids collected by the disengager and cyclone are recycled back to the gasifier mixing zone through the standpipe and a J-leg. The nominal Transport Gasifier operating temperature is 1,800°F. The gasifier system is designed to have a maximum operation pressure of 294 psig with a thermal capacity of about 41 MBtu/hr. Due to a lower oxygen supply pressure, the maximum operation pressure is about 180 psi in oxygen-blown mode.

For start-up purposes, a burner (BR0201) is provided at the gasifier mixing zone. Liquefied propane gas (LPG) is used as start-up fuel. The fuel and sorbent are separately fed into the Transport Gasifier through lockhoppers. Coal is ground to a nominal average particle diameter between 250 and 400 microns. Sorbent is ground to a nominal average particle diameter of 10 to 30 microns. Limestone or dolomitic sorbents are fed into the gasifier for sulfur capture. The gas leaves the Transport Gasifier cyclone and goes to the primary gas cooler which cools the gas prior to entering the Siemens-Westinghouse PCD barrier filter. The PCD uses ceramic or metal elements to filter out dust from the gasifier. The filters remove almost all the dust from the gas stream to prevent erosion of a downstream gas turbine in a commercial plant. The operating temperature of the PCD is controlled both by the gasifier temperature and by an upstream gas cooler. For test purposes, 0 to 100 percent of the gas from the Transport Gasifier can flow through the gas cooler. The PCD gas temperature can range from 700 to 1,600°F. The filter elements are back-pulsed by high-pressure nitrogen in a desired time interval or at a given maximum pressure difference across the elements. There is a secondary gas cooler after the filter vessel, to cool the gas before discharging to the atmospheric syngas combustor (thermal oxidizer) or flare. In a commercial process, the gas from the PCD would be sent to a gas turbine in a combined cycle package. The fuel gas is sampled for online analysis after traveling through the secondary gas cooler.

After exiting the secondary gas cooler, the gas is then let down to about 2 psig through a pressure control valve. The fuel gas is then sent to the atmospheric syngas burner to burn the gas and oxidize all reduced sulfur compounds (H_2S, COS, and CS_2) and reduced nitrogen

compounds (NH_3 and HCN). The atmospheric syngas burner uses propane as a supplemental fuel. The gas from the atmospheric syngas burner goes to the baghouse and then to the stack.

The Transport Gasifier produces both fine ash collected by the PCD and coarse ash extracted from the Transport Gasifier standpipe. The two solid streams are cooled using screw coolers, reduced in pressure in lock hoppers and then combined together. Any fuel sulfur captured by sorbent should be present as calcium sulfide (CaS). The gasification ash is processed in the atmospheric fluidized bed combustor (AFBC) to oxidize the CaS to calcium sulfate ($CaSO_4$) and burn any residual carbon on the ash. The waste solids are then suitable for commercial use or disposal. Depending on the fuel type and gasifier operating conditions, the gasification ash may be disposed of directly without sending it to the AFBC.

Table 2.2-1

Major Equipment in the Transport Reactor Train

TAG NAME	DESCRIPTION
BR0201	Reactor Start-Up Burner
BR0401	Syngas Combustor (Thermal Oxidizer)
BR0602	AFBC (Sulfator) Start-Up/PCD Preheat Burner
CO0201	Main Air Compressor
CO0401	Recycle Gas Booster Compressor
CO0601	AFBC (Sulfator) Air Compressor
CY0201	Primary Cyclone in the Reactor Loop
CY0207	Disengager in the Reactor Loop
CY0601	AFBC (Sulfator) Cyclone
DR0402	Steam Drum
DY0201	Feeder System Air Dryer
FD0206	Spent Solids Screw Cooler
FD0210	Coal Feeder System
FD0220	Sorbent Feeder System
FD0502	Fines Screw Cooler
FD0510	Spent Solids Transporter System
FD0520	Fines Transporter System
FD0530	Spent Solids Feeder System
FD0602	AFBC (Sulfator) Solids Screw Cooler
FD0610	AFBC (Sulfator) Sorbent Feeder System
FL0301	PCD — Siemens Westinghouse
FL0302	PCD — Combustion Power
FL0401	Compressor Intake Filter
HX0202	Primary Gas Cooler
HX0203	Combustor Heat Exchanger
HX0204	Transport Air Cooler
HX0402	Secondary Gas Cooler
HX0405	Compressor Feed Cooler
HX0601	AFBC (Sulfator) Heat Recovery Exchanger
ME0540	Heat Transfer Fluid System
RX0201	Transport Reactor
SI0602	Spent Solids Silo
SU0601	Atmospheric Fluidized Bed Combustor (AFBC)

Table 2.2-2 (Page 1 of 3)

Major Equipment in the Balance of Plant

TAG NAME	DESCRIPTION
BO2920	Auxiliary Boiler
BO2921	Auxiliary Boiler – Superheater
CL2100	Cooling Tower
CO2201A-D	Service Air Compressor A-D
CO2202	Air-Cooled Service Air Compressor
CO2203	High-Pressure Air Compressor
CO2601A-C	Reciprocating N_2 Compressor A-C
CR0104	Coal and Sorbent Crusher
CV0100	Crushed Feed Conveyor
CV0101	Crushed Material Conveyor
DP2301	Baghouse Bypass Damper
DP2303	Inlet Damper on Dilution Air Blower
DP2304	Outlet Damper on Dilution Air Blower
DY2201A-D	Service Air Dryer A-D
DY2202	Air-Cooled Service Air Compressor Air Dryer
DY2203	High-Pressure Air Compressor Air Dryer
FD0104	MWK Coal Transport System
FD0111	MWK Coal Mill Feeder
FD0113	Sorbent Mill Feeder
FD0140	Coke Breeze and Bed Material Transport System
FD0154	MWK Limestone Transport System
FD0810	Ash Unloading System
FD0820	Baghouse Ash Transport System
FL0700	Baghouse
FN0700	Dilution Air Blower
HO0100	Reclaim Hopper
HO0105	Crushed Material Surge Hopper
HO0252	Coal Surge Hopper
HO0253	Sorbent Surge Hopper
HT2101	MWK Equipment Cooling Water Head Tank
HT2103	SCS Equipment Cooling Water Head Tank
HT0399	60-Ton Bridge Crane
HX2002	MWK Steam Condenser
HX2003	MWK Feed Water Heater

Table 2.2-2 (Page 2 of 3)

Major Equipment in the Balance of Plant

TAG NAME	DESCRIPTION
HX2004	MWK Subcooler
HX2103A	SCS Cooling Water Heat Exchanger
HX2103C	MWK Cooling Water Heat Exchanger
LF0300	Propane Vaporizer
MC3001-3017	MCCs for Various Equipment
ME0700	MWK Stack
ME0701	Flare
ME0814	Dry Ash Unloader for MWK Train
ML0111	Coal Mill for MWK Train
ML0113	Sorbent Mill for Both Trains
PG0011	Oxygen Plant
PG2600	Nitrogen Plant
PU2000A-B	MWK Feed Water Pump A-B
PU2100A-B	Raw Water Pump A-B
PU2101A-B	Service Water Pump A-B
PU2102A-B	Cooling Tower Make-Up Pump A-B
PU2103A-D	Circulating Water Pump A-D
PU2107	SCS Cooling Water Make-Up Pump
PU2109A-B	SCS Cooling Water Pump A-B
PU2111A-B	MWK Cooling Water Pump A-B
PU2300	Propane Pump
PU2301	Diesel Rolling Stock Pump
PU2302	Diesel Generator Transfer Pump
PU2303	Diesel Tank Sump Pump
PU2400	Fire Protection Jockey Pump
PU2401	Diesel Fire Water Pump #1
PU2402	Diesel Fire Water Pump #2
PU2504A-B	Waste Water Sump Pump A-B
PU2507	Coal and Limestone Storage Sump Pump
PU2700A-B	Demineralizer Forwarding Pump A-B

Table 2.2-2 (Page 3 of 3)

Major Equipment in the Balance of Plant

TAG NAME	DESCRIPTION
PU2920A-B	Auxiliary Boiler Feed Water Pump A-B
SB3001	125-V DC Station Battery
SB3002	UPS
SC0700	Baghouse Screw Conveyor
SG3000-3005	4160-V, 480-V Switchgear Buses
SI0101	MWK Crushed Coal Storage Silo
SI0103	Crushed Sorbent Storage Silo
SI0111	MWK Pulverized Coal Storage Silo
SI0113	MWK Limestone Silo
SI0114	FW Limestone Silo
SI0810	Ash Silo
ST2601	N_2 Storage Tube Bank
TK2000	MWK Condensate Storage Tank
TK2001	FW Condensate Tank
TK2100	Raw Water Storage Tank
TK2300A-D	Propane Storage Tank A-D
TK2301	Diesel Storage Tank
TK2401	Fire Water Tank
XF3000A	230/4.16-kV Main Power Transformer
XF3001B-5B	4160/480-V Station Service Transformer No. 1-5
XF3001G	480/120-V Miscellaneous Transformer
XF3010G	120/208 Distribution Transformer
XF3012G	UPS Isolation Transformer
VS2203	High-Pressure Air Receiver

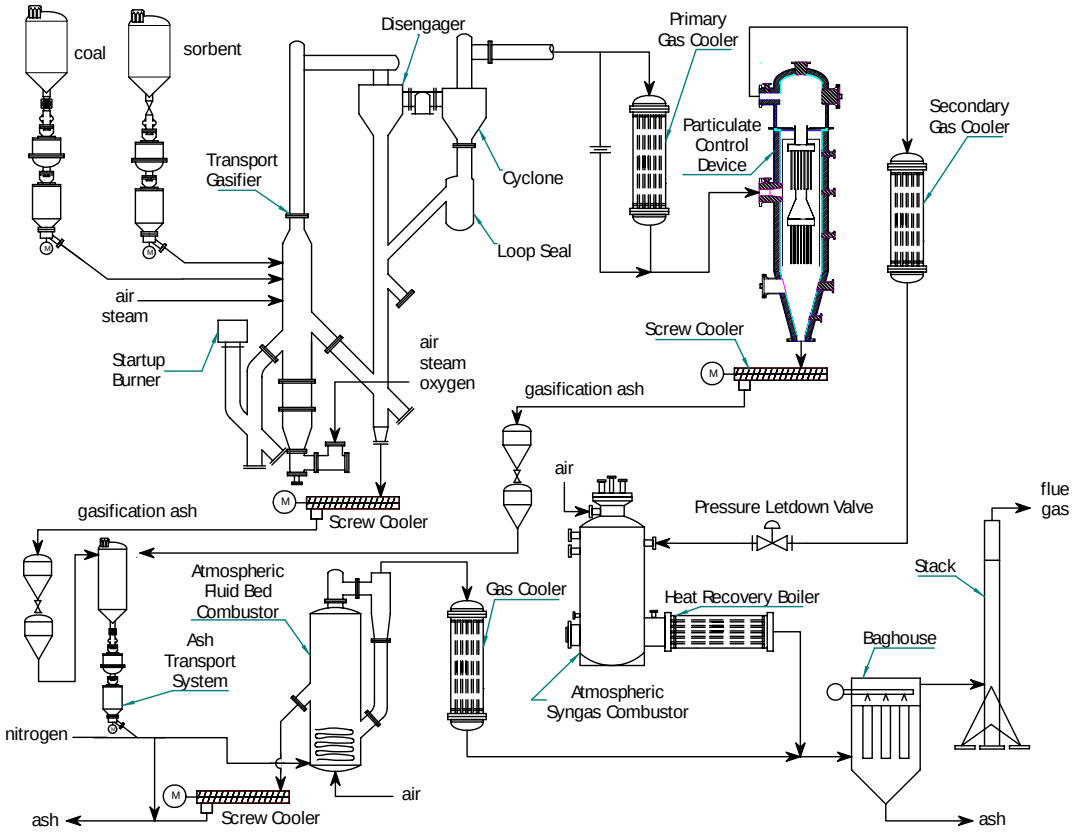

Figure 2.2-1 Flow Diagram of the Transport Gasifier Train

2.3 SIEMENS WESTINGHOUSE PARTICULATE CONTROL DEVICE

Different PCDs will be evaluated on the Transport Reactor train. The first PCD that was commissioned in 1996 has been used in all of the testing to date was the filter system designed by Siemens Westinghouse. The dirty gas enters the PCD below the tube sheet, flows through the filter elements, and the ash collects on the outside of the filter. The clean gas passes from the plenum/filter element assembly through the plenum pipe to the outlet pipe. As the ash collects on the outside surface of the filter elements, the pressure drop across the filter system gradually increases. The filter cake is periodically dislodged by injecting a high-pressure gas pulse to the clean side of the filter elements. The cake then falls to the discharge hopper.

Until the first gasification run in late 1999, the Transport Reactor had been operated only in the combustion mode. Initially, high-pressure air was used as the pulse gas for the PCD; however, the pulse gas was changed to nitrogen early in 1997. The pulse gas was routed individually to the two-plenum/filter element assemblies via injection tubes mounted on the top head of the PCD vessel. The pulse duration was typically 0.1 to 0.5 seconds.

A sketch of the Siemens Westinghouse PCD is shown in Figure 2.3-1.

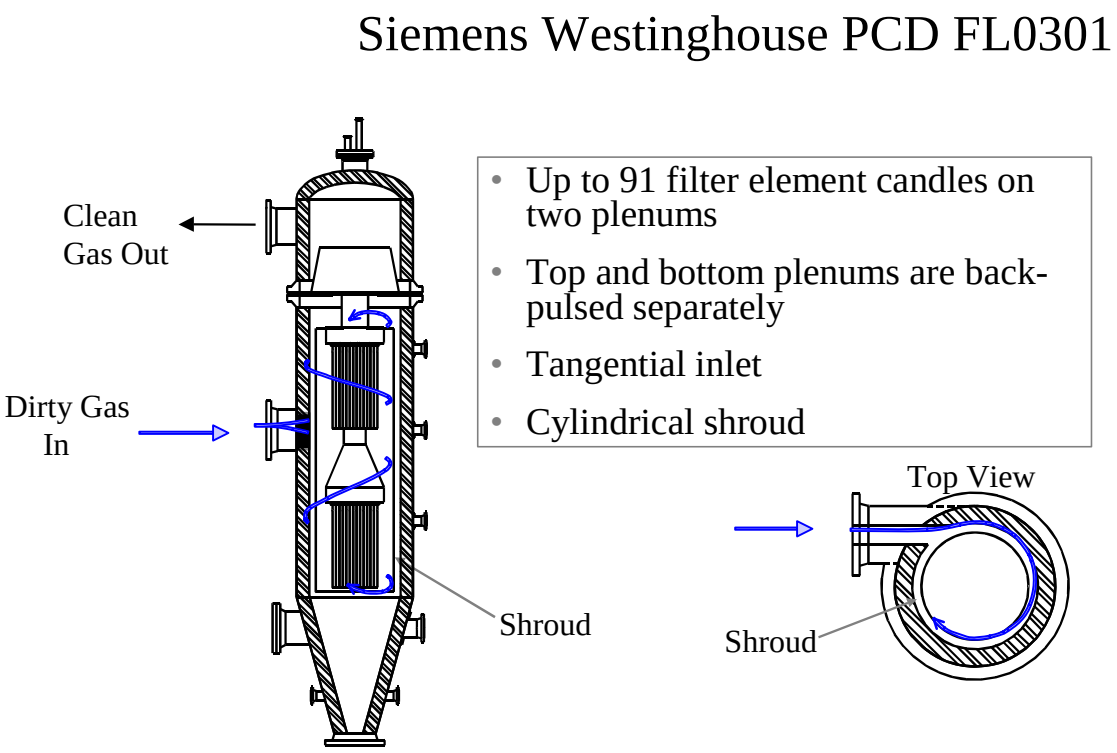

Figure 2.3-1 Siemens Westinghouse PCD

2.4 OPERATION HISTORY

Conversion of the transport reactor train to gasification mode of operation was performed from May to September 1999. The first gasification test run, GCT1, was planned as a 250-hour test run to commission the Transport Gasifier and to characterize the limits of operational parameter variations. GCT1 was started on September 9, 1999, with the first part completed on September 15, 1999 (GCT1A). The second part of GCT1 was started on December 7, 1999 and completed on December 15, 1999 (GCT1B-D). This test run provided the data necessary for preliminary analysis of gasifier operations and for identification of necessary modifications to improve equipment and process performance. Five different feed combinations of coal and sorbent were tested to gain a better understanding of the gasifier solids collection system efficiency.

GCT2, planned as a 250-hour characterization test run, was started on April 10, 2000, and completed on April 27, 2000. Additional data was taken to analyze the effect of different operating conditions on gasifier performance and operability. A blend of several Powder River Basin (PRB) coals was used with Longview limestone from Alabama. In the outage following GCT2, the Transport Gasifier underwent a major modification to improve the operation and performance of the gasifier solids collection system. The most fundamental change was the addition of the loop seal underneath the primary cyclone.

GCT3 was planned as a 250-hour characterization with the primary objective to commission the loop seal. A hot solids circulation test (GCT3A) was started on December 1, 2000, and completed December 15, 2000. After a one-month outage to address maintenance issues with the main air compressor, GCT3 was continued. The second part of GCT3 (GCT3B) was started on January 20, 2001, and completed on February 1, 2001. During GCT3B, a blend of several PRB coals was used with Bucyrus limestone from Ohio. The loop seal performed well needing little attention and promoting much higher solids circulation rates and higher coal feed rates that resulted in lower relative solids loading to the PCD and higher char retention in the gasifier.

GCT4, planned as a 250-hour characterization test run, was started on March 7, 2001, and completed on March 30, 2001. A blend of several PRB coals with Bucyrus limestone from Ohio was used. More experience was gained with the loop seal operations, and additional data was collected to better understand gasifier performance.

TC06, planned as a 1000-hour test campaign was started on July 4, 2001, and completed on September 24, 2001. A blend of several PRB coals with Bucyrus limestone from Ohio was used. Both gasifier and PCD operations were stable during the test run with a stable baseline pressure drop. Due to its length and stability, the TC06 test run provided valuable data necessary to analyze long term gasifier operations and to identify necessary modifications to improve equipment and process performance as well as progressing the goal of many thousands of hours of candle exposure.

TC07, planned as a 500-hour test campaign was started on December 11, 2001, and completed on April 5, 2002. A blend of several PRB coals and a bituminous coal from the Calumet mine in Alabama were tested with Bucyrus limestone from Ohio. Due to operational difficulties with the gasifier (stemming from instrumentation problems), the unit was taken offline several times. PCD operations were relatively stable considering the numerous gasifier upsets.

TC08, planned as a 250-hour test campaign to commission the gasifier in oxygen blown mode of operation was started on June 9, 2002, and completed on June 29, 2002. A blend of several PRB coals was tested in air blown, enriched air- and oxygen-blown modes of operation. The transition from different modes of operation was smooth, and it was demonstrated that the full transition could be made within 15 minutes. Both gasifier and PCD operations were stable during the test run with a stable baseline pressure drop.

TC09 was planned as a 250-hour test campaign to characterize the gasifier and PCD operations in air- and oxygen-blown mode of operations using a bituminous coal. TC09 was started on September 3, 2002, and completed on September 26, 2002. A bituminous coal from the Sufco mine in Utah was successfully tested in air- and oxygen-blown modes of operation. Both gasifier and PCD operations were stable during the test run.

TC10 was planned as a 500-hour test campaign to conduct long-term tests which evaluate the gasifier and PCD operations in oxygen-blown mode of operations using a blend of several PRB coals. TC10 was started on November 16, 2002, and completed on December 18, 2002. Despite problems with the coal mills, coal feeder, pressure tap nozzles and the standpipe, the gasifier did experience short periods of stability during oxygen-blown operations. During these periods, the syngas quality was high. During TC10, over 609 tons of Powder River Basin subbituminous coal were gasified.

TC11, the subject of this report, was planned as a 250-hour test campaign to conduct short-term tests to evaluate the gasifier and PCD operations in air- and oxygen-blown modes of operation using lignite from North Dakota. TC11 was started on April 7, 2003, and completed on April 18, 2003. During this campaign, the lignite proved difficult to feed because of the mill operation problems resulting from the high moisture content in the fuel. However, the gasifier operated better using lignite than with any other feedstock used to date. The lignite allowed high circulation rates and riser densities. Consequently, the temperature distribution in both the mixing zone and the riser was more uniform than in any previous test run, varying less than 10°F throughout the gasifier.

Figure 2.4-1 gives a summary of operating test hours achieved with the Transport Reactor at the PSDF.

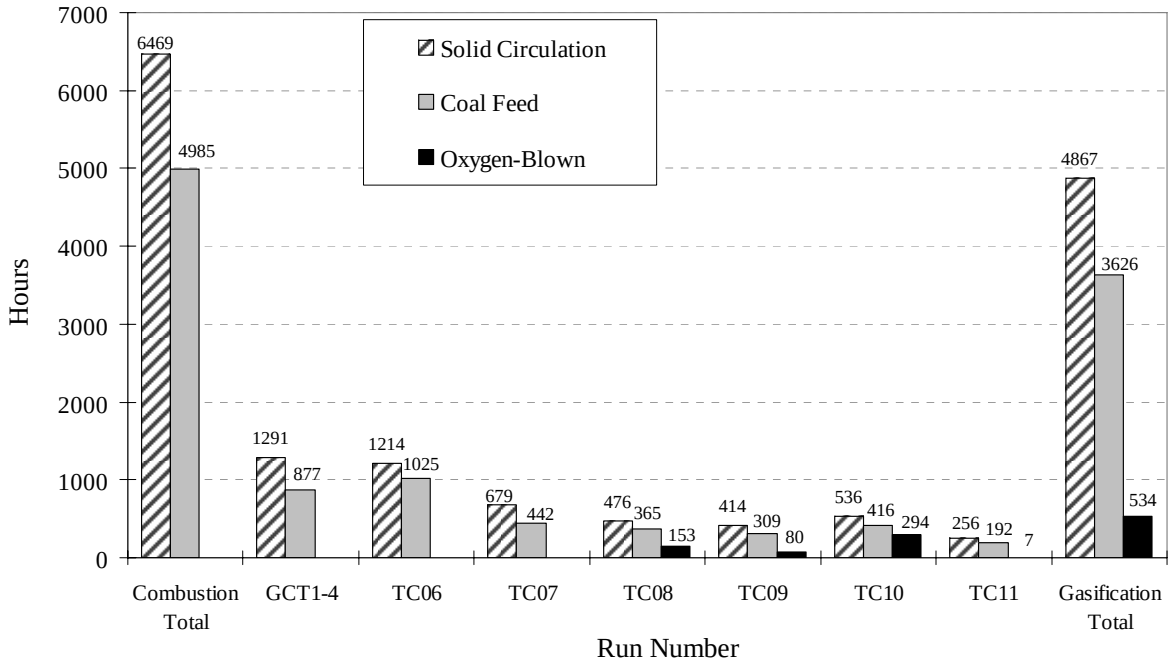

Figure 2.4-1 Operating Hours Summary for the Transport Reactor Train

3.0 TRANSPORT GASIFIER

3.1 TC11 RUN SUMMARY

Test run TC11 began on April 7, 2003, with the startup of the main air compressor and the lighting of the gasifier start-up burner. The Transport Gasifier operated until April 18, 2003, when a deposit formed in the mixing zone, due to a loss of solids circulation and forced the termination of the test run. Over the course of the entire test run, gasifier temperatures varied between 1,650 and 1,800°F using Falkirk lignite at pressures from 160 to 200 psig during air-blown operations and around 135 psig during enriched-air operations. Due to a restriction in the oxygen-fed lower mixing zone (LMZ), the majority of the test run featured air-blown operations.

The primary objectives of test run TC11 were:

- Operational stability – Characterize gasifier loop and PCD operations in both air- and oxygen-blown modes with short-term tests by varying coal-feed rate, oxygen/coal ratio, riser velocity, solids-circulation rate, system pressure, and oxygen distribution.
- Lignite operations – Evaluate the operation of the gasifier using lignite coal and study its effects on process performance, operational stability, and temperature profiles.

Secondary objectives included the following:

- Gasifier operations – Study the devolatilization and tar cracking effects from transient conditions during the transition from the start-up burner to coal feed. Evaluate the effect of process operations on heat release, heat transfer, and accelerated fuel particle heat-up rates. Study the effect of changes in gasifier conditions on transient temperature profiles, pressure balance, and product gas composition.
- Process performance – Continue to evaluate the effect of gasifier operating parameters such as steam/coal ratio, air distribution, solids-circulation rate, and gasifier temperature on CO/CO_2 ratio, carbon conversion, synthesis gas composition, synthesis gas lower heating value (LHV), sulfur and ammonia emissions, cold and hot gas efficiencies, tar cracking effects, transient temperature profiles, and the pressure balance.
- Fluidized-bed coal feeder commissioning – Commission and test the improved coal-feed system, and address the integration of the gasifier logic with the feeder logic.
- Ceramic ferrules – Continue to evaluate the performance of the ceramic ferrules in the syngas cooler.
- Particle size effects – Study the effect of particle size variations on standpipe operation including the effects of limestone and sand addition.
- Effect of moisture on the coal feed system – Study the effect of pulverized lignite moisture content on feed system operations.

The activities that occurred during the outage preceding test run TC11 included 45 equipment revisions. The revisions affecting the process the most were the installation and modifications listed below:

- Maintenance added a bypass line around the spent fines conveying system for the emergency removal of PCD solids in the event of a problem with the spent fines screw cooler or conveying system.
- Two new standpipe nuclear density gauges were installed to detect upsets in standpipe operation.
- New automation systems allowed for multiparameter gasifier temperature and standpipe level control as well as velocity controls for many of the gasifier fluidization nozzles in the loop seal and J-leg.

The gasifier start-up burner was lit on April 7. When the gasifier temperature reached 1,100°F (at 09:45 on April 8), coke breeze feed began. A few hours later, a problem with the plant electrical system tripped all plant equipment, delaying the start of coal feed. After the problem was resolved, the gasifier heat-up process continued until 15:50, when coal feed began. Since the gasifier temperatures were still below 1,650°F, the coal feeder fed at a minimum rate to prevent tar formation, producing a syngas of less than 1-percent carbon monoxide. When temperatures exceeded 1,650°F, the coal-feed rate increased, and syngas quality improved.

Shortly after normal gasifier operations were established, the coal feeder began to plug with the high moisture lignite. Eventually (at 19:12) the feeder tripped on high conveying line differential pressure. Blowing out the dispense vessel and conveying line allowed the feeder to restart, but it plugged again shortly thereafter, requiring further cleaning to unplug the line.

The feeder continued to plug continuously during the night. Although the line was relatively easy to clear, the unstable feed rate caused the gasifier temperature to fluctuate, and steady conditions were difficult to achieve. Occasionally, when the temperatures dropped below 1,650°F, feeding coke breeze was necessary to avoid producing tar. At 23:46, the fluidized-bed coal feeder was started in hopes that it would perform well with the high moisture coal, but it experienced the same problems that plagued the coal rotofeeder.

The period of unstable operation came to an end when a leak in one of the high-pressure nitrogen compressors allowed nitrogen to enter the cooling water system. The subsequent upset in the cooling water system allowed the instrument air compressors to become hot and trip. The loss of instrument air tripped all plant systems and caused all valves to go to their fail state, forcing a temporary shutdown. When the cooling water and instrument air systems returned to normal, the test run resumed using a different high pressure nitrogen compressor.

On April 9, at 21:28, once the start-up burner, along with coke breeze feed, heated the gasifier to a temperature above 1,650°F, coal feed resumed using the new fluidized-bed coal feeder. The new feeder contained a large amount of lignite that was relatively dry, that had been tested for a long period of time in the offline feed system. The dry lignite fed very well through the feeder for almost 3 hours. At the same time, however, the spent fines conveying line plugged, causing

material to accumulate in the PCD. At 00:23 on April 10, coal feed was stopped to allow the PCD cone to empty. Coke breeze kept the gasifier warm while the PCD emptied.

The PCD cone was empty by 04:48 on April 10, at which point coal feed resumed through the fluidized-bed feeder. Since the feeder had fed all of the dry lignite, it began to experience problems with plugging. Although easily corrected, the problems were frequent enough that constantly feeding coke breeze became necessary to minimize the wide variations in gasifier temperature. Since the fluidized-bed feeder plugged more frequently than the original rotofeeder, the operators stopped the fluidized-bed coal feeder and restarted the coal rotofeeder.

The coal feeder continued to plug for the remainder of the test run, making stable gasifier operations rare. Under normal operations, the coal feeder fed between 2,000 and 4,000 pph. To accommodate the unreliable coal-feed rate, the gasifier ran at lower temperatures than usual (around 1,700°F). The system pressure was around 190 psig for a majority of the testing. Occasionally, the feeder ran for longer periods of time (up to 3 or 4 hours) without plugging. At 07:30 on April 12, unplugging the coal feeder caused a large amount of lignite to enter the mixing zone, causing the gasifier temperatures to plummet below 1,200°F. After using the start-up burner to increase the gasifier temperatures, coal feed resumed at 13:01 the same day.

Coal feed was unsteady over the remainder of the test run. On April 14, in an attempt to improve stability, the coke breeze screw feeder fed coal to the gasifier in tandem with the coal rotofeeder. Although the screw feeder did not plug as often at lower feed rates, it used a disproportionate amount of nitrogen that diluted the syngas. Coal feed through the screw feeder ended at 19:22 on April 15 as high moisture content limited the coal-feed rate. The coal rotofeeder remained the only active coal feeder for the remainder of the test run.

At 18:50 on April 16, the transition to oxygen-blown operations began. A complete transition was impossible, however, due to a restriction in the LMZ that limited the oxygen-flow rate. Thus, the gasifier ran at 135 psig in enriched-air mode for a period of time. Meanwhile, the coal feeder continued to exhibit problems feeding, and the coal milling systems also began to plug with wet lignite.

On the morning of April 18 the restriction in the LMZ dislodged itself and the transition to oxygen-blown mode could continue. Only a few hours later, however, at 16:40 a bubble formed in the standpipe when workers were using high-pressure nitrogen to clear a plugged pressure port when the solids inventory was high. The bubble was large enough to cause a gasifier upset, which resulted in a loss of circulation that caused temperatures in the mixing zone to increase rapidly and form an agglomeration that ended the test run.

Although the coal feeder had difficulty feeding the lignite, the gasifier operated well during the short periods in which the coal-feed rate was steady. During the test run, the gasifier accumulated 192 hours of coal feed, 18 of which were in enriched-air mode and 7 of which were in oxygen-blown mode, bringing the total gasification time to 3,625 hours. The typical operating conditions, Falkirk ignite coal analysis, and steady-state operating periods selected for data analysis are given in Tables 3.1-1 through 3.1-3.

The postrun inspections revealed that the gasifier refractory continued to show only minor wear since starting gasification. A few pieces of the hexagonal refractory hex-mesh had fallen from the cyclone roof into the loop seal, but otherwise both the cyclone and disengager were in good order as was the primary gas cooler. The deposit in the lower mixing zone was large (about 5 ft high) and covered the entire LMZ with the exception of a few paths in which the air and oxygen could flow. Other than the LMZ, the remainder of the gasifier appeared clear of any significant deposits.

The test run contained the following steady-state test periods:

Name	Comments
TC11-1	First period. Air-blown. Dry lignite.
TC11-2	First period with wet coal.
TC11-3	Increased temperatures, circulation.
TC11-4	Slightly higher temperatures.
TC11-5	Increased pressure, coal-feed rate.
TC11-6	Increased pressure, lowered coal feed.
TC11-7	Decreased pressure.
TC11-8	Increased circulation.
TC11-9	Resumed operations after trip.
TC11-10	Using both FD0210 and FD0252.
TC11-11	Decreased temperatures.
TC11-12	Increased coal-feed rate, pressure
TC11-13	Increased circulation rate.
TC11-14	Reduced temperatures, coal feed.
TC11-15	Reduced circulation. Increased coal.
TC11-16	Increased temperatures.
TC11-17	First enriched air period.
TC11-18	Increased circulation.
TC11-19	Enriched air.
TC11-20	Increased temperatures.
TC11-21	First oxygen-blown period
TC11-22	Lowered temperatures.

Table 3.1-1

TC11 Operating Conditions for Transport Gasifier

Startup Bed Material	Sand, ~ 120 μm
Startup Fuel	Coke Breeze
Fuel Type	Falkirk Lignite (North Dakota)
Fuel Particle Size (mmd)	200 - 320 μm
Average Fuel Feed Rate, pph	1,800 - 5,000
Sorbent Type	None
Gasifier Temperature, °F	1,650 - 1,800
Gasifier Pressure Mixing Zone, psig	140 - 200
Riser Gas Velocity, fps	35 - 55
Riser Mass Flux, lb/s·ft^2	350 - 450 (average slip ratio = 2)
Standpipe Level, in. H_2O (LI339)	100 - 220
Primary Gas Cooler Bypass	0%
PCD Temperature, °F	650 - 800
Total Gas Flowrate, pph	14,000 - 26,000
Oxygen/coal mass ratio, lb/lb	0.6 - 1.0
Oxygen/steam mass ratio, lb/lb	0.0 - 2.0
Steam/coal mass ratio, lb/lb	0.0 to 0.5

Table 3.1-2

Coal Analyses as Fed[1]

	Falkirk Lignite	
	Value	Standard Deviation
Moisture, wt%	27.95	0.70
Carbon, wt%	42.53	0.59
Hydrogen[2], wt%	2.73	0.10
Nitrogen, wt%	0.69	0.02
Oxygen, wt%	12.04	0.86
Sulfur, wt%	0.76	0.12
Ash, wt%	13.07	1.35
Volatiles, wt%	29.67	3.30
Fixed Carbon, wt%	29.08	3.97
Higher Heating Value, Btu/lb	6,973	105
Lower Heating Value, Btu/lb	6,429	107
CaO, wt %	1.82	0.10
SiO_2, wt %	5.17	0.86
Al_2O_3, wt %	1.62	0.15
MgO, wt %	0.48	0.01
Fe_2O_3, wt %	1.13	0.17
Ca/S, mole/mole	1.30	0.28
Fe/S, mole/mole	0.56	0.12

Notes:

1. All analyses are as sampled at FD0210.
2. Hydrogen in coal is reported separately from hydrogen in moisture.

Table 3.1-3

Operating Periods

			Mixing Zone Temp	Riser Temp	Pressure	Coal Feed Rate[1]	Air Flow Rate	Oxygen Flow Rate	Steam Flow Rate
	Start	End	°F	°F	(psig)	(lb/hr)	(lb/hr)	(lb/hr)	(lb/hr)
TC11-1	4/9/2003 23:00	4/10/2003 00:15	1,669	1,713	180	3,769	11,300	0	0
TC11-2	4/10/2003 13:45	4/10/2003 14:45	1,636	1,647	160	2,502	9,400	0	810
TC11-3	4/10/2003 20:15	4/11/2003 00:15	1,678	1,690	170	2,406	10,400	0	740
TC11-4	4/11/2003 02:30	4/11/2003 03:45	1,687	1,699	170	2,530	10,800	0	730
TC11-5	4/11/2003 15:00	4/11/2003 16:30	1,682	1,702	190	4,203	13,400	0	760
TC11-6	4/12/2003 05:30	4/12/2003 07:15	1,676	1,681	196	2,360	10,100	0	730
TC11-7	4/12/2003 20:30	4/12/2003 22:00	1,680	1,692	190	2,617	10,700	0	750
TC11-8	4/14/2003 04:15	4/14/2003 05:15	1,659	1,664	190	2,463	10,200	0	760
TC11-9	4/14/2003 07:00	4/14/2003 08:30	1,664	1,673	190	2,466	10,200	0	760
TC11-10	4/15/2003 02:15	4/15/2003 06:00	1,665	1,689	190	3,828	11,000	0	760
TC11-11	4/15/2003 12:30	4/15/2003 16:30	1,654	1,682	190	2,526	10,600	0	760
TC11-12	4/15/2003 20:30	4/15/2003 22:00	1,713	1723	194	4,846	13,400	0	750
TC11-13	4/15/2003 22:30	4/16/2003 05:30	1,715	1,751	194	4,847	13,200	0	750
TC11-14	4/16/2003 08:15	4/16/2003 10:30	1,669	1,707	194	3,272	9,900	0	750
TC11-15	4/16/2003 12:15	4/16/2003 13:15	1,688	1,709	194	4,847	12,200	0	750
TC11-16	4/16/2003 17:00	4/16/2003 18:00	1,712	1,711	194	4,847	12,500	0	740
TC11-17	4/16/2003 22:15	4/17/2003 01:00	1,677	1,727	136	3,527	2,400	2,022	1,700
TC11-18	4/17/2003 13:00	4/17/2003 16:00	1,675	1694	136	1,872	8,100	0	910
TC11-19	4/18/2003 00:00	4/18/2003 04:00	1,648	1,668	136	2,941	4,300	1,090	1,290
TC11-20	4/18/2003 04:45	4/18/2003 07:15	1,711	1,734	136	2,941	4,200	1,272	1,280
TC11-21	4/18/2003 10:30	4/18/2003 12:30	1,734	1,675	136	4,156	0	2,282	1,140
TC11-22	4/18/2003 15:00	4/18/2003 16:00	1,655	1,605	136	4,817	0	2,357	1,140

[1] Based on coal feeder speed and conveying gas flow rate.

3.2 GASIFIER TEMPERATURE PROFILES

Section 3.2 describes the temperature profiles in TC11. A schematic of the gasifier with relative thermocouple locations is given in Figure 3.2-1. The gasifier was operated in air- and oxygen-blown modes during TC11 with lignite coal from the Falkirk mine in North Dakota. In this section, the temperature profile for air- and oxygen-blown operations are discussed and the effect of coal-feed rate and circulation rate on the temperature profile is evaluated.

The temperature profiles for steady-state periods for air- and oxygen-blown modes are shown in Figures 3.2-2 and -3. Summary data for the steady-state operating periods used are listed in Table 3.2-1. In air-blown mode in TC11, the temperature in the lower mixing zone (LMZ), T1-T2, increases quickly as the heat released from char combustion heats the air, steam, and solids in the LMZ. The temperature, T3, then decreases when the carbon in the LMZ is consumed and the solids from the J-leg, T17, back-mix with solids in the LMZ. The temperature then increases due to additional char combustion as the solids enter the upper mixing zone (UMZ), T4-T5. Air and steam added in the UMZ decrease the temperature, T6, slightly. The temperature in the UMZ, T7-T8, begins to increase as char combustions occurs again. Coal is added just before the UMZ transitions into the riser (see Figure 3.2-1). Coal and conveying gas heatup, coal devolatilization and endothermic gasification reactions combined with heat losses decrease the temperature, T9-T12, as the gas and solids flow up through the riser. The solids removed by the disengager and cyclone cool as they flow down the standpipe (T13-T16). The solids are heated as they reenter the UMZ by the hot gases and solids in the LMZ.

The temperature profile for the oxygen-blown case is shown in Figure 3.2-3. Similar to air mode the LMZ temperature, T1-T2, increases quickly as the heat released from char combustion heats the oxygen, steam, and solids in the LMZ. The temperature, T3, then decreases when the carbon in the LMZ is consumed and the solids from the J-leg, T17, back-mix with solids in the LMZ. The temperature then increases due to additional char combustion as the solids enter the upper mixing zone (UMZ), T4-T5. Steam added in the UMZ decrease the temperature, T6, slightly. The temperature in the UMZ, T7-T8, begins to increase as further char combustion occurs. Coal is added just before the UMZ transitions into the riser (see Figure 3.2-1). Coal and conveying gas heat-up, coal devolatilization, and endothermic gasification reactions combined with heat losses decrease the temperature, T9-T12, as the gas and solids flow up through the riser. The solids removed by the disengager and cyclone cool as they flow down the standpipe, T13-T16. The solids are heated as they reenter the UMZ by the hot gases and solids in the LMZ, T17.

Several operating parameters influence the temperature profile: coal-feed rate, amount of carbon in circulating solids, solids circulation rate, and oxygen and steam flow rates and distribution. The temperature profiles for a steady-state period with lower and higher coal feed rates (TC11-11, -12) during air-blown mode are shown in Figure 3.2-4. At low coal-feed rates the carbon conversion is high, resulting in a low carbon content in the circulating solids as well as lower temperatures in the LMZ and UMZ. Due to insufficient carbon, some of the oxygen reacts with the fresh coal added resulting in a temperature increase as the gas and solids flow up the riser. Since the riser exit temperature is higher, the standpipe temperatures are also high. At high

coal-feed rates, there is sufficient carbon in the circulating solids to consume all of the oxygen in the LMZ and UMZ resulting in higher temperatures.

The temperature profiles for a steady-state period with medium and high circulation rates (TC11-16, -12) during air blown mode are shown in Figure 3.2-5. The temperature profile trends for medium and high circulation rates are similar. However, at lower circulation rates, the effect of coal and conveying gas heat-up, coal devolatilization, endothermic gasification reactions, and heat losses in the riser is greater resulting in a greater decrease in the temperature, T9-T12. This results in lower standpipe temperatures. Thus, the solids reentering the UMZ are cooler resulting in lower UMZ temperatures at a similar set of operating conditions, i.e., coal-feed rate, air-flow rate, steam-flow rate, etc.

Table 3.2-1 Operating Periods

			Mixing Zone Temp	Riser Temp	Pressure	Coal Feed Rate[1]	Air Flow Rate	Oxygen Flow Rate	Steam Flow Rate
	Start	End	°F	°F	(psig)	(lb/hr)	(lb/hr)	(lb/hr)	(lb/hr)
TC11-11	4/15/2003 12:30	4/15/2003 16:30	1,654	1,682	190	2,526	10,600	0	760
TC11-12	4/15/2003 20:30	4/15/2003 22:00	1,713	1723	194	4,846	13,400	0	750
TC11-16	4/16/2003 17:00	4/16/2003 18:00	1,712	1,711	194	4,847	12,500	0	740
TC11-21	4/18/2003 10:30	4/18/2003 12:30	1,734	1,675	136	4,156	0	2,282	1,140

[1] Based on coal feeder speed and conveying gas flow rate.

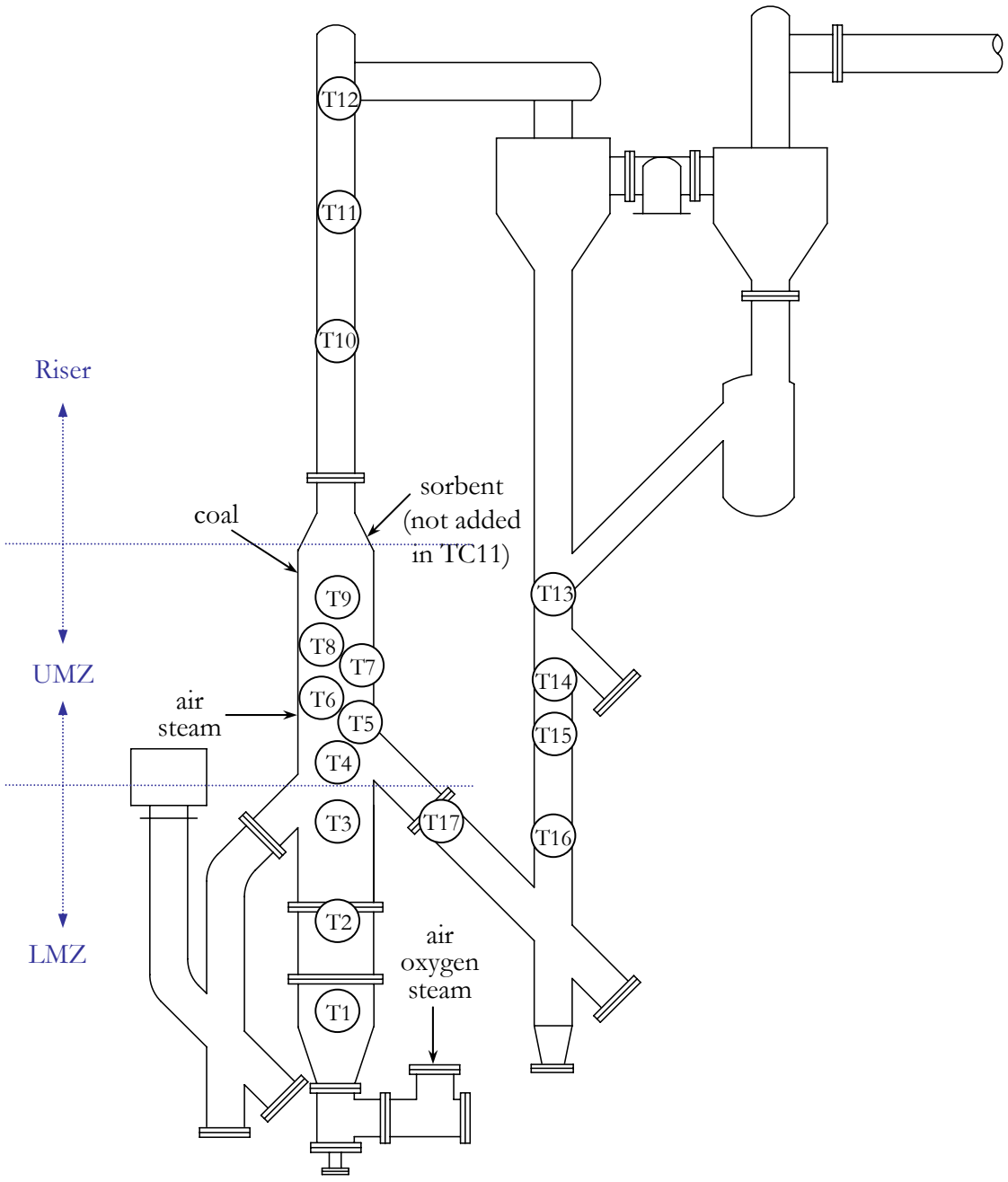

Figure 3.2-1 Transport Gasifier Schematic

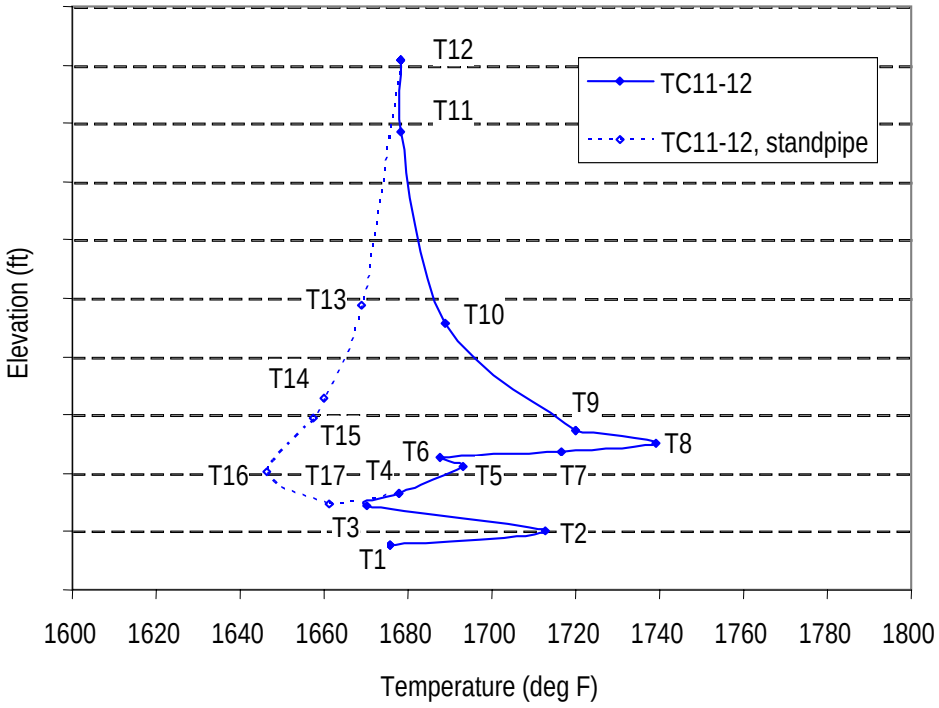

Figure 3.2-2 Temperature Profile in Air-Blown Mode in TC11 (TC11-12)

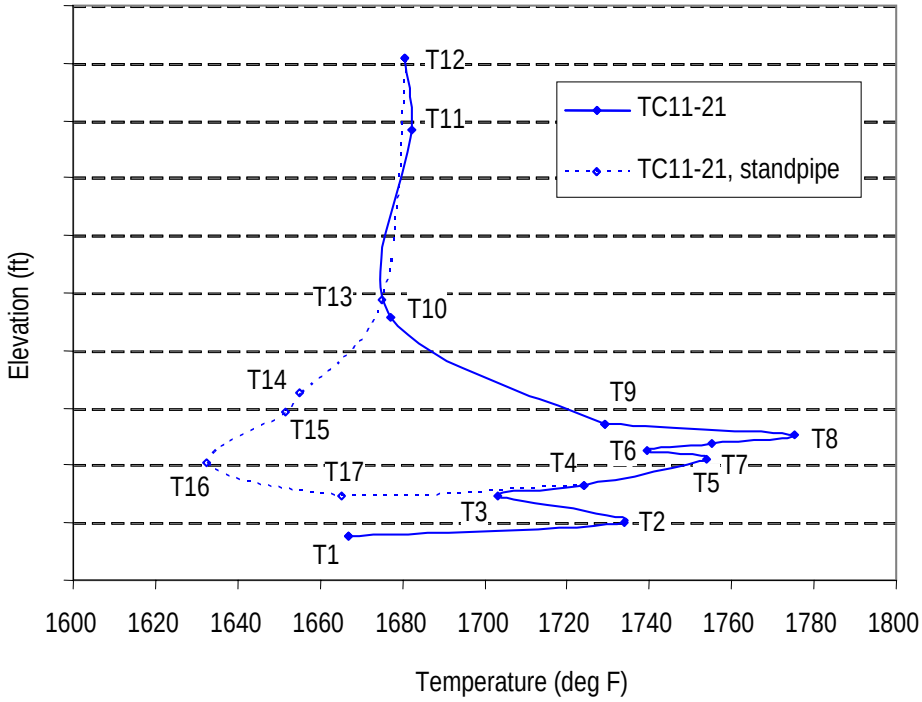

Figure 3.2-3 Temperature Profile in Oxygen-Blown Mode in TC11 (TC11-21)

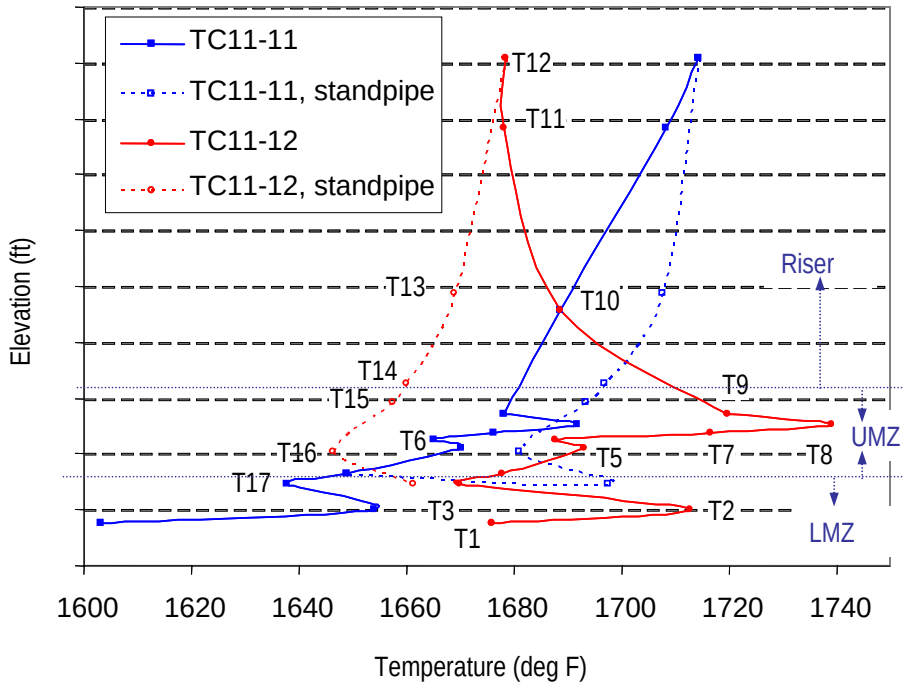

Figure 3.2-4 Temperature Profile in TC11 for Lower and Higher Coal-Feed Rates (TC11-11 and -12)

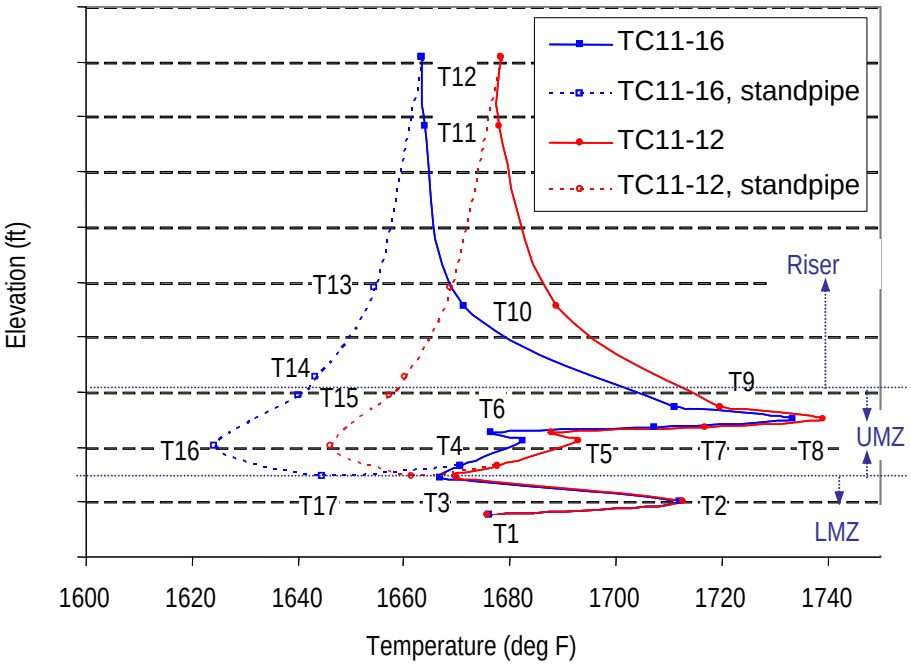

Figure 3.2-5 Temperature Profile in TC11 for Medium and High Circulation Rates (TC11-16 and -12)

3.3 GAS ANALYSIS

3.3.1 Summary and Conclusions

- The raw synthesis gas lower heating values (LHVs) were between 15 and 50 Btu/scf for air-blown operation, between 40 and 57 Btu/scf for enhanced-air operation, and either 80 or 81 Btu/scf for oxygen-blown operation.
- The LHVs for both modes of operation were strong functions of the relative amount of oxygen fed to the Transport Gasifier.
- The nitrogen-corrected, adiabatic synthesis gas LHVs were between 45 and 105 Btu/scf for air-blown operation, between 137 and 143 Btu/scf for enhanced-air, and either 209 or 215 Btu/scf for oxygen-blown operation.
- Total reduced sulfur (TRS, mostly H_2S) emissions were between 459 and 1,380 ppm. Synthesis gas analyzer data for CO was excellent, with all six analyzers in agreement for most of TC11.
- Synthesis gas analyzer data for H_2 was good with both gas chromatographic analyzers in agreement for most of TC11.
- Synthesis gas analyzer data for CH_4 was good in that two of the CH_4 analyzers were in agreement for most of TC11.
- Synthesis gas analyzer data for C_2^+ was acceptable in that AI419 read about 0.275 percent, while AI464 was erratic.
- Synthesis gas analyzer data for CO_2 was excellent in that three of the four analyzers were in agreement for most of TC11.
- Synthesis gas analyzer data for N_2 was good in that both GCs (AI464 and AI419) were in agreement for most of TC11.
- The synthesis gas H_2O measured by AI475H agreed with the in situ H_2O measurements.
- The sum of the dry gas analyzer concentrations were between 98 and 104 percent.
- The syngas H_2S analyzer gave good agreement when compared to the sulfur emissions by the syngas combustor SO_2 analyzer for the last 100 hours of TC11.
- The total reduced sulfur (TRS) was two to four times higher than the minimum equilibrium H_2S concentration.
- Wet chemistry data indicated 700 to 1,300 ppm NH_3 for air-blown operation and 1,900 ppm NH_3 for oxygen-blown operation.
- Both NH_3 gas analyzers agreed with each other for most of TC11 and were 200 to 500 ppm NH_3 lower than the wet chemistry data.
- The NH_3 emissions agreed with equilibrium calculations at 110ºF plus the PCD inlet temperature.
- The NH_3 emissions were lower for Falkirk lignite than for Powder River Basin and Hiawatha bituminous coals.
- Wet chemistry analyses measured about 10 ppm HCN.
- The Naphthalene analyzer indicated about 50 ppm $C_{10}H_8$ for air-blown operation and was erratic for enhanced air- and oxygen-blown operation.
- The CO/CO_2 ratio was between 0.2 and 1.1 for air-blown mode and between 0.7 and 1.2 for enhanced air- and oxygen-blown modes.

- The water-gas shift constants using the in situ H_2O measurements were between 0.65 and 0.84, despite large variations in H_2O, H_2, CO, and CO_2 concentrations.
- The water-gas shift constants using the H_2O analyzer were between 0.59 and 0.85 (one outlier), despite large variations in H_2O, H_2, CO, and CO_2 concentrations.
- The synthesis gas molecular weight was between 26.6 and 28.0 pounds/mole for air-blown mode and between 25.1 and 26.4 pounds/mole for enhanced air- and oxygen-blown modes.
- The synthesis gas combustor oxygen balance was good.
- The synthesis gas combustor hydrogen balance was excellent.
- The synthesis gas combustor carbon balance was excellent.

3.3.2 Introduction

The major goal for TC11 was the demonstration of the Transport Gasifier with Falkirk lignite coal. TC11 was the first time that lignite coal was used in the PSDF Transport Gasifier. Lignite feed was first established with air on April 8, 2003. After about 10 hours, the Transport Gasifier was tripped due to a leak in one of the high temperature nitrogen compressors. Coal testing resumed on April 9, 2003, and operated for about 200 hours before the unit was tripped due to a gasifier upset on April 18, 2003. Steady operation was difficult because the wet feed coal continually plugged the coal feed systems.

There were 22 steady periods of operation between April 9 and 19. The steady periods of operation are given on Table 3.3-1. Due to the frequent coal feed trips, the longest steady-state operating period was 7 hours (TC11-13). There were three enhanced air-operating periods (TC11-17, -19, and -20) and two oxygen-blown operating periods (TC11-21 and TC11-22). The remainder of TC11 was air blown.

Sorbent was not injected into the Transport gasifier during TC11; all sulfur removal was from the alkali contained in the Falkirk lignite coal.

Table 3.3-2 lists some of the TC11 operating conditions, including mixing zone temperatures, pressure control valve pressures, PCD inlet temperatures, air rate, oxygen rate, syngas rate, steam rate, and nitrogen rate. The system pressure was 160 to 196 psig for the air-blown periods, with the exceptions of TC11-18 (136 psig). All of the enhanced air- and oxygen-blown periods were at 136 psig.

3.3.3 Raw Gas Analyzer Data

During TC11, Transport Gasifier and synthesis gas combustor outlet gas analyzers were continuously monitored and recorded by the Plant Information System (PI). Seven in situ grab samples of synthesis gas moisture content were measured during PCD outlet loading sampling.

The gas analyzer system analyzed synthesis gas for the following gases during TC11 using the associated analyzers:

CO	AI419C, AI425, AI434B, AI453G, AI464C, AI475C
CO_2	AI419D, AI434C, AI464D, AI475D
CH_4	AI419E, AI464E, AI475E
C_2^+	AI419F, AI464F
H_2	AI419G, AI464G
H_2O	AI419H, AI475H, AI479H, AI480H
N_2	AI419B, AI464B
H_2S	AI419J, AI480J
NH_3	AI475Q, AI480Q
HCl	AI479R
HCN	AI479S
COS	AI479T
CS_2	AI480W
$C_{10}H_8$	AI480X

The locations of the synthesis gas analyzers are shown on Figure 3.3-1. The AI464 and AI419 analyzers use a gas chromatograph and typically have about a 6-minute delay. The other three CO analyzers (AI425, AI434B, and AI453B) and CO_2 analyzer (AI434C) are infrared based and give more real-time measurements. All analyzers except the AI475, AI479, and AI480 bank of analyzers require that the gas sample be conditioned to remove water vapor; therefore, those analyzers report gas compositions on a dry basis.

The gas analyzers obtain synthesis gas samples from three different locations:

- Between the PCD and the secondary gas cooler (HX0202).
- Between the secondary gas cooler and the pressure letdown valve (PCV-287).
- Between the pressure letdown valve and the atmospheric syngas combustor (BR0401).

With six CO analyzers, there is a measure of self-consistency when all or several of the six analyzers read the same value. There is also the choice of which analyzer to use if all the analyzers do not agree. The TC11 hourly averages for the six CO analyzers are given in Figure 3.3-2. The CO analyzer AI475C data was corrected to a dry composition using the H_2O analyzer AI475H data to compare with the other CO analyzers that measured dry. For most of TC11, all six CO analyzers were in good agreement. The only analyzers that had some periods of disagreement with the other analyzers were AI464C and AI475C.

The analyzer selection for each operating period is given in Table 3.3-3. AI419 was used for about half of the operating periods. The good agreement between the CO analyzers gives confidence to the accuracy of the CO data. The low CO measurements are either periods when the gas analyzers were being calibrated or analyzer measurements made during coal feeder trips. The CO data used in calculations were interpolated for times when the gas analyzers were being calibrated. The unit outage at hour 51 and the enhanced air- and oxygen-blown periods of

operation are noted on Figure 3.3-2. Note when the air and coal rates were increased at hour 128 the CO concentration increased.

TC11 hourly averages data for the H_2 analyzers are shown on Figure 3.3-3. Analyzer AI419G gave reasonable results for the entire run, and there were several long periods where both AI464G and AI419G agreed with each other (from hour 55 to 130). Either analyzer was used for the operating periods, with AI419G being used more often. The analyzer used is given in Table 3.3-3. For TC11-1, neither hydrogen analyzer was in service, so the hydrogen concentration was calculated using the water-gas shift reaction, the mixing zone temperature, TI350, and gas analyzer data for H_2O (AI475H), CO, and CO_2.

The TC11 hourly average gas analyzer data for CH_4 are given in Figure 3.3-4. Analyzer AI419E and AI475E (dry) agreed with each other for nearly all of TC11. Analyzer AI464E was lower than AI419E for most of TC11. Analyzer AI419E was used for all but the first two operating periods. The choice of which analyzer used is given in Table 3.3-3.

The TC11 hourly average gas analyzer data for C_2^+ are given in Figure 3.3-5. Analyzer AI419F read about 0.275 percent for the first 190 hours of TC11, until oxygen-blown operation. Analyzer AI464F either read zero or read erratically for all of TC11. AI419F was used for all of TC11.

The TC11 carbon dioxide analyzer hourly data are given on Figure 3.3-6. Analyzers AI419D and AI434C agreed with each other for most of TC11. Analyzer AI464D agreed with AI419D and AI434C for some of TC11 (hours 32 to 104) and was erratic for the remainder of TC11. Analyzer AI475D (dry) was consistently higher than AI419D and AI434C and clearly out of calibration. Either AI419D or AI434C was used for the operating periods. The analyzers used for each operating period are given on Table 3.3-3.

The nitrogen analyzer data is given in Figure 3.3-7. Analyzer AI464B and AI419B agreed for most of TC11 with a few periods of disagreement. Analyzer AI464B was more erratic than analyzer AI419B. Analyzer AI419B was used for all of the operating periods except for the first two. The analyzer used is given in Table 3.3-3.

Since both GC analyzers AI419 and AI464 analyze for nearly the entire spectrum of expected gas components, a useful consistency check of each analyzer is to plot the sum of the gases measured by each bank of analyzers and evaluate how close the sums of compositions are to 100 percent. The sums of both GC analyzer banks are given on Figure 3.3-8. Analyzer AI419 was fairly consistent during TC11 after hour 12, usually between 98 and 100 percent. The analyzer AI464 sums were erratic for most of TC11 varying between 90 and 108 percent. This poor performance of the AI464 sums was the reason that AI419 was used for most analyses, rather than AI464.

The H_2O analyzer AI419H is part of the AI419 GC. Since AI419 operates dry, and the synthesis gas H_2O is removed prior to analysis, AI419H always read 0.0 percent and will not be discussed further.

The raw H_2S analyzer AI419J data is shown on Figure 3.3-9. The AI419J H_2S data seems reasonable in that it was lower during the air-blown mode than in oxygen-blown mode and seemed to be in the expected range for coal with no sorbent added. The AI480J data was not plotted since all of the reported concentrations were less than zero and clearly in error. The AI419J data will be compared with synthesis gas combustor SO_2 analyzer data in Section 3.3.8.

The raw ammonia analyzer AI475Q and AI480Q data are shown on Figure 3.3-10. Three extractive ammonia analyses were done during TC11 and are shown on Figure 3.3-10. The extractive ammonia analyses were reported as water saturated gas at ambient conditions, so the extractive ammonia analyses were corrected from 6.45 percent H_2O to the AI574H analyzer H_2O concentration and then plotted on Figure 3.3-10. All three extractive ammonia analyses were 200 to 500 ppm higher than both ammonia analyzers. The extractive ammonia analyses did follow the trends of the two ammonia analyzers. Both ammonia analyzers tracked each other very well and both produced the expected higher ammonia concentrations in enhanced-air- and oxygen-blown modes than in air-blown modes due to increased nitrogen dilution in air-blown mode. The ammonia concentrations in air-blown mode were about 400 to 1,200 ppm and were lower than during air-blown PRB and Hiawatha bituminous coal testing. The two enhanced air periods produced 1,000 and 1,500 ppm ammonia. During oxygen-blown mode, the two ammonia analyzers stopped reading the same, with AI475Q increasing from 1,000 to 3,200 ppm and AI480Q varying between 1,000 and 1,500 ppm. The TC11 oxygen-blown ammonia data was also lower than the oxygen-blown PRB and Hiawatha bituminous ammonia emissions.

The raw hydrogen cyanide analyzer AI479S data is shown on Figure 3.3-11, along with three wet chemistry HCN analyses. At the beginning of TC11, the analyzer data was very erratic with readings from 0 to 160 ppm. At hour 37, the analyzer stopped operating and read less than 0 ppm for the remainder of TC11. The two air-blown HCN extractive samples were at 7 and 11 ppm and were lower than air-blown PRB HCN extraction data and in about the same range as the air-blown Hiawatha bituminous HCN extraction data. The TC11 extraction data taken at the transition between enhanced air- and oxygen-blown data was 11 ppm, about the same as the second TC11 air-blown HCN. The TC11 oxygen-blown extractive HCN data was lower than the TC10 PRB oxygen-blown HCN extractive data and the TC09 Hiawatha bituminous oxygen-blown extractive data. Based on all the HCN extractive samples for the last three test runs, the HCN analyzer was probably reading a higher HCN than was actually in the syngas for the first 37 hours of TC11.

Analyzer AI479T reported COS data for all of TC11. The data varied from 300 to 350 ppm and did not respond to changes in H_2S concentrations when in different modes of operation. The values are also higher than the expected COS concentrations of about 60 to 120 ppm in air-blown mode and 140 to 180 ppm in oxygen-blown mode (10 percent of the H_2S concentrations). The poor response to mode changes and higher than expected values lead to the conclusion that the COS data from AI479T are not reliable and therefore should not be used for analysis.

Analyzer AI480W reported CS_2 data for all of TC11. The data varied from 0 to 20 ppm with one excursion up to 95 ppm. The analyzer did not respond to changes in H_2S concentrations due to changes from air- to enhanced-air- to oxygen-blown operation. The values were in the

expected range of CS_2 (1 percent of the H_2S concentrations). The poor response to mode changes leads to the conclusion that the COS data from AI480W are not reliable and therefore should not be used for analysis.

Analyzer AI479R reported HCl data for all of TC11. The data varied erratically from 0 to 180 ppm until hour 37 when the analyzer read less than zero for the remainder of TC11. The values are not in the expected range of syngas HCl. The maximum HCl syngas concentration can be determined from the Falkirk lignite chloride concentration, the coal rate, and the syngas rate. The maximum HCl syngas composition, assuming no HCl removal by the Transport Gasifier and PCD solids, is 16 ppm for air-blown mode and 22 ppm for oxygen-blown mode. The higher than possible HCl concentrations lead to the conclusion that the HCl data from AI479R are not reliable and therefore should not be used for analysis.

The raw naphthalene analyzer AI480X data is shown on Figure 3.3-12. The naphthalene analyzer was purchased to give guidance to how much hydrocarbons were being produced by the Transport Gasifier that were not being measured up by the C_2^+ component of the GCs. The amount of naphthalene also might indicate periods of tar formation. During air-blown operations, the analyzer reported naphthalene concentrations between 0 and 100 ppm, with one excursion up to 225 ppm at hour 133 and one excursion to 312 ppm at hour 171. The two excursions did not have an explanation by the other Transport Gasifier data. The naphthalene increased during the first enhanced air- and oxygen-blow periods but did not increase during the second enhanced air-blown period. The reliability of this measurement is not known at this time.

3.3.4 Gas Analysis Results

The dry, raw synthesis gas analyzer data was adjusted to produce the best estimate of the actual gas composition in three steps:

1. Choice of CO, H_2, CH_4, N_2, and CO_2 analyzer data to use (See Table 3.3-3).
2. Normalization of dry gas compositions (force to 100 percent total).
3. Conversion of dry compositions to wet compositions.

For the rest of this section, the data analysis will be based only on the TC11 operating periods (Table 3.3-1). The operating period averages of the sums of the dry gas analyses selected are shown on Figure 3.3-13. All of the operating periods have the sums of dry gas compositions between 98 and 104 percent. All of the data after hour 36 is biased low, in that the gas analyzers are not measuring up all of the syngas components. The average of all the operating sums of the dry gas composition is 100 percent, indicating that the few high bias sums balanced the more numerous low bias sums.

During the TC11 testing, there were two operating H_2O analyzers, AI475H and AI480H. The H_2O concentration was also measured at the PCD exit during PCD outlet particulate measurements. In previous gasification runs, the water-gas shift reaction was used to interpolate H_2O measurements between in situ H_2O measurements and to check the consistency of the H_2O analyzer data, if available. The water-gas shift equilibrium constant should be a function of a Transport Gasifier mixing zone or riser temperature.

The water-gas shift reaction (WGS) and equilibrium constant:

$$CO + H_2O \leftrightarrow H_2 + CO_2 \quad (1)$$

$$Kp = \frac{(H_2)(CO_2)}{(H_2O)(CO)} \quad (2)$$

Plotted on Figure 3.3-14 are the AI475H, AI480H, in situ H_2O concentrations, and the H_2O concentrations calculated from the water-gas shift equilibrium constant. The water-gas shift H_2O concentrations are based on the mixing zone temperature TI350 and the measured H_2, CO, and CO_2 concentrations. A zero approach temperature seemed to give the best fit of the in situ data.

Analyzer AI475 was close to the in situ data for most of the in situ H_2O analyses. A direct comparison of analyzer AI475H and in situ H_2O concentrations is given on Figure 3.3-15. The WGS or AI475H H_2O measurements agree with each other for TC11, and either could be used to determine the H_2O concentration. The AI475H H_2O concentrations will be used for further data analysis, except for TC11-5 (hour 46). During TC11-5, AI475H H_2O analyzer was out of service and gave erroneous results, so the WGS H_2O concentration was used for TC11-5.

Except for one operating period, analyzer AI480H was higher than AI475 by 5- to 15-percent H_2O, and did not agree with the in situ H_2O measurements. Analyzer AI480H was clearly giving erroneous results and will not be used for further analyses.

The H_2O concentrations used for the operating periods are given in Table 3.3-4. The H_2O concentration was erratic for the first two operating periods and then settled down to be fairly constant during the rest of the air-blown operating periods, varying between 10- and 14-percent H_2O. For the last six operating periods, the H_2O concentration varied between 14 and 24 percent as the steam rate was changed drastically and the unit transitioned from air- to enhanced-air-to-oxygen-blown mode.

The best estimates of the wet gas compositions for the TC11 operating periods are given on Table 3.3-4 and shown on Figure 3.3-16. Also shown on Table 3.3-4 are the synthesis gas molecular weights for each operating period.

During the first six operating periods, the CO concentration was varied significantly between 1.4 and 8.4 percent from the start of TC11 to hour 60. The CO was then fairly constant at about 4 percent until hour 120. The air and coal rates were increased at hour 132 and the CO increased from 3.5 to 7.0 percent. The CO did not change much during the first enhanced-air mode period at hour 159. In the final air-blown period at hour 174, the CO concentration dropped to 1.8 percent. In the second two enhanced-air periods, the CO was about 5 percent. During the oxygen-blown periods, the CO increased to between 9.9 and 10.7.

The H_2 concentration varied significantly at the start of TC11 to hour 60 from between 2 and 5 percent. The H_2 then leveled off at about 3 percent until hour 132 when the air and coal rates were increased. After the coal and air rates were increased, the H_2 concentration was about 5.5

percent until the first enhanced air period. During the first enhanced air period, the H_2 concentration increased to 9 percent due to the higher steam rate, which caused some of the extra H_2O to convert to H_2 via the water-gas shift reaction. During the second enhanced air period, the H_2 concentration increased to about 6 percent. During all three enhanced-air operating periods, the H_2 was higher than the CO concentration as contrasted to the air-blown periods, when the H_2 was lower than the CO. This difference was due to the higher steam rates during the enhanced air-blown periods which increased the H_2 concentration via the water-gas shift reaction. The final air-blown period had a H_2 concentration of 2 percent. The H_2 concentrations were about 10 percent during the two oxygen-blown periods. Note that the H_2 and CO concentrations were about the same during the oxygen-blown periods, because the steam rate was lower during the oxygen-blown periods than the enhanced-air periods.

The CO_2 concentration increased from 10 to 12 percent at the start of TC11. After hour 23, the CO_2 concentration decreased down about 9 percent and was steady at 9 percent until hour 132 when the air and coal rates increased. The CO_2 concentration then increased to 10 percent until the first enhanced-air period. The three enhanced-air periods CO_2 concentrations were between 10.8 and 13.0 percent. The final air-blown period CO_2 concentration was 9 percent. The two oxygen-blown periods CO_2 concentrations were about 13 percent.

The CH_4 concentration was between 0.1 and 0.9 percent for the air-blown and enhanced-air-blown operating periods. The CH_4 concentration increased when the air and coal rates were increased. During the oxygen-blown operating periods, the CH_4 concentration increased to about 1.5 percent.

The C_2^+ concentrations were between 0.2 and 0.3 percent during TC11.

The syngas molecular weight and nitrogen concentration are plotted on Figure 3.3-17. The air-blown molecular weights are all between 26 and 28 lb/lb mole. The three enhanced-air operating periods had molecular weights between 25 and 27 lb/lb mole, while the two oxygen-blown operating periods had molecular weights between 25 and 26 lb/lb mole. The molecular weights decrease in enhanced-air- and oxygen-blown modes because nitrogen is replaced by lower molecular compounds such as H_2 and H_2O.

The nitrogen trends follow the molecular weight trends, with the lower nitrogen concentrations in oxygen and enhanced-air-blown modes and higher nitrogen concentrations in air-blown mode.

The CO/CO_2 ratios were calculated from the gas data for each operating period and are listed on Table 3.3-4. The TC11 CO/CO_2 ratio varied from 0.1 to 0.8.

The lower heating value (LHV) for each gas composition was calculated and is given on Table 3.3-4 and plotted on Figure 3.3-18.

The LHVs value was calculated using the formula:

$$\mathrm{LHV(Btu/SCF)} = \left\{ \begin{array}{l} 275\times(\mathrm{H_2\%}) + 322\times(\mathrm{CO\%}) + \\ 913\times(\mathrm{CH_4\%}) + 1641\times(\mathrm{C_2^+\%}) \end{array} \right\} / 100 \qquad (3)$$

The raw LHVs cycled from between 15 and 50 Btu/scf from the beginning of TC11 until hour 36. Until the air and coal rates were increased at hour 132, the LHVs were fairly constant varying between 20 and 30 Btu/scf. When the air and coal rates were increased, the LHVs increased to between 40 and 50 Btu/scf. The large increase in the LHV between TC11-11 and TC11-12 (25 to 50 Btu/scf) was a result of the improved temperature profile and increased carbon in the recirculating solids which was produced by the increase in coal rates. The temperature profile changes between TC11-12 and TC11-16 due to solids circulation rates only increased the LHV from 47 to 49 Btu/scf. The LHV of the final air-blown operating period, TC11-18, was low at 16 Btu/scf, similar to TC11-2 at 15 Btu/scf due to lower coal or higher steam rates when compared to the other air-blown LHVs. The three enhanced-air-blown mode LHVs were either 40 or 57 Btu/scf. The TC11-17 LHV was higher than the other two enhanced-air LHVs due to lower steam and coal rates in TC11-17. The two oxygen-blown LHVs were about 80 Btu/scf.

Past test runs have indicated that LHV is most affected by coal rate and steam rate. The LHVs increase as the coal rate increases (see Figure 4.5-5 of TC06 Final Report). The coal-rate effect is due to the way that the Transport Gasifier is operated, in that the aeration and instrument nitrogen is maintained constant as coal rate increases. As coal rate increases, the syngas rate increases, but the nitrogen rate remains constant. The pure nitrogen part of the syngas concentration is thus lessened (less nitrogen dilution) and the syngas LHVs increase. When air is replaced by oxygen in enhanced-air- and oxygen-blown operation, the nitrogen content of the syngas is also decreased, increasing the LHVs. The syngas LHV is also decreased by increasing steam to the gasifier due to the increased syngas dilution with H_2O. A way to combine the effects of changes in steam, mode of operation, and coal rates is to determine the overall percent of oxygen of all the gas that is fed to the Transport Gasifier. This compensates for the different amounts of nitrogen and steam that are added to the gasifier. The overall percent O_2 is calculated by the following formula:

$$\text{Overall } \%O_2 = \frac{0.21 * \text{air} + \text{oxygen}}{\text{air} + \text{oxygen} + (\text{pure nitrogen}) + \text{steam}} \quad (4)$$

The air, oxygen, nitrogen, and steam flows are in moles per hour. At the PSDF, a large amount of pure nitrogen is fed to the gasifier for instrument purges, coal and sorbent transport, and equipment purges. In PSDF air-blown operation, about 50 percent of the synthesis gas nitrogen comes from air and 50 percent comes from the pure nitrogen system. In PSDF oxygen-blown operation, the removal of air nitrogen removes about the same amount of nitrogen as if the pure nitrogen was replaced by synthesis gas recycle. The TC11 overall percent O_2 are listed on Table 3.3-4 and range from 9.7 to 12.9 percent in air-blown mode, from 13 to 17.1 percent in enhanced-air-blown mode, and from 18.9 to 19.3 percent in oxygen-blown mode. As the overall percent O_2 increases, the LHV also increases.

The TC11 raw LHV's data are plotted against overall percent O_2 on Figure 3.3-19. The TC11 data are from 15 Btu/scf at 9.7 percent O_2 to 81 Btu/scf at 19.3 percent O_2 and follow a clear trend of increasing Btu/scf with percent O_2. All of the TC11 air-blown data are close to the

straight line fit on Figure 3.3-19, with five outliers, TC11-1, TC11-2, TC11-17, TC11-18, and TC11-20. TC11-1 was an operating period that was only 1.25 hours long and started about an hour after coal feed was started. Both H_2 analyzers were out of service, and the H_2 concentration had to be estimated from the water-gas shift equilibrium. TC11-1 is therefore a questionable operating period. TC11-2 was taken 12 hours after a coal restart and only lasted 1 hour. TC11-18 was a 3-hour operating period but also was taken about an hour after a coal restart. It would appear that the TC11-1, TC11-2, and TC11-18 were taken too soon after a coal trip to produce consistent data. TC11-17 lasted 2.75 hours and was started only 1 hour after the pressure had been reduced. During TC11-17, the gasifier temperatures were still increasing, and it is probable that TC11-17 had not reached steady operating conditions. The last two enhanced-air operating periods and both oxygen-blown operating periods were taken during the last 17 hours of lignite operation, when the PCD fines solids compositions were rapidly changing (see Figures 3.4-9, 3.4-10, and 3.4-11). TC11-19, however, seems consistent with the air-blown data and slightly lower.

All of the air-blown points on Figure 3.3-19 clearly above the Falkirk lignite line were operated at higher coal rates and probably had higher carbon in the recirculating solids which would lead to a higher LHV than would be predicted by the simple dilution of the syngas by less nitrogen to coal fed. TC11-12 is one of the air-blown LHVs at about 49 Btu/scf which is above the straight line fit of the data and benefited from higher carbon in the recirculating solids.

Also plotted on Figure 3.3-19 are the straight line correlation of TC06, TC07, TC08, and TC10 Powder River Basin coal data and TC09 Hiawatha bituminous data, which contains air-, enhanced-air, and oxygen-blown mode data. When the three coals are compared at the same level of percent O_2, the Falkirk lignite has lower LHVs at the same percent O_2 than the other two coals, possibly due to the higher moisture content of the Falkirk lignite.

3.3.5 Nitrogen- and Adiabatic-Corrected Synthesis Gas Lower Heating Values

The PSDF Transport Gasifier produces syngas of a lower quality than a commercially sized gasifier due to the use of recycle gas (in a commercial gasifier) rather than nitrogen (at the PSDF), for aeration and instrument purges as well as the lower heat loss per pound of coal gasified in a commercially sized gasifier when compared to the PSDF Transport Gasifier. The following corrections are made to the measured, raw synthesis gas composition to estimate the commercial synthesis LHVs.

1. All nonair nitrogen is subtracted from the syngas. This nitrogen is used for Transport Gasifier aeration and instrument purges. In a commercial plant, the instrument purges will be lower due to less commercial plant instrumentation and due to commercial instruments requiring the same purge rate independent of the plant size. This correction assumes that recycled syngas or steam will be used in a commercial plant for aeration and instrument purges to replace the nonair nitrogen. The nonair nitrogen was determined by subtracting the air nitrogen from the synthesis gas nitrogen. This correction increases all the nonnitrogen syngas compositions and decreases the nitrogen syngas composition. The syngas rate will decrease as a result of this correction. For oxygen-blown mode, this correction removes all the nitrogen from the syngas, thus oxygen-blown syngas will have 0 percent nitrogen. The water-gas shift

equilibrium constant and the CO/CO_2 ratios will not change.

2. The nonair nitrogen (that has been eliminated by using steam or recycle gas for aeration or instrument purges) no longer has to be heated to the maximum gasifier temperature. This eliminated heat is counteracted by the additional energy required to heat the recycle gas and steam that replaces the nonair nitrogen. A recent commercial design will be used to estimate the amount and temperature of the recycle gas and steam required. Since the total amount of instrument and aeration gas required is reduced, the coal and air rates will decrease by the amount of energy no longer required and result in decreased coal, air, and oxygen rates to the Transport Gasifier. It is assumed that this eliminated coal (to heat up the nonair nitrogen) is combusted to CO_2 and H_2O. Eliminating this additional coal reduces the syngas CO_2 and H_2O concentrations. The lower corrected air rates for air-blown mode also decrease the nitrogen in the corrected syngas. This correction decreases the synthesis gas flow rate. For this correction, the water-gas shift constant and the CO/CO_2 ratio both change due to the reduction in CO_2 and H_2O.

3. The PSDF higher heat loss per pound of coal gasified than a commercially sized plant is taken into account. Smaller scale pilot and demonstration units have higher surface-area-to-volume ratios than their scaled-up commercial counterparts, and hence the PSDF Transport Gasifier has a higher heat loss per pound of coal gasified than a commercial plant. Since the heat loss of a commercial plant is difficult to estimate, the corrected heat loss is assumed to be zero (adiabatic). The correction uses the same method to correct for the no longer required energy to heat up the decreased amounts of aeration and instrumentation gas. The coal, air, and oxygen rates are reduced; the syngas CO_2, H_2O, and N_2 concentrations are reduced; the water-gas shift equilibrium constant and the CO/CO_2 ratio change. This correction is reasonable since the commercial plant heat loss per pound of coal gasified is much smaller than the PSDF Transport Gasifier heat loss per pound of coal gasified.

4. The steam rates are reduced for oxygen-blown operation, since in oxygen-blown operation steam is added to control the gasifier temperature. As the oxygen rate is decreased in a commercial plant, the steam rate will also be decreased. It was assumed that the steam-to-oxygen ratio will be the same for the PSDF and the commercial Transport Gasifier, and hence the corrected steam rate will be lower than the original steam rate. The effect of lowering the steam rate will decrease the amount of H_2O in the syngas by the amount the steam rate was reduced. This correction reduces the steam rate and the H_2O content of the syngas, and hence, the LHVs and water-gas shift equilibrium constant also changes. The steam-to-oxygen ratio is a function of the detailed design of the Transport Gasifier. It is difficult to estimate what a commercial steam-to-oxygen ratio will be since typically in oxygen-blown mode steam is added to control local temperatures.

5. The water-gas shift is corrected to reflect the gasifier mixing zone temperature. Corrections #2, #3, and #4 all change the water-gas shift equilibrium constant without changing the mixing zone temperature. The commercial plant will operate at the PSDF mixing zone temperature, and hence, have the same water-gas shift equilibrium

constant as the commercial plant. The H_2O, CO_2, CO, and H_2 concentrations are then adjusted to return to the measured PSDF water-gas shift equilibrium for that particular operating period. In respect to LHV, the LHV could go up if H_2 and CO_2 are converted to H_2O and CO since the LHV for CO is higher than H_2. The LHV could decrease if H_2O and CO are converted to H_2 and CO_2. This correction is usually small on a LHV basis, but is important if the syngas is used for fuel cell or chemical production where the H_2 concentration is a critical design parameter.

For correction #2, it is assumed that the recycle gas is 2.4 percent of the syngas from the gasifier and is available at 234ºF. The recycle gas is taken from the exit of a cold syngas sulfur removal system which decreases the syngas temperature to 150ºF, prior to sulfur removal. Decreasing the syngas temperature to 150ºF will condense most of the syngas H_2O out as liquid water, which is then removed from the syngas. For the commercial design at 388 psia, the syngas water composition is 0.96 percent. In a commercial plant, the cleaned syngas would be sent to a gas turbine, fuel cell, or for chemical production. For correction #2, is it assumed that the aeration steam is 1.45 percent of the syngas from the gasifier and available at 660ºF. For correction #3, it is assumed that the heat loss for the PSDF Transport gasifier is 3.5 million Btu/hr. This heat loss will be discussed further in Section 3.5.

The sum of all five corrections is the adiabatic nitrogen-corrected LHV. Correction #1 (removing the nonair nitrogen) adds an average of 15 Btu/scf to the raw LHV for air-blown LHV, an average of 29 Btu/scf to the enhanced air-blown LHV, and an average of 69 Btu/scf to the oxygen-blown LHV. Correction #2 (correcting the Transport Gasifier energy balance for the commercial amount and type of aeration and instrument gas) adds an average of 9 Btu/scf to the raw LHV for air-blown LHV, an average of 25 Btu/scf to the enhanced air-blown LHV, and an average of 15 Btu/scf to the oxygen-blown LHV. Correction #1 and #2 both increase the oxygen-blown LHV more than for the air-blown LHV because 100 percent of the syngas nitrogen is removed in the oxygen-blown correction, while only about 50 percent of the syngas nitrogen is removed for the air-blown correction. The sum of correction #3 and #4 (adiabatic gasifier and correcting the steam rate) adds an average of 18 Btu/scf to the raw LHV for air-blown LHV, an average of 41 Btu/scf to the enhanced air-blown LHV, and an average of 47 Btu/scf to the oxygen-blown LHV. Correction #5 (water-gas shift correction) subtracts an average of 0.4 Btu/scf for air-blown LHV, subtracts an average 0.3 Btu/scf for enhanced air-blown LHV, and adds an average of 0.6 Btu/scf to the oxygen-blown LHV.

These calculations are an oversimplification of the gasification process. A more sophisticated model is required to correctly predict the effects of decreasing pure nitrogen and gasifier heat loss. It should be noted that the corrected syngas compositions are based on a corrected coal rate, corrected air rate, corrected oxygen rate, corrected steam rate, and a corrected syngas rate. The adiabatic N_2-corrected LHVs for each operating period are given in Table 3.3-5 and plotted on Figure 3.3-20. The N_2-corrected LHVs were between 45 and 105 Btu/scf for air-blown operation, between 137 and 143 Btu/scf for enhanced air, and either 209 or 215 Btu/scf for oxygen-blown operation. The average increase for the all the corrections was 42 Btu/scf for air-blown, 94 for the enhanced air-blown, and 131 Btu/scf for the oxygen-blown LHVs. The correction is higher for oxygen-blown because there is less syngas in the oxygen-blown mode of operation, so taking about the same amount of pure nitrogen out of the syngas has a larger effect.

For comparing the raw LHVs with the adiabatic N_2-corrected LHVs, an equivalent to the overall percent O_2 is defined as:

$$\text{Corrected Overall \%O}_2 = \frac{0.21*(\text{corrected air}) + (\text{corrected oxygen})}{(\text{corrected air}) + (\text{corrected oxygen}) + (\text{corrected steam})} \quad (5)$$

All flow rates are expressed as moles per hour. The corrected air rate, corrected oxygen rate, and corrected steam rate are used in the determination of the corrected LHVs. The corrected overall percent O_2 for oxygen-blown mode is a direct function of the steam-to-oxygen ratio, since the corrected air rate is zero.

The adiabatic N_2-corrected LHVs are plotted against the adiabatic overall percent O_2 in Figure 3.3-20. Also plotted are the raw TC11 LHV data. The TC11-corrected LHVs seem to form a straight line, with a few outliers. The corrected LHVs are larger than the raw LHVs at equivalent percent O_2. Two of the smaller corrected LHVs are consistent with the raw LHV.

3.3.6 Synthesis Gas Water Gas-Shift Equilibrium

The water-gas-shift (WGS) equilibrium constants (K_p) were calculated for the seven in situ moisture measurements and are given on Table 3.3-6. Of the seven in situ moisture measurements, only one was taken completely during an operating period (May 17 in situ sample, TC11-18). The equilibrium constants varied from 0.64 to 0.84. Lower equilibrium constants would tend to have less H_2 and CO_2 and higher H_2O and CO. The WGS was constant despite the wide range of H_2O (9.3 to 18.4 percent), dry CO (3.9 to 12.6 percent), dry H_2 (3.1 to 12.1 percent), and dry CO_2 (10.0 to 16.2 percent) during TC11. This constant figure would indicate that the water-gas shift reaction is controlling the relative H_2, H_2O, CO, and CO_2 concentrations in the Transport Gasifier.

The thermodynamic equilibrium temperature for each equilibrium constant was calculated from thermodynamic data and is shown on Table 3.3-6. The thermodynamic equilibrium temperature varied from 1,584 to 1,758°F. These temperatures are all within 100°F of the mixing zone temperatures, which are listed in Table 3.3-6 for the in situ sampling periods. The WGS equilibrium constants calculated from the mixing zone temperatures are compared with the measured WGS equilibrium constants in Figure 3.3-21 using the same approach temperature used to estimate the syngas H_2O concentration in Figure 3.3-14 (0°F). The oxygen-blown equilibrium constants and air-blown equilibrium constants were plotted separately on Figure 3.3-21. Both calculated and measured oxygen-blown K_ps agree well with each other, as does two of the air-blown K_ps (4/14/03 and 4/16/03 in situ sample.) Of the remaining air-blown K_ps, two had higher mixing zone K_ps than measured and one had a higher measured K_p than the mixing zone K_p.

The WGS constants determined from the mixing zone temperature have less variation than the measured WGS constants.

The measured K_ps were calculated for 20 of the 22 operating periods and are given in Table 3.3-7. For TC11-1, neither hydrogen analyzer was in operation, so the syngas water-gas shift equilibrium constant could not be calculated. For TC11-5, the moisture analyzer, AI475H, was not in operation, so again the syngas water-gas shift equilibrium constant could not be calculated. The remaining measured equilibrium constants varied from 0.51 to 0.85, with one outlier at 1.23 (TC11-2). Operating period TC11-2 was a short, 1-hour operating period during which some of the syngas compositions were not constant. TC11-2 was also about 12 hours after a coal feed trip, and the Transport Gasifier did not seem to be at constant conditions. The remaining WGS K_ps were constant despite the wide range of H_2O (10.4 to 24.3 percent), CO (1.8 to 10.7 percent), H_2 (1.9 to 10.2 percent), and CO_2 (8.6 to 13.3 percent) concentrations during TC11. This constant figure would indicate that the water-gas shift reaction is controlling the relative H_2, H_2O, CO, and CO_2 concentrations in the Transport Gasifier.

The thermodynamic equilibrium constants for each operating period are shown in Table 3.3-7. The thermodynamic equilibrium constants were calculated from the mixing zone temperature TI350. The operating period WGS equilibrium constants calculated from the mixing zone temperatures are compared with the measured WGS equilibrium constants in Figure 3.3-22. For 19 of the 20 measured K_ps, there was good agreement between the measured equilibrium constants and the equilibrium constants based on the mixing zone temperature. The WGS constants determined from the mixing zone temperature have slightly less variation than the measured WGS constants, since the mixing zone temperature was fairly constant during TC11.

The ability to predict the water-gas shift constant is important in the process design of a commercial Transport Gasifier, since the water-gas shift constant should be a function of the mixing zone temperature. The water-gas shift constant then can be used to determine the concentrations of the H_2, CO, CO_2, and H_2O if the carbon conversion, LHV, and CH_4 are known.

3.3.7 Synthesis Gas Combustor Oxygen, Carbon, and Hydrogen Balance Calculations

The synthesis gas compositions and synthesis gas flow rate can be checked by oxygen balances, hydrogen balances, and carbon balances around the synthesis gas combustor since the synthesis gas combustor flue gas composition is measured by the following syngas combustor flue gas analyzers (See Figure 3.3-1 for the analyzer location):

- AI8775 - O_2
- AI476H - H_2O
- AI476D - CO_2

The above analyzers all measure wet and do not have to be corrected for syngas H_2O.

The synthesis gas combustor gas composition was calculated for each operating period by using synthesis gas composition synthesis gas flow rate, FI463, and the following syngas combustor flow rate tags:

- Primary air flow, FI8773

- Secondary air flow, FI8772
- Quench air flow, FI8771
- Propane flow, FI8753

The O_2 measured by AI8775 and O_2 calculated by mass balance concentrations are shown in Figure 3.3-23 and Table 3.3-8. The measured and calculated synthesis gas combustor O_2 concentrations agreed well for all of the operating periods, with all of the measured concentrations within 15 percent of the calculated oxygen concentrations. There was no difference between the air-blown, enhanced-air, and oxygen-blown syngas combustor oxygen data. There was a slight bias to having higher calculated oxygen concentrations than measured oxygen concentrations. A higher calculated oxygen concentration than measured oxygen concentration would indicate that the assumed synthesis gas composition had fewer combustibles than the actual synthesis gas and that the actual syngas LHV was higher than the syngas analyzers would indicate. The comparisons for the measured and calculated oxygen concentrations are consistent with previous testing.

The CO_2 concentration measured by AI476D and the CO_2 concentration calculated by synthesis gas combustor mass balance are shown in Figure 3.3-24 and Table 3.3-8. In September 2003 it was discovered that the carbon dioxide analyzer AI476D was reading 2 percent too low. For TC11, 2 percent was added to the actual AI476D. The calculated CO_2 concentrations agreed well with the measured CO_2 concentrations with all of the measured carbon dioxide concentrations agreeing within 10 percent of the calculated carbon dioxide concentrations.

Analyzer AI475H measured and mass balance calculated H_2O values are shown in Figure 3.3-25 and Table 3.3-8. The calculated H_2O agreed very well with the analyzer H_2O with the measured and calculated H_2O within 10 percent for all operating periods. Note that the high syngas H_2O concentration for the enhanced air operating periods TC11-17 had the highest steam rate.

The results of the synthesis gas combustor (SGC) flue gas analyzers indicate that the syngas compositions and flow rates are consistent with the syngas combustor flow rates and flue gas compositions.

The synthesis gas LHVs can be estimated by doing an energy balance around the synthesis gas combustor. The SGC energy balance is done by estimating the SGC heat loss to make the synthesis gas LHVs calculated by the SGC energy balance agree with LHVs calculated from the synthesis gas analyzer data. In some of the commissioning tests (GTC test series), the gas analyzers were not operational during the entire run, and the SGC energy balance determined LHVs was used to estimate synthesis gas LHVs during periods when there was no gas analyzer data. A comparison between the measured TC11 LHVs and the SGC energy balance LHVs using a SGC heat loss of 2 million Btu/hr is given on Figure 3.3-26. This heating loss was consistent with previous test campaigns. The syngas combustor energy balance LHVs and analyzer LHVs were within 10 percent of each other except for two air-blown operating periods which had very low LHV (TC11-2 & TC11-18). TC11-2 was a 1-hour operating period and probably not at steady conditions. TC11-18 was a 3-hour operating period that started 1 hour after a coal trip, and the gasifier was probably not at steady conditions.

3.3.8 Sulfur Emissions

For the TC11 operating periods, the wet H_2S concentration measured by AI419J is plotted on Figure 3.3-27 and compared with the SGC SO_2 analyzer AI476P, and the synthesis gas total reduced sulfur (TRS). The wet H_2S concentration measured by AI419J and the synthesis gas TRS are listed on Table 3.3-8. The AI419 analyzers measure the gas composition dry, so the values from AI419J were corrected to allow for the H_2O in the syngas. The SGC SO_2 analyzer, AI476P, measures the total sulfur emissions from the Transport Gasifier. The higher range of the two AI476 SO_2 analyzers was used since the low range SO_2 analyzer, AI476N, has a maximum of 500 ppm SO_2. The Transport Gasifier sulfur emissions consist of H_2S, COS, and CS_2. The main sulfur species in coal gasification are considered to be H_2S and carbon oxysulfide (COS). There should also be a minor amount of carbon disulfide (CS_2).

The H_2S analyzer AI419J was less than the TRS during for the first 60 hours of TC11. After hour 92, the H_2S analyzer AI419J agreed well with the TRS. The operating periods when the AI419J analyzer H_2S was equal to the TRS would indicate zero COS and CS_2 emissions. Operating periods when the AI419J was less than the TRS would indicate that there was some COS and CS_2 emissions. It is expected that there should be about 100 ppm of COS emissions, based on previous work on other gasifiers. The measured TRS is plotted against the wet AI419J data on Figure 3.3-28. Except for the air-blown data before hour 60 and one of the enhanced-air operating periods, the measured and AI419J agree within 10 percent, the best H_2S analyzer data performance to date. Since TC11 AI419J readings were not always consistent with AI476P, H_2S analyzer AI419J data will not be used for the remainder of this report.

At the beginning of TC11, the TRS emissions were about 460 ppm and then increased to 848 ppm at 36 hours. The TRS then decreased to 650 ppm at hour 52. The increase in coal and air rates at hour 132 also increased the TRS. By the end of the air-blown operating periods, the TRS had increased to between 900 and 1,100 ppm. The enhanced-air-blown operating periods had TRS from between 1,045 and 1,215 ppm, while the two oxygen-blown mode operating periods had TRS emissions of about 1,375 ppm.

The calculation of the minimum equilibrium synthesis H_2S concentration has been described in previous PSDF reports. In summary, the minimum equilibrium H_2S concentration is a function of the partial pressures of H_2O and CO_2, as long as there is calcium sulfide present in the solids. (The equilibrium H_2S concentration is a function of system temperature, while the minimum equilibrium H_2S concentration is not a function of temperature.) As the partial pressures of H_2O and CO_2 increase, the H_2S concentration should increase. Using Aspen simulations, the minimum equilibrium H_2S concentrations determined for all of the operating periods are listed in Table 3.3-7.

Figure 3.3-29 plots the TRS and equilibrium H_2S directly against each other for TC11. The data is expected to all fall above the 45-degree line since the minimum equilibrium H_2S concentration should be the lowest H_2S concentration in a system with calcium sulfide present. All of the data indicate sulfur emissions greater than equilibrium, as expected. Sulfur emissions greater than the equilibrium H_2S concentration and small amounts of sulfur in the reactor solids would indicate very little Transport Gasifier sulfur capture.

TC11 was operated without sorbent addition for the entire run to determine the amount of sulfur removal that could be obtained by the Falkirk lignite ash alkalinity. This topic will be discussed further in Section 3.5.

3.3.9 Ammonia Equilibrium

At the high temperature of the Transport Gasifier mixing zone, thermodynamic equilibrium predicts that there is minimal ammonia present. The presence of ammonia in the syngas is therefore a result of ammonia production while the syngas cools to the location where the ammonia is sampled. The ammonia formation reaction and equilibrium constant:

$$\left(\frac{1}{2}\right)N_2 + \left(\frac{3}{2}\right)H_2 \leftrightarrow NH_3 \tag{6}$$

$$Kp = \frac{P_{NH_3}}{\left(P_{N_2}\right)^{.5}\left(P_{H_2}\right)^{1.5}} \tag{7}$$

where P is the partial pressure of ammonia, hydrogen, or nitrogen. The equilibrium ammonia concentration was estimated using the PCD inlet temperature TI458 and an approach temperature of 110ºF. The AI475Q measured ammonia concentrations and the equilibrium calculated ammonia concentrations are compared on Figure 3.3-30 and Table 3.3-7. All but 2 of the 21 operating period equilibrium calculation ammonia concentrations are within 20 percent of the measured ammonia concentrations. (The equilibrium ammonia concentration can not be calculated for TC11-1 because neither H_2 analyzer was in operation.) The correlation is good, especially since the ammonia concentrations ranged from 200 ppm to 2,875 ppm. The two outliers are TC11-5 and TC11-21. Both were short-duration operating periods of either 1.5 or 2.0 hours, and the ammonia concentration may not have had time to reach a steady concentration. Using equilibrium calculations may permit the estimation of syngas ammonia concentrations for commercial reactors.

Table 3.3-1 Operating Periods

Operating Period	Start Time	End Time	Duration Hours	Operating Period Average Time	Operating Period Relative Hours
TC11-1	4/9/2003 23:00	4/10/2003 0:15	1:15	4/9/2003 23:37	1
TC11-2	4/10/2003 13:45	4/10/2003 14:45	1:00	4/10/2003 14:15	10
TC11-3	4/10/2003 20:15	4/11/2003 0:15	4:00	4/10/2003 22:15	18
TC11-4	4/11/2003 2:30	4/11/2003 3:45	1:15	4/11/2003 3:07	23
TC11-5	4/11/2003 15:00	4/11/2003 16:30	1:30	4/11/2003 15:45	36
TC11-6	4/12/2003 5:30	4/12/2003 7:15	1:45	4/12/2003 6:22	50
TC11-7	4/12/2003 20:30	4/12/2003 22:00	1:30	4/12/2003 21:15	60
TC11-8	4/14/2003 4:15	4/14/2003 5:15	1:00	4/14/2003 4:45	92
TC11-9	4/14/2003 7:00	4/14/2003 8:30	1:30	4/14/2003 7:45	95
TC11-10	4/15/2003 2:15	4/15/2003 6:00	3:45	4/15/2003 4:07	115
TC11-11	4/15/2003 12:30	4/15/2003 16:30	4:00	4/15/2003 14:30	126
TC11-12	4/15/2003 20:30	4/15/2003 22:00	1:30	4/15/2003 21:15	132
TC11-13	4/15/2003 22:30	4/16/2003 5:30	7:00	4/16/2003 2:00	137
TC11-14	4/16/2003 8:15	4/16/2003 10:30	2:15	4/16/2003 9:22	144
TC11-15	4/16/2003 12:15	4/16/2003 13:15	1:00	4/16/2003 12:45	148
TC11-16	4/16/2003 17:00	4/16/2003 18:00	1:00	4/16/2003 17:30	153
TC11-17	4/16/2003 22:15	4/17/2003 1:00	2:45	4/16/2003 23:37	159
TC11-18	4/17/2003 13:00	4/17/2003 16:00	3:00	4/17/2003 14:30	174
TC11-19	4/18/2003 0:00	4/18/2003 4:00	4:00	4/18/2003 2:00	185
TC11-20	4/18/2003 4:45	4/18/2003 7:15	2:30	4/18/2003 6:00	189
TC11-21	4/18/2003 10:30	4/18/2003 12:30	2:00	4/18/2003 11:30	195
TC11-22	4/18/2003 16:00	4/18/2003 17:00	1:00	4/18/2003 16:30	200

Note: TC11-1 to TC11-16 and TC11-18 were air blown; TC11-17, TC11-19, and TC11-20 were enhanced air; TC11-21 and TC11-22 were oxygen blown.

Table 3.3-2 Operating Conditions

Operating Periods	Average Relative Hours	Mixing Zone Temperature TI350 °F	Pressure PI287 psig	PCD Inlet Temperature TI458 °F	Air Rate lb/hr	Oxygen Rate lb/hr	Synthesis Gas Rate lb/hr	Steam Rate lb/hr	Nitrogen Rate lb/hr
TC11-1	1	1,659	180	705	11,253	0	21,539	770	7,603
TC11-2	10	1,644	160	734	9,388	0	20,609	812	9,299
TC11-3	18	1,672	170	737	10,394	0	21,545	739	8,866
TC11-4	23	1,676	170	736	10,766	0	21,973	735	8,723
TC11-5	36	1,673	190	751	13,433	0	26,232	761	8,931
TC11-6	50	1,667	196	729	10,085	0	21,453	727	8,853
TC11-7	60	1,677	190	733	10,724	0	21,713	747	8,406
TC11-8	92	1,639	190	713	10,236	0	21,581	756	9,124
TC11-9	95	1,650	190	720	10,187	0	21,389	756	8,898
TC11-10	115	1,673	190	751	11,011	0	23,185	759	9,209
TC11-11	126	1,665	190	745	10,604	0	21,724	757	8,754
TC11-12	132	1,688	194	740	13,401	0	24,808	749	6,971
TC11-13	137	1,712	194	756	13,247	0	24,098	754	7,004
TC11-14	144	1,680	194	725	9,917	0	19,250	751	7,026
TC11-15	148	1,675	194	730	12,169	0	22,265	751	6,440
TC11-16	153	1,676	194	724	12,542	0	23,132	744	6,769
TC11-17	159	1,698	136	687	2,360	2,022	16,340	1,698	6,457
TC11-18	174	1,676	136	709	8,054	0	16,617	913	6,430
TC11-19	185	1,648	136	675	4,271	1,090	16,024	1,294	6,888
TC11-20	189	1,711	136	690	4,237	1,272	16,299	1,280	6,826
TC11-21	195	1,740	136	648	0	2,282	14,327	1,141	6,674
TC11-22	200	1,739	136	663	0	2,371	15,560	1,151	7,205

Notes:

1. TC11-1 to TC11-16 and TC11-18 were air blown; TC11-17, TC11-19, and TC11-20 were enhanced air; TC11-21 and TC11-22 were oxygen blown.

Table 3.3-3 Gas Analyzer Choices

Operating Periods	Average Relative Hours	Gas Compound						
		H_2O	CO	H_2	CO_2	CH_4	C_2^+	N_2
TC11-1	1	475	453	X[2]	434	475	419	464
TC11-2	10	475	434	464	434	464	X[1]	464
TC11-3	18	475	453	419	434	419	419	419
TC11-4	23	475	453	419	434	419	419	419
TC11-5	36	X[3]	434	464	434	419	419	419
TC11-6	50	475	453	419	419	419	419	419
TC11-7	60	475	419	419	419	419	419	419
TC11-8	92	475	464	419	419	419	419	419
TC11-9	95	475	419	419	419	419	419	419
TC11-10	115	475	419	419	419	419	419	419
TC11-11	126	475	419	419	419	419	419	419
TC11-12	132	475	419	419	419	419	419	419
TC11-13	137	475	419	419	419	419	419	419
TC11-14	144	475	419	419	419	419	419	419
TC11-15	148	475	419	419	419	419	419	419
TC11-16	153	475	419	419	419	419	419	419
TC11-17	159	475	419	464	419	419	419	419
TC11-18	174	475	419	464	419	419	419	419
TC11-19	185	475	419	464	419	419	419	419
TC11-20	189	475	419	419	419	419	419	419
TC11-21	195	475	425	419	419	419	419	419
TC11-22	200	475	419	419	419	419	419	419

Notes:

1. Both GC's out of service, used TC11-1 value.
2. H_2 calculated from water gas shift equilibrium using TI350, and H_2O, CO, and CO_2 data.
3. H_2O calculated from water gas shift equilibrium using TI350, and H_2, CO, and CO_2 data.

Table 3.3-4 Gas Compositions, Molecular Weight, and Heating Value

Operating Period	Average Relative Hour	H_2O Mole %	CO Mole %	H_2 Mole %	CO_2 Mole %	CH_4 Mole %	C_2H_6 Mole %	N_2 Mole %	Total Mole %	Syngas LHV Btu/SCF	Syngas TRS[1] ppm	Syngas MW lb./Mole	O_2 in Feed %	Syngas CO/CO_2 Ratio
TC11-1	1	7.3	8.4	4.2	10.5	0.9	0.2	68.5	100.0	50	496	27.7	11.6	0.8
TC11-2	10	12.6	1.5	2.1	11.3	0.1	0.2	72.1	100.0	15	665	28.0	9.7	0.1
TC11-3	18	11.2	3.7	2.8	11.7	0.3	0.2	70.1	100.0	26	825	28.0	10.5	0.3
TC11-4	23	10.9	4.4	3.3	11.9	0.4	0.2	69.0	100.0	30	871	27.9	10.8	0.4
TC11-5	36	11.2	5.6	4.9	9.4	0.6	0.2	68.1	100.0	41	956	27.0	11.8	0.6
TC11-6	50	10.7	3.2	2.7	8.6	0.3	0.2	74.3	100.0	25	770	27.6	10.4	0.4
TC11-7	60	11.7	4.2	3.3	8.8	0.4	0.2	71.5	100.0	30	902	27.4	10.9	0.5
TC11-8	92	10.4	3.9	3.1	8.7	0.4	0.3	73.3	100.0	29	725	27.5	10.3	0.4
TC11-9	95	10.7	3.8	3.1	8.8	0.4	0.2	73.0	100.0	28	769	27.5	10.4	0.4
TC11-10	115	12.5	3.3	2.9	8.7	0.3	0.2	72.2	100.0	25	1039	27.4	10.6	0.4
TC11-11	126	12.1	3.4	3.0	8.8	0.3	0.2	72.3	100.0	25	930	27.4	10.7	0.4
TC11-12	132	13.6	6.7	5.7	9.8	0.8	0.2	63.1	100.0	49	1104	26.6	12.9	0.7
TC11-13	137	13.1	6.4	5.1	9.7	0.6	0.2	65.0	100.0	43	1231	26.8	12.8	0.7
TC11-14	144	12.6	4.4	3.7	9.2	0.4	0.2	69.4	100.0	32	1021	27.2	11.3	0.5
TC11-15	148	11.6	6.6	5.6	10.0	0.7	0.2	65.3	100.0	47	1147	26.9	12.8	0.7
TC11-16	153	12.6	6.6	5.6	9.9	0.8	0.2	64.4	100.0	47	1113	26.8	12.7	0.7
TC11-17	159	24.3	6.4	9.4	13.0	0.8	0.2	45.9	100.0	57	1605	25.1	17.1	0.5
TC11-18	174	14.1	1.8	1.9	9.1	0.1	0.2	72.7	100.0	16	872	27.5	10.5	0.2
TC11-19	185	18.1	4.6	6.5	10.8	0.5	0.2	59.3	100.0	41	1294	26.2	13.0	0.4
TC11-20	189	19.0	5.1	5.5	11.1	0.6	0.2	58.5	100.0	40	1284	26.4	14.0	0.5
TC11-21	195	18.0	10.7	10.1	13.3	1.6	0.2	46.1	100.0	81	1674	25.5	19.3	0.8
TC11-22	200	18.4	9.9	10.2	13.3	1.7	0.3	46.1	100.0	80	1693	25.4	18.9	0.7

Notes:

1. Synthesis gas total reduced sulfur (TRS) estimated from Synthesis gas combustor SO_2 analyzer data.

2. TC11-1 to TC11-16 and TC11-18 were air blown; TC11-17, TC11-19, and TC11-20 were enhanced air; TC11-21 and TC11-22 were oxygen blown.

3. For TC11-1, the water gas shift equilibrium was used to estimate the H_2 concentrration.

3. For TC11-5, the water gas shift equilibrium was used to estimate the H_2O concentrration.

Table 3.3-5 Corrected Gas Compositions, Molecular Weight, and Heating Value

Operating Period	Average Relative Hour	H_2O Mole %	CO Mole %	H_2 Mole %	CO_2 Mole %	CH_4 Mole %	C_2H_6 Mole %	N_2 Mole %	Total Mole %	Syngas LHV Btu/SCF	Syngas MW lb./Mole	O_2 in Feed %	Syngas CO/CO_2 Ratio	Clean Syngas LHV[3] Btu/SCF
TC11-1	1	10.6	17.2	9.3	14.3	1.8	0.5	46.3	100.0	105	26.6	16.8	1.2	117
TC11-2	10	26.8	4.0	6.6	20.1	0.4	0.6	41.4	100.0	45	26.8	14.8	0.2	61
TC11-3	18	20.3	8.6	7.3	18.7	0.7	0.6	43.7	100.0	64	27.0	16.2	0.5	79
TC11-4	23	18.8	9.6	8.0	18.5	0.8	0.5	43.7	100.0	69	26.9	16.5	0.5	84
TC11-5	36	18.4	10.8	11.1	13.0	1.2	0.5	45.1	100.0	84	25.2	17.3	0.8	102
TC11-6	50	22.5	8.5	9.7	13.3	1.1	0.7	44.3	100.0	75	25.2	15.4	0.6	96
TC11-7	60	21.7	9.5	9.6	12.8	1.0	0.6	44.9	100.0	76	25.3	16.1	0.7	96
TC11-8	92	20.4	9.9	10.1	13.4	1.1	0.7	44.5	100.0	81	25.4	15.6	0.7	101
TC11-9	95	21.1	9.6	10.0	13.4	1.1	0.7	44.2	100.0	79	25.3	15.6	0.7	99
TC11-10	115	25.0	7.8	9.0	13.0	0.8	0.6	43.9	100.0	67	25.2	16.0	0.6	88
TC11-11	126	23.7	7.9	9.2	12.9	0.7	0.6	45.0	100.0	67	25.2	15.9	0.6	87
TC11-12	132	20.1	11.0	10.9	12.4	1.5	0.4	43.6	100.0	86	25.0	17.7	0.9	107
TC11-13	137	19.6	10.9	10.2	12.3	1.0	0.4	45.6	100.0	79	25.3	17.6	0.9	98
TC11-14	144	22.0	9.4	10.0	12.8	0.9	0.5	44.3	100.0	75	25.1	16.0	0.7	95
TC11-15	148	17.3	11.6	11.2	12.9	1.3	0.4	45.3	100.0	87	25.3	17.3	0.9	104
TC11-16	153	18.8	11.2	11.0	12.7	1.4	0.5	44.5	100.0	87	25.1	17.5	0.9	106
TC11-17	159	38.3	15.7	23.4	20.2	2.0	0.5	0.0	100.0	141	21.1	36.9	0.8	227
TC11-18	174	31.1	4.5	7.1	13.7	0.4	0.7	42.4	100.0	49	25.2	13.3	0.3	71
TC11-19	185	38.3	15.0	23.7	20.5	1.8	0.8	0.0	100.0	143	21.1	29.1	0.7	229
TC11-20	189	40.2	16.4	19.7	21.0	1.9	0.8	0.0	100.0	137	22.0	32.6	0.8	226
TC11-21	195	21.7	30.0	25.3	18.1	4.1	0.7	0.0	100.0	215	21.6	46.6	1.7	272
TC11-22	200	23.8	26.9	25.3	18.8	4.3	0.8	0.0	100.0	209	21.5	46.9	1.4	272

Notes:

1. Correction is to assume that only air nitrogen is in the synthesis gas and that the reactor is adiabatic
2. TC11-1 to TC11-16 and TC11-18 were air blown; TC11-17, TC11-19, and TC11-20 were enhanced air; TC11-21 and TC11-22 were oxygen blown.
3. Clean syngas LHV is the LHV after cold sulfur cleanup where the syngas H_2O is decreased to 1%.

Table 3.3-6 Water-Gas Shift Equilibrium Constants

In-situ Start	In-situ End	Run Time Hours	Operating Period	Dry CO %	Dry H_2 %	Dry CO_2 %	In-situ H_2O %	Kp	WGS Eqm. Temp. F	Mixing Zone Temp. F	Mixing Zone Kp^2
4/11/2003 8:45	4/11/2003 12:45	31	None[1]	5.8	4.4	12.1	9.8	0.84	1,584	1,651	0.75
4/14/2003 9:45	4/14/2003 14:09	99	None[1]	4.2	3.1	10.0	9.3	0.72	1,678	1,684	0.72
4/15/2003 9:35	4/15/2003 13:35	123	TC11-11[4]	3.9	3.4	10.1	11.9	0.65	1,746	1,659	0.74
4/16/2003 13:00	4/16/2003 17:14	150	TC11-15[4] & 16[4]	6.8	5.9	11.0	11.7	0.72	1,681	1,667	0.73
4/17/2003 13:30	4/17/2003 15:30	174	TC11-18	2.1	2.2	10.7	15.2	0.64	1,758	1,680	0.72
4/18/2003 9:15	4/18/2003 11:15	193	TC11-21[4]	12.6	12.1	16.2	18.1	0.70	1,695	1,733	0.67
4/18/2003 13:15	4/18/2003 15:16	197	None[1]	12.1	12.1	16.0	18.4	0.71	1,693	1,717	0.68

Notes:

1. Data not taken during operating period.
2. Equilibrium constant calculated at mixing zone temperature (TI350), with an 0ºF approach.
3. April 11 to 17 data taken during air operation. April 18 data taken during oxygen operation.
4. In-situ sample was taken during part of the indicated operating period.

Table 3.3-7 Transport Gasifier Equilibrium Calculations

Operating Period	Average Relative Hour	Measured Syngas Kp[1]	Mixing Zone Equilibrium Temperature Kp[2]	Wet AI419J H_2S ppm	Syngas Total Reduced Sulfur[3] ppm	Equilibrium H_2S[4] ppm	AI475Q Ammonia ppm	PCD Equilibrium Ammonia[5] ppm
TC11-1	1	(6)	0.74	1	459	168	715	(6)
TC11-2	10	1.23	0.76	192	581	408	146	199
TC11-3	18	0.78	0.73	544	733	273	399	313
TC11-4	23	0.81	0.72	635	776	278	402	393
TC11-5	36	(7)	0.73	605	848	(7)	246	723
TC11-6	50	0.68	0.73	357	688	215	371	366
TC11-7	60	0.59	0.72	574	797	212	456	454
TC11-8	92	0.67	0.77	629	650	198	619	478
TC11-9	95	0.67	0.75	645	686	208	544	461
TC11-10	115	0.61	0.73	912	909	231	350	341
TC11-11	126	0.63	0.74	819	817	230	404	367
TC11-12	132	0.61	0.71	969	954	272	1,101	966
TC11-13	137	0.59	0.69	1,069	1,070	260	688	747
TC11-14	144	0.62	0.72	889	893	245	504	588
TC11-15	148	0.72	0.73	973	1,014	263	826	997
TC11-16	153	0.66	0.72	886	973	266	974	1,029
TC11-17	159	0.79	0.70	1,311	1,215	590	1,574	1,743
TC11-18	174	0.69	0.72	667	749	269	190	175
TC11-19	185	0.85	0.76	1,093	1,059	414	1,025	1,217
TC11-20	189	0.63	0.69	1,049	1,040	379	976	852
TC11-21	195	0.70	0.66	1,417	1,374	430	1,778	2,504
TC11-22	200	0.74	0.66	1,353	1,380	456	2,875	2,295

Notes:

1. Syngas Kp determined by measured syngas hydrogen, water, carbon dioxide, and carbon monoxide concentrations.
2. Mixing zone Kp determined by equilibrium calculations using the mixing zone temperature (TI350).
3. Synthesis gas total reduced sulfur (TRS) estimated from Synthesis gas combustor SO_2 analyzer data
4. Minimum equilibrium H_2S determined by equilibrium calculations and the carbon dioxide and water partial pressures.
5. Equilibrium ammonia concentrations determined by equilibrium calculations and the partial pressures of hydrogen and nitrogen.
6. Hydrogen analyzer not in operation so syngas Kp and equilibrium ammonia concentration could not be determined
7. Moisture analyzer not in operation so syngas Kp and minimum H_2S equilibrium concentration could not be determined.
8. TC11-1 to TC11-16 and TC11-18 were air blown; TC11-17, TC11-19, and TC11-20 were enhanced air; TC11-21 and TC11-22 were oxygen blown.

Table 3.3-8 Synthesis Gas Combustor Calculations

Operating Period	Average Relative Hour	Syngas Combustor Exit AI8775 O_2 M %	Syngas Combustor Exit Calculated O_2 M %	Syngas Combustor Exit AI476D CO_2 M %	Syngas Combustor Exit Calculated CO_2 M %	Syngas Combustor Exit AI476H H_2O M %	Syngas Combustor Exit Calculated H2O M %	Gas Analyzer LHV Btu/SCF	Energy Balance LHV[1] Btu/SCF	Combustor SO_2 AI476P ppm	Syngas Total Reduced Sulfur[2] ppm
TC11-1	1	6.0	6.0	9.6	10.2	8.2	8.7	50	48	217	459
TC11-2	10	5.2	5.2	8.0	8.8	12.2	11.9	15	11	254	581
TC11-3	18	6.2	6.5	8.2	8.8	11.1	10.5	26	25	287	733
TC11-4	23	6.6	6.9	8.2	8.7	10.8	10.2	30	29	292	776
TC11-5	36	5.7	5.8	9.2	8.7	11.4	11.2	41	42	388	848
TC11-6	50	5.3	5.7	8.6	7.8	11.0	10.7	25	26	303	688
TC11-7	60	5.1	5.5	8.9	8.3	11.6	11.2	30	32	370	797
TC11-8	92	5.0	5.4	8.9	8.2	10.8	10.7	29	30	300	650
TC11-9	95	5.0	5.5	8.9	8.2	11.0	10.9	28	30	315	686
TC11-10	115	5.0	5.1	8.6	8.2	12.1	11.8	25	24	419	909
TC11-11	126	5.0	5.5	8.9	8.1	11.9	11.5	25	28	373	817
TC11-12	132	5.0	4.8	10.1	9.9	12.7	13.2	49	49	510	954
TC11-13	137	5.0	5.1	9.9	9.7	12.4	12.5	43	44	553	1070
TC11-14	144	5.0	5.6	9.1	8.5	12.1	11.7	32	35	415	893
TC11-15	148	5.0	5.1	10.0	9.8	12.1	11.9	47	47	522	1014
TC11-16	153	5.0	5.1	10.1	9.8	11.9	12.4	47	49	512	973
TC11-17	159	5.0	4.5	10.4	11.2	19.6	20.4	57	55	636	1215
TC11-18	174	5.0	5.7	8.4	7.7	12.7	12.1	16	19	315	749
TC11-19	185	5.0	5.3	9.5	9.2	15.8	15.5	41	43	514	1059
TC11-20	189	5.0	5.5	9.8	9.6	15.9	15.4	40	44	507	1040
TC11-21	195	6.0	6.0	10.9	11.4	15.5	15.3	81	79	585	1374
TC11-22	200	6.4	6.7	10.5	10.6	15.1	15.0	80	83	555	1380

Notes:

1. Energy LHV calculated assuming the synthesis gas combustor heat loss was 2 million Btu/hr.
2. Synthesis gas total reduced sulfur (TRS) estimated from Synthesis gas combustor SO_2 analyzer data
3. TC11-1 to TC11-16 and TC11-18 were air blown; TC11-17, TC11-19, and TC11-20 were enhanced air; TC11-21 and TC11-22 were oxygen blown.

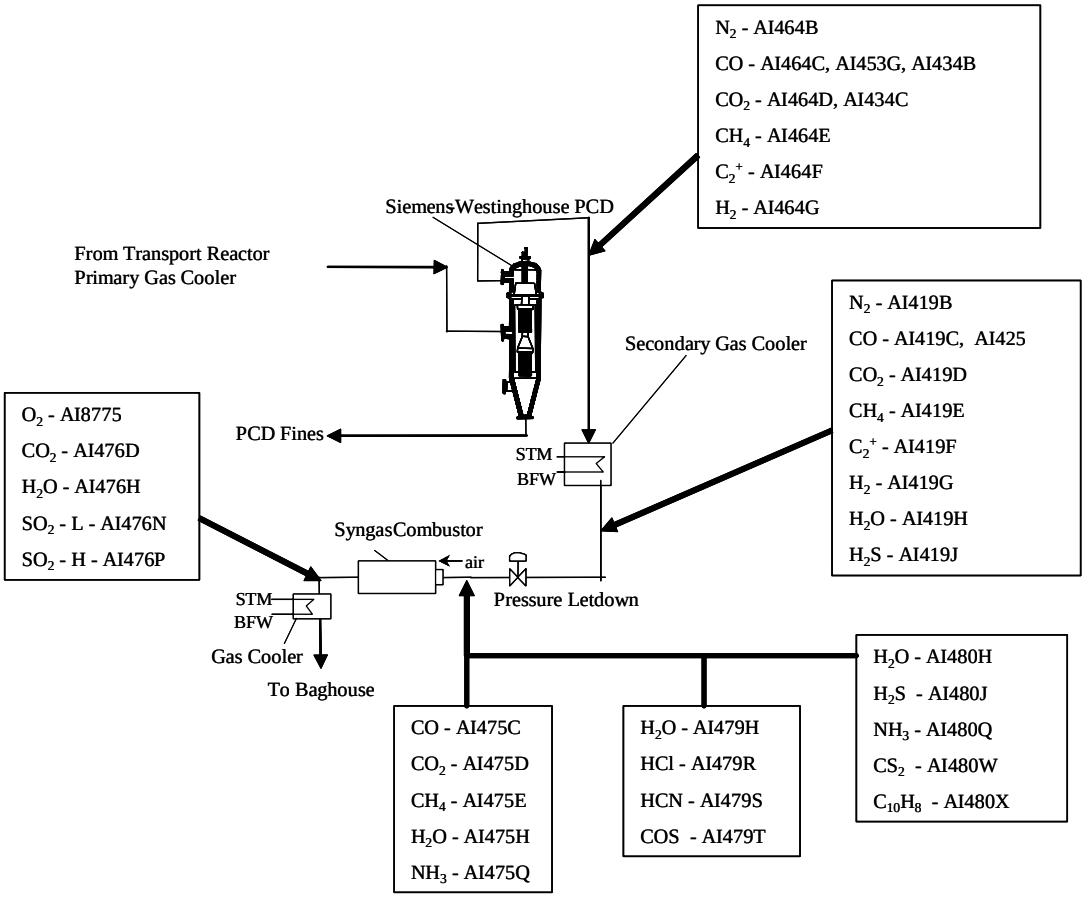

Figure 3.3-1 Gas Sampling Locations

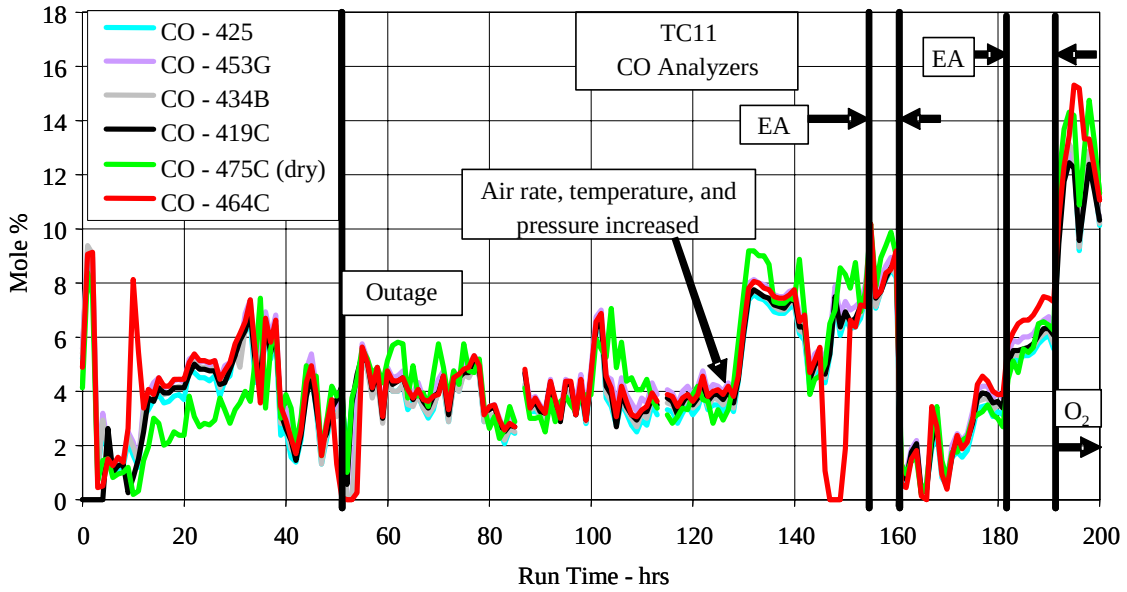

Figure 3.3-2 Carbon Monoxide Analyzer Data

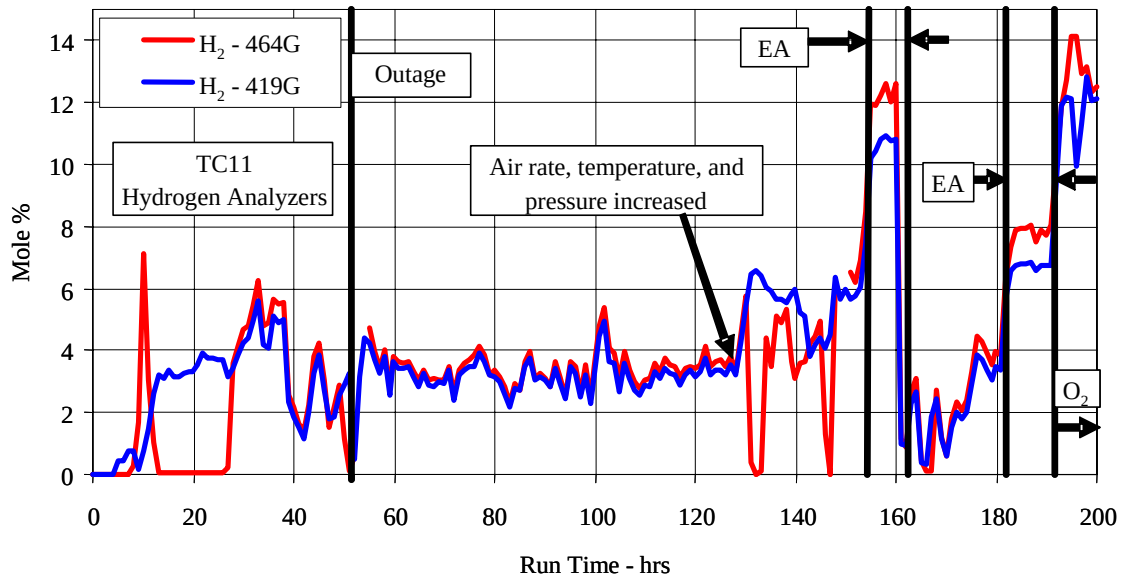

Figure 3.3-3 Hydrogen Analyzer Data

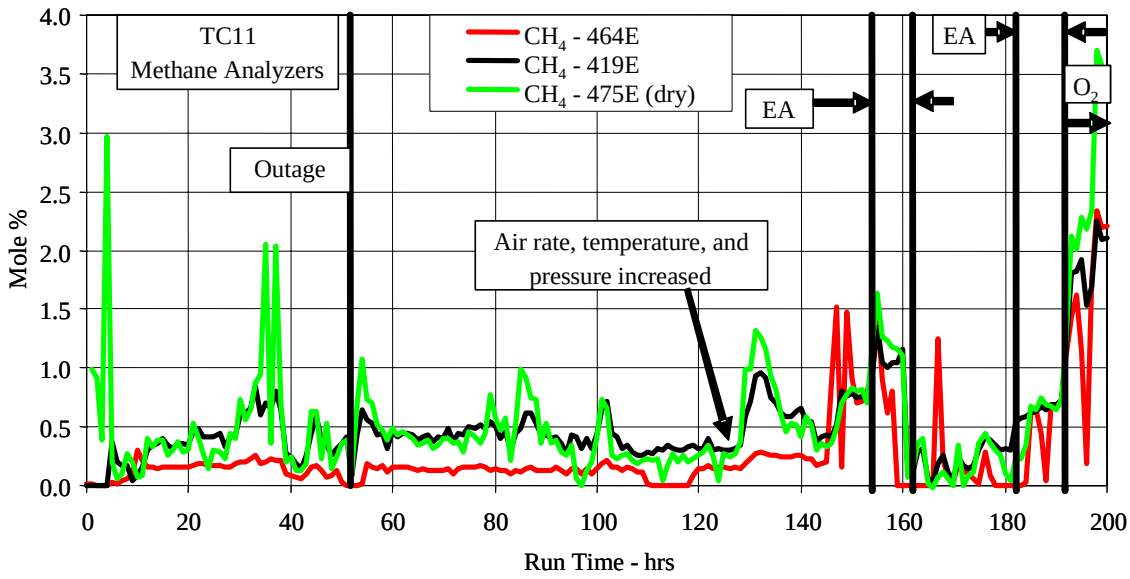

Figure 3.3-4 Methane Analyzer Data

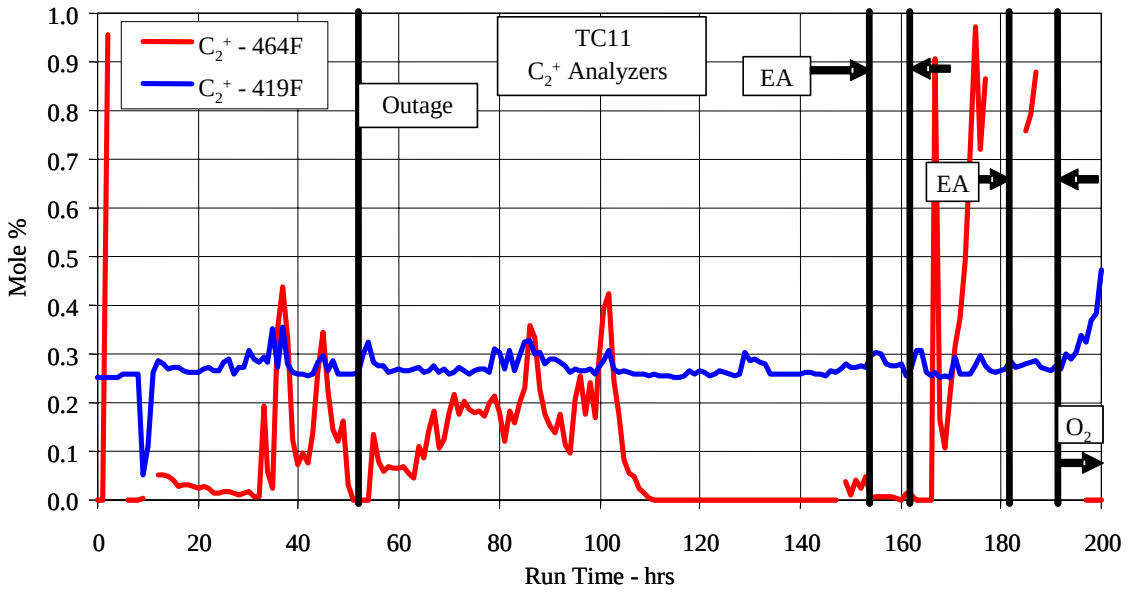

Figure 3.3-5 C_2^+ Analyzer Data

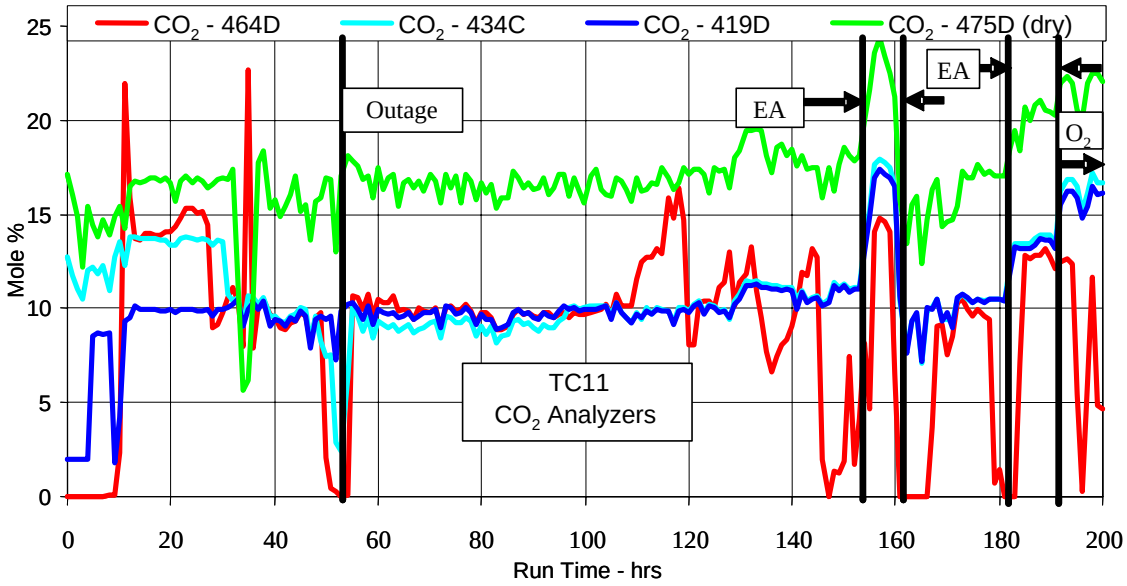

Figure 3.3-6 Carbon Dioxide Analyzer Data

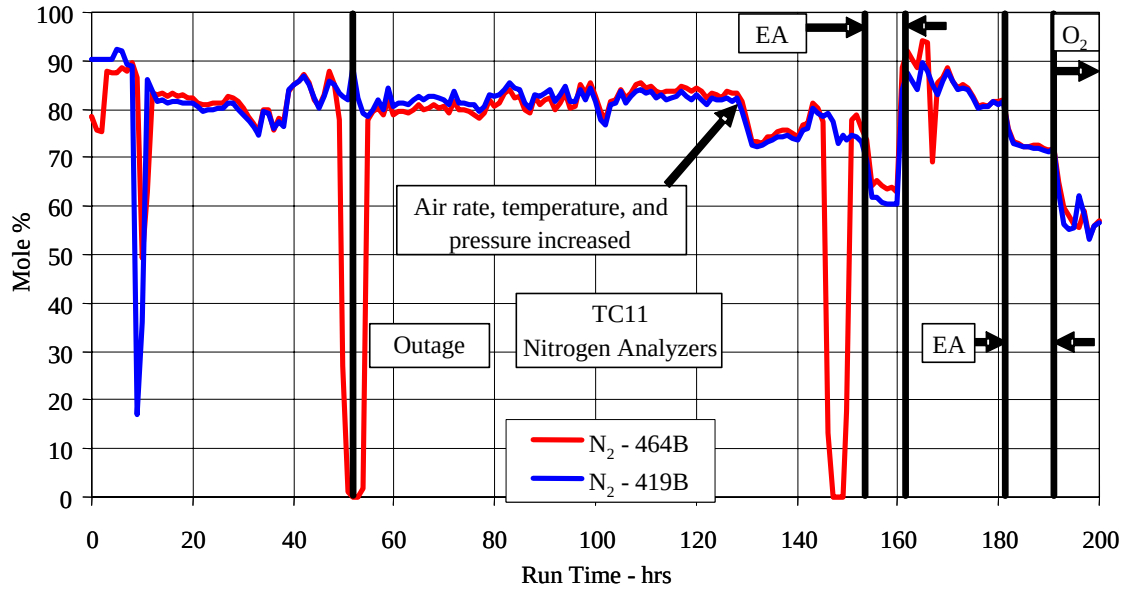

Figure 3.3-7 Nitrogen Analyzer Data

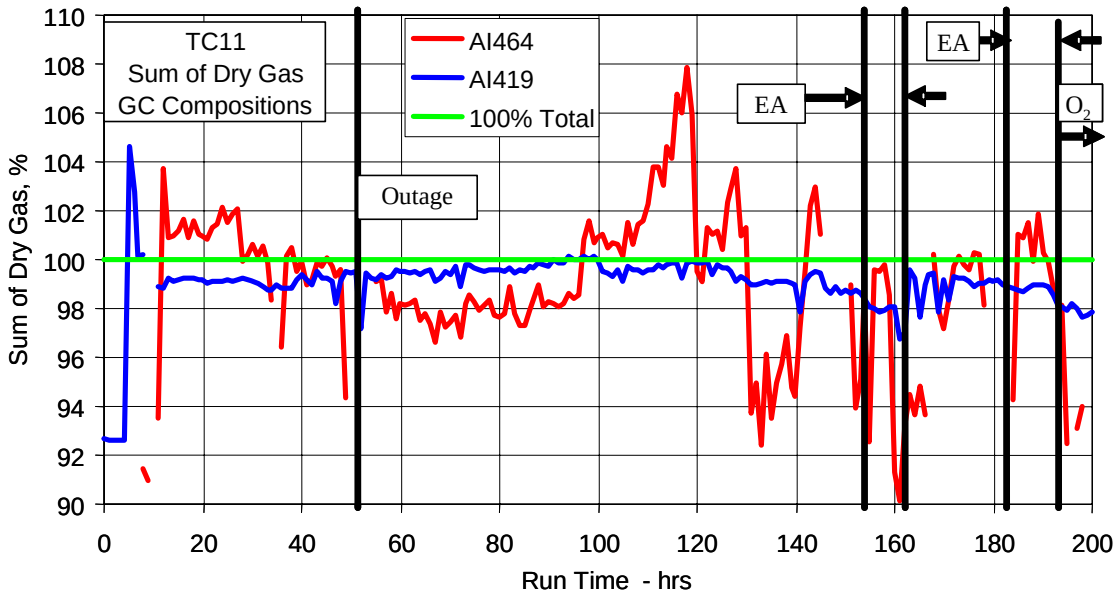

Figure 3.3-8 Sums of GC Gas Compositions (Dry)

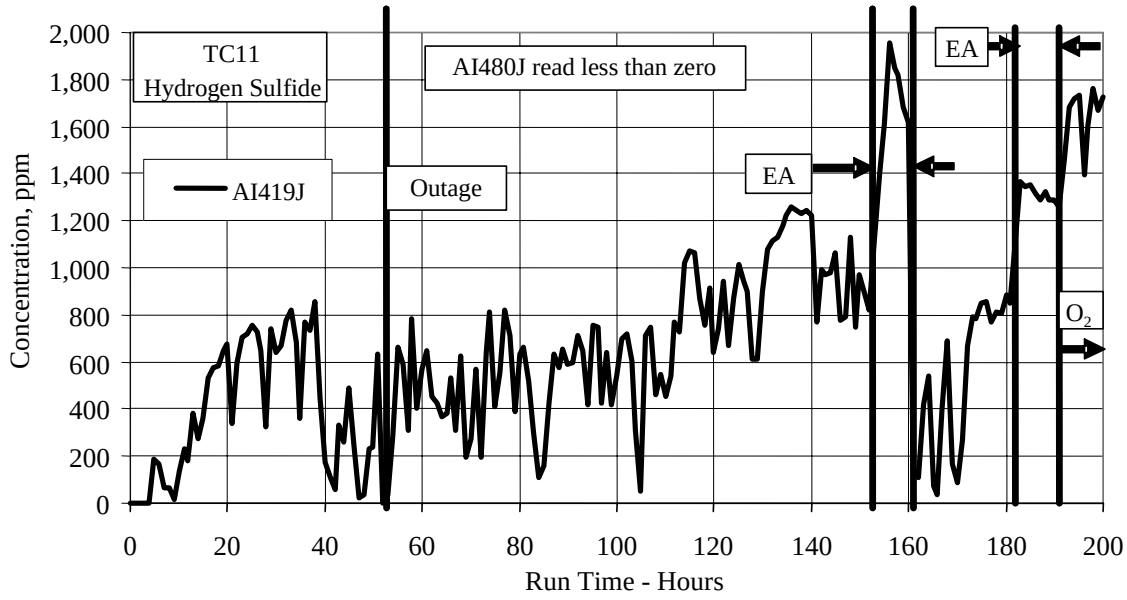

Figure 3.3-9 Hydrogen Sulfide Analyzer Data

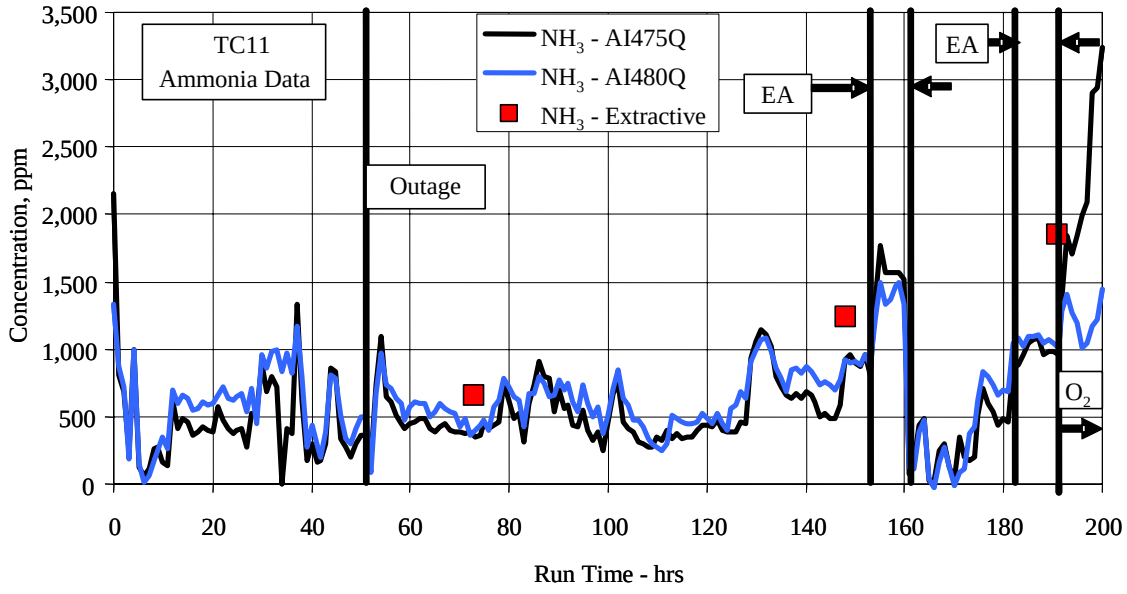

Figure 3.3-10 Ammonia Data

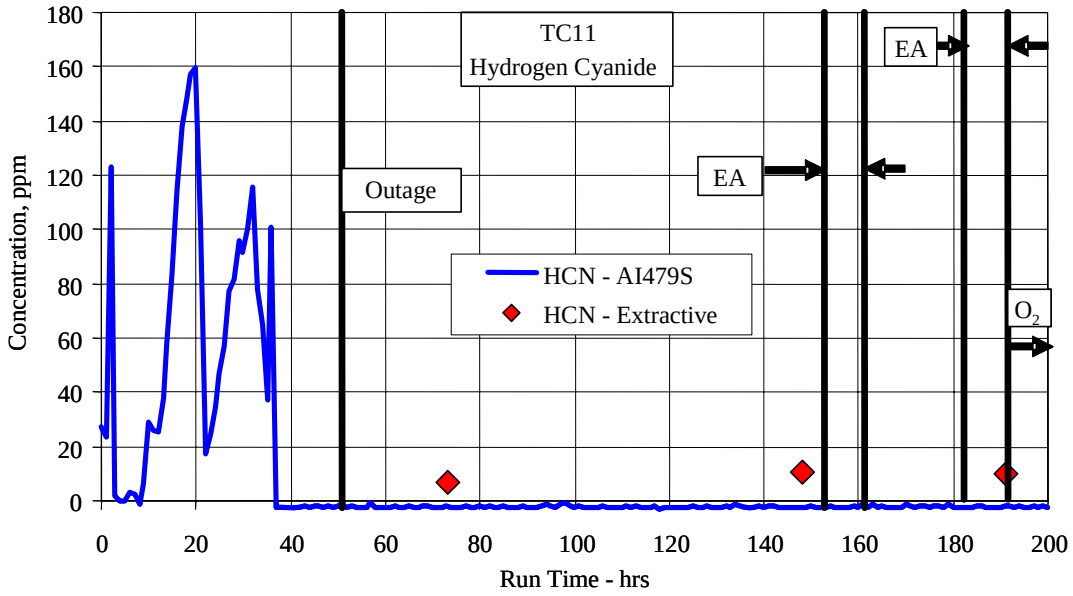

Figure 3.3-11 Hydrogen Cyanide Data

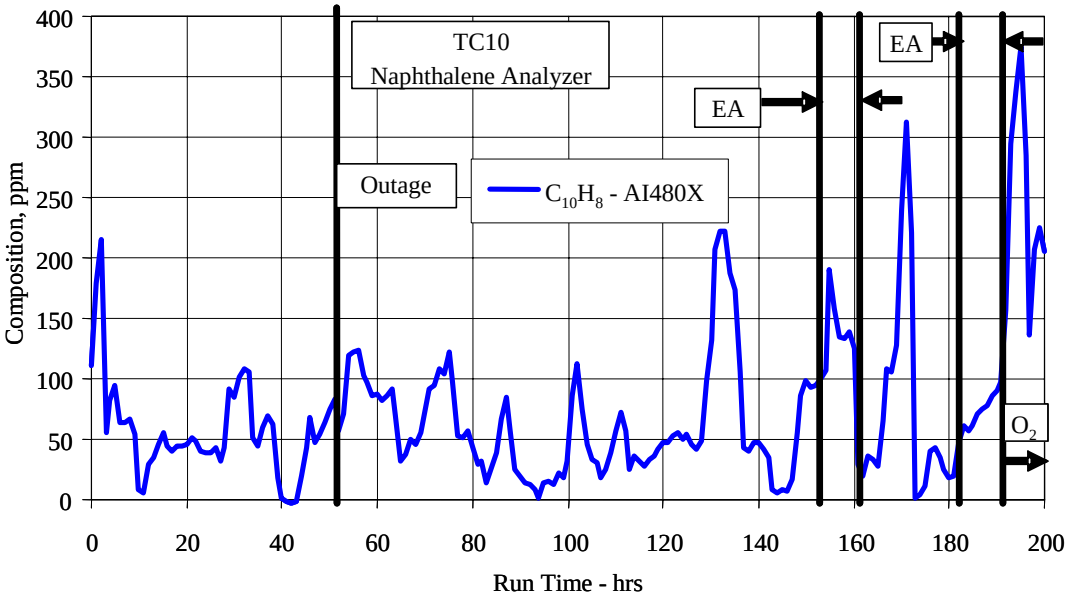

Figure 3.3-12 Naphthalene Data

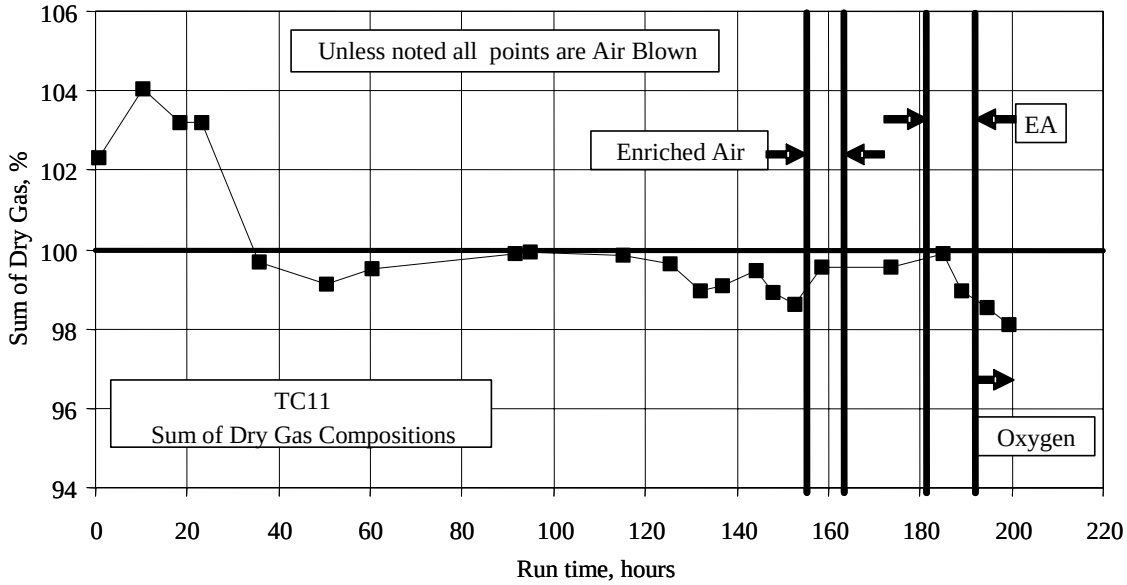

Figure 3.3-13 Sums of Dry Gas Compositions

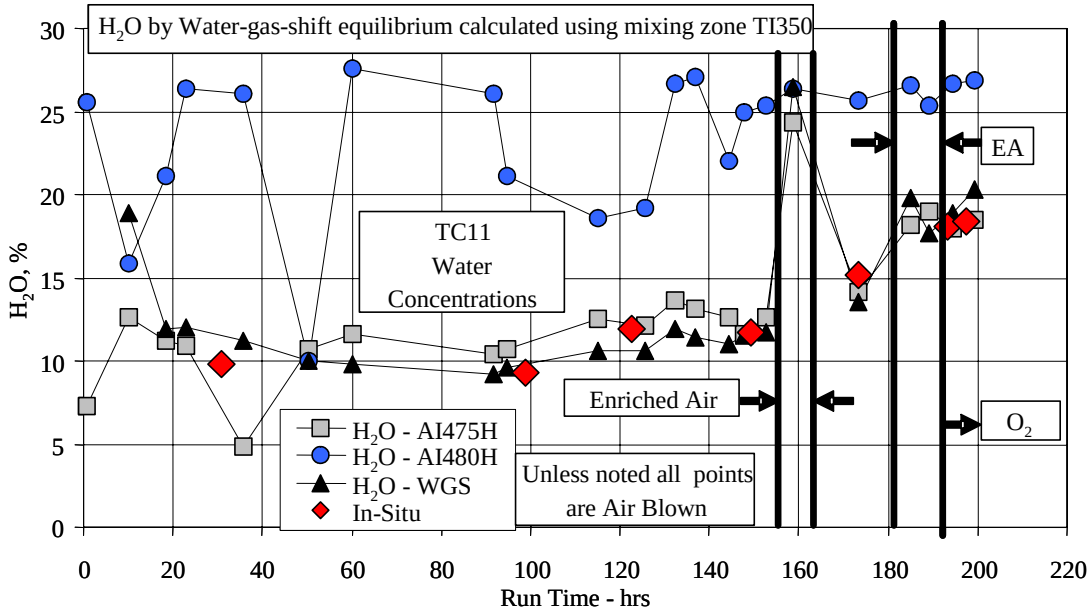

Figure 3.3-14 H_2O Data

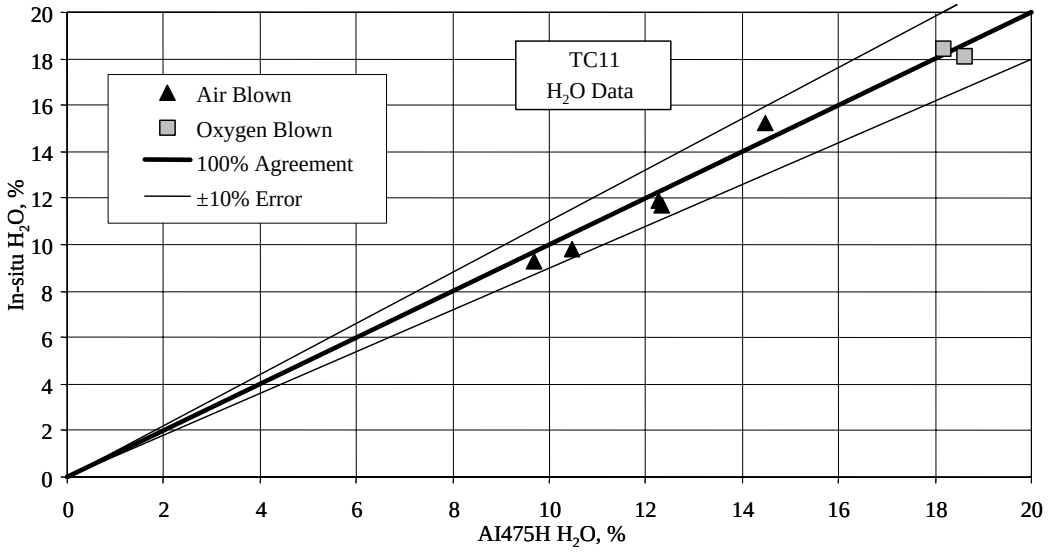

Figure 3.3-15 H_2O Data

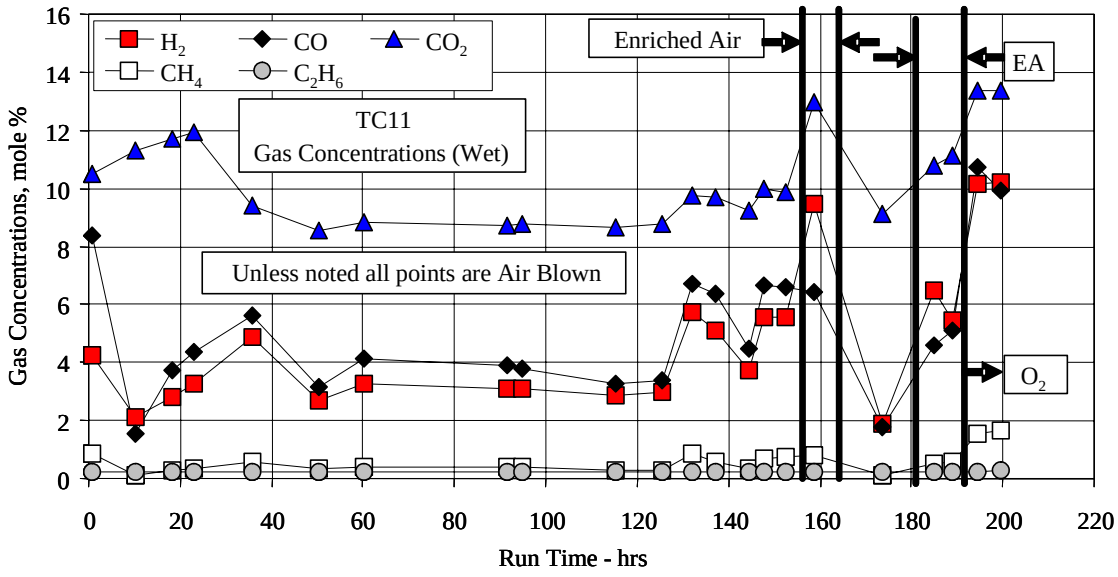

Figure 3.3-16 Wet Synthesis Gas Compositions

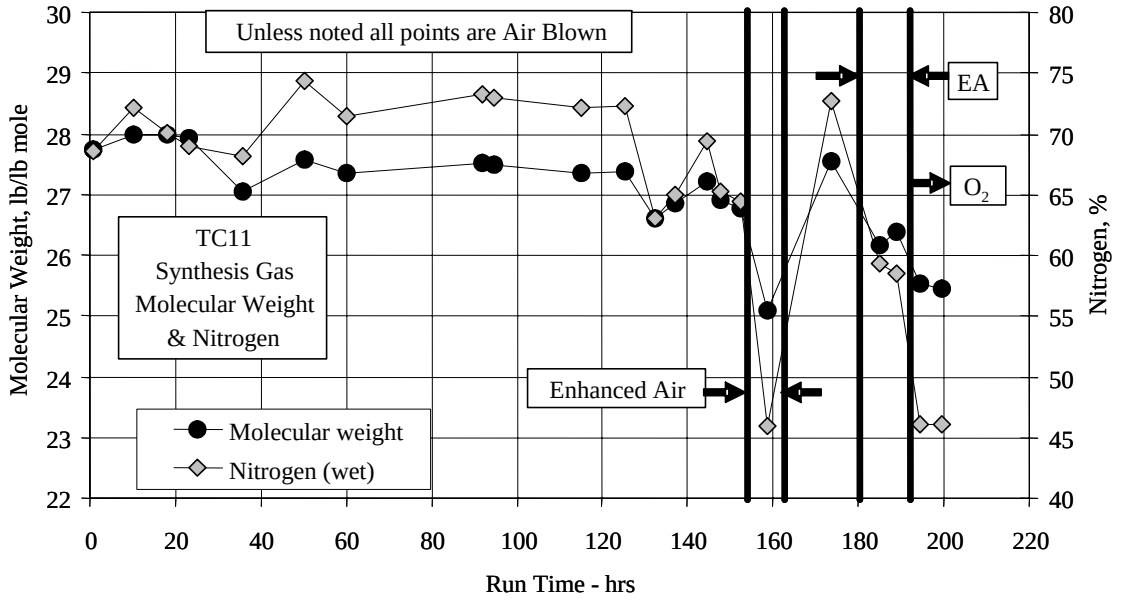

Figure 3.3-17 Syngas Molecular Weight and Nitrogen Concentration

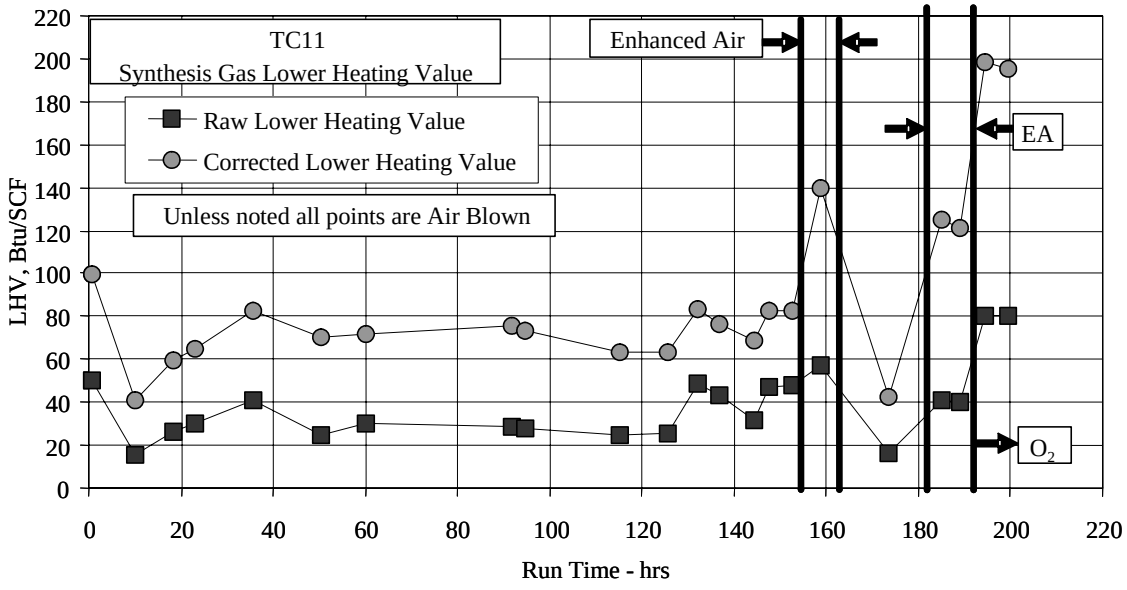

Figure 3.3-18 Synthesis Gas Lower Heating Values

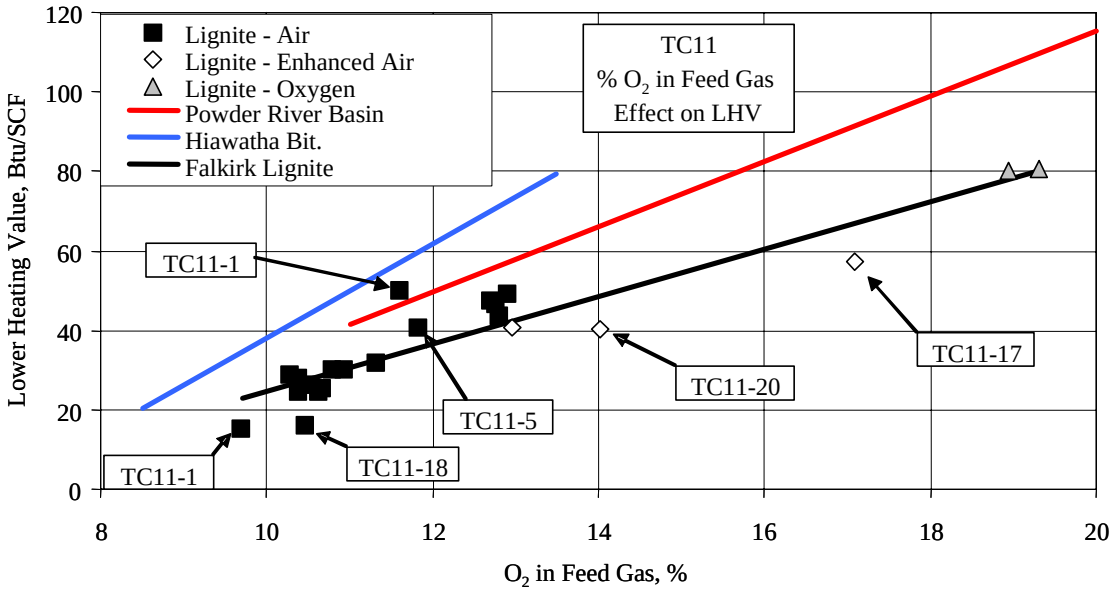

Figure 3.3-19 Raw Lower Heating Value and Overall Percent O_2

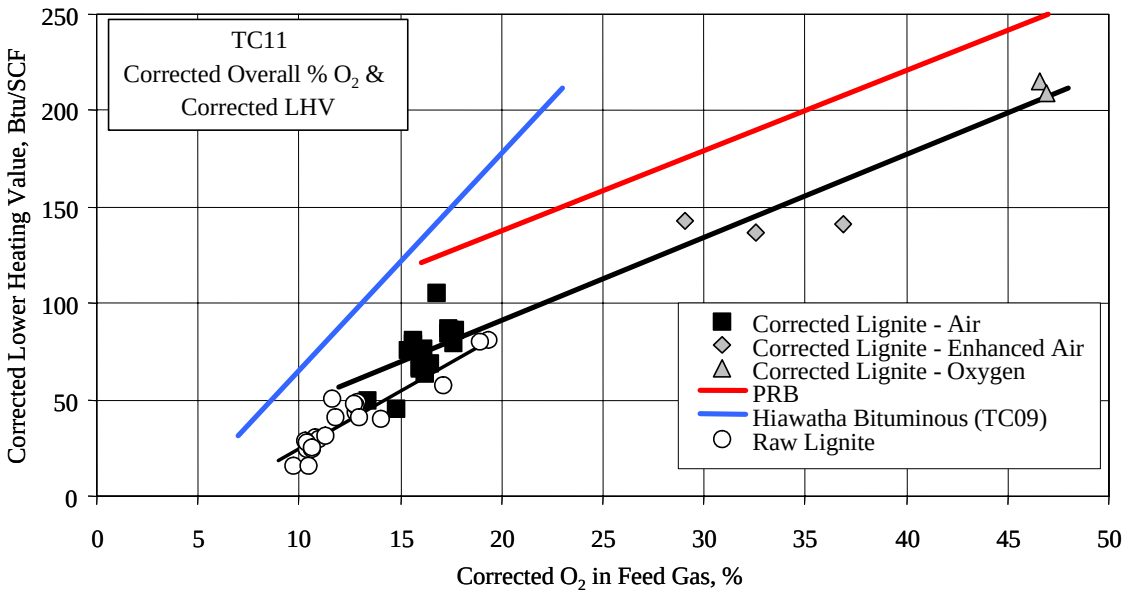

Figure 3.3-20 Corrected LHVs and Overall Percent O_2

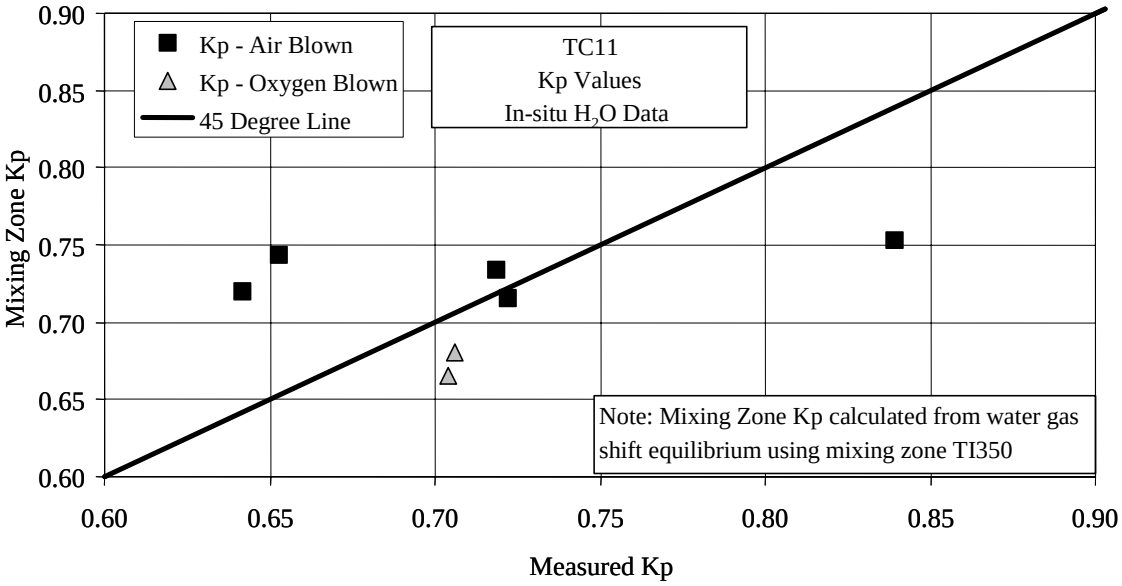

Figure 3.3-21 Water-Gas Shift Constants (In situ H_2O)

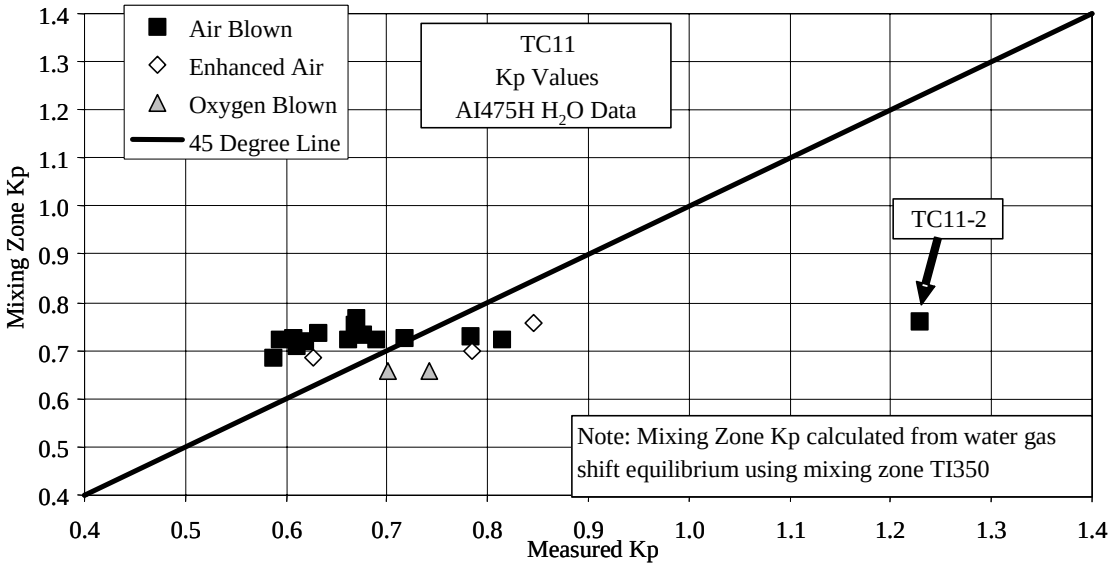

Figure 3.3-22 Water-Gas Shift Constants (AI475H H_2O)

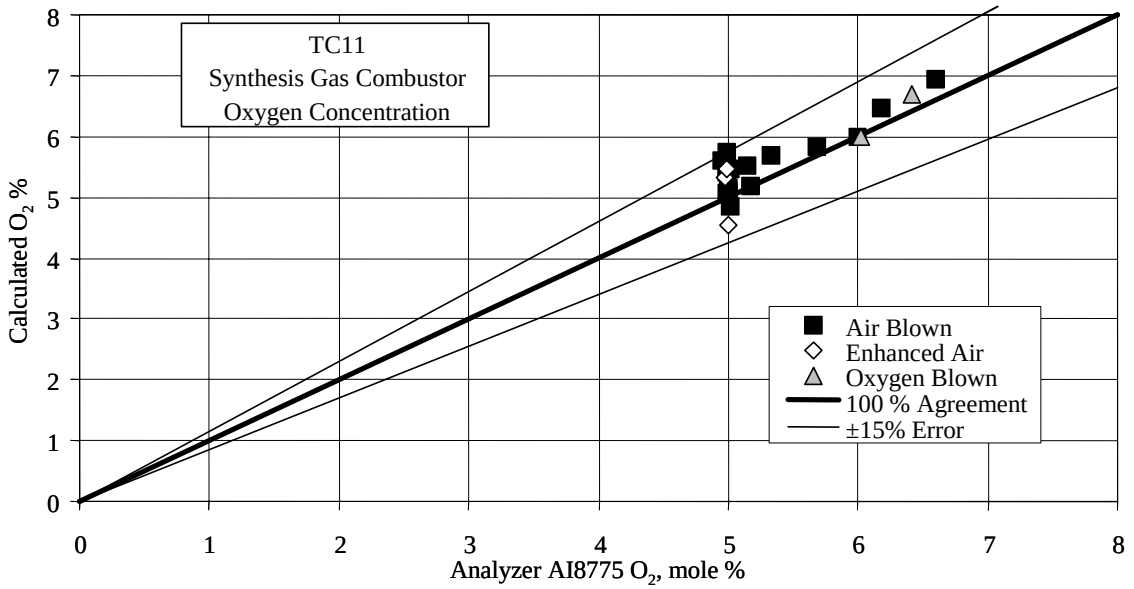

Figure 3.3-23 Synthesis Gas Combustor Outlet Oxygen

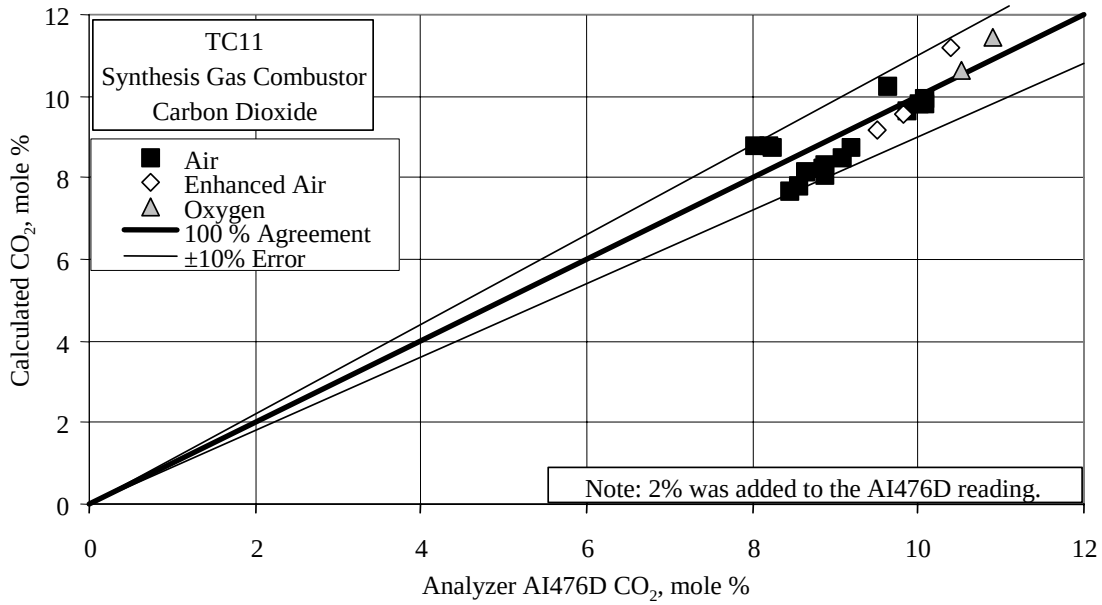

Figure 3.3-24 Synthesis Gas Combustor Outlet Carbon Dioxide

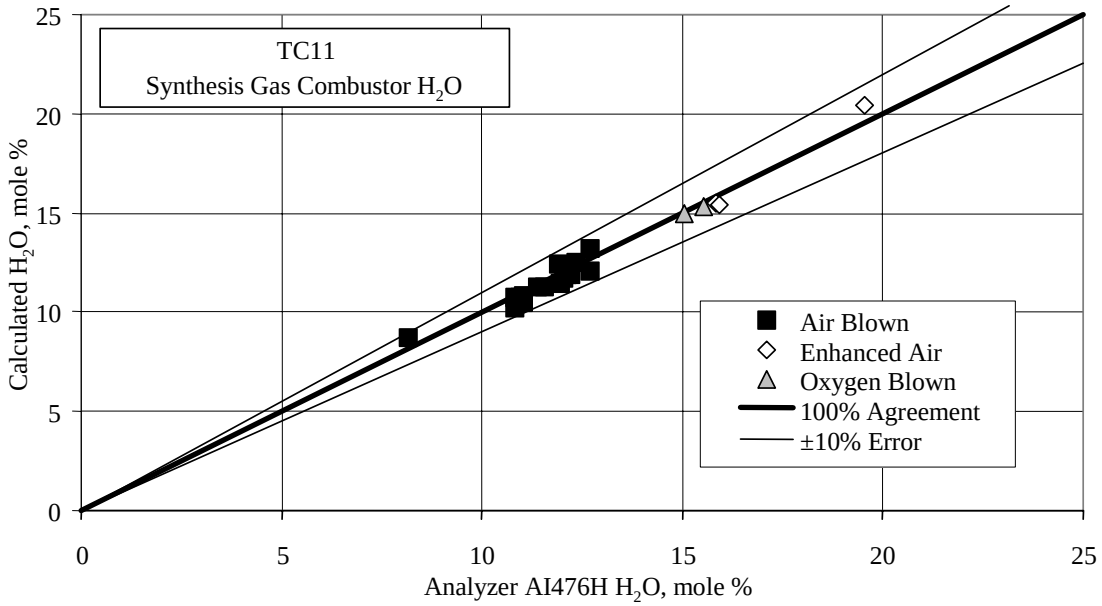

Figure 3.3-25 Synthesis Gas Combustor Outlet Moisture

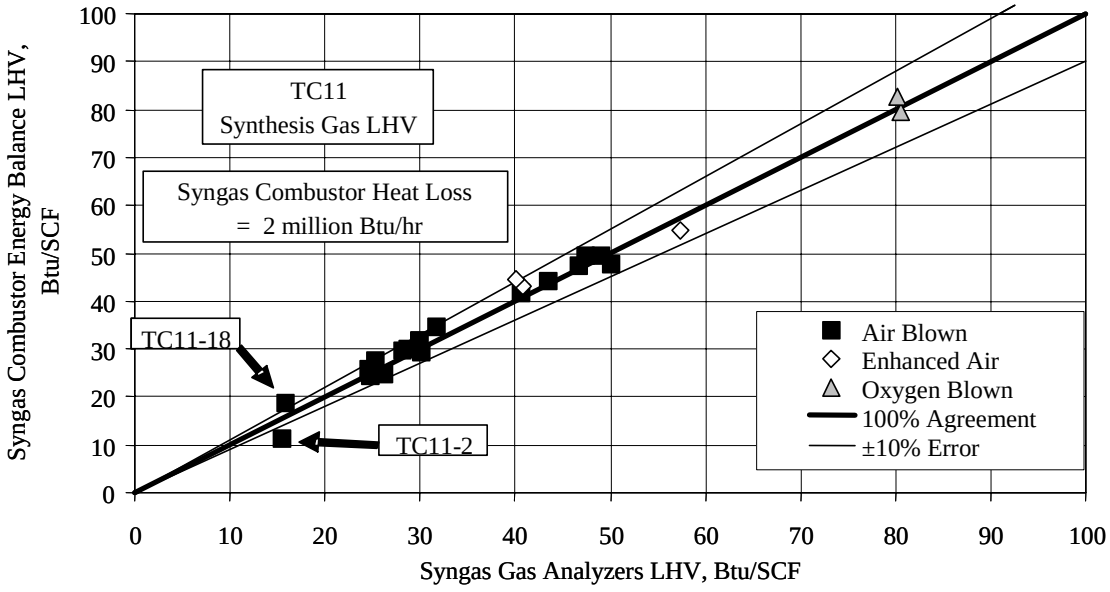

Figure 3.3-26 Synthesis Gas LHV

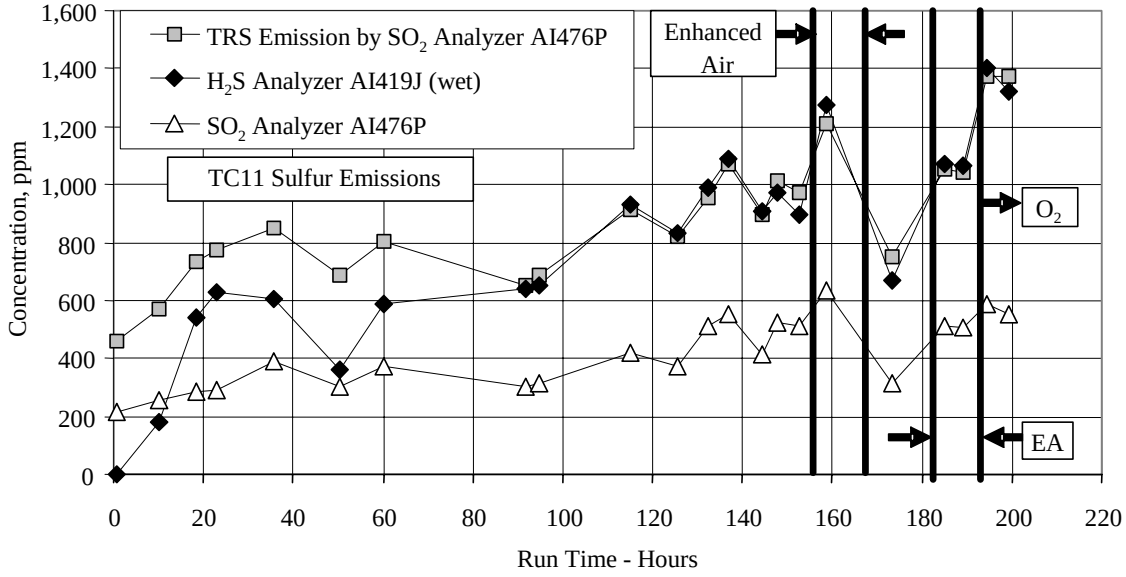

Figure 3.3-27 Sulfur Emissions

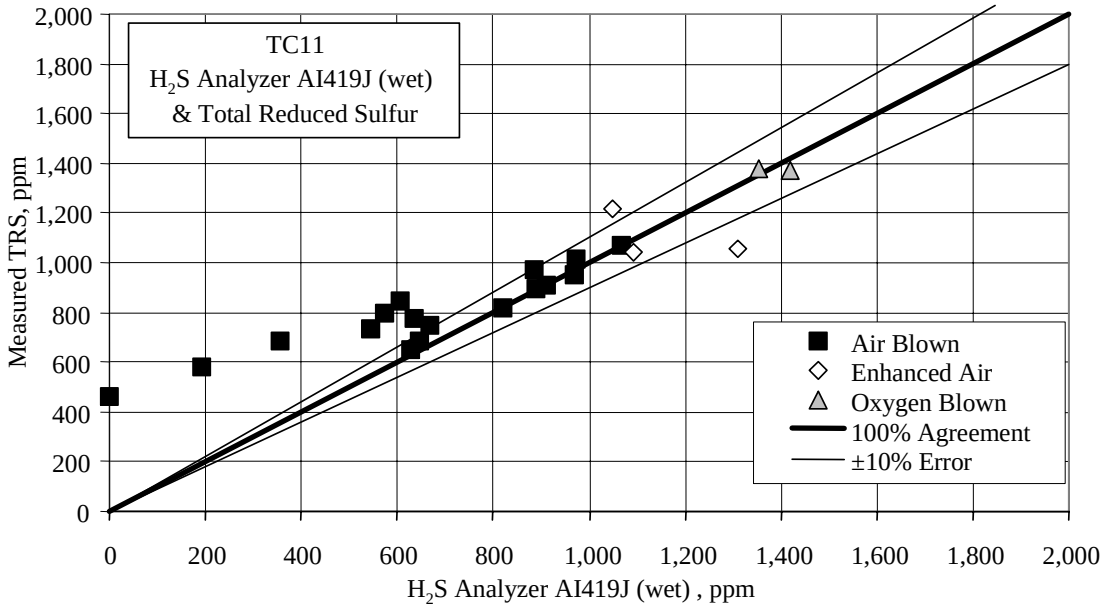

Figure 3.3-28 H_2S Analyzer AI419J and Total Reduced Sulfur

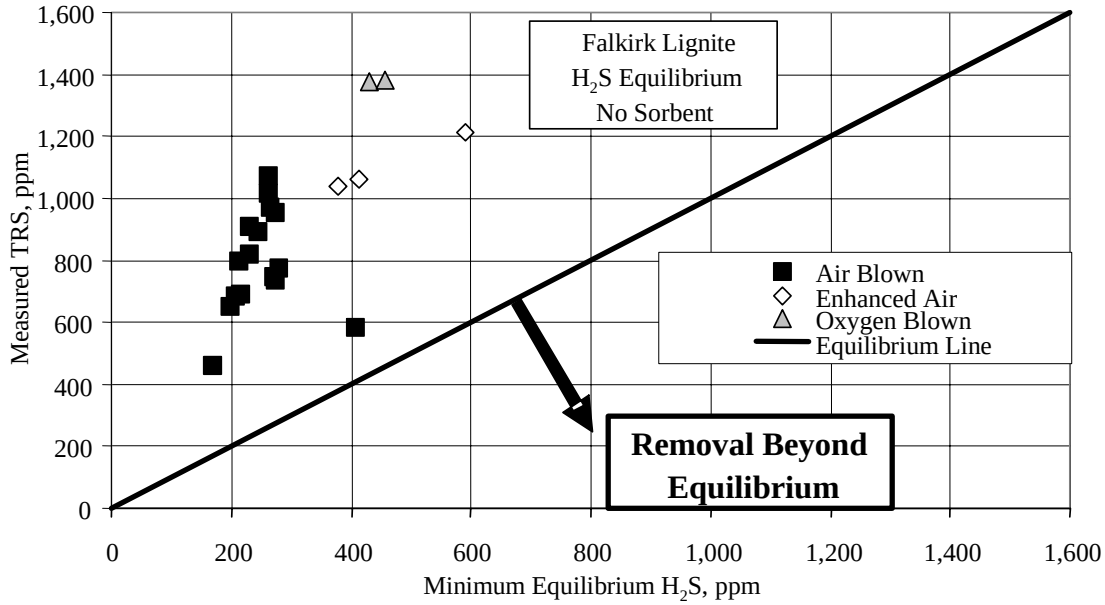

Figure 3.3-29 Minimum Equilibrium H_2S and Total Reduced Sulfur

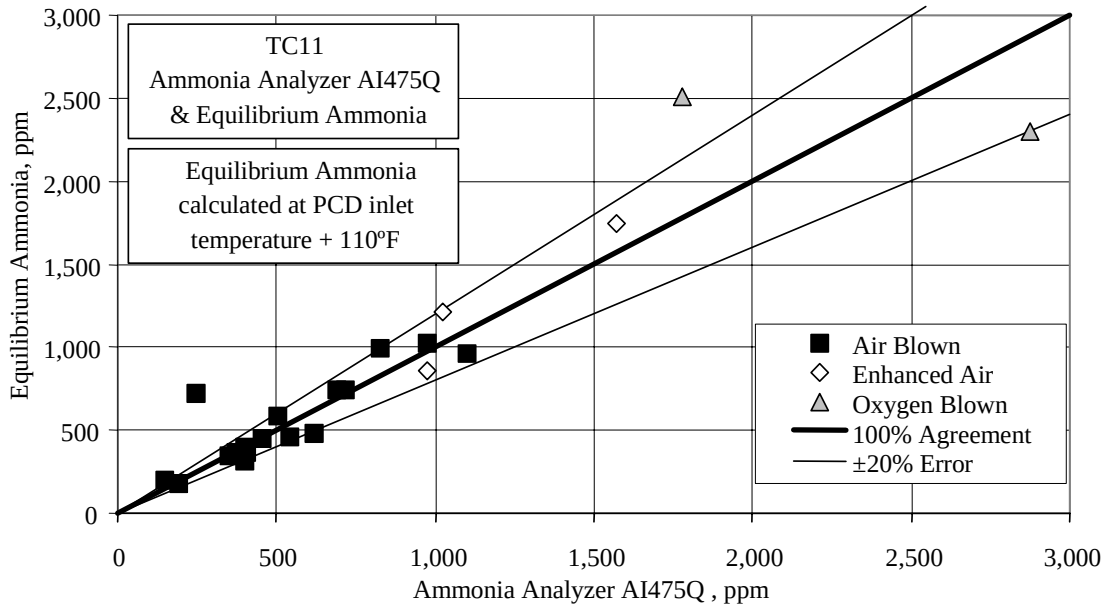

Figure 3.3-30 NH_3 Analyzer AI475Q and Equilibrium NH_3

3.4 SOLIDS ANALYSES

3.4.1 Summary and Conclusions

- Falkirk lignite coal moisture, sulfur and ash compositions were not constant during TC11 testing. Other coal properties were constant during TC11.
- Standpipe carbon was as high as 0.7-weight percent for periods with coal feed. The standpipe carbon was not effected by coal and coke breeze feed.
- Standpipe solids contained negligible amounts of CaS.
- Standpipe solids contained negligible $CaCO_3$; standpipe calcium was totally calcined.
- Loopseal downcomer carbon was as high as 3.2-weight percent.
- Loopseal downcomer solids contained negligible amounts of CaS.
- Loopseal downcomer solids contained negligible $CaCO_3$; loopseal downcomer calcium was totally calcined.
- PCD inlet in situ samples carbon, $CaCO_3$, CaO, CaS, and SiO_2 concentrations were consistent with FD0520 samples concentrations.
- The PCD fines sulfur and standpipe solids sulfur content indicate some Transport Gasifier sulfur capture.
- In air- and enhanced-air-blown modes, the PCD fines calcium was 80- to 95-percent calcined, while in oxygen-blown mode the PCD fines calcium was 70- to 80-percent calcined.
- Loopseal downcomer carbon, silica, and calcium compositions were similar to the standpipe compositions during air-blown operation.
- Loopseal downcomer and standpipe silica and calcium compositions approached the PCD fines compositions as TC11 progressed.
- Coal feed particle size decreased from 250 to 150 μ Sauter mean diameter (SMD) for the first 50 hours, then leveled off at 150 μ SMD. The mass mean coal particle size leveled off at 250 to 320 μ.
- The coal feed percent fines increased during TC11.
- Standpipe solids particle size reached a steady state value of 200 μ SMD.
- Standpipe solids bulk density decreased from 90 to 75 lb/ft^3.
- Standpipe solids particle sizes were larger than in previous PRB air-blown and Hiawatha bituminous air-blown testing.
- Loopseal downcomer solids particle size slowly increased to 175 μ SMD during air-blown testing, then decreased to 50 μ SMD during oxygen-blown testing.
- Loopseal downcomer solids bulk density decreased from 85 to 75 lb/fr^3.
- PCD solids particle size was nearly constant at between 10 and 15 μ.
- In situ PCD fines particle sizes were within 5 μ of the FD0520 samples particle sizes.
- PCD solids bulk density was constant at 30 to 40 lb/ft^3.
- In situ PCD fines bulk densities were consistent with the FD0520 bulk densities.
- Loopseal downcomer samples particle sizes were the same as the standpipe particle sizes until the enhanced-air testing, when the loopseal downcomer samples particle sizes decreased, approaching the PCD fines particle sizes.

3.4.2 Introduction

During TC11, solid samples were collected from the original fuel feed system (FD0210), the sorbent feed system (FD0220), the Transport Gasifier standpipe, the Transport Gasifier loopseal downcomer, and the PCD fine solids transport system (FD0520). In situ solids samples were also collected from the PCD inlet. The sample locations are shown in Figure 3.4-1. These solids were analyzed for chemical composition and particle size. During TC11, coke breeze and sand were added through FD0220. Sorbent was not added through FD0220.

3.4.3 Feeds Analysis

Table 3.4-1 gives the average coal composition for the samples analyzed as sampled from FD0210 during TC11. Coal was also fed to the gasifier from FD0252, and FD0200, but samples were not taken from those feed systems. FDO252 is normally used to feed char to the Transport Gasifier. FD0200 is a new coal feeder which uses a fluidized bed feeder to feed coal into the Transport Gasifier. The coal carbon and moisture contents are shown in Figure 3.4-2. The average Falkirk lignite coal carbon was 42.5-weight percent and the average Falkirk lignite moisture was 28-weight percent. The carbon contents of the coal were essentially constant, while the moisture contents had some slight variations. The moisture content variations were due to the difficulty in grinding the high moisture Falkirk lignite coal. The Falkirk lignite coal was the highest moisture coal gasified in the PSDF Transport Gasifier, higher than the 22-weight percent moisture PRB fuel.

Figure 3.4-3 shows the fuel sulfur and ash as sampled from FD0210 during TC11. The average values are given on Table 3.4-1; the Falkirk lignite coal average sulfur was 0.76-weight percent and the average ash was 13.07-weight percent. The Falkirk lignite coal sulfur and ash analyses show more variation than previous Powder River Basin analyses. The maximum measured TC11 coal sulfur was 1.0-weight percent and the maximum coal ash was 16-weight percent.

The coal higher heating value (HHV) and lower heating value (LHV) are given on Figure 3.4-4 with the TC11 average values given in Table 3.4-1. Coal HHV is determined by a bomb calorimeter which condenses all the coal combustion moisture as liquid water. The heat of vaporization of the coal hydrogen moisture is then counted as part of the coal HHV. The LHV is determined by subtracting the heat vaporization of the H_2O produced by the coal elemental hydrogen from the HHV. Since heat recovery steam generators do not recover the coal syngas moisture heat of vaporization, the LHV is a more realistic measure of coal heating value. The average HHV was 6,973 Btu/lb and the average LHV was 6,719 Btu/lb. The Falkirk lignite heating values were constant during TC11. The Falkirk lignite was the lowest heating value fuel gasified to date at the PSDF Transport Gasifier.

Average values for TC11 coal moisture, carbon, hydrogen, nitrogen, oxygen, sulfur, ash, volatiles, fixed carbon, higher heating value, lower heating value, CaO, SiO_2, Al_2O_3, MgO, and Fe_2O_3 are given in Table 3.4-1. Also given in Table 3.4-1 are the molar ratios for coal calcium-to-sulfur (Ca/S) and coal iron-to-sulfur (Fe/S). Falkirk lignite has sufficient alkalinity in the ash to remove all of the coal sulfur. The Falkirk lignite coal alkalinity has less relative alkalinity than Powder River Basin coal.

FD0220 was used during TC11 to feed coke breeze or sand into the Transport Gasifier, but no FD0220 solids samples were taken. Limestone sorbent was not fed to the Transport Gasifier during TC11.

3.4.4 Gasifier Solids Analysis

The chemical compositions of the solid compounds produced by the Transport Gasifier were determined using the solids chemical analysis and the following assumptions:

1. All carbon dioxide measured came from $CaCO_3$, hence moles CO_2 measured = moles $CaCO_3$.
2. All sulfide sulfur measured came from CaS.
3. All calcium not taken by CaS and $CaCO_3$ came from CaO.
4. All magnesium came from MgO.
5. Total carbon is measured, which is the sum of organic and inorganic (CO_2) carbon. The organic carbon is the total carbon minus the inorganic carbon (CO_2).
6. All iron reported as Fe_2O_3 is assumed to be present in the gasifier and PCD solids as FeO.
7. Inerts are the sum of the P_2O_5, K_2O, Na_2O, and TiO_2 concentrations.

It will be assumed that all iron in both the standpipe and PCD solids is in the form of FeO and not in the form of Fe_3O_4 or Fe_2O_3. Thermodynamically, the mild reducing conditions in the Transport Gasifier should reduce all Fe_2O_3 to FeO, however, the assumption of iron as FeO seemed to give solids compositions totals that add up to around 100 percent.

It will also be assumed that no FeS is formed in the Transport Gasifier and that all the sulfur in the standpipe and PCD fines solids is present as CaS. It is thermodynamically possible that some FeS is formed. Most of the captured sulfur should be in the form of CaS due to the larger amount of calcium than iron in the system.

Table 3.4-2 gives the results from the standpipe analyses. The standpipe solids are solids that recirculate through the mixing zone, riser, and standpipe and change slowly with time, since a small amount of solids are taken out of the standpipe via the standpipe spent solids transporter system (FD0510). FD0510 was operated intermittently during TC11 to control the standpipe level. The flow rates for FD0510 and FD0520 solids during the stable operating periods are given in Section 4.5.

On startup, the standpipe solids mainly contained sand at 96.7-percent SiO_2. The standpipe did not contain pure sand at zero run-time hours since there were several periods of coal and coke breeze operation prior to the starting of the clock for the test, which diluted the standpipe sand.

As the run progressed, the start-up sand was slowly replaced by CaO, Al_2O_3, Fe_2O_3, and other inerts. This data is shown in Figure 3.4-5 which plots SiO_2, CaO, and Al_2O_3 and run time. The SiO_2 content slowly decreased and both the Al_2O_3 and the CaO slowly increased to replace the SiO_2. Sand was added at hour 61, but did not increase the SiO_2 content or decrease the Al_2O_3 and the CaO as in previous testing. It is possible that the gasifier did reach constant conditions at

the end of TC11 as the standpipe solids SiO_2, Al_2O_3, and CaO were all leveling out for the last two standpipe samples taken.

The standpipe organic carbon content is plotted in Figure 3.4-6. The average standpipe organic carbon content during coal operation was 0.4 percent and varied between 0.1 and 0.7 percent carbon. This level of carbon was consistent with previous PRB standpipe samples that were taken during steady operations. Coke breeze was fed to the gasifier for most of TC11. The samples that were taken during coal operation are noted on Figure 3.4-6. The addition of coke breeze did not seem to influence the amount of carbon in the standpipe solids as it did in previous test runs. The low standpipe carbon at hour 141 seems to contradict the conclusion that the increase in coal rates at hour 132 increased the recirculating carbon. However, the same effect would have been seen if the solids circulation rate increased at hour 132 with the same amount of carbon in the recirculating solids.

The standpipe solids sulfur level in the solids was very low, with all values essentially zero (except for one 0.2-percent CaS analysis), for all of the samples taken during coal feed. The high standpipe temperatures and low syngas H_2S concentrations would tend to favor low CaS formation in the standpipe. This low level indicates that all of the sulfur removed from the synthesis gas is removed via the PCD solids and is not accumulating in the gasifier or leaving with the gasifier solids.

The standpipe $CaCO_3$ was 0.0 for most of TC11, indicating that there was no inorganic carbon in the gasifier solids. The standpipe calcium was about 100 percent calcined to CaO. Since there was no sorbent calcium, all the standpipe solids calcium came from the fuel calcium.

The MgO, Fe_2O_3, and other inerts contents are not plotted on Figure 3.4-5, but they follow the same trends as the CaO and Al_2O_3, that is, they are accumulating in the gasifier as the start-up sand is replaced by feed solids. The standpipe analyses consistency was quite good with a low bias as the total sum of the compounds in Table 3.4-2 averaged 99.3 percent with a standard deviation of only 0.3 percent.

Table 3.4-3 gives the results from the loopseal downcomer analyses. The loopseal downcomer solids are solids that recirculate through the mixing zone, riser, disengager, and loopseal downcomer and change slowly with time, since a small amount of solids are taken out of the gasifier via FD0510. The loopseal downcomer solids are a portion of the standpipe solids and are the solids that are not collected by the disengager, but are collected by the cyclone. The standpipe solids consist of solids collected by both the disengager and the cyclone.

On startup, the loopseal downcomer solids mainly contained sand at 96.7-percent SiO_2. The loopseal downcomer did not contain pure sand at zero run-time hours since there were several periods of coal and coke breeze operation prior to the starting of the clock for the test, which diluted the loopseal downcomer sand.

As the run progressed, the start-up sand was slowly replaced by CaO, Al_2O_3, Fe_2O_3, and other inerts. This is shown in Figure 3.4-7 which plots loopseal downcomer SiO_2, CaO, and Al_2O_3 with run time. The SiO_2 content slowly decreased and both the Al_2O_3 and the CaO increased to replace the SiO_2. Sand was added at hour 61, and slightly increased the SiO_2 content. The

loopseal downcomer did not reach constant conditions at the end of TC11 as the loopseal downcomer solids SiO_2 was decreasing for the last four samples analyzed.

The loopseal downcomer organic carbon content is plotted in Figure 3.4-8. The average loopseal downcomer organic carbon content during coal operation was 0.9 percent and varied between 0.1- and 3.2-percent carbon. The loopseal downcomer average carbon was higher than that of the average standpipe carbon.

The loopseal downcomer solids sulfur level in the solids was very low, with all values less than 0.2-percent CaS, slightly higher than the standpipe CaS. The loopseal downcomer $CaCO_3$ was 0.0 for all of the TC11 samples (except for one at 0.1-percent $CaCO_3$), indicating that there was no inorganic carbon in the loopseal downcomer solids. The loopseal downcomer calcium was 100-percent calcined to CaO. Since there was no sorbent calcium, all the loopseal downcomer solids calcium came from the fuel calcium. The volatile loopseal downcomer compounds (sulfur and carbon) were all very low in the loopseal downcomer solids and were slightly higher than the sulfur and carbon in the standpipe solids.

The MgO, Fe_2O_3, and other inerts contents are not plotted on Figure 3.4-7, but they follow the same trends as the CaO and Al_2O_3, that is, they are accumulating in the gasifier as the start-up sand is replaced by feed solids. The loopseal downcomer analyses consistency was good with a low bias as the total sum of the compounds in Table 3.4-2 averaged 98.8 percent with a standard deviation of 0.6 percent.

3.4.5 Gasifier Products Solids Analysis

Figure 3.4-9 plots the organic carbon (total carbon minus CO_2 carbon) for the PCD solids sampled from FD0520. The organic carbon content for every PCD fines sample analyzed is also given on Table 3.4-4. Since FD0520 ran continuously during TC11, solid samples were taken often, with a goal of one sample every 4 hours. Of the TC11 PCD solids that were sampled, 35 percent were analyzed. In situ PCD inlet particulate solids recovered were also analyzed.

The in situ carbon contents are compared with the FD0520 solids on Figure 3.4-9. The in situ solids organic carbon analyses were in agreement with the FD0520 solids for five of the six in situ solid samples. The only in situ sample not in agreement was at hour 171 during air-blown operation. There is no apparent reason why this sample should be in such disagreement with the FD0520 samples. Three composite FD0520 samples were also analyzed on April 16, 2003, and are plotted at hour 149. The organic carbon for these composite samples agreed well with both the FD0520 and in situ samples organic carbon.

The TC06, TC07, and TC10 in situ and FD0520 solids organic carbon compared very well for most of the solids (see Figures 4.4-7 in the TC06 and TC07 reports). The TC08 in situ and FD0520 solids organic carbon compared well for only half of the in situ samples (see Figure 4.4-6 in the TC08 report). The in situ organic carbon was higher than the FD0520 organic carbon in the solids that did not agree well. In TC09 all of the in situ organic carbons were higher than the FD0520 PCD fines organic carbons by 10 to 40 percent, a significant difference.

Small amounts of coke breeze were added to the gasifier through FD0220 from hours 70 to 124 and hours 141 and 201. There does not appear to be any effect of coke breeze addition on FD0520 samples organic carbon.

The PCD fines organic carbon was nearly constant at about 12 percent for the first 100 hours of TC11. This low organic carbon indicates excellent carbon conversion. Between 100 and 150 hours, the PCD fines organic carbon decreased down to 2 percent and then increased back up to 10-percent organic carbon. The organic carbon was increasing once the gasifier was placed in oxygen-blown mode, deceasing the carbon conversion. Carbon conversions will be discussed in Section 3.5.5.

Figure 3.4-10 and Table 3.4-4 gives the amounts of SiO_2 and CaO in the PCD solids as sampled from FD0520. Also plotted on Figure 3.4-10 are the in situ solids concentrations for SiO_2 and CaO. All six in situ CaO concentrations showed good agreement with the FD0520 solids. The CaO concentrations were constant at around 10 to 15 percent until oxygen-blown mode began at hour 193 and the CaO dropped from 14 to 5 percent. In TC06, TC07 TC08, TC09, and TC10 the in situ and FD0520 CaO analyses compared very well, as they did in TC11. The TC11 FD0520 solids CaO concentrations were about half of the PRB runs TC06 and TC07 concentrations due to the lack of sorbent feed in TC11, as limestone sorbent feed was used in TC06 and TC07. The CaO concentrations in TC11 were about twice the CaO concentrations in TC09 due to the lower calcium in the TC09 fuel (Hiawatha bituminous - 1.3-percent calcium) when compared to Falkirk lignite (1.82-percent calcium). The TC08 and TC10 tests (PRB with no limestone operation) PCD fines calcium were equivalent to the TC11 Falkirk lignite PCD fines CaO despite a lower PRB calcium (0.87 percent) than the Falkirk lignite (1.82 percent).

Four of the six TC11 SiO_2 in situ solids analyses compared well with the FD0520 SiO_2 samples. During TC06, TC07, and TC10, there were periods of good agreement and periods of poor agreement between in situ and FD0520 SiO_2 analyses. During the first half of TC06 and TC08 and all of TC07, the in situ and FD0520 SiO_2 analyses compared very well. During the last half of TC06 and TC09, all of TC08 and the first 75 hours of TC10, the in situ SiO_2 were lower than the FD0520 analyses.

The SiO_2 concentrations were between 39 and 48 percent for the first 185 hours of TC11. During the oxygen-blown testing, the SiO_2 decreased from 36 to 31 percent.

Figure 3.4-11 and Table 3.4-4 give the concentrations of $CaCO_3$ and CaS in the PCD solids as sampled from FD0520. Also plotted on Figure 3.4-11 are the in situ solids concentrations for $CaCO_3$ and CaS.

All of the in situ samples $CaCO_3$ concentrations agreed well with FD0520 solids $CaCO_3$. In TC06 and TC10, the in situ $CaCO_3$ concentrations were consistently higher than the FD0520 $CaCO_3$ concentrations, while in TC07 the in situ $CaCO_3$ concentrations were either equal to or slightly higher than the FD0520 $CaCO_3$ concentrations. In TC08 the in situ $CaCO_3$ agreed well with the FD0520 $CaCO_3$ until 100 hours, when the in situ $CaCO_3$ was higher than the FD0520 $CaCO_3$ by 1 to 2 percent. The TC09 in situ $CaCO_3$ concentrations were usually higher than the FD0520 $CaCO_3$ concentrations.

The TC11 PCD fines $CaCO_3$ concentrations (1- to 5-percent $CaCO_3$) were lower than the PRB tests with limestone (TC06 and TC07 at 2- to 10-percent $CaCO_3$) and about the same as the PRB test without limestone (TC08 at 1- to 4-percent $CaCO_3$) and the last 250 hours of the Hiawatha bituminous tests without limestone (TC09 – 1.5- to 3.0-percent $CaCO_3$).

Five of the six in situ CaS concentrations agreed well with the FD0520 solids CaS concentrations. This data is consistent with TC06, TC07, TC08, and TC08 data, where all of the in situ solids CaS analyses agreed with the FD0520 CaS analyses. The TC09 (Hiawatha bituminous) in situ CaS concentrations were higher than the FD0520 CaS concentrations from 0.5 to 1.0 percent. The FD0520 CaS varied from 0.3 to 3.8 percent during TC11 indicating some sulfur removal by the PCD fines solids. The mode of operation did not seem to affect the amount of sulfur in the PCD fines.

The PCD fines calcination is defined as:

$$\%\,\text{Calcination} = \frac{\text{M}\%\,\text{CaO}}{\text{M}\%\,\text{CaO} + \text{M}\%\,\text{CaCO}_3} \qquad (1)$$

The PCD fines calcination is plotted on Figure 3.4-12. The PCD fines calcination was fairly constant at 80 to 90 percent for the first 185 hours of TC11. During the oxygen-blown mode operation (last 16 hours), the calcination was 70 to 80 percent. The lower calcination during oxygen-blown testing might be the result of higher syngas CO_2 concentrations which would tend to form more $CaCO_3$ and thus decrease calcination. All previous runs with both PRB and Hiawatha bituminous with and without sorbent all had 80 to 90 percent calcination, consistent with the air- and enhanced-air-blown TC11 Falkirk lignite calcinations.

The calcium sulfation is defined as:

$$\%\text{Sulfation} = \frac{\text{M}\%\text{CaS}}{\text{M}\%\text{CaO} + \text{M}\%\text{CaCO}_3 + \text{M}\%\text{CaS}} \qquad (2)$$

The PCD fines sulfation is plotted on Figure 3.4-12 with the PCD fines calcination. The PCD fines sulfation started TC11 at about 10 percent and then decreased to nearly zero at hour 95. The calcium sulfation then increased slowly to 15 percent at hour 153, just before the first enhanced-air mode. The sulfation then decreased to about 5 percent until hour 185. The sulfation then increased to 20 percent during the oxygen-blown mode operation. All previous runs with both PRB and Hiawatha bituminous with and without sorbent had 0- to 10-percent sulfations, consistent with the air- and enhanced-air TC11 Falkirk lignite sulfations.

Table 3.4-4 gives the PCD fines compositions for the samples collected in FD0520. The consistency is not as good as the standpipe solids in that the totals usually add up to between 97 and 104 percent. The average of the totals was 98.9 percent with a standard deviation of 1.7, indicating a very slight negative bias. Additional components on Table 3.4-4, other than those plotted on Figures 3.4-6, 3.4-7, and 3.4-8, are MgO, FeO, and Al_2O_3. The MgO concentrations were between 2.3 and 4.2 percent. The Al_2O_3 concentrations were between 10 and 14 percent with the last sample during oxygen-blown operation at a lower Al_2O_3 concentration. Also given in Table 3.4-4 are the higher heating value (HHV), lower heating value (LHV), and organic

carbon for the PCD fines. As expected, the trend of heating values follows the carbon content of the PCD fines. Note the very low heating values taken at hours 113, 125, and 141 samples.

No FD0510 solid samples were analyzed during TC11 because the standpipe samples should give a more accurate view of the circulating solids composition.

3.4.6 Gasifier Solids Analysis Comparison

With the addition of the loopseal downcomer solids sampling system, it is now possible to sample solids at three different points in the Transport Gasifier. By comparing the various species concentrations with run time, the operation of the Transport Gasifier may be better understood for different feeds and operating conditions.

A comparison of the total organic carbon contents for the standpipe, loopseal downcomer, and spent fines samples is shown in Figure 3.4-13. The PCD solids contained the highest amounts of organic carbon at about 10 percent, with lower amounts in the loopseal downcomer solids and the standpipe solids. The standpipe and loopseal downcomer solids organic carbon were nearly indistinguishable until the oxygen-blown operation at the end of TC11, when the higher PCD solids organic carbon concentration seemed to increase the loopseal downcomer carbon content. The TC11 loopseal downcomer carbon content is not consistent with the TC10 (PRB coal) carbon content. During TC10, the loopseal downcomer carbon content was significantly higher than the standpipe carbon content and often was nearly as high as the PCD fines carbon content. (See Figure 3.4-13, TC10 report.) TC11 seems to indicate that the loopseal downcomer solids are very similar to the standpipe solids, while TC10 data seems to indicate that the loopseal downcomer solids are made up of a mixture of the standpipe and PCD fines. Further testing will be required to determine whether this difference in loopseal downcomer carbon is a result of the different coals tested, different modes of operation, feed fuel size, or mill operating conditions. (TC10 was nearly all oxygen-blown, while TC11 was nearly all air-blown.)

Figure 3.4-14 compares the silica (SiO_2) content between the standpipe, loopseal downcomer, and PCD solids samples. Consistent with the relative carbon contents discussed above, the standpipe solids have the highest SiO_2 content, and the PCD solids contain the lowest SiO_2 content with the loopseal downcomer solids usually containing silica contents between that of the PCD solids and that of the standpipe solids. Like the TC11 organic carbon content, the standpipe and loopseal downcomer silica concentration are quite close to each other until the oxygen-blown mode. The loopseal downcomer and standpipe silica concentrations also appear to be asymptotically approaching the steady-state value of the PCD fines, which might indicate that the steady-state standpipe solids concentration is the PCD fines concentration. The gasifier solids silica concentration with time was quite different for TC10 and TC11. In TC10, the loopseal downcomer and standpipe silica were consistently higher than the PCD fines silica and did not asymptotically approach the PCD fines silica. The loopseal downcomer silica was also always lower than the standpipe silica. This difference possibly may have been due to the several large sand additions during TC10, while there were minimal sand additions during TC11.

Figure 3.4-15 compares the calcium concentration between the standpipe, loopseal downcomer, and PCD solids samples. Note that the calcium is distributed between CaO, $CaCO_3$, and CaS. Consistent with the relative carbon and silica contents discussed above, the PCD solids have the

highest calcium content, and the standpipe solids contain the lowest calcium content with the loopseal downcomer solids usually containing calcium contents between that of the PCD solids and that of the standpipe solids. In the standpipe and loopseal downcomer, the start-up sand (silica) is slowly being replaced with calcium from the coal ash. Like the TC11 organic carbon and silica, the standpipe and loopseal downcomer calcium concentrations are quite close to each other until oxygen-blown mode. The loopseal downcomer and standpipe calcium concentrations also appear to be asymptotically approaching the steady-state value of the PCD fines, which might indicate that the steady-state standpipe calcium solids concentration is the PCD fines calcium concentration. The gasifier solids calcium concentration profile with time was slightly different for TC10 and TC11. In TC10 the loopseal downcomer and standpipe calcium concentrations were nearly the same for all of TC10. The three calcium contents were about equal after only 100 hours of TC10 and stayed nearly equal within the variability of the data.

3.4.7 Feeds Particle Size

The TC11 SMD and mass mean diameter (D_{50}) particle sizes of the coal sampled from FD0210 are plotted on Figure 3.4-16. The Falkirk lignite coal SMD particle size decreased from 250 to 150 μ during the first 50 hours of TC11. After hour 50, the SMD was fairly constant during TC11 with values between 140 and 170 μ. The Falkirk lignite coal D_{50} followed the same trends as the TC11 SMD, decreasing from 370 to 200 μ in the first 50 hours of TC11 and afterwards varying between 250 to 320 μ. The D_{50} varied from 60 to 150 μ larger than the SMD. The leveling out of the coal particle size was probably due to the improvements in the coal mill operation as more experience was gained in grinding Falkirk lignite. Consistency in coal feed size has not been identified as a source of coal feeder problems. The TC11 D_{50} data was consistent with previous tests TC06 to TC09. TC10 had a slightly higher D_{50} particle size than TC11.

In past testing, a high fines content in the feed coal resulted in an increased number of coal feeder outages due to the packing of coal fines in the coal feed system lock vessel. A measure of the amount of fines in the coal is the percent of the smallest size fraction. To show the level of fines in the coal feed, the percent of ground coal less than 45 μ is plotted in Figure 3.5-17. During TC11, the percent coal fines increased from 5 to about 17 percent during the first 50 hours of TC11. The percent fines were then between 13 and 15 percent up to hour 125. After hour 125, the percent fines less than 45 μ was between 15 and 22 percent which may have increased the difficulty in feeding coal. Both periods in enhanced air modes had high fines. The fines were below 15 percent for the oxygen-blown mode. The high coal fines may have contributed to the coal feeder trips during the last 75 hours of TC11. However, the major cause of coal feed trips during TC11 was the high coal feed moisture.

3.4.8 Gasifier Solids Particle Size

The TC11 standpipe solids particle sizes are given in Figure 3.4-18. The particle size of the solids increased as the start-up sand is replaced by coal ash. When the gasifier lost solids during a gasifier excursion, the bed material was replaced by 122 μ D_{50} sand, which had a smaller particle size. The SMD of the gasifier solids slowly increased from 160 μ at hour 14 to 180 μ at hour 57. The standpipe particle size decreases as expected due to the sand addition at hour 61 during the outage. After the sand addition, the standpipe SMD decreased slightly and then increased up to 200 μ at hour 137. The standpipe particle size remained constant at about 200 μ until oxygen-blown operation at hour 193, when the SMD increased to 226 μ.

The standpipe solids reached a steady-state particle size of about 200 μ for air-blown operation. Due to the short duration of TC11 oxygen-blown mode, there was insufficient run time to determine the oxygen-blown mode steady-state particle size. The TC06 SMD steady-state particle size was about 160 μ (see TC06 report Figure 4.4-14) and the steady-state TC07 SMD was about 170 μ (see TC07 report Figure 4.4-14). The TC08 SMD steady-state particle size was about 160 μ during the initial air-blown testing. The TC08 oxygen-blown standpipe solid's particle size were generally increasing during oxygen-blown testing and reached as high as 250 μ SMD. The TC09 (Hiawatha bituminous) air-blown steady-state standpipe SMD was about 180 μ. During TC09 oxygen-blown mode, the standpipe SMD was still increasing above 220 μ when the run was terminated. TC10 oxygen-blown standpipe solids SMD increased several times until outages; subsequent sand additions then lowered the standpipe particle sizes TC10 never attained steady-state particle sizes with several SMD particle sizes over 250 μ. The Falkirk lignite standpipe solids had a higher steady-state standpipe particle size than for the air-blown PRB and air-blown Hiawatha bituminous testing.

The TC11 mass mean diameter (D_{50}) was about 20 μ less than the TC11 SMD and followed the same trend as the SMD.

The TC11 loopseal downcomer solids particle sizes are given in Figure 4.3-19. Only one TC11 loopseal downcomer solid sample was analyzed for particle size for the first 120 hours of TC11 due to insufficient amounts of solids sampled. The TC11 loopseal downcomer solid samples particle sizes fell on the dividing line between performing a Microtrac particle size analysis or a sieve particle size analysis. The dividing line seemed to be 140 μ SMD, where above 140 μ SMD, a sieve analysis was done and below 140 μ SMD, a Microtrac particle size analysis was done. The loopseal downcomer solids increased from 120 μ at hour 120 to 175 μ SMD at hour 140. After hour 140, the loopseal downcomer solids particle size decreased during the enhanced-air and oxygen-blown operation. The loopseal downcomer solids decreased down to 52 μ at the end of TC11. For the nine loopseal downcomer particle sizes:

- the SMD is smaller than the MMD (below 140 μ) for three points.
- the SMD is larger than the MMD (above 157 SMD) for three points.
- the SMD is equal to the MMD (between 142 and 156 SMD) for three points.

This is a result of the loopseal downcomer solids being a mixture of sand and coal ash which resulted in a bimodal particle size distribution.

TC10 loopseal downcomer particle sizes cycled between 20 and 150 μ and appeared to be either like PCD fines or the standpipe solids. Several of the TC10 particle sizes decreased down to 20 μ which seemed to correspond to most periods of sand addition. It would appear that the TC11 decrease in particle size after hour 160 was quite consistent with the TC10 decreases in particle size. For all of the TC10 SMD less than about 120, the SMD was less than the MMD, consistent with TC11. Most, but not all, of the larger TC10 particle sizes follow the same trend as in TC11.

Figure 3.4-20 plots the SMD and D_{50} for the PCD solids sampled from FD0520 and the six in situ solids recovered during the PCD inlet sampling. None of the six in situ solids particle size agreed with the particle size of the solids collected by FD0520, although all were within 5 μ. In previous tests, TC06 to TC09, the FD0520 PCD fines particle size usually agreed with the in situ PCD inlet particle size. In TC10, the in situ and FD0520 solids particle sizes agreed with each other for the first half of TC10 and then were in poorer agreement for the last half of TC10.

The PCD fines SMD was fairly constant at between 10 and 15 μ for TC11 during all three modes of operation. There were a few SMD above 15 and below 10 μ. Previous testing with PRB and Hiawatha indicate PCD fines in about the same range as in TC11. PRB tests TC08 and TC10 had a few finer particle sizes (under 10 μ SMD), while the Hiawatha bituminous test TC09 had a few more courser particle sizes (over 20 μ SMD).

The D_{50} was about 5 μ larger than the SMD and follows the same trends as the SMD particle sizes. The in situ PCD inlet D_{50} solids particle size also showed the same trend of slight disagreement with the FD0520 solids D_{50} particle size as the SMD particles sizes.

3.4.9 Particle Size Comparison

Figure 3.4-21 plots all the solids SMD particle sizes. The Transport Gasifier is fed with an average of 150 μ SMD coal and produces an average of 185 μ SMD gasifier solids and 12 μ SMD PCD fines. It is surprising that the SMD of the standpipe was higher than the coal feed for the last half of TC11. The decrease in loopseal downcomer particles sizes during enhanced-air and oxygen-blown mode is also clear.

The D_{50} diameters were larger than the SMD for the FD210 (coal), and FD0520 (PCD fines), while the TC11 SMD particle sizes are larger than the D_{50} particle sizes for the standpipe solids. This trend was also seen in TC06 to TC10. The standpipe solids have a non-Gaussian distribution (bimodal) which probably caused the standpipe SMD to be larger than the standpipe D_{50}. The loopseal downcomer solid samples particle sizes had either the SMD larger than the D_{50}, or the D_{50} larger than the SMD, as was also seen in TC10.

3.4.10 Standpipe and PCD Fines Bulk Densities

The TC11 standpipe, loopseal downcomer, and PCD fines bulk densities are given in Figure 3.4-22. The standpipe bulk density of the solids decreased slowly as the start-up sand was replaced by ash after both the original startup and the sand additions at hour 61. The standpipe solids bulk density decreased from 90 to 75 lb/ft^3 in about 150 hours after startup. The standpipe solids bulk density then increased to 80 lb/ft^3 and decreased down to 75 lb/ft^3 during the oxygen-blown mode. TC06 through TC10 standpipe solids bulk density behaved as did the TC11 standpipe bulk density, at 90 lb/ft^3 just after sand addition and then decreasing to about 80 lb/ft^3. At the end of TC10, however, the standpipe solids bulk density increased to 100 lb/ft^3.

The loopseal downcomer solids bulk densities were identical to the standpipe densities from the first loopseal downcomer sample at hour 46 until hour 161 during the first enhanced-air mode. The final two loopseal downcomer solids bulk densities were slightly lower than the standpipe bulk densities. Not all of the loopseal downcomer sample bulk densities could be measured because there were insufficient amounts of solids sampled. The TC10 loopseal downcomer bulk densities varied between the standpipe and the FD0520 PCD fines bulk densities.

The bulk densities for the FD0520 PCD solids samples from both FD0520 and the in situ PCD inlet are plotted on Figure 3.4-22. The FD0520 and in situ solid samples bulk densities agreed very well with each other. The bulk densities of the FD0520 PCD fines were nearly constant, varying from 30 to 40 lb/ft^3 from the start of TC11 to the beginning of the oxygen-blown mode at hour 193. During the oxygen-blown mode, the PCD solids bulk density decreased down to 25 lb/ft^3.

TC06, PCD fines bulk densities were in the range of 20 to 30 lb/ft^3. TC07 and TC08 bulk densities were constant at 22 lb/ft^3 with periods of wide variation in bulk density up to 60 lb/ft^3. TC09 FD0520 solid samples bulk densities slowly decreased during the run from 40 to 20 lb/ft^3. There were wide variations in the TC09 FD0520 bulk densities. The TC10 bulk densities were fairly constant usually between 15 and 40 lb/ft^3. The TC11 bulk densities were consistent with previous gasification tests.

In TC06, the in situ PCD inlet solids bulk density slowly decreased from 20 to 15 lb/ft^3 and agreed with the FD0520 bulk density during the first 600 hours of TC06. TC07 in situ and FD0520 PCD fines bulk densities agreed. TC08 in situ PCD inlet bulk densities were lower than the FD0520 bulk densities. TC09 in situ PCD inlet bulk densities were fairly constant at between 15 and 20 lb/ft^3 and were lower than the TC09 bulk densities until the end of TC09. TC10 PCD in situ PCD fines bulk density were constant at about 18 lb/ft^3 and agreed well with the TC10 FD0520 solid samples bulk densities. TC11 in situ bulk densities varied between 25 and 40 lb/ft^3 and agreed well with the TC11 FD0520 PCD fines bulk densities.

Table 3.4-1 Coal Analyses[1]

	Falkirk Lignite	
	Value	Standard Deviation
Moisture, wt%	27.95	0.70
Carbon, wt%	42.53	0.59
Hydrogen,[2] wt%	2.73	0.10
Nitrogen, wt%	0.69	0.02
Oxygen, wt%	12.04	0.86
Sulfur, wt%	0.76	0.12
Ash, wt%	13.07	1.35
Volatiles, wt%	29.67	3.30
Fixed Carbon, wt%	29.08	3.97
Higher Heating Value, Btu/lb	6,973	105
Lower Heating Value, Btu/lb	6,719	108
CaO, wt %	1.82	0.10
SiO_2, wt %	5.17	0.86
Al_2O_3, wt %	1.62	0.15
MgO, wt %	0.48	0.01
Fe_2O_3, wt %	1.13	0.17
Ca/S, mole/mole	1.30	0.28
Fe/S, mole/mole	0.56	0.12

Notes:

1. All analyses are as sampled at FD0210.
2. Hydrogen in coal is reported separately from hydrogen in moisture.

Table 3.4-2 Standpipe Solids Analyses

Sample Number	Sample Date & Time	Sample Run Time Hours[2]	SiO_2 Wt. %	Al_2O_3 Wt. %	FeO Wt. %	Other Inerts[1] Wt. %	$CaCO_3$ Wt. %	CaS Wt. %	CaO Wt. %	MgO Wt. %	Organic Carbon Wt. %	Total Wt. %
AB10664	4/10/2003 18:00	14	85.5	4.3	3.1	2.3	0.0	0.1	3.0	0.9	0.4	99.5
AB10667	4/11/2003 18:00	38	78.8	5.1	4.7	3.4	0.0	0.2	5.2	1.4	0.3	99.2
AB10668	4/12/2003 18:00	57	77.4	5.5	5.3	3.3	0.0	0.1	5.7	1.5	0.6	99.3
AB10669	4/13/2003 10:00	73	75.2	6.8	5.5	3.9	0.0	0.1	6.0	1.7	0.7	99.9
AB10670	4/14/2003 2:00	89	73.6	7.8	5.7	4.3	0.0	0.0	6.0	1.8	0.1	99.3
AB10679	4/15/2003 10:00	121	70.1	8.5	6.5	4.8	0.0	0.0	7.0	2.1	0.2	99.2
AB10680	4/16/2003 6:00	141	63.7	9.6	7.6	5.8	0.0	0.0	9.4	2.7	0.1	98.9
AB10681	4/17/2003 6:00	165	60.7	10.4	8.4	6.1	0.1	0.1	9.9	2.9	0.6	99.2
AB10703	4/18/2003 10:00	193	59.2	10.6	8.7	6.2	0.0	0.0	10.5	3.1	0.5	98.9

Notes:

1. Other inerts consist of P_2O_5, Na_2O, K_2O, & TiO_2

2. Hours 14 to 165 were air blown; hour 193 was oxygen blown.

Table 3.4-3 Loopseal Downcomer Solids Analyses

Sample Number	Sample Date & Time	Sample Run Time Hours[2]	SiO_2 Wt. %	Al_2O_3 Wt. %	FeO Wt. %	Other Inerts[1] Wt. %	$CaCO_3$ Wt. %	CaS Wt. %	CaO Wt. %	MgO Wt. %	Organic Carbon Wt. %	Total Wt. %
AB12524	4/10/2003 18:00	14	83.8	4.3	3.5	2.3	0.0	0.1	3.3	1.0	0.8	99.1
AB12567	4/11/2003 18:00	38	79.9	4.9	4.6	3.3	0.0	0.1	5.3	1.4	0.1	99.5
AB12570	4/12/2003 18:00	57	72.5	6.7	5.6	3.8	0.1	0.2	6.2	1.7	1.6	98.2
AB12572	4/13/2003 10:00	73	73.7	6.8	5.5	4.0	0.0	0.1	6.4	1.8	0.7	99.2
AB12609	4/15/2003 10:00	121	68.4	9.0	6.8	5.1	0.0	0.1	7.5	2.2	0.1	99.0
AB12621	4/16/2003 6:00	141	62.2	10.3	7.7	6.0	0.0	0.2	9.8	2.7	0.3	99.1
AB12654	4/17/2003 6:00	165	56.1	12.2	8.7	6.4	0.1	0.1	11.1	3.1	0.8	98.6
AB12690	4/18/2003 10:00	193	49.6	13.2	8.9	6.5	0.0	0.0	12.8	3.5	3.2	97.7

Notes:

1. Other inerts consist of P_2O_5, Na_2O, K_2O, & TiO_2

2. Hours 14 to 165 were air blown; hour 193 was oxygen blown.

Table 3.4-4 PCD Fines Solids From FD0520 Analyses

Sample Number	Sample Date & Time	Sample Run Time Hours[2]	SiO_2 Wt. %	Al_2O_3 Wt. %	FeO Wt. %	Other Inerts[1] Wt. %	$CaCO_3$ Wt. %	CaS Wt. %	CaO Wt. %	MgO Wt. %	Organic C (C-CO_2) Wt. %	Total Wt. %	HHV Btu/lb.	LHV Btu/lb.
AB12527	4/10/2003 22:00	18	43.9	12.1	7.4	4.8	1.7	1.6	10.1	3.2	13.9	98.7	1,747	1,727
AB12529	4/11/2003 6:00	26	42.8	13.6	8.4	5.8	1.8	1.8	12.2	3.7	8.1	98.2	1,567	1,558
AB12574	4/11/2003 18:00	38	44.6	11.4	7.1	5.3	2.9	2.2	10.2	3.3	11.6	98.6	1,822	1,803
AB12577	4/12/2003 6:00	50	41.4	13.0	7.7	5.6	1.7	2.0	11.0	3.5	11.5	97.3	1,675	1,654
AB12580	4/12/2003 22:00	61	43.0	13.7	7.2	5.8	2.5	2.0	10.5	3.5	11.8	99.9	1,505	1,494
AB12588	4/14/2003 8:15	95	43.1	13.5	7.4	5.7	1.7	0.3	12.0	3.5	11.0	98.2	1,614	1,606
AB12599	4/15/2003 2:00	113	44.4	14.4	7.5	6.0	0.7	1.2	13.0	3.7	6.1	96.9	754	738
AB12610	4/15/2003 14:00	125	46.1	14.2	8.8	6.0	0.8	0.8	15.1	4.2	2.6	98.6	252	244
AB12627	4/15/2003 22:00	133	42.6	12.3	7.5	5.6	3.4	2.3	10.6	3.8	11.6	99.7	1,747	1,733
AB12632	4/16/2003 6:00	141	48.0	13.1	7.3	6.2	2.1	1.3	11.7	3.7	6.6	100.0	825	822
AB12655	4/16/2003 18:00	153	39.0	12.8	7.8	5.7	4.0	2.9	9.8	3.8	12.9	98.7	1,998	1,974
AB12657	4/17/2003 2:00	161	43.1	13.7	7.9	6.2	1.7	0.9	14.0	4.1	7.5	99.1	1,057	1,044
AB12678	4/17/2003 18:00	177	42.2	13.9	8.3	6.3	0.9	1.0	12.6	3.6	9.2	98.1	1,230	1,220
AB12680	4/18/2003 2:00	185	42.5	14.2	8.6	6.1	1.2	0.9	13.3	3.8	7.7	98.2	1,027	1,019
AB12692	4/18/2003 10:00	193	36.7	11.6	7.9	4.5	2.9	1.8	14.3	4.4	13.5	97.5	1,892	1,881
AB12693	4/18/2003 12:30	196	32.4	10.0	6.5	4.0	6.2	3.8	8.2	3.7	24.4	99.3	3,756	3,724
AB12700	4/18/2003 14:00	197	32.4	10.0	6.7	4.0	4.7	3.4	9.6	3.8	23.7	98.3	3,351	3,310
AB12701	4/18/2003 18:00	201	30.6	8.3	5.1	3.9	3.1	2.2	5.0	2.3	43.8	104.3	6,205	6,124

Notes:

1. Other inerts consist of P_2O_5, Na_2O, K_2O, & TiO_2.

2. Hours 18 to 177 were air blown; hour 185 was enhanced air, hours 193 to 201 were oxygen blown.

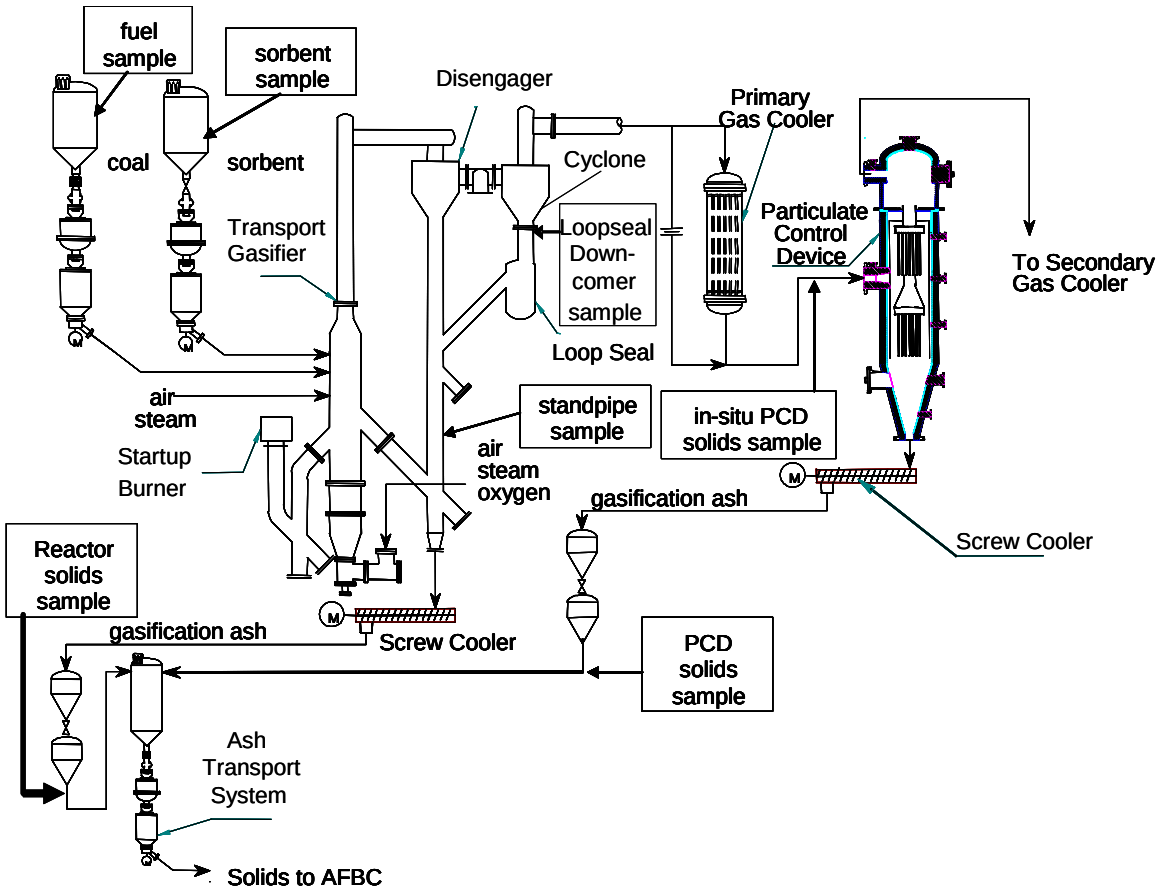

Figure 3.4-1 Solid Sample Locations

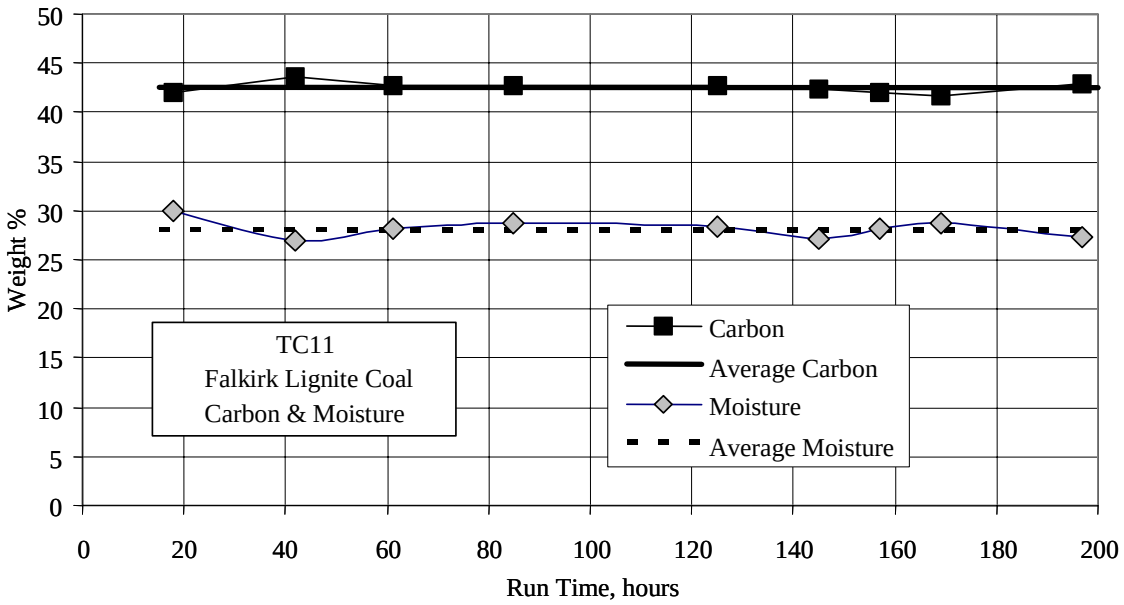

Figure 3.4-2 Coal Carbon and Moisture

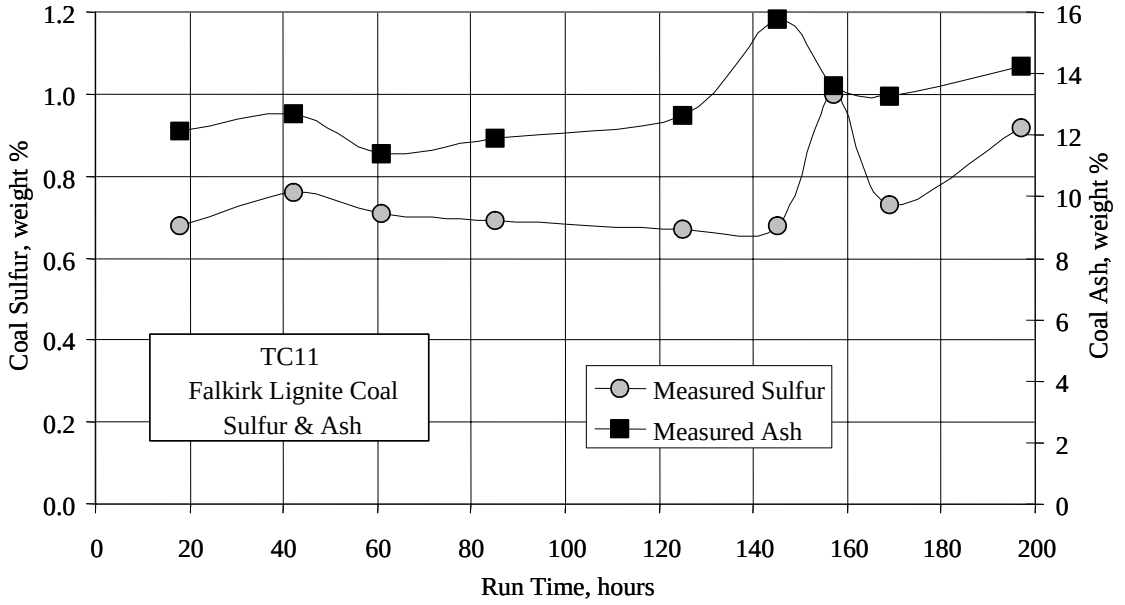

Figure 3.4-3 Coal Sulfur and Ash

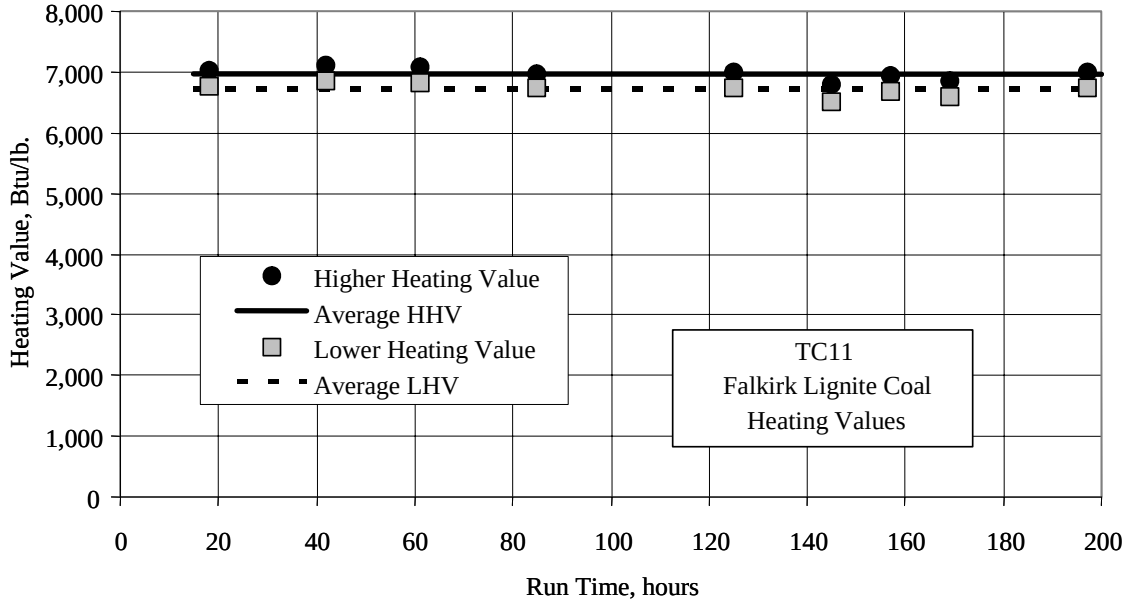

Figure 3.4-4 Coal Heating Value

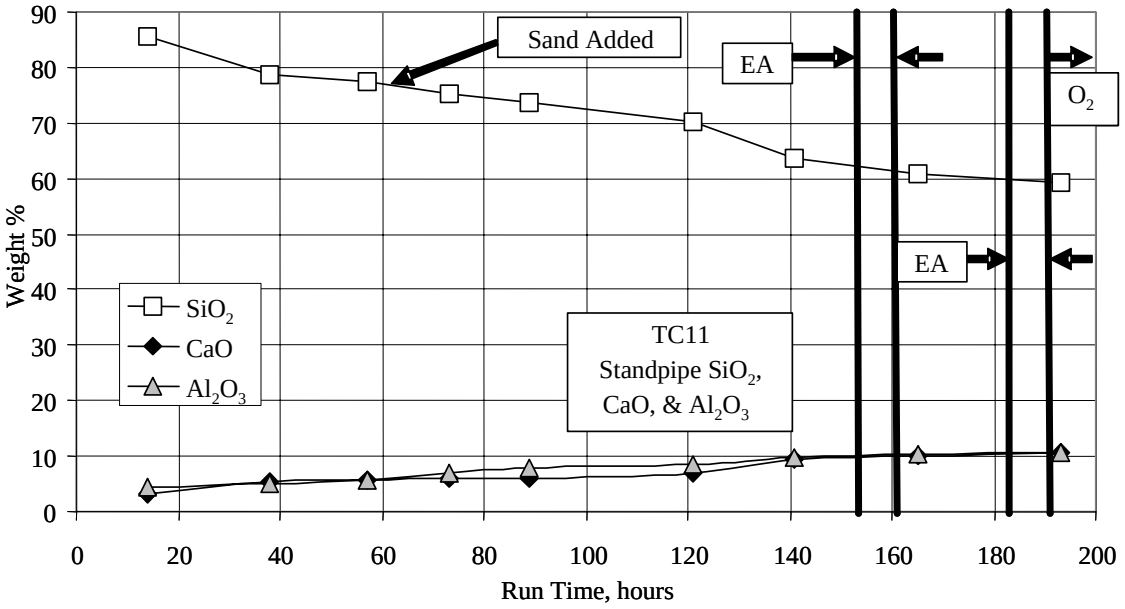

Figure 3.4-5 Standpipe SiO_2, CaO, and Al_2O_3

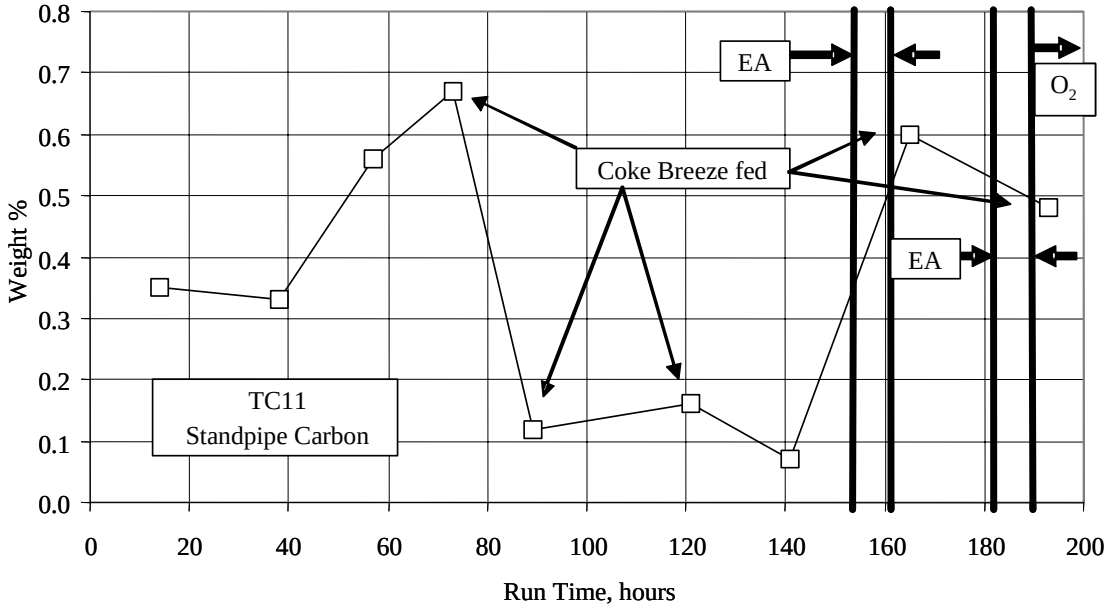

Figure 3.4-6 Standpipe Organic Carbon

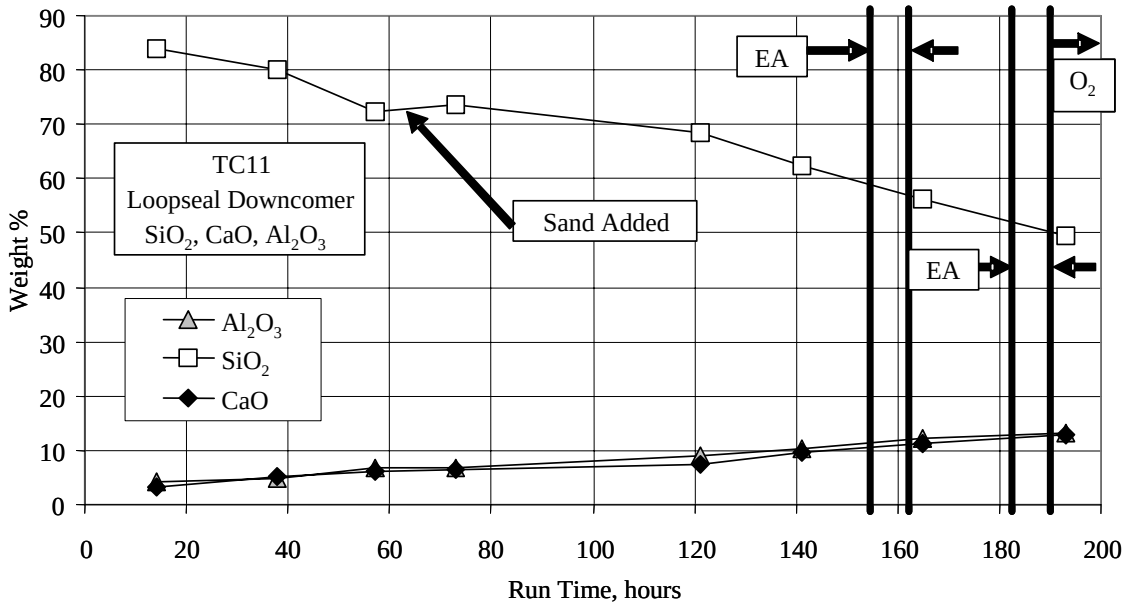

Figure 3.4-7 Loopseal Downcomer SiO_2, CaO, and Al_2O_3

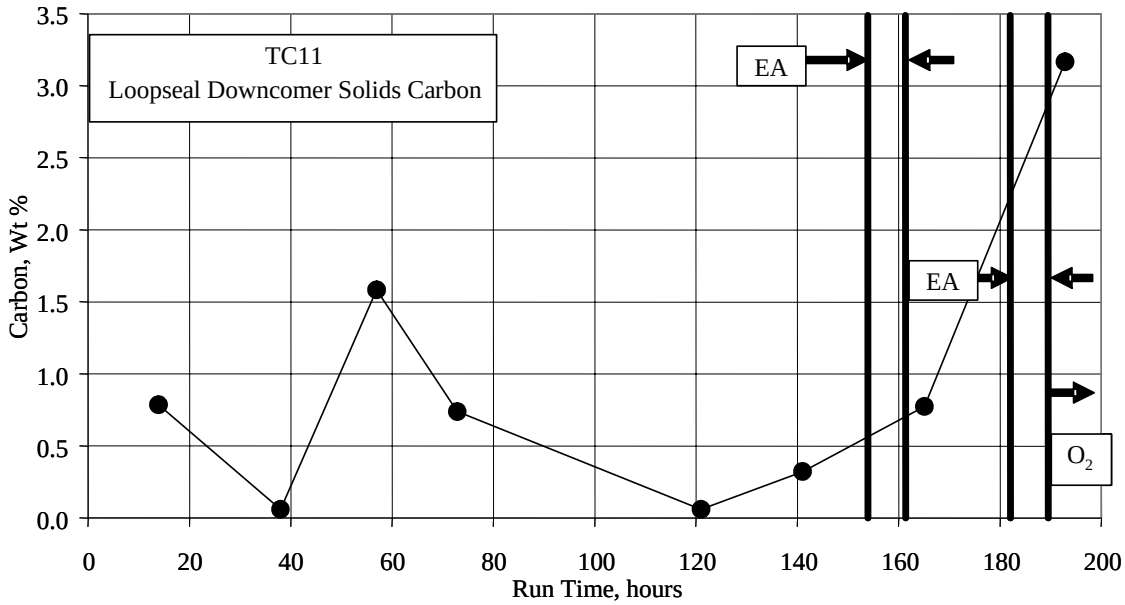

Figure 3.4-8 Loopseal Downcomer Organic Carbon

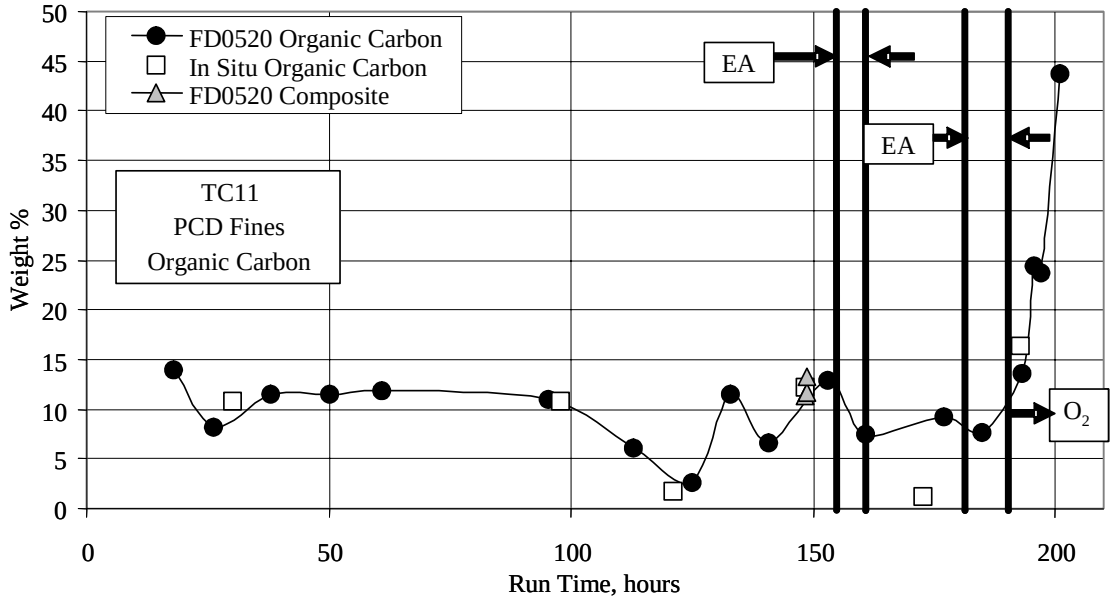

Figure 3.4-9 PCD Fines Organic Carbon

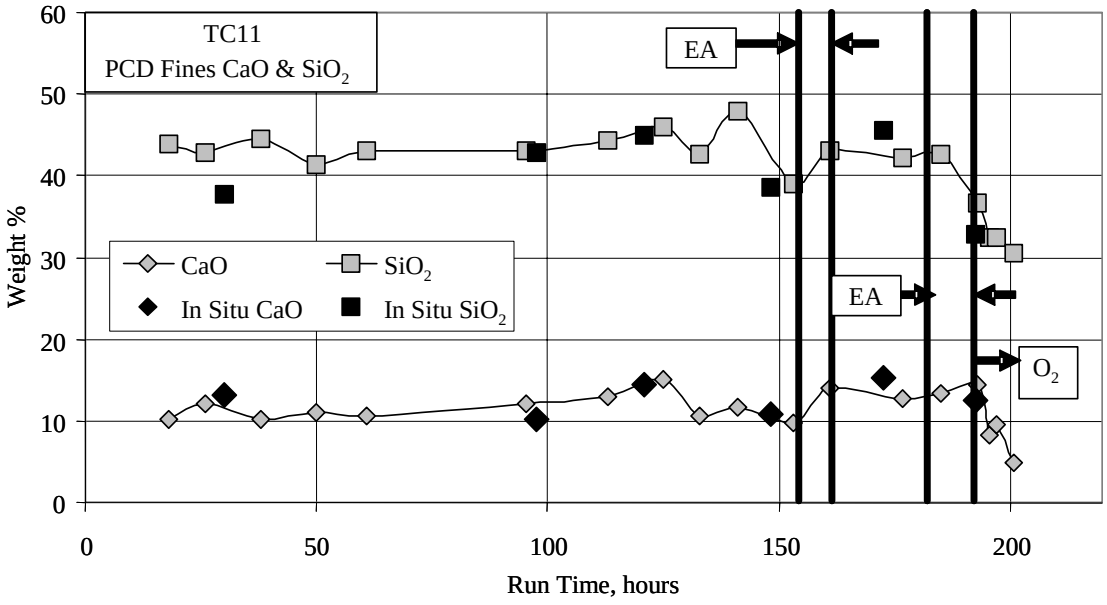

Figure 3.4-10 PCD Fines SiO_2 and CaO

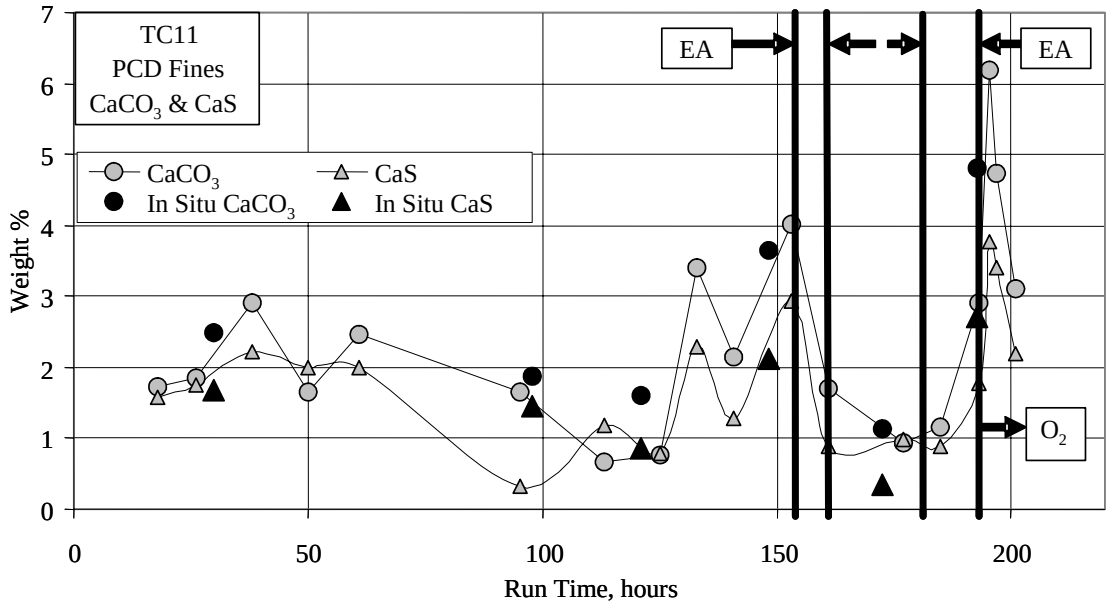

Figure 3.4-11 PCD Fines $CaCO_3$ and CaS

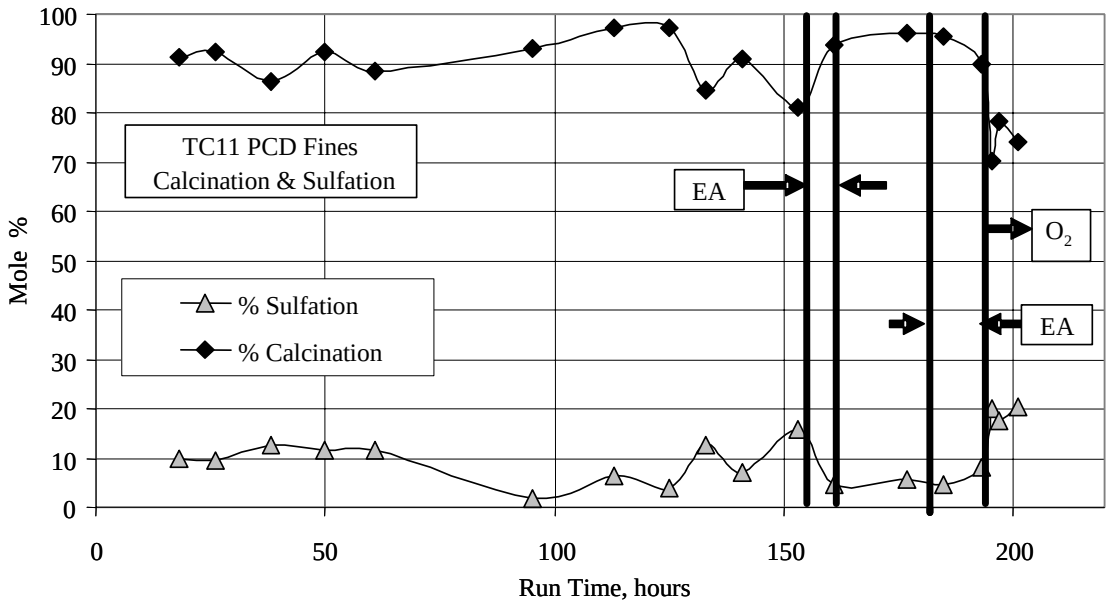

Figure 3.4-12 PCD Fines Calcination and Sulfation

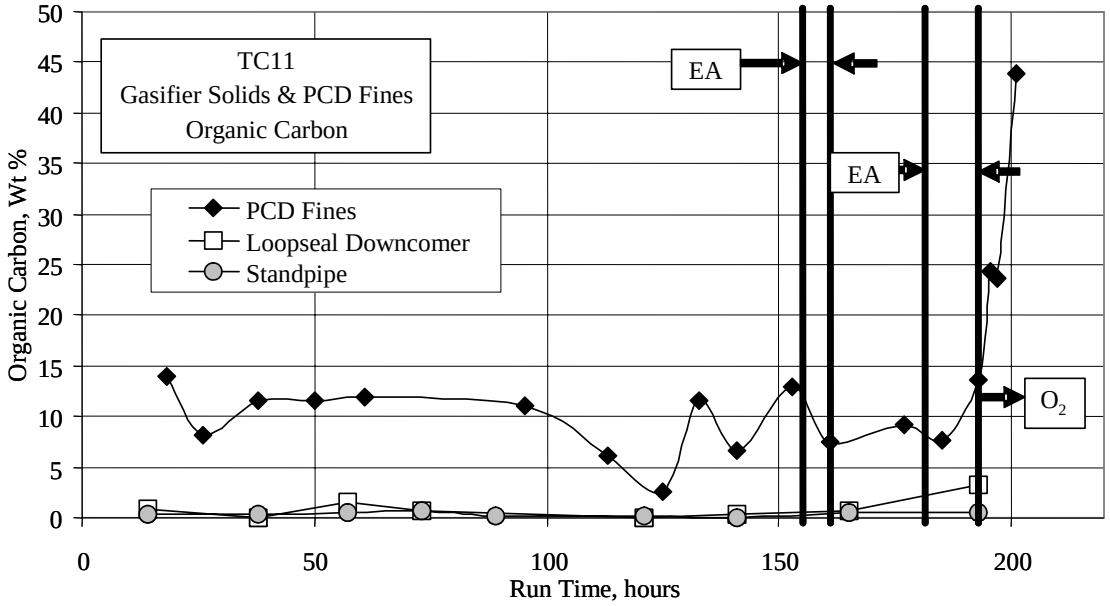

Figure 3.4-13 Gasifier Solids and PCD Fines Organic Carbon

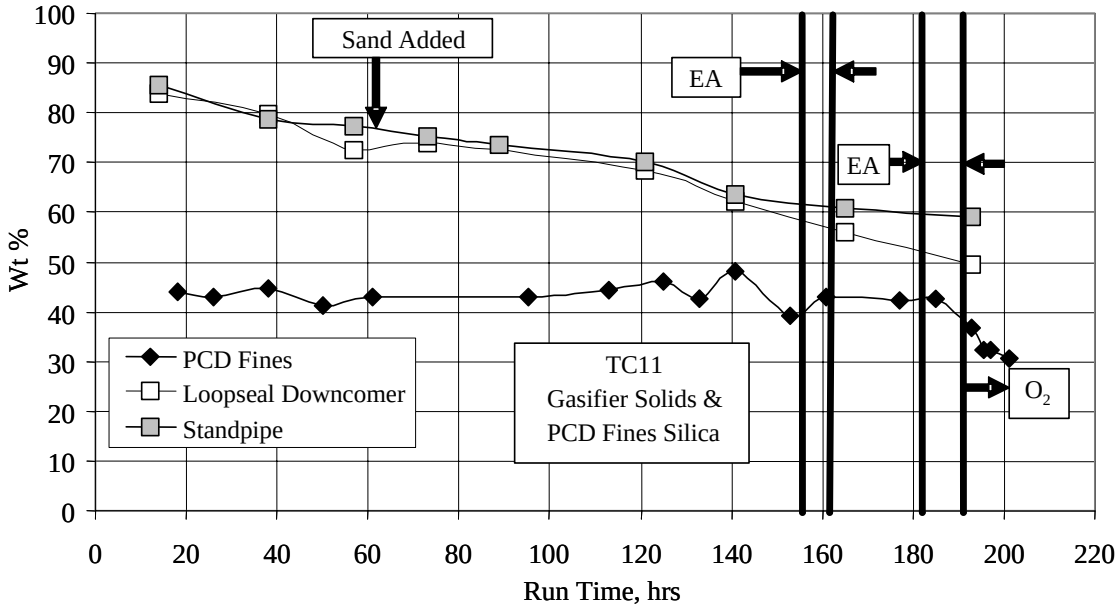

Figure 3.4-14 Gasifier Solids and PCD Fines Silica

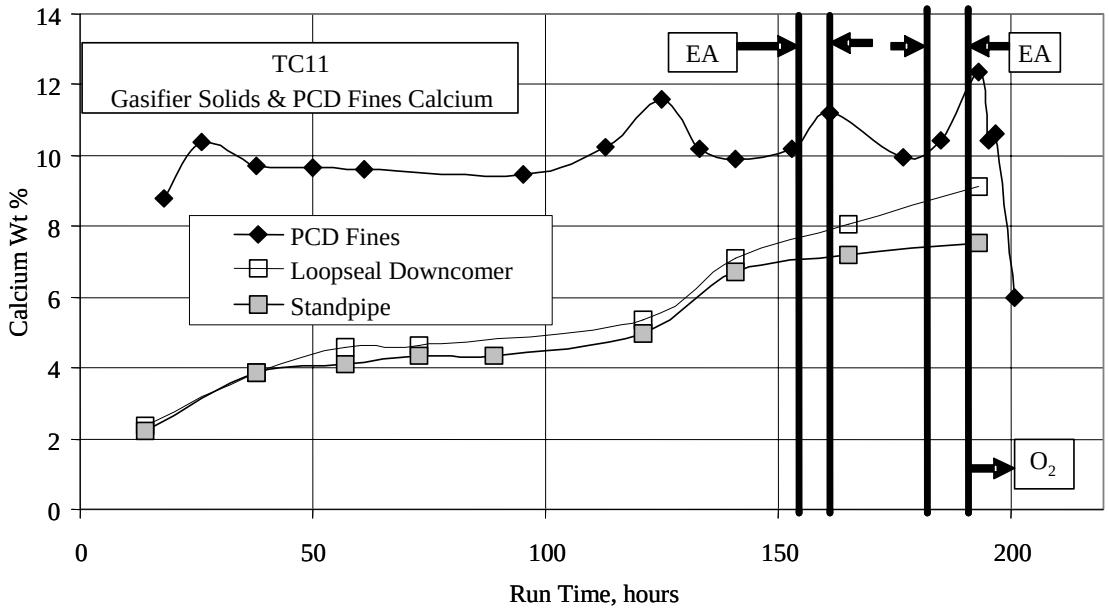

Figure 3.4-15 Gasifier Solids and PCD Fines Calcium

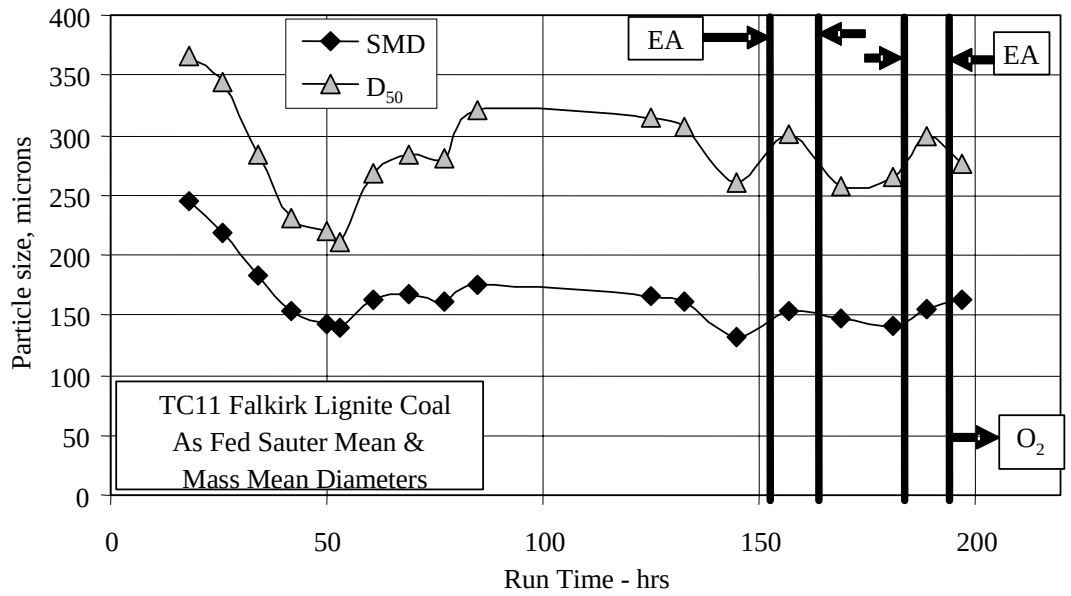

Figure 3.4-16 Coal Particle Size

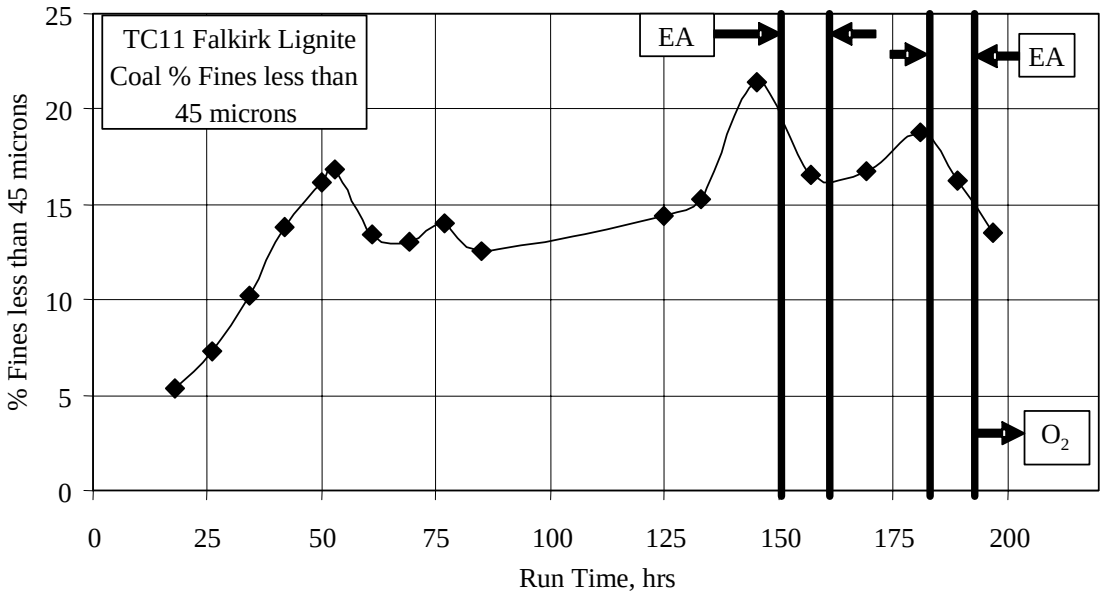

Figure 3.4-17 Percent Coal Fines

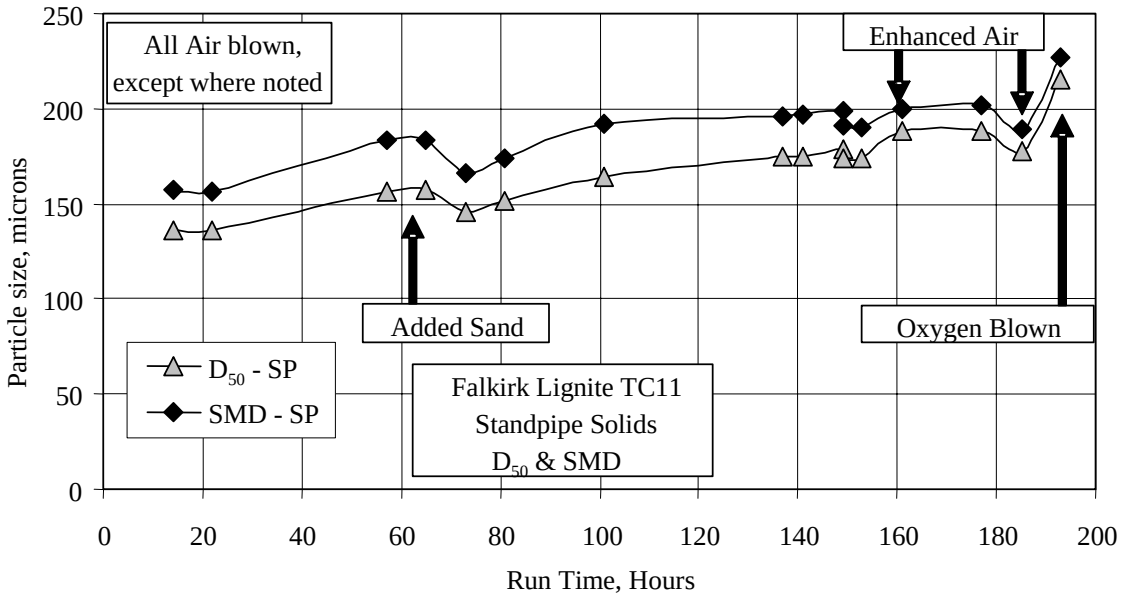

Figure 3.4-18 Standpipe Solids Particle Size

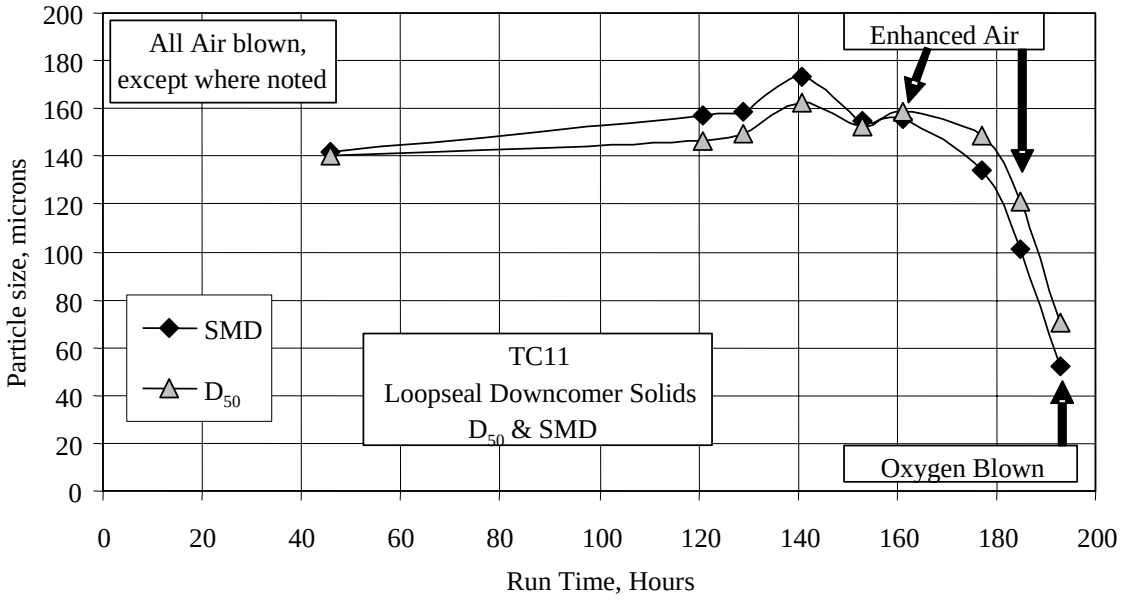

Figure 3.4-19 Loopseal Downcomer Particle Size

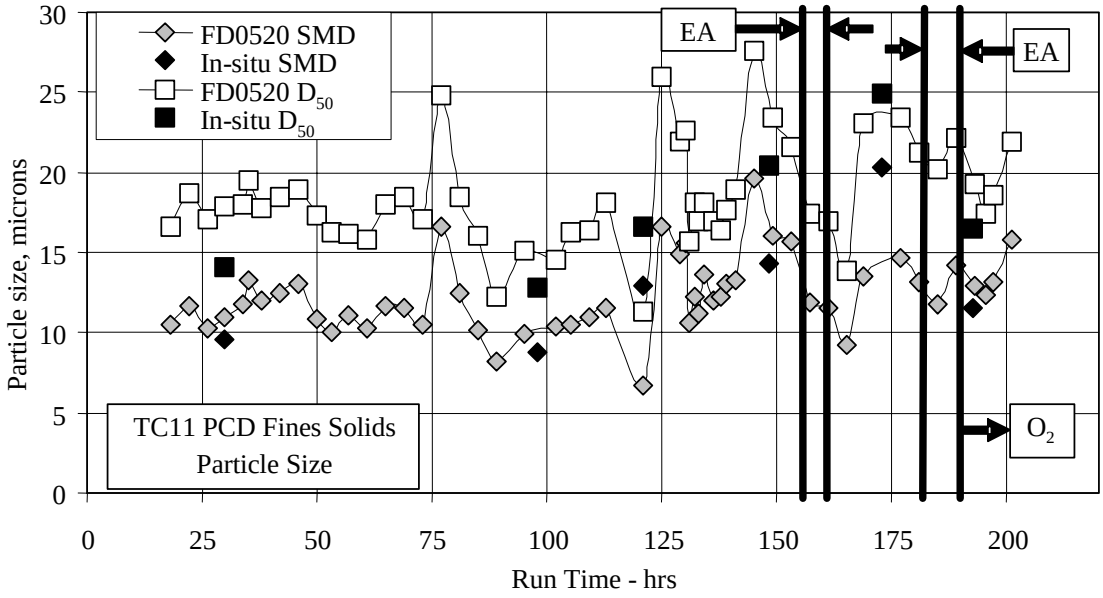

Figure 3.4-20 PCD Fines Particle Size

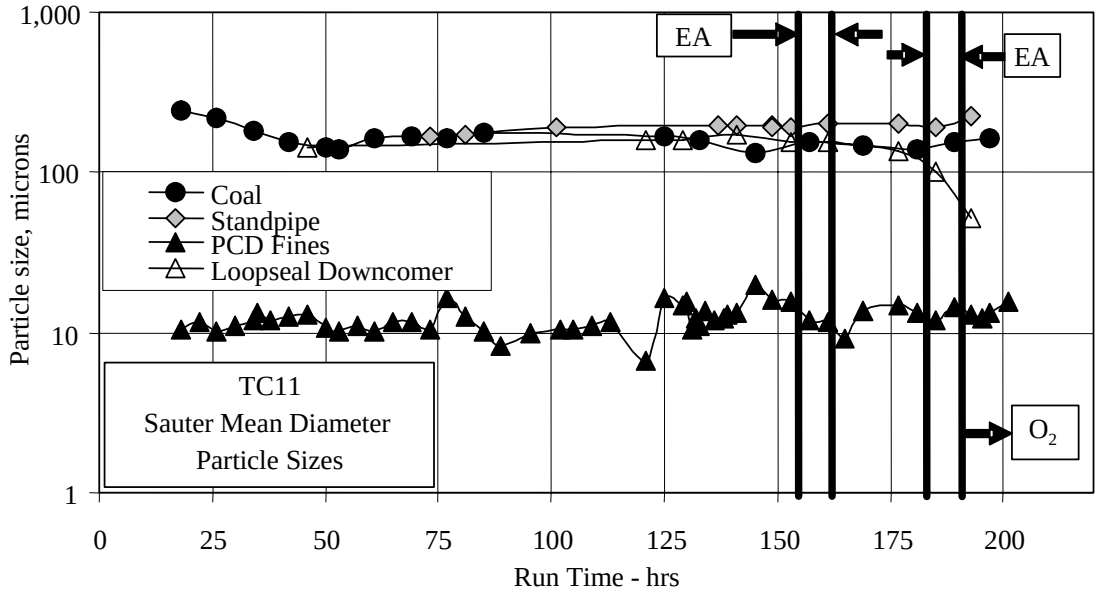

Figure 3.4-21 Particle Size Distribution

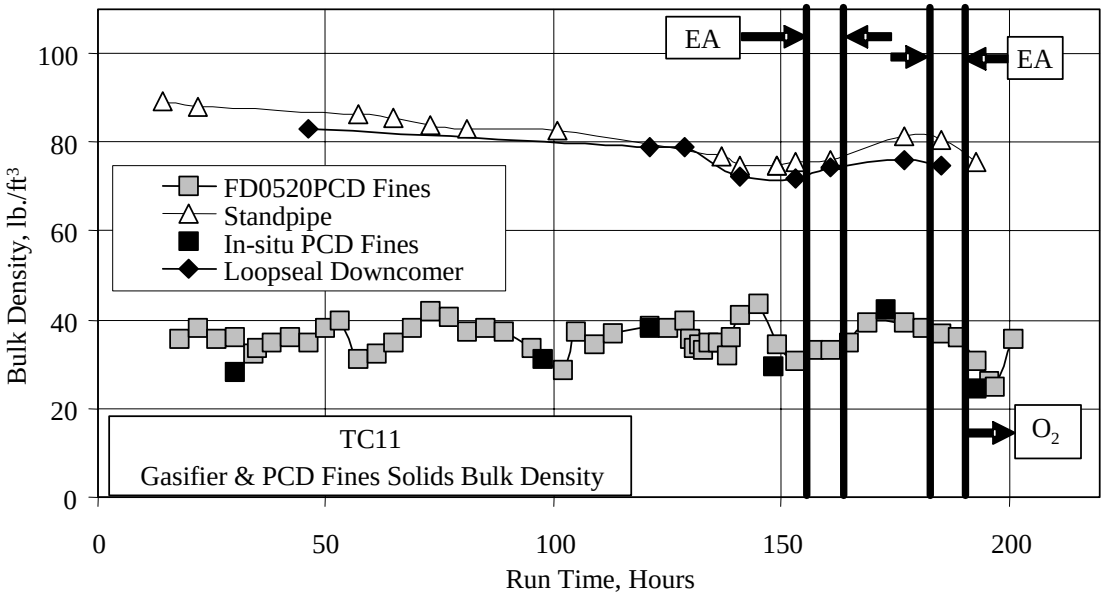

Figure 3.4-22 Gasifier Solids and PCD Fines Bulk Density

3.5 MASS AND ENERGY BALANCES

3.5.1 Summary and Conclusions

- Carbon conversions were between 95 and 99 percent in air-blown mode, between 97 and 98 in enhanced-air-blown mode, and 93 and 96 percent in oxygen-blown mode.
- Carbon balances were good at ±15 percent.
- Coal rates were varied from 2,300 to 4,800 lb/hr.
- Oxygen-to-coal ratio (pound per pound) was 0.60 to 0.84.
- Overall mass balance was good at ±9 percent.
- Nitrogen balances were good at ±10 percent.
- Fuel nitrogen conversion to ammonia was 20 to 50 percent, which was less than the PRB fuel nitrogen conversion.
- Sulfur balance was acceptable at ±20 percent (five outliers).
- Sulfur removal averaged 12.5 percent. All removal came from the Falkirk coal alkalinity, since no sorbent was added.
- Sulfur emissions were from 0.76 to 2.16 pounds SO_2 per MBtu coal.
- Equilibrium H_2S calculations indicated that sulfur capture did not reach equilibrium concentrations.
- Hydrogen balances were good at ±15 percent (three outliers).
- Oxygen balances were good at ±10 percent (one outlier).
- Calcium balances were poor at ±40 percent for air-blown mode and +70 percent in oxygen-blown mode.
- Silica balances were poor at ±30 percent (three outliers).
- Energy balances were good at 0 to 12 percent.
- The raw cold gasification efficiency was 24 to 52 percent for air-blown mode, 44 to 53 percent in enhanced-air-blown mode, and 59.5 percent for oxygen-blown mode.
- The raw hot gasification efficiency was between 74 and 85 percent for air-blown mode, 81 to 82 percent for enhanced-air-blown mode, and 83 to 84 percent for oxygen-blown mode.
- The corrected cold gas efficiency was 50 to 72 percent for air-blown, 75 to 76 percent for enhanced-air-blown mode, and 79 to 81 percent for oxygen-blown.

3.5.2 Introduction

The process flows into the Transport Gasifier process are:

- Coal flow through FD0210.
- Coal flow through FD0220.
- Coke breeze flow through FD0220.
- Air flow measured by FI205.
- Oxygen flow measured by FI726.
- Pure nitrogen flow measured by FI609.

- Steam flow measured by the sum of FI204, FI727b, FI734, and FI733.

Sand was added through FD0220 to increase the Transport Gasifier standpipe level both during outages and coal feed. Limestone was not fed to the Transport Gasifier during TC11.

The process flows from the Transport Gasifier process are:

- Synthesis gas-flow rate from the PCD measured by FI465.
- PCD solids flow through FD0520.
- Gasifier solids flow through FD0510.

3.5.3 Feed Rates

The coal flow through FD0210 can be determined by three different methods:

- FD0210 surge bin weigh cell.
- Transport Gasifier carbon balance.
- Syngas Combustor carbon balance.

The FD0210 surge bin weigh cell uses the time between filling cycles and the weigh differential between dumps to determine the coal rate. This method was used to determine the coal rate in GCT4 and resulted in both the carbon and energy balance being 10- to 20-percent high. It appeared that the coal rates determined from the FD0210 weigh cell data were consistently higher than actual coal rate for test runs TC06 to TC10. During TC11, there were several periods when the FD0210 surge bin weigh cell could not be used to determine the coal rate due to numerous FD0210 trips. Although the FD0210 weigh cell coal rates were consistent with the other two coal rates, the FD0210 surge bin weigh cell coal rates will not be used for TC11.

The Transport Gasifier carbon balance method uses the syngas carbon rate from the syngas flow rate and composition plus the PCD carbon rate from the PCD fines carbon concentration and PCD solids flow rate. This method was used in TC06, TC07, TC08 and TC10. Using this method forces the Transport Gasifier carbon balance to be perfect.

The syngas combustor carbon balance method uses the syngas combustor flue gas CO_2 analyzer and the syngas combustor flue gas rate to determine the carbon in the synthesis gas. The coal rate is determined by adding the carbon in the PCD fines to the carbon in the synthesis gas. The TC11 energy balance was better for the syngas combustor carbon balance method than the other two coal rate methods so the syngas combustor carbon balance coal rate was used for TC11. The coal rates used for the further analysis are listed in Table 3.5-1 for each operating period.

The Transport Gasifier carbon balance coal rates, syngas combustor carbon balance coal rates, and FD0210 weigh cells coal rates for the operating periods are compared on Figure 3.5-1. The values for the FD0210 weigh cell were averaged for each operating period. There were several operating periods during which the weigh cell coal-feed rate could not be determined, TC11-1, and TC011-8 through TC11-11.

For the first 23 hours of TC11, the Transport Gasifier carbon balance coal rate was higher than the syngas combustor carbon balance coal rate, while the weigh cell coal rate was lower than both of the other coal rates. At 36 hours, all three coal rates agreed with each other. Between hours 50 and 126 hours, the Transport Gasifier carbon balance coal rate was lower than the syngas combustor coal rate. Between hours 132 and the rest of TC11, the syngas combustor coal rate and the Transport Gasifier coal rate agreed with each other. The weigh cell carbon rate agreed with the syngas combustor coal rate for several of the operating periods.

The Transport Gasifier carbon balance coal flow rates for the operating periods are given in Table 3.5-1. The coal rate at the beginning of TC11 was 4,300 lb/hr, and then it was decreased to 2,600 lb/hr at hour 10. The coal rate was then increased to 4,700 lb/hr at hour 36. The coal rate was constant from hour 60 to hour 126 at about 3,300 lb/hr (except for TC11-5 at 4,700 lb/hr). At hour 132, the coal rate was increased to 4,850 lb/hr which caused an increase in CO and H_2 syngas concentrations. The coal rate was held between 4,300 and 4,800 lb/hr for the rest of the air-blown testing (except for TC11-14 at 3,200 lb/hr). The coal rate for the first enhanced-air-blown test was 3,500 lb/hr, while the final two enhanced-air coal rates were about 3,000 lb/hr. The two oxygen-blown operating periods had coal rates of 4,000 and 4,500 lb/hr.

The coke breeze flow through sorbent feeder FD0220 was determined from a correlation between feeder speed and dumps from the FD0220 storage bin between fills. The correlation is based on data taken during the steady operating periods during a previous test campaign, TC09. The correlation for the sorbent feeder is:

$$\text{FD0220 rate} = 47.924(\text{rpm}) \qquad (1)$$

The coke breeze rates are shown on Table 3.5-1 for each operating period. The rates were from 0 to 77 lb/hr. Coke breeze was fed to the Transport Gasifier during about one-half of the TC11 operating periods at a very low rate.

The operating period air, steam, oxygen, and nitrogen flow rates are shown in Figure 3.5-2 and on Table 3.5-1. The small amount of nitrogen added via FI6080 to the Transport Gasifier through the coke breeze feed line to keep the line clear between periods of coke breeze feed is included in the feed nitrogen.

The nitrogen rate for TC11-1 was 7,600 lb/hr and was then increased and held steady at about 9,000 lb/hr until hour 126. The nitrogen rate was then decreased down to about 7,000 lb/hr for the remainder of TC11. The low TC11-1 nitrogen rate contributed to the high TC11-1 LHV, since decreasing the nitrogen rate increases the LHV. For the first 126 hours of TC11, about 1,000 lb/hr of nitrogen were fed to the unit via FI6080.

The oxygen rate was 0 for air-blown mode. For enhanced-air, the oxygen rate was 1,000 to 2,000 lb/hr, and for oxygen-blown mode, the oxygen rate was about 2,300 lb/hr.

The total steam rate to the Transport Gasifier is calculated by the sum of FI204 (total steam flow to the upper mixing zone), FI727b (steam mixed with the air fed to the lower mixing zone), FI734 (steam fed into the lower mixing zone), and FI733 (steam fed to a shroud into the lower mixing zone). The steam-feed rates for each operating period are shown in Figure 3.5-2 and

listed on Table 3.5-1. The steam rate was held constant at about 700 to 825 lb/hr steam for the first 153 hour of TC11 (first 16 air-blown operating periods). The steam rate was 1,700 lb/hr for the first enhanced-air-blown operating period (TC11-17), 900 lb/hr for the last air-blown period (TC11-18), 1,330 lb/hr for the last two enhanced-air operating periods, and 1,150 lb/hr for the oxygen-blown periods. The higher steam rate in air-blown TC11-18 decreased the LHV compared to the other air-blown operating periods. The higher steam rate in enhanced-air operating period TC11-17 also resulted in a lower LHV than in the other two enhanced-air LHVs.

The operating period air feed rates are shown on Figure 3.5-2 and 3.5-3 and are listed in Table 3.5-1. The air rate during the first 16 air-blown runs was either about 10,000 lb/hr or about 13,000 lb/hr tracking the coal rate. The air-to-coal ratio determines the gasifier temperature at given process conditions. When the coal rate is increased, the air rate is increased to provide for additional carbon combustion to heat up the addition coal that is added to the gasifier to maintain gasifier temperature constant. Therefore, the coal rate and air rate increase and decrease together if the gasifier temperature is maintained as a constant. The lowest air rate was during the last air-blown operating period, TC11-18, which also had the lowest air-blown coal rate. The air rates for the three enhanced-air operating periods were either 2,300 or 4,200 lb/hr. During oxygen-blown mode, there was no air fed to the Transport Gasifier.

3.5.4 Product Rates

The synthesis gas rates for each operating period are shown on Figure 3.5-3 and listed on Table 3.5-1. The synthesis gas rates were taken from FI465.

The synthesis gas rate was checked for all the operating periods using an oxygen, carbon, and hydrogen balance around the synthesis gas combustor and found to be in good agreement with the synthesis gas combustor data for most of the operating periods (see Section 3.3 Figures 3.3-23, 24, and 25). The synthesis gas rate was from 19,000 to 26,000 lb/hr for the first 16 air-blown operating periods. The last air-blown operating period had a synthesis gas rate of 16,600 lb/hr. The syngas rate during all three enhanced air-operating periods was about 16,300 lb/hr. During the two oxygen-blown operating periods, the synthesis gas rate was either 14,300 or 15,600 lb/hr. The synthesis gas rate is a strong function of the air and oxygen rates and a weak function of the steam and nitrogen rates. The air-blown TC11 syngas rates track the air rates very closely.

The solids flow from the PCD can be determined from two different methods by using:

- In situ particulate sampling data upstream of the PCD.
- Spent solids feeder system (FD0530) weigh cell data.

The best measurements of the PCD solids flow are the in situ PCD inlet particulate determinations. Using the synthesis gas flow rate and the in situ PCD inlet particulate measurement, the solids flow to the PCD can be determined, since the PCD captures all of the solids. Because there was no sorbent feed operation in TC11, the PCD fines rate should be a strong function of the coal rate (coal ash) and carbon conversion.

The FD0530 weigh cell data can be used to determine the PCD solids flow only if both the FD0530 feeder and the FD0510 feeder (standpipe solids) are off, because FD0520 and FD0510 both feed into FD0530, and FD0530 feeds the atmospheric fluidized-bed combustor. This method assumes that the solids level in the PCD and fines screw cooler (FD0502) are constant. A good check on the PCD fines rates is the calcium and silica balances because calcium and silica are only present in the feed coal and the PCD fines. The two PCD fines rates methods are compared on Figure 3.5-4 where the five in situ rates are plotted against rates determined by the FD0530 weigh cells at about the same time. The in situ rates were higher than the FD0530 weigh cell rates by 80 to 235 lb/hr (average of 160 lb/hr).

The results for all of the FD0530 weigh cell data are compared with the in situ data in Figure 3.5-5. The FD0530 weigh cell measurements had a large scatter and were usually lower than the in situ samples PCD fines rates. Because the in situ PCD fines rate are more reliable than the FD0530 weigh cell PCD fines rate, the in situ PCD fines solids rates were used for further analyses. Also plotted on Figure 3.5-5 are the interpolated PCD solids rates used for the operating periods.

The operating periods PCD fines rates were from 400 to 500 lb/hr and did not change during the first 16 air-blown operating periods. Unfortunately no in situ PCD inlet measurements were taken for the first 97 hours of TC11, so the first 98 hours of PCD fines rates were based on the in situ PCD fines rate taken at 98 hours. In fact, the PCD fines rates certainly would have varied with the coal rates during the first 98 hours of TC11, but further analyses will assume that the PCD fines rate was constant at 421 lb/hr. The PCD fines rate then decreased to 195 lb/hr during the final air-blown operating period, which was also the lowest coal rate. The oxygen-blown PCD fine rates were about 350 lb/hr. The PCD fines rates for each operating period used in the mass balances are shown in Table 3.5-2.

FD0510 was operated during several of the operating periods. It was difficult to estimate the amount of solids removed during those operating periods due to frequent plugging of LI339, since the amounts of solids removed from the gasifier were determined by differences in the standpipe level using LI339 before and after FD0206 and FD0510 operation. Because the amount of reactor solids removed during an operating period is usually small and it was difficult to estimate, it was assumed that the FD0510 rates were zero for all operating periods.

3.5.5 Carbon Balances and Carbon Conversion

The carbon balances are given on Figure 3.5-6 and in Table 3.5-2. All but two of the air-blown carbon balances were between ±12-percent error, with TC11-2 and TC11-18, having a carbon balance error larger than 12 percent. TC11-2 and TC11-18 were the two lowest coal rates during operating periods. All three of the enhanced-air-blown mode carbon balances had carbon balance errors between ±10 percent, while both oxygen-blown carbon balances were less than ±5 percent error. The carbon balance was sacrificed slightly to obtain the best possible energy balance by choosing the syngas combustor carbon balance coal rate. The carbon balance is dominated by the coal carbon rates and the syngas carbon rates.

Carbon conversion is defined as the percent fuel carbon that is gasified to CO, CO_2, CH_4, C_2H_6, and higher hydrocarbons. The carbon conversion is a measure of how much carbon is rejected by the gasifier with the PCD and gasifier solids. For the coke breeze addition periods of TC11, the coke breeze carbon was considered potential carbon for gasification. The rejected carbon to the gasifier or PCD fines solids in a typical IGCC flow sheet is burned in a less efficient combustor or sent for disposal.

The carbon conversion can be calculated at least three different ways due to inconsistencies in the carbon balance. Because the carbon balance is off by up to 14 percent (TC11-2 and TC11 18), each result could be different. If there were a perfect carbon balance, all three calculations would produce the same result (as in TC11-22). Three calculation methods were used to determine carbon conversion:

1. Based on the feed carbon (coal plus coke breeze) and the carbon in the syngas. This method assumes that the feed carbon and the synthesis gas carbon are correct. (Gas analyses method)
2. Based on the feed carbon and the synthesis gas carbon determined by a Transport Gasifier carbon balance, not the gas analyses. This method assumes that the synthesis gas carbon is incorrect. (Solids analyses)
3. Based on the feed carbon determined by Transport Gasifier carbon balance and the synthesis gas carbon. This method assumes that the coal feed is in error. (Products analyses)

The carbon conversions using all three methods are plotted on Figure 3.5-7. The products method carbon conversions for each operating period are given in Table 3.5-2. The carbon conversions by the solids and products method are approximately the same for TC11. The carbon conversion by the gas method is larger than the carbon conversion by the products method when the carbon balance error is less than zero and is greater than the products method when the carbon balance error is greater than zero. The carbon conversion by the gas method has about 25 percent of the carbon conversions above 100 percent, which is a result of the syngas carbon being larger than the coal carbon for over half of the operating periods. Clearly these are unrealistic carbon conversions. The products method is the most reasonable because it is not based on the coal rate but on the syngas and PCD solids rates.

The products method carbon conversion was about 96 percent during the first 95 hours of TC11, and then increased to about 98 percent for a few operating periods (hours 115 to 137). From hours 144 to 153, the carbon conversions were about 97 percent. There does not seem to be any process changes at the appropriate times to indicate why the carbon conversions changes, so the differences may be due to data scatter and inaccuracies in the coal and PCD fines rates. The carbon conversions remained constant during the first enhanced-air-blown period (TC11-17), the last air-blown period (TC11-18), and the second enhanced-air-blown period (TC11-19) at about 98 percent. For the last three operating periods, one enhanced-air (TC11-20) and the two oxygen-blown periods (TC11-21 and 22), the carbon conversion was decreasing rapidly from 97 to 93 percent. Note from Section 3.4, Figure 3.4-9, the organic carbon increased from about 10 to 45 percent during the last 18 hours of TC11, which includes the entire oxygen-blown mode testing at the end of TC11. Due to the short duration of the last two operating

periods (2.0 and 1.0 hours) and the rapidly changing carbon content of the solids, the last two carbon conversions are probably not representative of steady, repeatable behavior.

The carbon conversion should be a function of gasifier temperature, with the carbon conversion increasing as the temperature increases. The TC11 products method carbon conversions are plotted against riser exit temperature, TI360, in Figure 3.5-8. With most of the carbon conversions in such a narrow range (95 to 99 percent) it is difficult to determine whether there is a temperature effect on carbon conversions from this data. The air-blown data shows a slight increase in carbon conversion with temperature. The 80ºF temperature range of operation (1,650 to 1,730ºF) is probably too small to notice the effect of temperature on carbon conversion. The small variation and the inherent errors in the carbon conversion probably obscured any temperature effect on carbon conversion. This is consistent with TC06 to TC10 data where the temperature range was small, and the data sometimes showed that increasing temperatures slightly decreased carbon conversions.

The carbon conversions of Powder River Basin, Hiawatha bituminous, and Falkirk Lignite coal are compared on Figure 3.5-9 for both air and oxygen operation. The oxygen and enhanced-air carbon conversions are shown separately. The Falkirk Lignite had higher carbon conversions than both PRB and the Hiawatha bituminous in both air- and oxygen-blown modes.

3.5.6 Overall Material Balance

Material balances are useful in checking the accuracy and consistency of data as well as determining periods of operation where the data is suitable for model development or commercial plant design. Total material balances for each operating period are given on Figure 3.5-10 which compares the total mass in and the total mass out. The overall material balance was good, with all of the relative differences at ±9 percent, and most of the relative differences less than ±5 percent. The relative difference (relative error) is defined as the Transport Gasifier feeds in minus products out divided by the feeds ({In-Out}/In). Note that the air-blown operating periods had higher overall mass flow rates than the oxygen-blown operating periods due to additional nitrogen fed to the Transport Gasifier.

The details of the overall mass balance are given in Table 3.5-1 with the relative differences and the absolute differences. The absolute difference (absolute error) is defined as the difference between the feeds and the products (In-Out).

The main contributors to the material balance are the synthesis gas rate (14,000 to 25,000 lb/hr), air rate (0 to 13,500 lb/hr), oxygen rate (0 to 2,400 lb/hr), steam rate (700 to 1,700 lb/hr), nitrogen rate (6,500 to 9,100 lb/hr), and coal rate (2,300 to 4,850 lb/hr).

The oxygen-to-coal ratios are listed on Table 3.5-1. The oxygen-to-coal ratio varied from 0.60 to 0.84 for air-blown operation and from 0.71 or 0.72 for enhanced-air operation. The oxygen-to-coal ratio was either 0.57 or 0.52 for oxygen-blown operation.

3.5.7 Nitrogen Balance

TC11 operating period nitrogen balances are plotted on Figure 3.5-11 by comparing the nitrogen in and the nitrogen out and are listed in Table 3.5-3. Detailed nitrogen flows for a typical air-blown test (TC11-13) are shown in Table 3.5-4 and for a typical oxygen-blown test (TC11-21) are shown on Table 3.5-5. The air-blown mode nitrogen balances were good with errors less than 11 percent for all operating periods and a positive bias (feeds larger than the products). The enhanced-air nitrogen balances were excellent with errors in all three balances less than 1 percent. Both oxygen-blown mode nitrogen balances were acceptable with a negative bias at either -8.1 or -9.2 percent. Note that air-blown mode nitrogen rates were much higher than the enhanced-air and oxygen-blown nitrogen rates.

The nitrogen flows as shown in Tables 3.5-4 and 3.5-5 are dominated by the air, nitrogen, and synthesis gas flows. Previous gasification tests TC06 to TC10 assumed that from 500 to 1,250 pounds of nitrogen per hour were lost due to seals and lock hoppers. This loss was not assumed, and it is possible that the system was improved to eliminate nitrogen leaks.

None of the solid streams contribute significantly to the nitrogen balance. The TC11 nitrogen balances were consistent with previous nitrogen balances which ranged from a maximum of 10-percent error.

Using the ammonia analyzer data, the coal rates, and the coal nitrogen concentration, the amount of fuel nitrogen converted to NH_3 can be calculated. The amount of fuel nitrogen converted to NH_3 is shown on Figure 3.5-12. The amount of fuel nitrogen converted to ammonia varied from 20 to 40 percent during air- and oxygen-blown operation, and varied between 40 and 55 percent during enhanced-air operation. The percent coal nitrogen converted to ammonia for PRB was much higher during TC07 at about 80 percent.

The trends of several process parameters against percent fuel nitrogen conversion to ammonia were briefly investigated. The PCD inlet and Transport Gasifier temperatures did not seem to effect the percent fuel nitrogen-to-ammonia conversion. The only parameters found were the coal-feed rate and the overall percent O_2. The trend of the fuel nitrogen conversion with overall the percent O_2 is shown in Figure 3.5-13. The fuel nitrogen conversion to ammonia increases as the percent O_2 is increased for both the air-blown and enhanced-air, with the data on the same line. This trend with percent oxygen would imply that the fuel nitrogen conversion to ammonia is a function of the amount of syngas dilution similar to the LHV. The oxygen-blown fuel nitrogen conversions are lower than the air and enhanced-fuel nitrogen conversions at the same overall percent O_2 and are lower than the straight line fit of the air and enhanced-air data, possibly due to the short duration of the two oxygen-blown operating periods.

The trend of the fuel nitrogen-to-ammonia conversion with coal rate is not shown in this report. The fuel nitrogen conversion to ammonia increases as coal rate is increased for both air-blown and enhanced-air modes. However, the air-blown and enhanced-air data do not fall on the same line, with the enhanced-air fuel nitrogen-to-ammonia conversions about 15 percent higher than the air-blown fuel nitrogen-to-ammonia conversions at the same coal rate. The oxygen-blown fuel nitrogen conversions are consistent with the air fuel nitrogen conversions at the same coal rate and are lower than the enhanced-air fuel nitrogen conversions at the same coal rate.

3.5.8 Sulfur Balance and Sulfur Removal

Sulfur balances for all the TC11 operating periods are given in Figure 3.5-14 and Table 3.5-6. The synthesis gas sulfur compounds were not directly measured but estimated from syngas combustor SO_2 analyzer data and synthesis gas combustor flue gas flow. The coal sulfur values were interpolated between the solids sampling times. The TC11 sulfur balances were acceptable with all but two (TC11-1 and TC11-22) sulfur balances with relative errors of less than ±25 percent with no bias. The sulfur balances were better than the sulfur balances for TC06 through TC10, probably because the Falkirk Lignite was the highest sulfur fuel to data gasified during the gasification test campaign (TC) series of tests (TC06 to TC11). The higher sulfur level makes it easier to accurately measure the solid and gaseous sulfur concentrations. TC11-1 was only a 1-hour operating period, which started 1 hour after a coal startup. TC11-22 was a 1-hour operating period at the end of TC11 when the operating temperatures were decreasing prior to shut down.

With the errors in the sulfur balances, it is difficult to determine the correct sulfur removal. Similar to the coal conversions calculations, there are three different methods to determine Transport Gasifier sulfur removals:

1. From synthesis gas sulfur emissions (using the synthesis gas combustor flue gas rate and synthesis gas combustor flue gas SO_2 measurement) and the feed sulfur rate (using the feed coal rate and coal sulfur content) (gas analyses method).
2. From PCD solids analysis (using PCD solids flow rate and PCD solids sulfur content) and the feed sulfur rate (solids analyses method).
3. From the gas analysis data and the PCD solids data (product analyses method).

The three sulfur removal methods are plotted on Figure 3.5-15 and given on Table 3.5-6. The sulfur in the fuel is an inaccurate measurement due to the multiplication of a very small number (coal sulfur) by a large number (coal-feed rate). The coal rate for mass balances is determined by the Transport Gasifier carbon balance rather than the actual weigh cell measurement. The gaseous sulfur flow should be accurate, although it is also the product of a small number (syngas combustor SO_2) and a large number (syngas combustor flue gas rate). The syngas H_2S was measured by the H_2S analyzer AI419J and seemed to be in agreement with the TRS by the syngas combustor AI476P from hours 92 to 201. The PCD fines sulfur rates have inaccuracies due to the low sulfur in the PCD solids. There is no accumulation of sulfur-containing solids in the gasifier during TC11 because the standpipe and FD0510 gasifier samples contained negligible amounts of sulfur.

The TC11 results indicate that the gas method is less accurate than the product and the solids methods. The solids and products method methods usually agreed with each other and seemed to change slowly and consistently during the run. The gas method varied greatly during the run, and there was one period (TC11-10) of negative gas method sulfur removals. The negative sulfur removals were because the sulfur flows out were larger than the sulfur flows in. The sulfur removal by the products is probably the most reliable sulfur removal.

The sulfur removal by products started TC11 at 20 percent and then decreased to 13 percent at hour 36. After two operating periods (hours 50 and 60) at about 17 percent, the sulfur removal then decreased to 3 percent at hour 95. The sulfur removal then slowly increased to 18 percent by the end of the first air-blown operating periods (hour 153). The sulfur removal was 5 to 10 percent for the next three operating periods (hours 159 to 185) which was the first enhanced-air period, the last air-blown operating period and the second enhanced-air operating period. At hour 189, sulfur removal increased to above 10 percent. Due to the errors in the sulfur balance, all that can be concluded from the data is that the sulfur removal was between 0 and 20 percent for TC11 and did not seem to change with mode of operation.

The synthesis gas combustor SO_2 data was used for the sulfur emissions shown in Table 3.5-6. The sulfur emissions were from 1.41 to 2.16 pounds SO_2 per MBtu coal fed with one outlier (TC11-1) at 0.76 pounds SO_2 per MBtu coal fed.

Figure 3.5-16 plots the measured sulfur emissions against the sulfur out of the reactor (sulfur emissions plus the PCD fines sulfur). On Figure 3.5-16, the 45-degree line is the 0-percent sulfur removal line (PCD fines sulfur equals 0) and the X-axis is the 100-percent sulfur removal line (0 sulfur emissions). This plot is a replotting of the products method sulfur removal calculation because it is based on the PCD fines sulfur and the syngas sulfur. The average sulfur capture is 12.5 percent and is plotted on Figure 3.5-16. There does not seem to be any difference in sulfur capture based on the mode of operation.

3.5.9 Hydrogen Balance

Operating period hydrogen balances are given in Figure 3.5-17 and Table 3.5-3. Typical hydrogen flows for air-blown tests (TC11-13) are shown in Table 3.5-4, and typical hydrogen flows for oxygen-blown test, (TC11-21) are shown in Table 3.5-5. The hydrogen balance is acceptable with 17 of the 22 operating periods within ±15 percent of perfect agreement. The worst hydrogen balance is TC11-1 at 36-percent error. TC11-1 was only a 1-hour operating period, which started 1 hour after a coal startup. Both hydrogen analyzers were out of service during TC11-1, which required the TC11-1 hydrogen concentration to be estimated from the water-gas shift equilibrium and the CO, CO_2, and H_2O concentrations. The coal, steam, and synthesis gas streams dominate the hydrogen balance. The TC11 hydrogen balances are better than previous test campaigns such as TC07 and TC08, where the hydrogen and oxygen balances indicated that the steam flow meters were reading 500 lb/hr low. Test campaigns TC09 and TC10 used the hydrogen balance to determine a reasonable steam rate rather than using the measured steam rate.

The steam rate for each operating period was calculated using a hydrogen balance, which is essentially the difference in hydrogen between the coal feed and synthesis gas rate. The hydrogen balance steam rate is compared with the measured steam rate on Figure 3.5-18. Note the lower steam rates in air-blown mode. Only about one half of the measured steam rates are within 20 percent of the hydrogen balance steam rates. The air-blown mode differences are balanced around the 0-percent error line indicating there is no systematic error at a measured rate of 750 lb/hr steam. The TC11-1 steam rate is not shown on Figure 3.5-18 because the hydrogen balance calculated steam rate was less than zero. TC11-17 has both the largest steam rate and the largest error.

In TC07 and TC10, the hydrogen balance indicated that there was about 500 pounds more steam per hour than measured being fed to the Transport Gasifier. During TC08, the enhanced-air and oxygen-blown modes the steam rate by hydrogen balance was less than the measured steam rate by about 200 to 500 lb/hr of steam. The second air-blown mode indicates that about 500 pounds more steam per hour is being fed to the gasifier than reported by the measured steam rate. In TC09 the hydrogen balance steam rates were 30 to 50 percent larger than the measured steam rates.

3.5.10 Oxygen Balance

Operating period oxygen balances are given in Figure 3.5-19 and Table 3.5-3. Typical oxygen flows for an air-blown mode test (TC-13) are shown in Table 3.5-4 and typical oxygen flows for an oxygen-blown mode test (TC11-21) are shown in Table 3.5-5. The oxygen balance will help determine if the steam and oxygen or air rates are consistent with the synthesis gas rate and composition.

The TC11 operating periods oxygen balances for air-blown mode were acceptable with all but three operating periods with less than ±10 percent relative error (TC11-2, TC11-3, and TC11-4). All of the three operating periods had a low bias. Acceptable oxygen balances indicate that the measured steam rates are consistent with the other oxygen flows (air, oxygen, and synthesis gas).

The TC11 oxygen balances were better than two previous test campaigns oxygen (TC06 and TC07) balances that used the measured steam rate. TC06 oxygen balances were off by -20 to -4 percent and the TC07 oxygen balances were off by -20 to -5 percent. The TC11 oxygen balances were about as good as the TC08 oxygen balances which were off from 0 to 12 percent. The TC11 oxygen balances were not as good as TC09 and TC10, which used the hydrogen balance to determine the steam rate.

3.5.11 Calcium Balance

Operating period calcium balances are given in Figure 3.5-20 and Table 3.5-3. Typical calcium flows for an air-blown mode test (TC11-13) are shown in Table 3.5-4, and typical calcium flows for an oxygen-blown mode test (TC11-21) are shown on Table 3.5-5. The calcium balances are essentially a comparison between the coal calcium and the PCD fines calcium. Because there was no sorbent fed to the gasifier during TC11, there was minimal flow through FD0510, and the gasifier accumulation term was assumed to be small.

The TC11 calcium balances were acceptable with 15 of the 22 having errors less than 30 percent, with a high bias. This is acceptable because essentially the comparison is between two solid streams that are difficult to measure. Both oxygen-blown operating periods had high errors, up to 74 percent (40 lb/hr calcium). One of the enhanced-air operating periods (TC11-20) had a high error of 40 percent (16 lb/hr calcium). Due to the lack of sorbent feed, the calcium flows were fairly low, and any errors in flow rates would tend to magnify the errors.

The TC11 calcium balances were better than previous calcium balances for most of the previous test campaigns. TC11 calcium rates were consistent with TC08 and TC09 which also had no

sorbent feed. In TC06, the calcium balances were off by -50 to +40 percent; in TC07, the calcium balances were off by -100 to +40 percent, and the TC08 calcium balances were off by ±40 percent. The TC09 calcium balance was from ±40 percent (±40 pounds calcium per hour). The TC10 calcium balances were slightly better than the TC11 at ±20 percent.

Figure 3.5-21 plots TC11 sulfur removal by products method as a function of calcium-to-sulfur molar ratio (Ca/S, molecular weight) measured in the PCD solids samples from FD0520. The sulfur removals were 5 to 20 percent. Removals were consistent with TC08, TC09, and TC10 PRB sulfur removals with no sorbent addition. The trends in PCD solids Ca/S with sulfur emissions on Figure 3.5-21 are opposite of what are expected if the amount of excess calcium is limiting sulfur capture. (It is expected that increased sorbent should lead to increased sulfur removal.) The sulfur removal should increase with Ca/S. The results seen on Figure 3.5-21 demonstrate that when the PCD solids contain very little sulfur (high Ca/S), the sulfur removals are low, which is reasonable by sulfur balance. The calcium sulfation percent is the reciprocal (times 100) of the Ca/S ratio based on the PCD fines solids. TC06 had 10- to 55-percent sulfur removal; TC07 had 5- to 50-percent sulfur removal, both with sorbent addition. The lower sulfur removals during TC08, TC09, TC10, and TC11 were due to the absence of limestone feed.

Figure 3.5-22 plots TC11 sulfur emissions (expressed as pounds SO_2 emitted per MBtu coal fed) as a function of calcium to sulfur ratio (Ca/S) measured in the PCD solids sampled from FD0520. The sulfur emissions varied from 1.41 to 2.16 pounds SO_2 emitted per MBtu coal fed (one outlier at 0.76 pounds SO_2 emitted per MBtu coal fed) independent of Ca/S ratio. Since the Falkirk lignite had a higher sulfur level than the previously tested PRB and Hiawatha bituminous, the sulfur emissions were higher. PRB sulfur emissions ranged from 0.13 to 0.7 pounds SO_2 per MBtu, while Hiawatha bituminous sulfur emissions ranged from 0.6 to 1.01 pounds SO_2 per MBtu.

3.5.12 Silica Balance

Operating period silica balances are given in Figure 3.5-23 and Table 3.5-3. Typical silica flows for an air-blown mode test (TC11-13) are shown in Table 3.5-4, and typical silica flows for an oxygen-blown test (TC11-21) are shown on Table 3.5-5. The silica balances are essentially a comparison between the coal silica and the PCD fines silica, since those two streams are the only significant streams which contain silica.

The TC11 silica balances were good with 16 of the 22 having errors less than 25 percent, with no bias. This is acceptable because essentially the comparison is between two solid streams that are difficult to measure. Three of the operating period silica balances are identified on Figure 3.5-23. The TC11 silica balances were better than previous silica balances.

3.5.13 Energy Balance

The TC11 Transport Gasifier energy balance is given in Figure 3.5-24 with standard conditions chosen to be 1.0 atmosphere pressure and 80°F temperature. Table 3.5-7 breaks down the individual components of the energy balance for each operating period. The energy consists of the coal, air, and steam fed to the Transport Gasifier. The nitrogen, oxygen, and sorbent fed to the gasifier were considered to be at standard conditions (80°F) and hence have zero enthalpy. The nitrogen and oxygen feeds actually enter the gasifier at a higher temperature than standard conditions, but compared to the other feed enthalpies, this neglected input energy is not significant. The energy out consisted of the synthesis gas and PCD solids. The lower heating value of the coal and PCD solids were used in order to be consistent with the lower heating value of the synthesis gas. The energy of the synthesis gas was determined at the Transport Gasifier cyclone exit. About 1,200 pounds of N_2 per hour fed to the PCD inlet and outlet particulate sampling trains has been subtracted from the synthesis gas rate to determine the actual syngas rate from the cyclone. The sensible enthalpy of the syngas was determined by the overall gas heat capacity from the synthesis gas compositions and the individual gas heat capacities. The synthesis gas and PCD solids energy consists of both latent and sensible heat. The heat loss from the Transport Gasifier was estimated to be 3.5 MBtu/hr.

The TC11 energy balances were within 0- to 12-percent error. There was a positive bias in the TC11 energy balances, especially for all of the air-blown energy balances. A gasifier heat loss of 5.02 MBtu/hr minimizes the TC11 operating period's energy balance errors.

3.5.14 Gasification Efficiencies

Gasification efficiency is defined as the percent of the energy in (coal energy and steam energy) that is converted to potentially useful synthesis gas energy. Two types of gasification efficiencies have been defined, which are the cold gas efficiency and the hot gas efficiency. The cold gas efficiency is the amount of energy fed that is available to a gas turbine as synthesis gas latent heat. The hot gasification efficiency is the amount of feed energy that is available to a gas turbine plus a heat recovery steam generator.

The cold gas efficiency can be calculated at least three different ways, similar to sulfur removal and carbon conversion. Since the energy balance is off by up to 12 percent, each result could be different. If there were a perfect energy balance, all three calculations would produce the same result. Three calculation methods were performed for cold gasification efficiency consistent with the three methods of sulfur removal:

1. Based on the feed heat (coal latent heat plus steam heat) and the latent heat of the synthesis gas. This method assumes that the feed heat and the synthesis gas latent heat are correct. (gas analyses)
2. Based on the feed heat (coal latent heat plus steam heat) and the latent heat of the synthesis gas determined by a Transport Gasifier energy balance, not the gas analyses. This method assumes that the synthesis gas latent heat is incorrect. (solids analyses)

3. Based on the feed heat determined by Transport Gasifier energy balance and the synthesis gas sensible heat. This method assumes that the coal feed or the steam rate is in error. (products analyses)

The cold gas gasification efficiencies for the three calculation methods are plotted in Figure 3.5-25. For all of the operating periods, the products method is between the solids and gas methods. The gas method is lower than the solids method and the products method for all TC11 operating periods that the energy balances are biased high. The three methods agree with each other whenever the energy balance is off by less then 1.5 percent (hours 159 and 195). Only the products method is listed in Table 3.5-6 because the products method is the most accurate method since it does not use the coal rate determined by Syngas Combustor carbon balance.

The products analyses cold gas gasification efficiencies started TC11 at 52 percent due to the high coal rate and low steam rate. The cold gas efficiency then decreased as the coal rate decreased. The lowest efficiency (24 percent) was during the lowest coal rates at hours 10 and 174 in the air-blown mode. In the air-blown mode, the efficiency was 48 to 52 percent when the coal rate was above 4,000 lb/hr and 35 to 40 percent when the coal rate was at 3,000 lb/hr. The enhanced-air efficiencies were from 44 to 53 percent and dependent on both the steam rate and coal rate. The enhanced-air efficiencies were the only efficiencies to show a dependence on steam rate, since the steam rate was changed significantly only in the enhanced-air modes operations. The oxygen-blown cold gas efficiencies were at 59 to 60 percent. The steam rate effect on cold gas efficiency is not due to steam dilution but due to the increased loss in efficiency of heating steam to the Transport Gasifier temperature. An increase in steam rate decreases the syngas LHV and increases the syngas sensible heat such that the total syngas enthalpy remains the same.

Figure 3.5-26 shows the trend in cold gas efficiency with steam-to-coal ratio, that is, as the steam-to-coal ratio increases, the cold gas efficiency decreases. The oxygen-blown and enhanced-air operating periods had higher cold gas efficiency than the air-blown modes at the same steam-to-coal ratio by about 20 to 25 percent because the air-blown modes had the inefficiency of heating the air nitrogen.

The hot gasification efficiency is the amount of feed energy that is available to a gas turbine plus a heat recovery steam generator. The hot gas efficiency counts both the latent and sensible heat of the synthesis gas. Similar to the cold gasification efficiency and the sulfur removal, the hot gas efficiency can be calculated at least three different ways. The three calculation methods for hot gasification are identical to the three methods of cold gasification efficiency calculation except for the inclusion of the synthesis gas sensible heat into the hot gasification efficiency.

The hot gasification efficiency assumes that the sensible heat of the synthesis gas can be recovered in a heat recovery steam generator, so the hot gasification efficiency is always higher than the cold gasification efficiency. The three hot gasification calculation methods are plotted in Figure 3.5-27, and the products analysis hot gasification efficiencies are shown in Table 3.5-7.

For all of the operating periods, the products method is essentially equal to the solids method, because the amount of inlet coal heat is about the same as the total synthesis gas heat, and it

makes little difference whether the synthesis gas heat is corrected (solids analysis method) or the coal heat (products analysis method). The gas method is lower than the solids and products when the energy balance has a high bias.

As with the cold gasification efficiencies, the products method hot gasification efficiencies started TC11 high (at 85 percent) due to low steam and high coal rates and generally followed the coal rate, since for most of TC11, the steam rate was fairly constant. The air-blown hot gas efficiencies were between 74 and 85 percent. The enhanced-air hot gas efficiencies were 81 to 85 percent; the two oxygen-blown hot gasification efficiencies were 83 and 84 percent.

Figure 3.5-28 plots the hot gas efficiency against the steam-to-coal ratio. The air-blown trend of decreasing gasification efficiency with increasing steam-to-coal ratio is clear, but not as pronounced as the cold gasification trend. The enhanced-air and oxygen-blown hot gasification efficiencies do not seem to be a function of steam-to-coal ratio. The oxygen-blown hot gas efficiencies are consistent with the air-blown hot gas efficiencies at the same steam-to-coal ratios, while the enhanced-air-blown hot gas efficiencies were higher than the air-blown hot gas efficiencies at the same steam-to-coal ratios.

The two main sources in efficiency losses are the gasifier heat loss and the latent heat of the PCD solids. The gasifier heat loss of 3.5 MBtu/hr was about 13 percent of the feed energy, while the total energy of the PCD solids was about 3 percent of the feed energy. The heat loss percentage decreased as the gasifier size is increased. While the Transport Gasifier does not recover the latent heat of the PCD solids, this latent heat could be recovered in a combustor. The total enthalpy of the PCD solids can be decreased by decreasing both the PCD solids carbon content (heating value) and the PCD solids rate.

Gasification efficiencies can be calculated from the adiabatic nitrogen-corrected gas heating values and corrected flow rates that were determined in Section 3.3. The products adiabatic nitrogen-corrected cold gasification efficiencies are plotted on Figure 3.5-29 against the corrected steam-to-coal ratio and are listed on Table 3.5-7 for all of the operating periods. Only the cold gasification efficiencies based on the products are given in Figure 3.5-29 and Table 3.5-7 because they are the most representative of the actual gasification efficiencies. Because the nitrogen and adiabatic syngas LHV corrections reduce the coal rate and the steam rate (for oxygen-blown only), the corrected coal rates and the corrected steam rates were used in Figure 3.5-29. The corrected efficiencies are calculated assuming an adiabatic gasifier, because zero heat loss was one of the assumptions in determining the corrected LHV in Section 4.3. The corrected cold gas efficiencies were from 50 to 72 percent for air-blown mode, from 75 to 77 percent for enhanced-air, and 79 and 81 percent for oxygen-blown mode, with a decreasing trend of efficiency with increasing steam-to-coal ratio. As for the raw cold gas efficiencies, the corrected oxygen-blown and enhanced-air-blown modes were higher than the corrected air-blown mode at equivalent steam-to-coal ratios. The nitrogen and adiabatic corrections increased the cold gasification efficiencies by about 23 percent in air-blown mode and by about 28 percent in enhanced-air-blown mode, and by about 21 percent in oxygen-blown mode due to the use of recycle gas rather than nitrogen for aeration and instrument purges.

The adiabatic nitrogen correction does not increase the hot gasification efficiency because the deleted nitrogen lowers the synthesis gas sensible heat and increases the synthesis gas latent heat. Both changes effectively cancel each other.

Table 3.5-1 Feed Rates, Product Rates, and Mass Balances

		Feeds (In)							Products (Out)						
Operating Period	Average Relative Hours	Coal[1] lb/hr	Coke Br. FD0220 lb/hr	Air FI205 lb/hr	Oxygen FI726 lb/hr	Nitrogen[2] lb/hr	Steam lb/hr	Total lb/hr	Syngas FI465 lb/hr	PCD Solids FD0520 lb/hr	SP Solids FD0510 lb/hr	Total lb/hr	In - Out lb/hr	(In- Out)/In %	Oxygen to Coal Ratio lb/lb
TC11-1	1	4,334	0	11,253	0	7,603	770	23,960	21,539	421	0	21,960	2,000	8.3	0.60
TC11-2	10	2,593	0	9,388	0	9,299	812	22,092	20,609	421	0	21,030	1,062	4.8	0.84
TC11-3	18	3,344	0	10,394	0	8,866	739	23,343	21,545	421	0	21,966	1,378	5.9	0.72
TC11-4	23	3,629	0	10,766	0	8,723	735	23,853	21,973	421	0	22,394	1,459	6.1	0.69
TC11-5	36	4,704	0	13,433	0	8,931	761	27,829	26,232	421	0	26,653	1,176	4.2	0.66
TC11-6	50	3,166	0	10,085	0	8,853	727	22,830	21,453	421	0	21,874	957	4.2	0.74
TC11-7	60	3,425	32	10,724	0	8,406	747	23,334	21,713	421	0	22,134	1,201	5.1	0.73
TC11-8	92	3,311	39	10,236	0	9,124	756	23,465	21,581	421	0	22,002	1,463	6.2	0.72
TC11-9	95	3,300	29	10,187	0	8,898	756	23,171	21,389	421	0	21,810	1,360	5.9	0.72
TC11-10	115	3,268	21	11,011	0	9,209	759	24,268	23,185	380	0	23,565	703	2.9	0.78
TC11-11	126	3,293	0	10,604	0	8,754	757	23,408	21,724	390	0	22,114	1,294	5.5	0.75
TC11-12	132	4,857	0	13,401	0	6,971	749	25,979	24,808	426	0	25,234	744	2.9	0.64
TC11-13	137	4,536	0	13,247	0	7,004	754	25,540	24,098	449	0	24,548	993	3.9	0.68
TC11-14	144	3,219	24	9,917	0	7,026	751	20,937	19,250	488	0	19,738	1,199	5.7	0.71
TC11-15	148	4,320	39	12,169	0	6,440	751	23,719	22,265	506	0	22,771	949	4.0	0.65
TC11-16	153	4,491	77	12,542	0	6,769	744	24,623	23,132	449	0	23,580	1,043	4.2	0.65
TC11-17	159	3,566	39	2,360	2,022	6,457	1,698	16,143	16,340	366	0	16,706	-563	-3.5	0.72
TC11-18	174	2,270	42	8,054	0	6,430	913	17,709	16,617	195	0	16,812	897	5.1	0.82
TC11-19	185	2,937	39	4,271	1,090	6,888	1,294	16,519	16,024	286	0	16,310	209	1.3	0.71
TC11-20	189	3,126	40	4,237	1,272	6,826	1,280	16,780	16,299	319	0	16,618	162	1.0	0.72
TC11-21	195	4,024	39	0	2,282	6,674	1,141	14,161	14,327	352	0	14,679	-519	-3.7	0.57
TC11-22	200	4,546	46	0	2,371	7,205	1,151	15,319	15,560	352	0	15,912	-593	-3.9	0.52

Notes:

1. Coal Rate by Syngas Combustor carbon balance.

2. Nitrogen is the sum of FI609 and FI6080

3. TC11-1 to TC11-16 and TC11-18 were air blown; TC11-17, TC11-19, and TC11-20 were enhanced air; TC11-21 and TC11-22 were oxygen blown.

Table 3.5-2 Carbon Balances

Operating Period	Average Relative Hours	Carbon In (Feed)			Carbon Out (Products)				In - Out	(In- Out)/In	Carbon Conversion[2]
		Coal[1] lb/hr	Coke B. lb/hr	Total lb/hr	Syngas lb/hr	Standpipe lb/hr	PCD Solids lb/hr	Total lb/hr	lb/hr	%	%
TC11-1	1	1,819	0	1,819	1,878	0.0	60	1,938	-119	-7	96.9
TC11-2	10	1,089	0	1,089	1,184	0.0	60	1,244	-155	-14	95.2
TC11-3	18	1,405	0	1,405	1,492	0.0	57	1,549	-144	-10	96.3
TC11-4	23	1,535	0	1,535	1,616	0.0	44	1,660	-125	-8	97.3
TC11-5	36	2,030	0	2,030	1,867	0.0	48	1,915	115	6	97.5
TC11-6	50	1,379	0	1,379	1,172	0.0	49	1,221	158	11	96.0
TC11-7	60	1,465	24	1,489	1,320	0.0	51	1,371	118	8	96.3
TC11-8	92	1,416	30	1,446	1,271	0.0	47	1,318	128	9	96.4
TC11-9	95	1,411	22	1,434	1,256	0.0	47	1,304	130	9	96.4
TC11-10	115	1,398	16	1,414	1,289	0.0	21	1,310	104	7	98.4
TC11-11	126	1,408	0	1,408	1,225	0.0	14	1,239	169	12	98.9
TC11-12	132	2,070	0	2,070	1,992	0.0	46	2,038	31	2	97.7
TC11-13	137	1,927	0	1,927	1,840	0.0	42	1,882	45	2	97.7
TC11-14	144	1,362	18	1,380	1,232	0.0	43	1,275	105	8	96.6
TC11-15	148	1,823	30	1,853	1,762	0.0	54	1,816	37	2	97.0
TC11-16	153	1,890	59	1,949	1,834	0.0	60	1,894	54	3	96.8
TC11-17	159	1,495	30	1,525	1,608	0.0	33	1,641	-116	-8	98.0
TC11-18	174	951	32	984	832	0.0	18	849	135	14	97.9
TC11-19	185	1,246	30	1,277	1,199	0.0	26	1,225	51	4	97.9
TC11-20	189	1,332	30	1,363	1,278	0.0	46	1,324	39	3	96.5
TC11-21	195	1,725	30	1,756	1,758	0.0	83	1,841	-85	-5	95.5
TC11-22	200	1,954	35	1,990	1,875	0.0	132	2,007	-17	-1	93.4

Notes:

1. Coal carbon determined by Syngas Combustor carbon balance.
2. Carbon Conversion based on Products method.
3. TC11-1 to TC11-16 and TC11-18 were air blown; TC11-17, TC11-19, and TC11-20 were enhanced air; TC11-21 and TC11-22 were oxygen blown.

Table 3.5-3 Nitrogen, Hydrogen, Oxygen, Calcium, and Silica Mass Balances

Operating Period	Average Relative Hours	Nitrogen		Hydrogen		Oxygen		Calcium		Silica	
		(In- Out) In	In - Out	(In- Out) In	In - Out	(In- Out) In	In - Out	(In- Out) In	In - Out	(In- Out) In	In - Out
		%	lb/hr	%	lb/hr	%	lb/hr	%	lb/hr	%	lb/hr
TC11-1	1	8.2	1,325	36.0	122	6.1	297	34.3	19	17.6	39
TC11-2	10	9.8	1,608	4.9	12	-13.4	-518	-9.8	-3	-37.7	-51
TC11-3	18	10.2	1,708	15.5	43	-10.5	-453	13.4	6	-6.6	-11
TC11-4	23	10.4	1,765	16.8	50	-10.6	-475	12.6	6	3.0	6
TC11-5	36	3.8	721	3.1	11	-0.8	-44	32.5	20	23.3	57
TC11-6	50	2.3	377	13.3	35	5.9	246	1.3	1	-6.5	-11
TC11-7	60	4.4	726	7.8	22	2.8	124	9.0	4	-1.7	-3
TC11-8	92	5.1	857	15.1	42	5.8	248	7.5	3	-5.4	-9
TC11-9	95	4.8	794	14.0	39	5.0	212	7.4	3	-5.9	-10
TC11-10	115	2.9	503	-2.1	-6	-2.1	-92	6.6	3	-0.1	0
TC11-11	126	4.8	816	6.3	18	2.6	113	-3.9	-2	-4.8	-8
TC11-12	132	4.4	763	-10.3	-38	-7.6	-425	30.0	19	27.0	68
TC11-13	137	4.8	816	-2.9	-10	-3.8	-208	23.3	14	13.2	31
TC11-14	144	5.9	867	7.5	20	2.0	83	-16.6	-7	-32.5	-54
TC11-15	148	4.0	623	5.1	17	-0.4	-20	9.2	5	3.6	8
TC11-16	153	4.9	801	-2.2	-8	-3.6	-190	21.6	13	25.2	59
TC11-17	159	-1.0	-85	-17.8	-71	-9.9	-534	13.5	6	16.9	31
TC11-18	174	2.4	306	12.4	29	5.8	204	32.4	10	30.2	36
TC11-19	185	0.0	3	-2.0	-6	-1.1	-49	25.1	10	19.0	29
TC11-20	189	-0.3	-34	0.3	1	-1.5	-67	39.9	16	7.1	12
TC11-21	195	-8.0	-537	1.0	4	-4.6	-220	74.3	39	9.2	19
TC11-22	200	-9.1	-660	-2.1	-8	-6.7	-342	69.2	41	42.5	100

Notes:

1. TC11-1 to TC11-16 and TC11-18 were air blown; TC11-17, TC11-19, and TC11-20 were enhanced air; TC11-21 and TC11-22 were oxygen blown.

Table 3.5-4 Typical Air-Blown Component Mass Balances

	Nitrogen	Hydrogen	Oxygen	Calcium	Silica
Operating Period	TC11-13	TC11-13	TC11-13	TC11-13	TC11-13
Date Start	4/15/2003	4/15/2003	4/15/2003	4/15/2003	4/15/2003
Time Start	22:30	22:30	22:30	22:30	22:30
Time End	5:30	5:30	5:30	5:30	5:30
Fuel	Fal. Lig.	Fal. Lig.	Fal. Lig.	Fal. Lig.	Fal. Lig.
Riser Temperature, ^{O}F	1,723	1,723	1,723	1,723	1,723
Pressure, psig	194	194	194	194	194
In, pounds/hr					
Fuel	31	266	1,682	59	235
Coke Breeze			0		0
Air	10,105		3,070		
Nitrogen	7,004				
Steam		84	670		
Total	17,139	350	5,422	59	235
Out, pounds/hr					
Synthesis Gas	16,323	359	5,576		
PCD Solids	1	1	54	45	203
Reactor			0	0	0
Total	16,323	360	5,630	45	203
(In-Out)/In, %	4.8%	-2.9%	-3.8%	23.3%	13.2%
(In-Out), pounds per hour	816	-10	-208	14	31

Table 3.5-5 Typical Oxygen-Blown Component Mass Balances

	Nitrogen	Hydrogen	Oxygen	Calcium	Silica
Operating Period	TC11-21	TC11-21	TC11-21	TC11-21	TC11-21
Date	4/18/2003	4/18/2003	4/18/2003	4/18/2003	4/18/2003
Time Start	10:30	10:30	10:30	10:30	10:30
Time End	12:30	12:30	12:30	12:30	0:00
Fuel	Fal. Lig.	Fal. Lig.	Fal. Lig.	Fal. Lig.	Fal. Lig.
Riser Temperature, ^{O}F	1,682	1,682	1,682	1,682	1,682
Pressure, psig	136	136	136	136	136
In, pounds/hr					
Fuel	28	236	1,493	52	208
Coke Breeze			5		1
Oxygen			2,282		
Nitrogen	6,674				
Steam		127	1,014		
Total	6,702	363	4,794	52	209
Out, pounds/hr					
Synthesis Gas	7,238	359	4,973		
PCD Solids	0	1	42	13	190
Reactor			0	0	0
Total	7,238	359	5,014	13	190
(In-Out)/In, %	-8.0%	1.0%	-4.6%	74.3%	9.2%
(In-Out), pounds per hour	-537	4	-220	39	19

Table 3.5-6 Sulfur Balances

Operating Period	Average Relative Hours	Feeds (In)	Products (Out)				In - Out	(In- Out)/In	Sulfur Removal			Sulfur
		Coal	Syngas[1]	PCD Solids	SP Solids	Total			Gas[4]	Products	Solids	Emissions
		lb/hr	lb/hr	lb/hr	lb/hr	lb/hr	lb/hr	%	%	%	%	lb SO_2/MMBtu
TC11-1	1	29.5	11.4	2.9	0.0	14.4	15.1	51.3	61	20	10	0.76
TC11-2	10	17.6	13.7	2.9	0.0	16.6	1.0	5.7	22	18	17	1.51
TC11-3	18	22.8	18.1	3.0	0.0	21.0	1.8	7.9	21	14	13	1.55
TC11-4	23	25.3	19.5	3.2	0.0	22.7	2.6	10.2	23	14	12	1.54
TC11-5	36	34.8	26.3	4.0	0.0	30.3	4.5	12.8	24	13	12	1.61
TC11-6	50	24.1	17.1	3.7	0.0	20.9	3.2	13.2	29	18	16	1.55
TC11-7	60	24.3	20.2	3.7	0.0	24.0	0.3	1.4	17	16	15	1.70
TC11-8	92	22.7	16.3	0.9	0.0	17.2	5.5	24.4	28	5	4	1.41
TC11-9	95	22.6	17.1	0.6	0.0	17.7	4.9	21.8	24	3	3	1.49
TC11-10	115	22.1	24.7	1.9	0.0	26.5	-4.5	-20.3	-12	7	9	2.16
TC11-11	126	22.1	20.7	1.6	0.0	22.4	-0.3	-1.3	6	7	7	1.81
TC11-12	132	32.7	28.4	4.0	0.0	32.4	0.3	0.9	13	12	12	1.68
TC11-13	137	30.7	30.7	3.6	0.0	34.3	-3.6	-11.8	0	10	12	1.94
TC11-14	144	21.9	20.2	3.8	0.0	24.0	-2.1	-9.8	8	16	17	1.80
TC11-15	148	32.8	26.8	5.0	0.0	31.9	1.0	2.9	18	16	15	1.78
TC11-16	153	40.1	26.9	5.8	0.0	32.7	7.4	18.5	33	18	15	1.72
TC11-17	159	34.1	25.3	2.3	0.0	27.6	6.5	19.0	26	8	7	2.04
TC11-18	174	17.3	14.5	0.8	0.0	15.3	2.0	11.4	16	5	5	1.83
TC11-19	185	24.6	20.7	1.3	0.0	22.1	2.6	10.4	16	6	5	2.03
TC11-20	189	27.1	20.6	2.6	0.0	23.2	3.9	14.4	24	11	10	1.89
TC11-21	195	36.3	24.7	4.9	0.0	29.6	6.7	18.5	32	17	14	1.76
TC11-22	200	41.8	27.0	4.0	0.0	31.0	10.8	25.8	35	13	10	1.70

Notes:

1. Synthesis gas sulfur emissions determined from synthesis gas combustor SO_2 analyzer.
2. There was no sorbent feed to the Transport Gasifier during TC11.
3. TC11-1 to TC11-16 and TC11-18 were air blown; TC11-17, TC11-19, and TC11-20 were enhanced air; TC11-21 and TC11-22 were oxygen blown.
4. Negative sulfur removals were assumed to actually be 0% sulfur removal. (TC11-10, gas method)

Table 3.5-7 Energy Balances

Operating Period	Average Relative Hours	Feeds (In)				Products (Out)						In - Out	(In- Out)/In	Efficiency[5]		
						Latent	Sensible	PCD	Reactor	Heat				Raw		Corrected[4]
		Coal	Air	Steam	Total	Syngas	Syngas	Solids	Solids	Loss	Total			Cold	Hot	Cold
		10^6 Btu/hr	10^6 Btu/hr	10^6 Btu/hr	10^6 Btu/hr	10^6 Btu/hr	10^6 Btu/hr	10^6 Btu/hr	10^6 Btu/hr	10^6 Btu/hr	10^6 Btu/hr	10^6 Btu/hr	%	%	%	%
TC11-1	1	29.1	0.6	1.0	30.7	14.8	9.2	0.8	0.00	3.5	28.3	2.4	7.9	52.3	84.7	72.1
TC11-2	10	17.4	0.5	1.1	19.1	4.3	8.9	0.8	0.00	3.5	17.6	1.5	7.8	24.6	75.4	49.5
TC11-3	18	22.5	0.6	1.0	24.0	7.6	9.5	0.8	0.00	3.5	21.5	2.6	10.6	35.5	79.8	59.2
TC11-4	23	24.4	0.6	1.0	26.0	9.0	9.7	0.7	0.00	3.5	22.9	3.1	12.0	39.3	81.7	62.2
TC11-5	36	31.6	0.8	1.0	33.4	14.9	11.9	0.9	0.00	3.5	31.2	2.2	6.7	47.9	86.0	67.7
TC11-6	50	21.3	0.6	1.0	22.8	7.3	9.4	0.9	0.00	3.5	21.1	1.7	7.5	34.5	79.1	62.5
TC11-7	60	23.0	0.6	1.0	24.6	9.0	9.9	0.8	0.00	3.5	23.2	1.5	6.0	38.9	81.6	64.2
TC11-8	92	22.2	0.6	1.0	23.8	8.6	9.3	0.7	0.00	3.5	22.1	1.7	7.3	38.7	80.9	66.2
TC11-9	95	22.2	0.6	1.0	23.8	8.3	9.4	0.8	0.00	3.5	22.0	1.8	7.4	37.8	80.6	65.0
TC11-10	115	22.0	0.7	1.0	23.6	8.0	10.7	0.4	0.00	3.5	22.6	1.1	4.5	35.3	82.5	62.3
TC11-11	126	22.1	0.6	1.0	23.8	7.6	10.1	0.3	0.00	3.5	21.5	2.3	9.7	35.5	82.4	63.2
TC11-12	132	32.6	0.8	1.0	34.4	17.3	11.7	0.7	0.00	3.5	33.2	1.2	3.5	52.1	87.2	68.8
TC11-13	137	30.5	0.8	1.0	32.3	14.8	11.7	0.7	0.00	3.5	30.6	1.6	5.0	48.3	86.4	66.2
TC11-14	144	21.6	0.6	1.0	23.2	8.5	9.0	0.5	0.00	3.5	21.6	1.6	7.1	39.4	81.3	64.2
TC11-15	148	29.0	0.7	1.0	30.8	14.7	10.5	0.8	0.00	3.5	29.4	1.4	4.4	49.9	85.5	68.5
TC11-16	153	30.2	0.8	1.0	31.9	15.6	10.6	0.9	0.00	3.5	30.6	1.3	4.2	50.9	85.6	68.4
TC11-17	159	24.0	0.1	2.3	26.4	14.2	8.5	0.6	0.00	3.5	26.7	-0.4	-1.4	53.0	84.7	75.9
TC11-18	174	15.3	0.5	1.2	17.0	3.6	7.7	0.4	0.00	3.5	15.3	1.7	9.8	23.8	74.4	53.3
TC11-19	185	19.7	0.2	1.7	21.7	9.5	7.5	0.4	0.00	3.5	20.9	0.8	3.6	45.3	81.2	76.3
TC11-20	189	21.0	0.2	1.7	23.0	9.4	7.9	0.3	0.00	3.5	21.2	1.8	7.9	44.4	81.8	75.3
TC11-21	195	27.0	0.0	1.5	28.6	17.2	7.1	1.1	0.00	3.5	28.9	-0.3	-1.1	59.4	84.0	81.0
TC11-22	200	30.5	0.0	1.5	32.1	18.6	7.3	1.7	0.00	3.5	31.2	0.9	2.7	59.7	83.2	79.3

Notes:

1. Nitrogen and sorbent assumed to enter the system at ambient temperature and therefore have zero enthalpy.
2. TC11-1 to TC11-16 and TC11-18 were air blown; TC11-17, TC11-19, and TC11-20 were enhanced air; TC11-21 and TC11-22 were oxygen blown.
3. Reference conditions are 80°F and 14.7 psia.
4. Correction is to assume that only air nitrogen is in the synthesis gas and that the reactor is adiabatic
5. Efficiencies based on the products method.

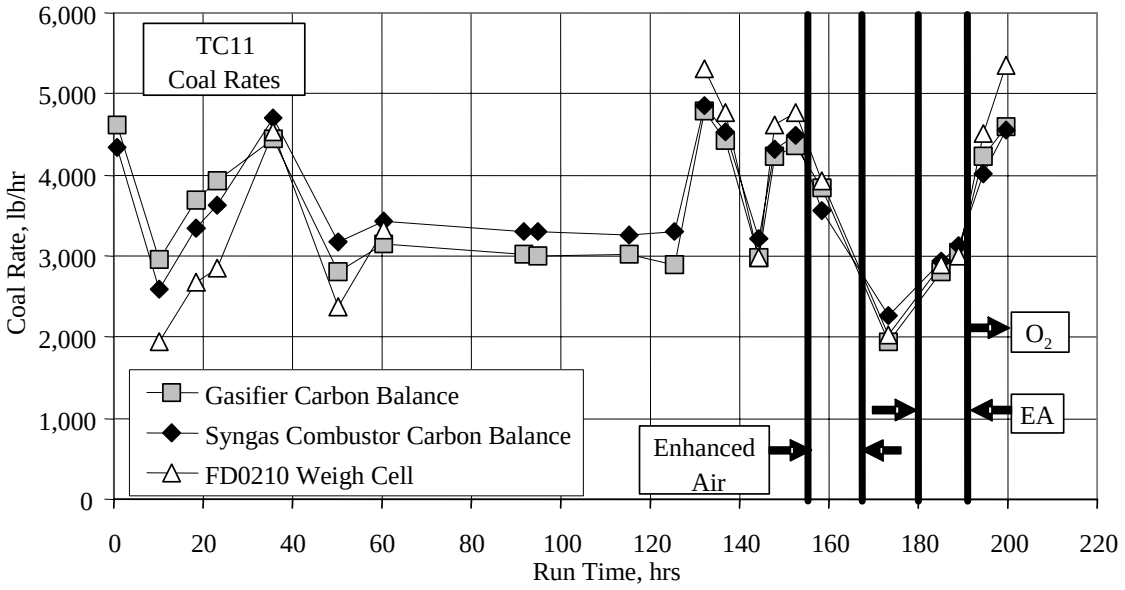

Figure 3.5-1 Coal Rates

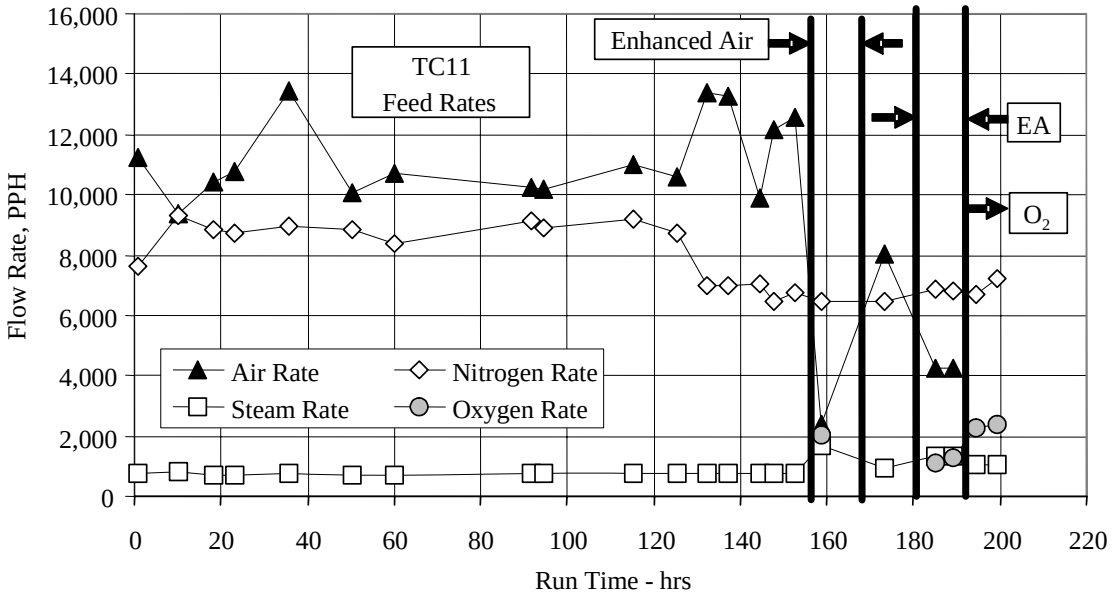

Figure 3.5-2 Air, Nitrogen, Oxygen, and Steam Rates

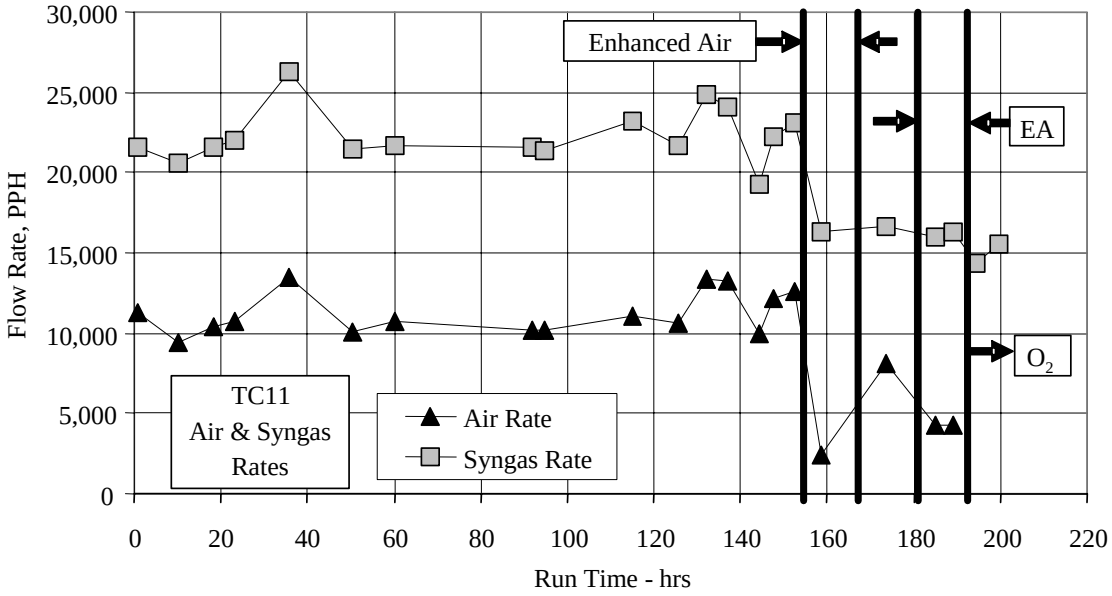

Figure 3.5-3 Air and Synthesis Gas Rates

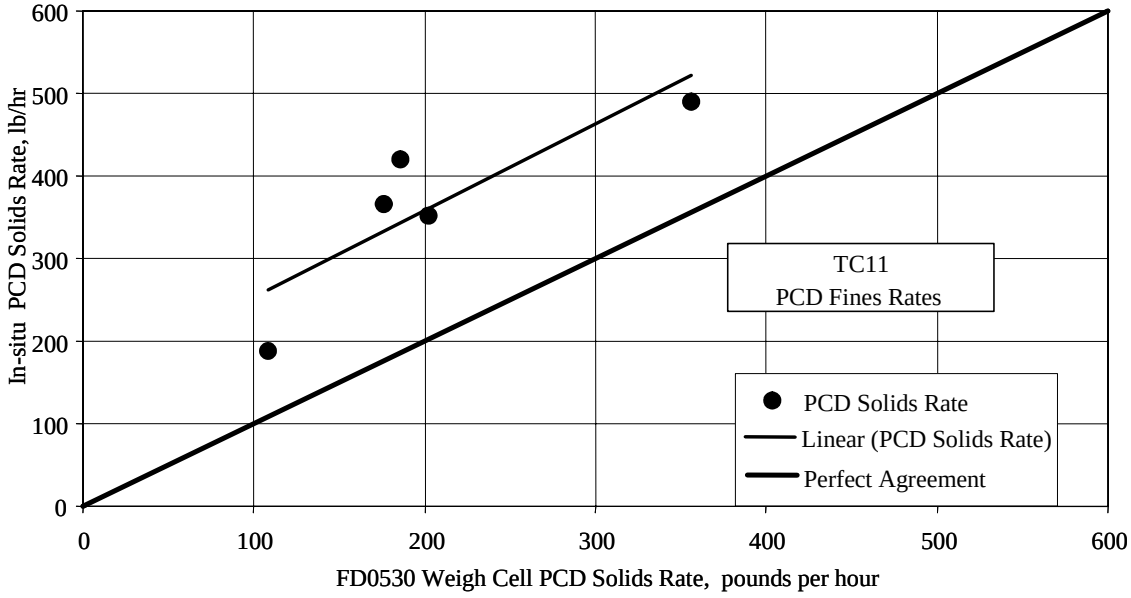

Figure 3.5-4 PCD Fines Rates

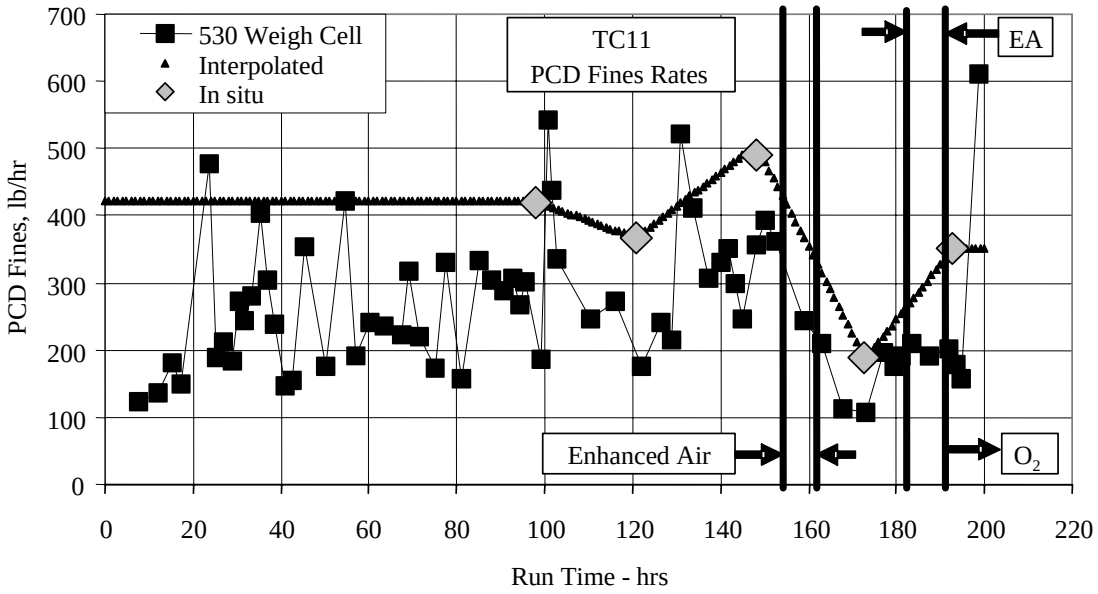

Figure 3.5-5 PCD Fines Rates

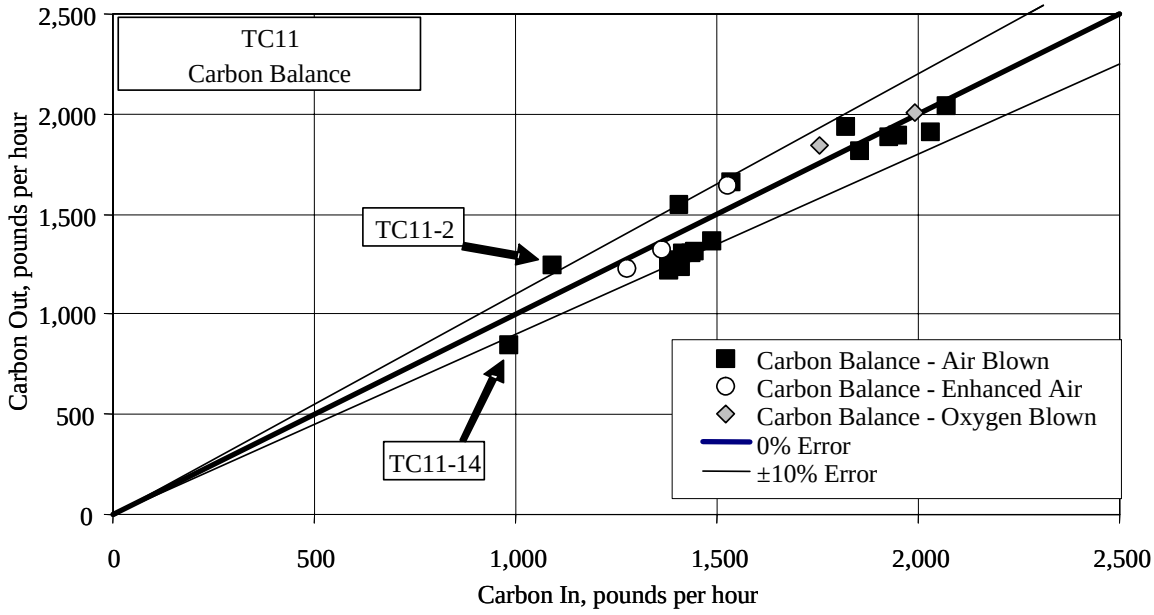

Figure 3.5-6 Carbon Balance

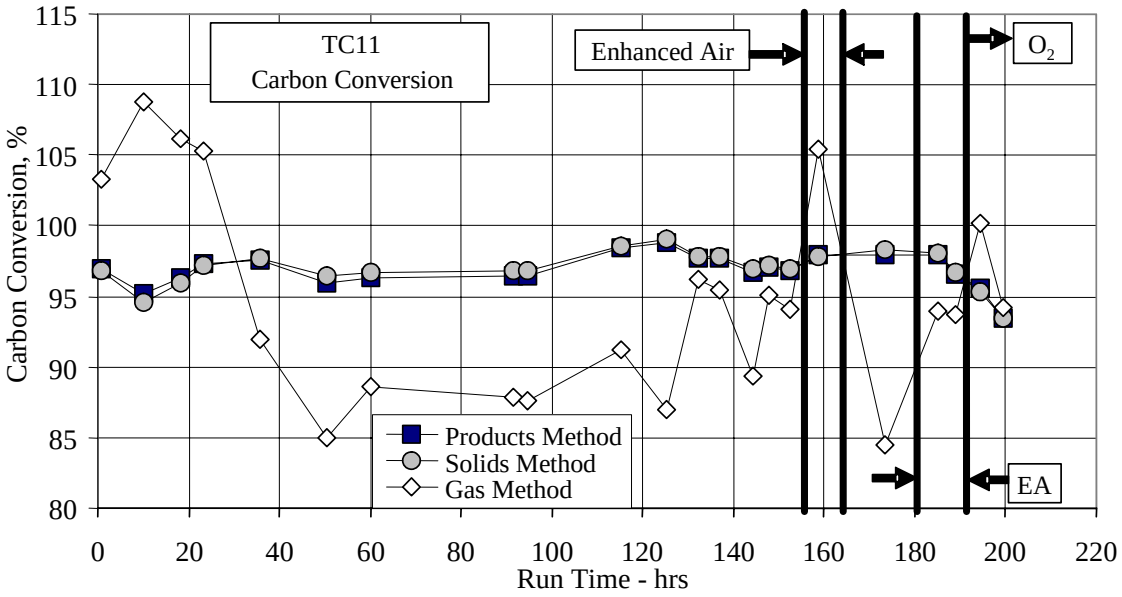

Figure 3.5-7 Carbon Conversion

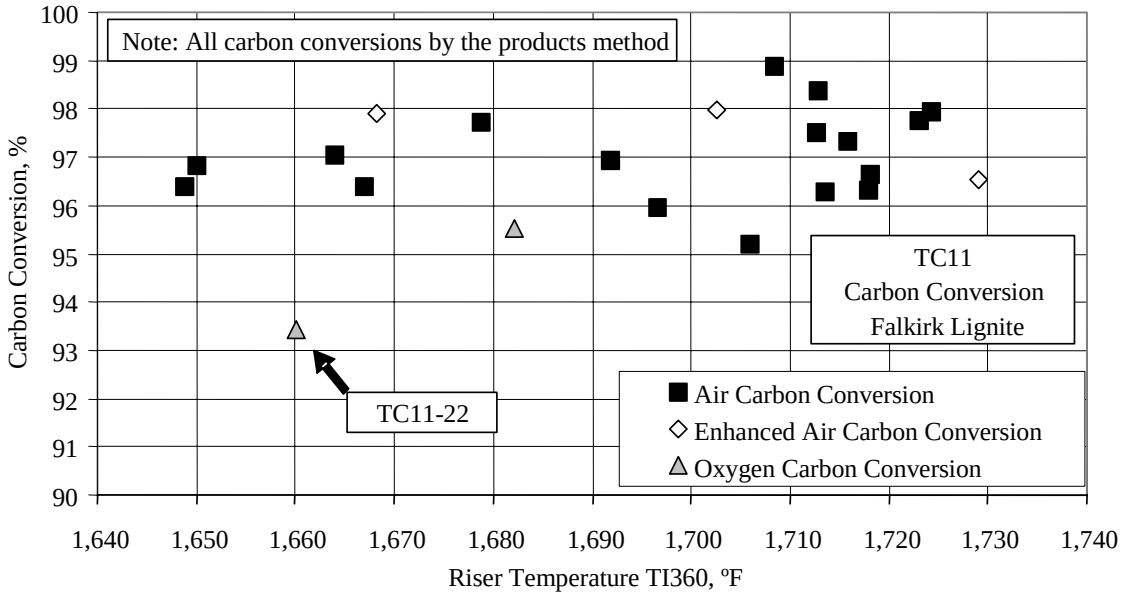

Figure 3.5-8 Carbon Conversion and Riser Temperature

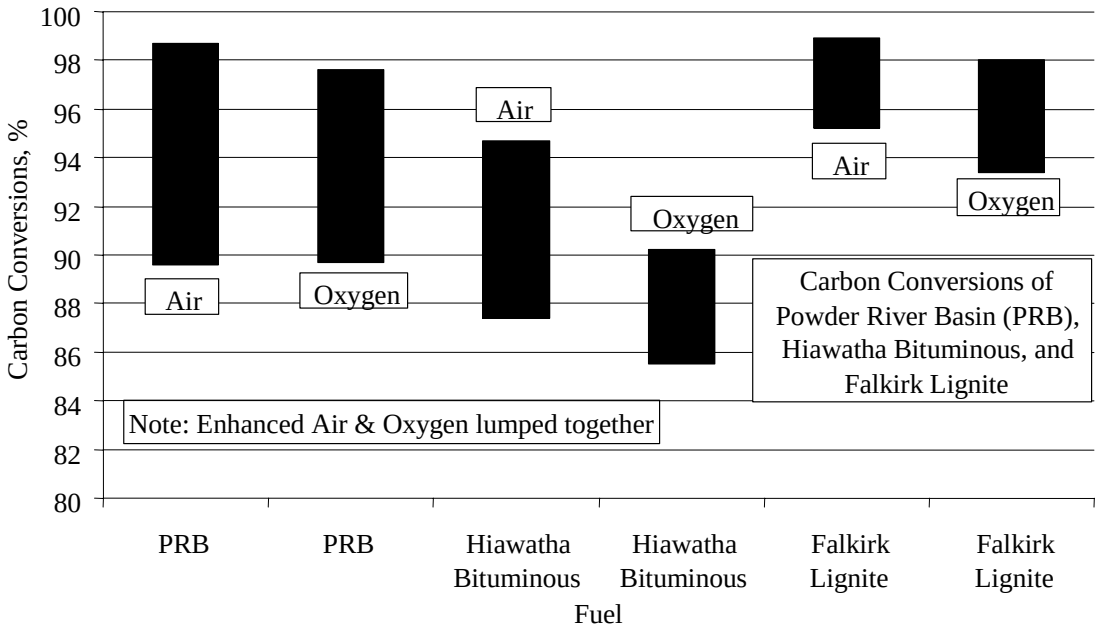

Figure 3.5-9 Carbon Conversion of Three Coals

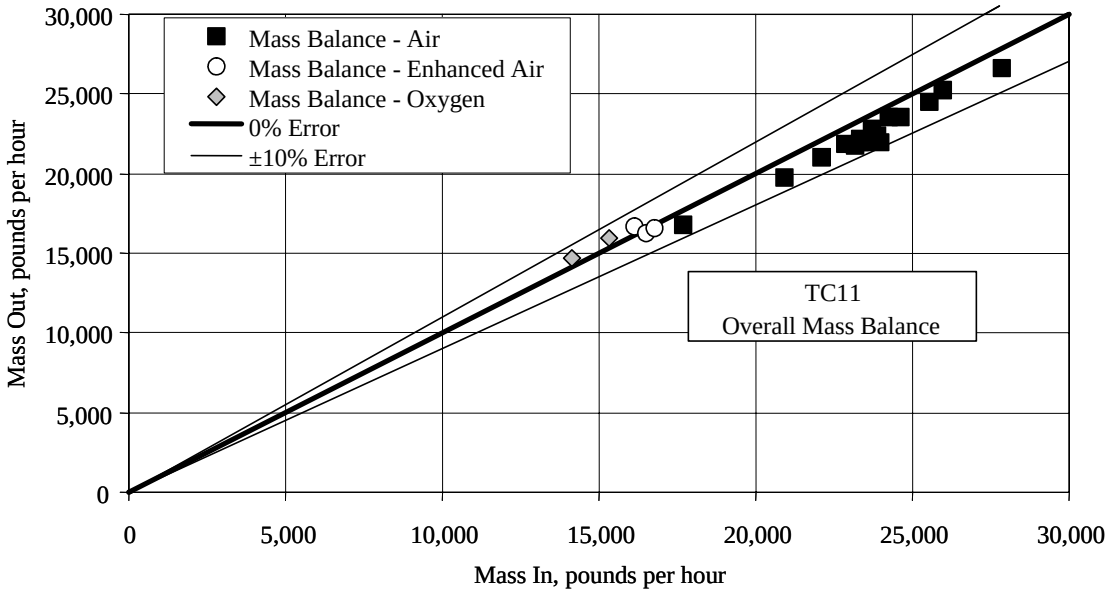

Figure 3.5-10 Overall Material Balance

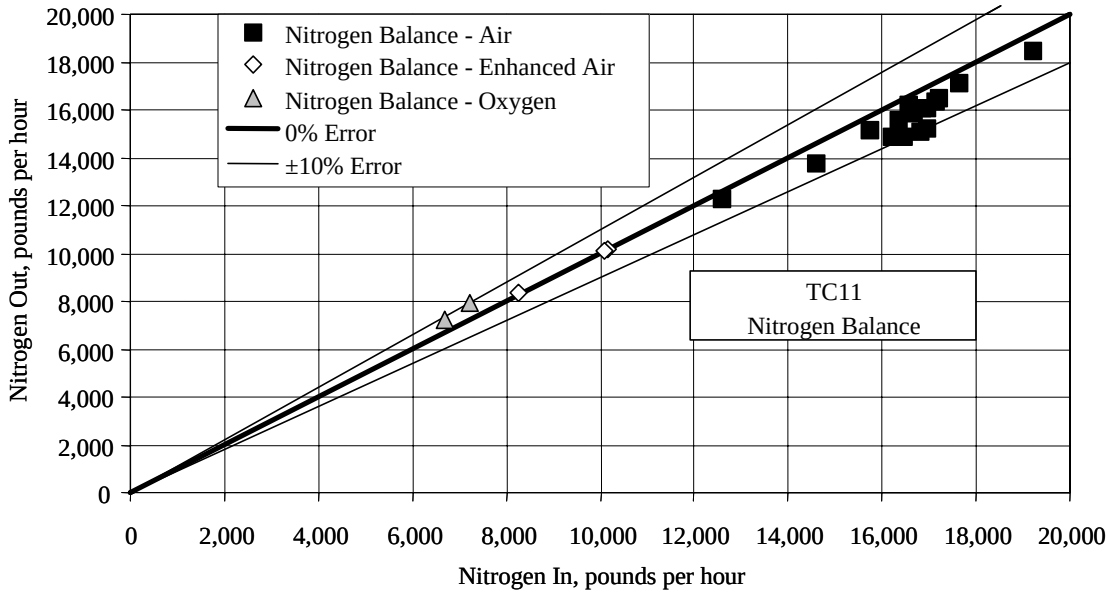

Figure 3.5-11 Nitrogen Balance

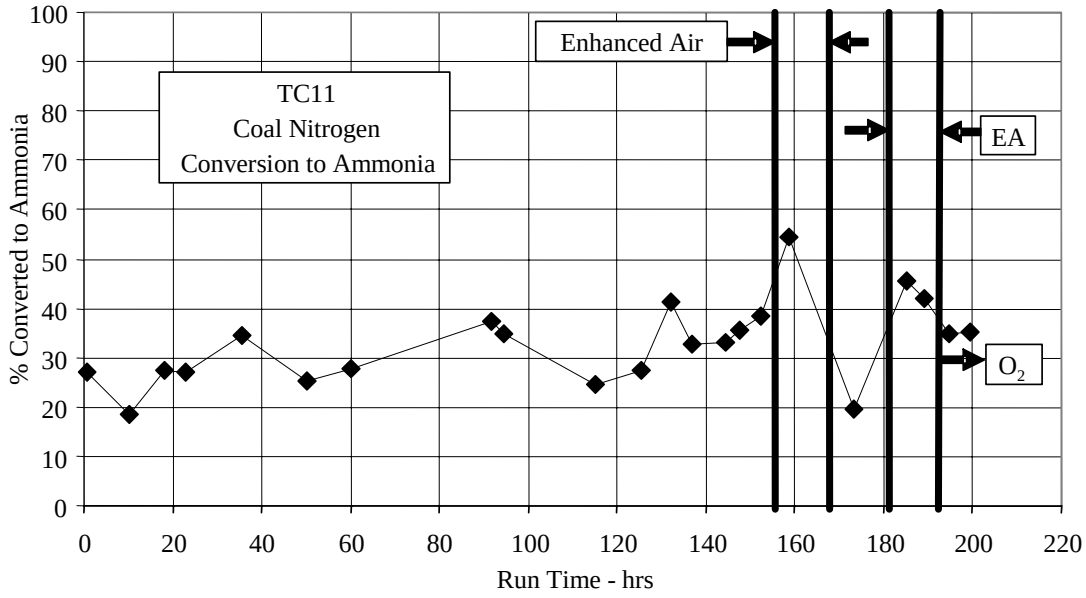

Figure 3.5-12 Coal Nitrogen Conversion to Ammonia

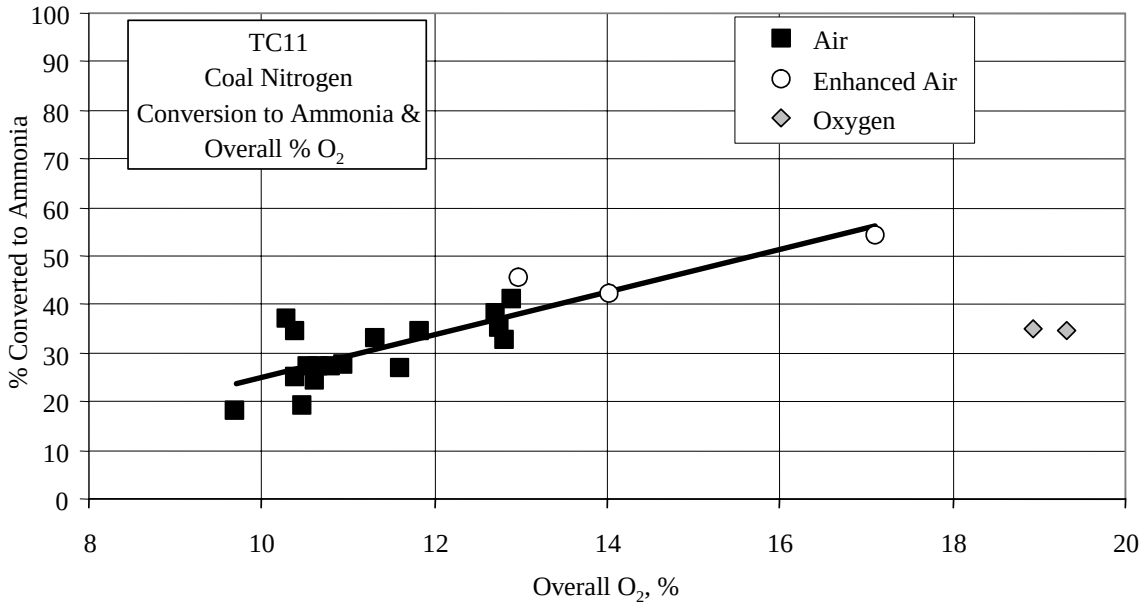

Figure 3.5-13 Coal Nitrogen Conversion to Ammonia and Percent Overall O_2

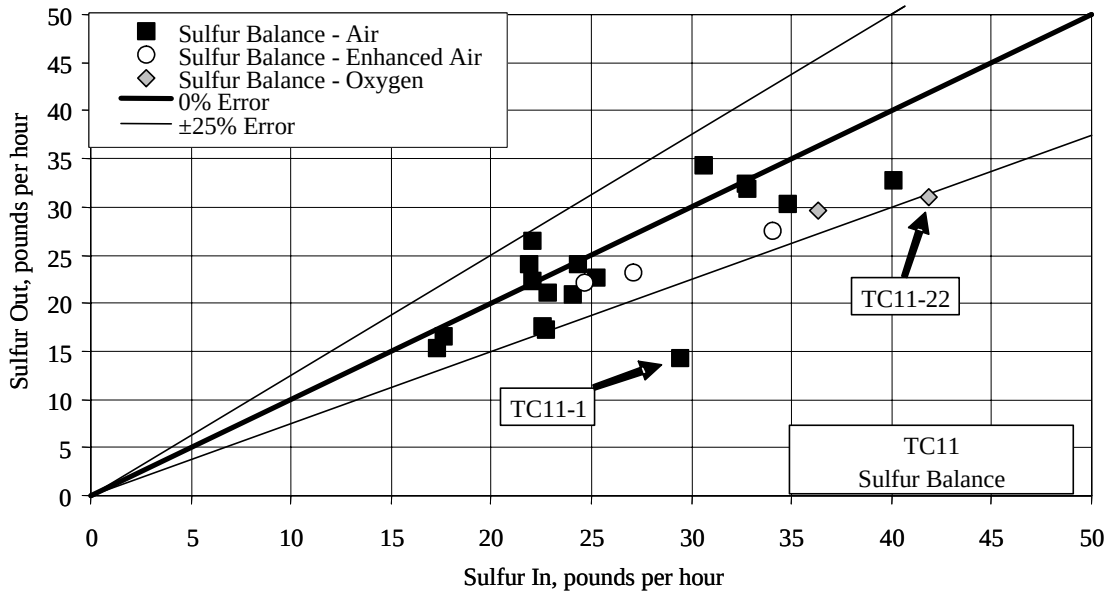

Figure 3.5-14 Sulfur Balance

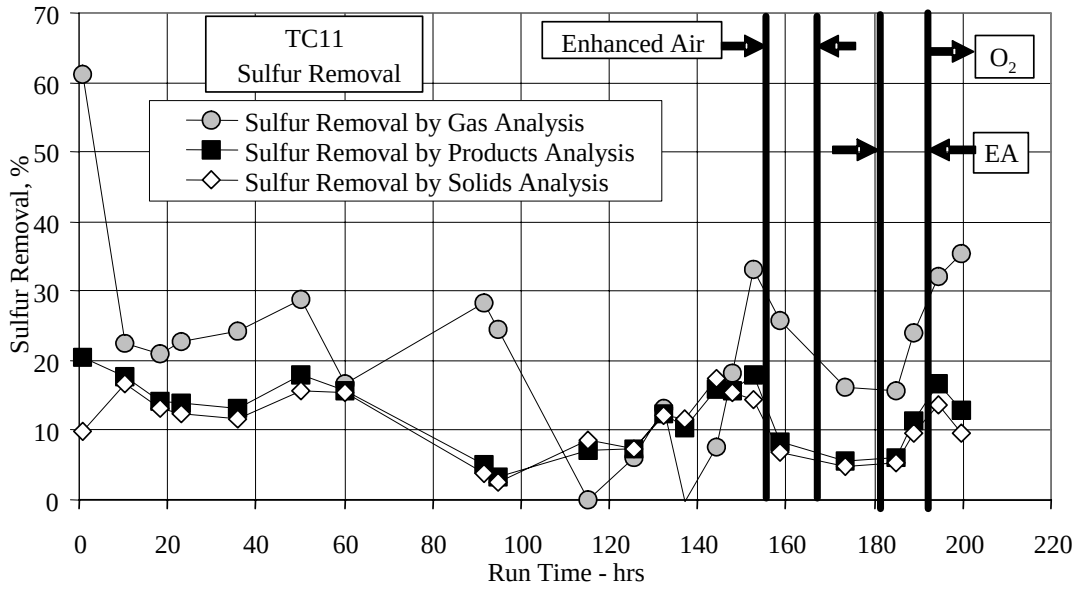

Figure 3.5-15 Sulfur Removal

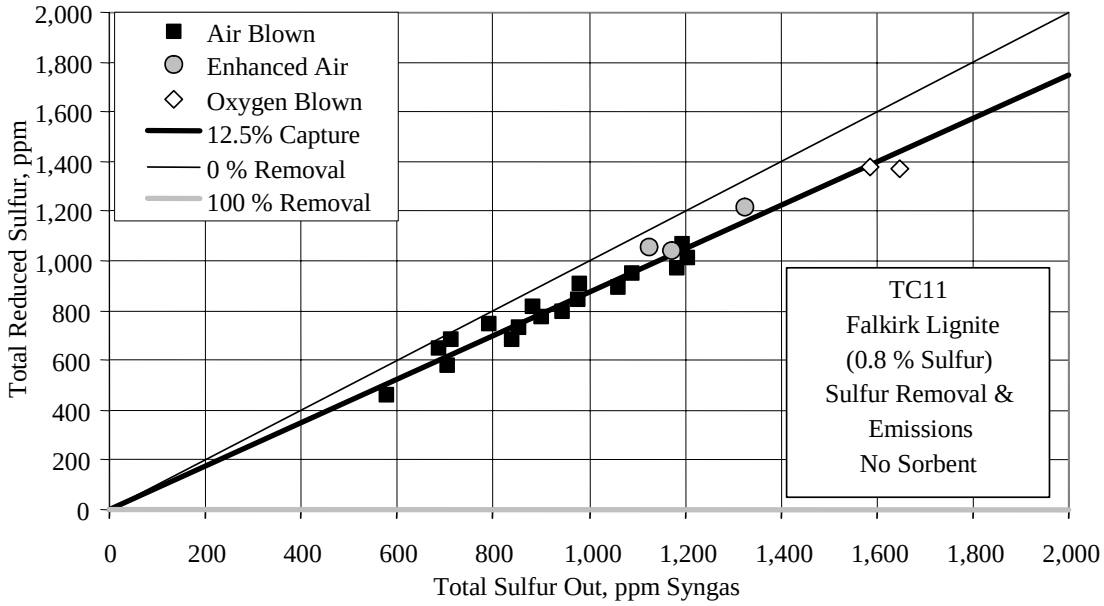

Figure 3.5-16 Sulfur Emissions

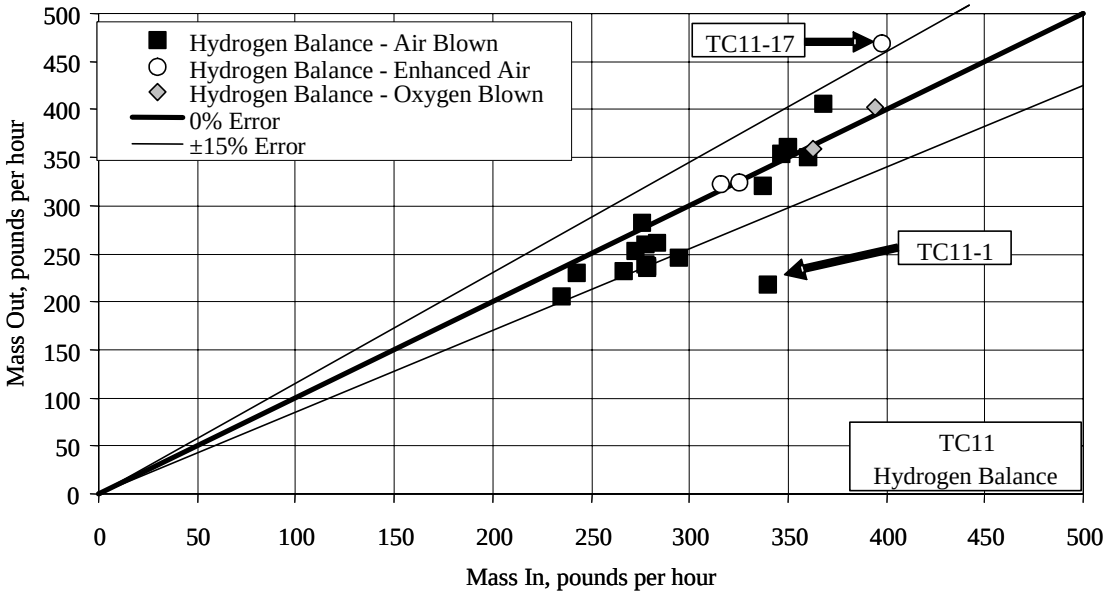

Figure 3.5-17 Hydrogen Balance

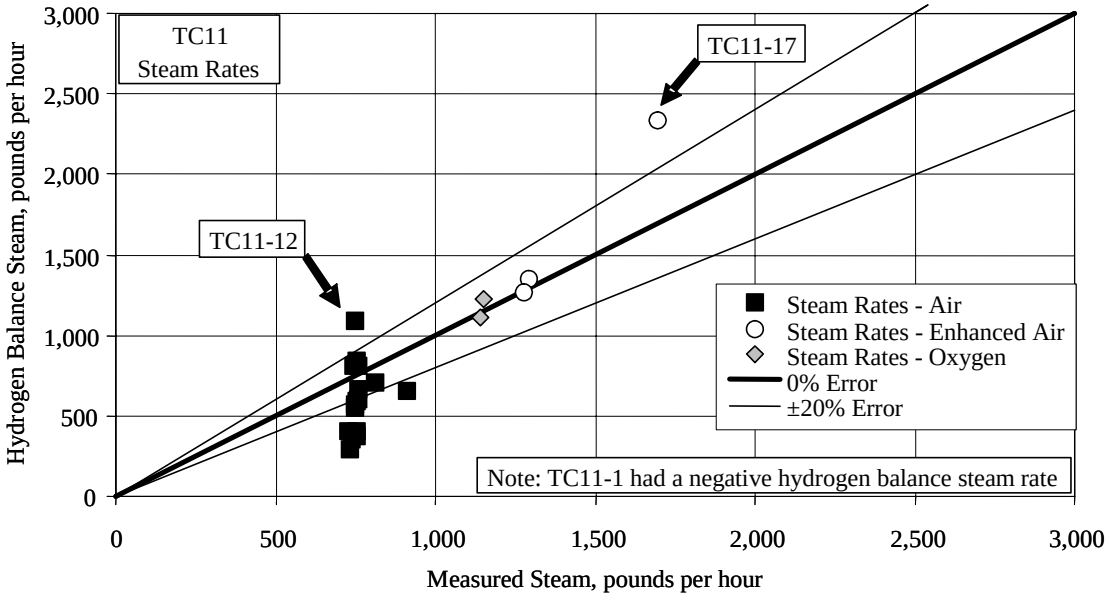

Figure 3.5-18 Steam Rates

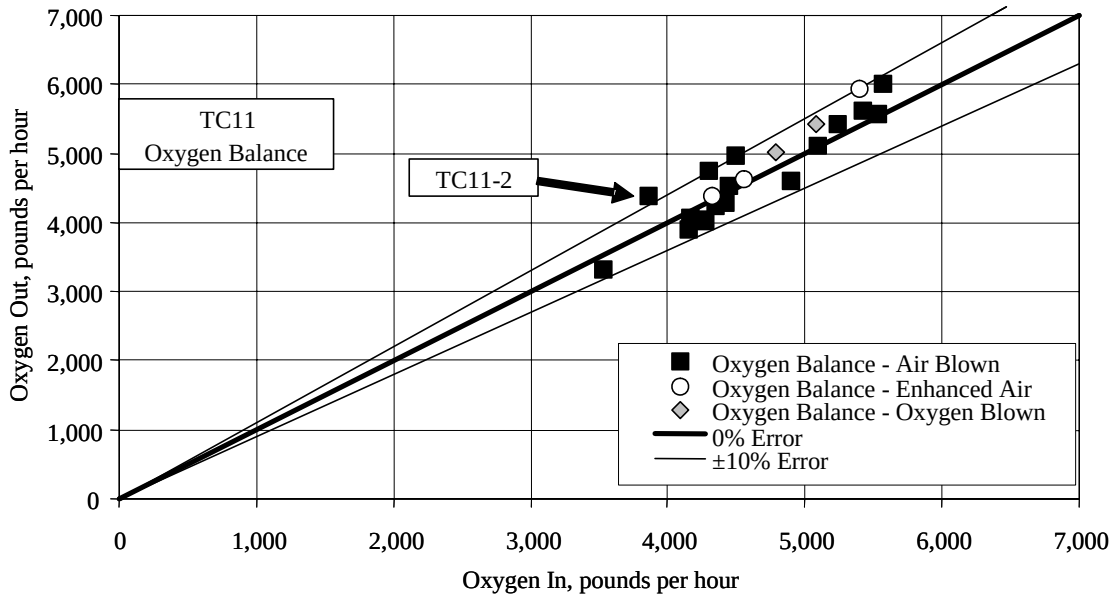

Figure 3.5-19 Oxygen Balance

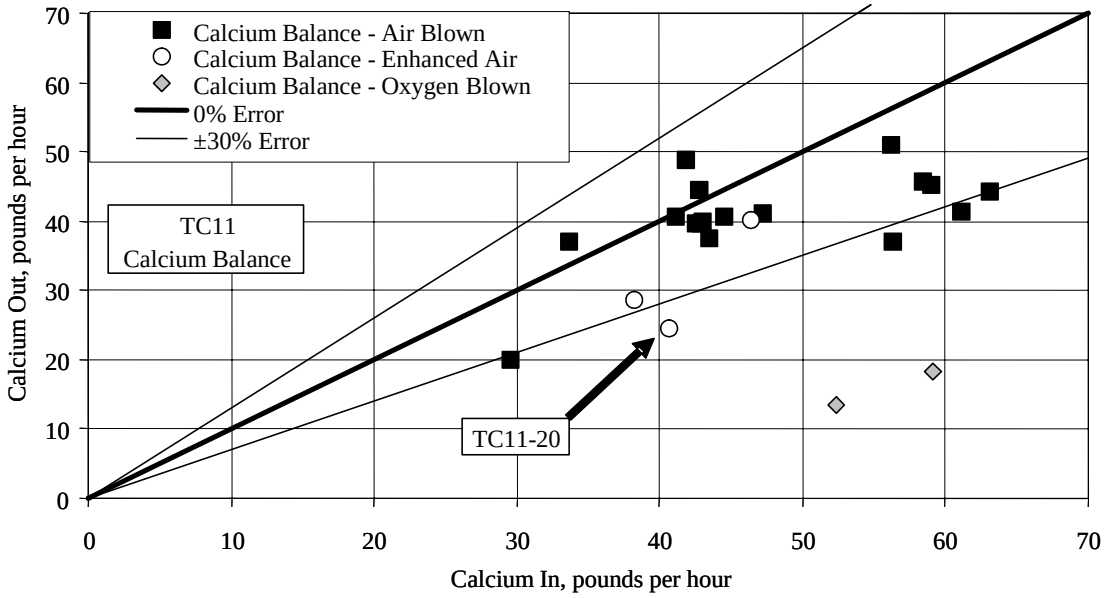

Figure 3.5-20 Calcium Balance

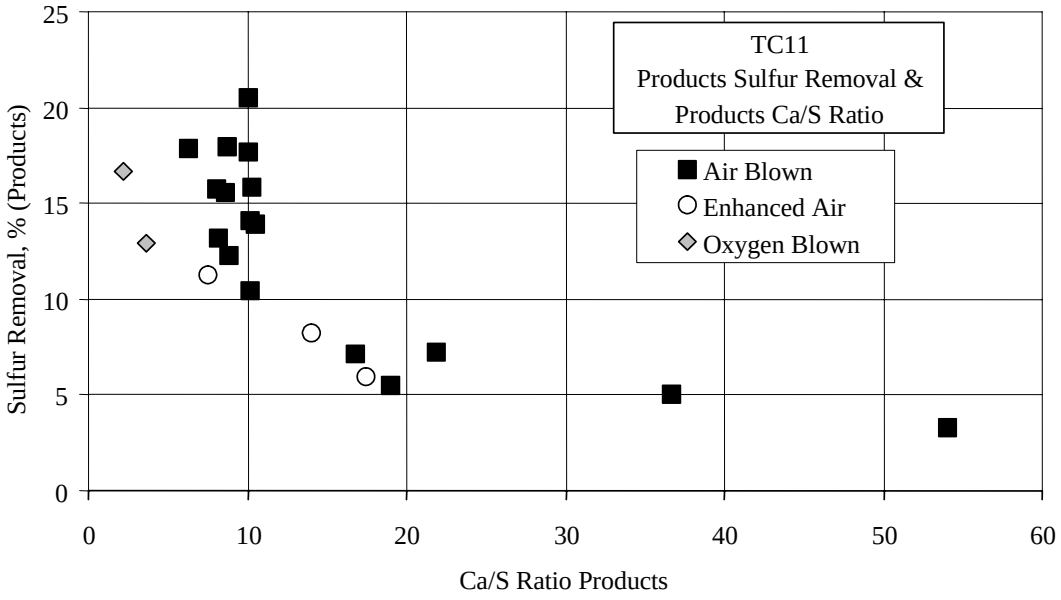

Figure 3.5-21 Sulfur Removal and PCD Solids Ca/S Ratio

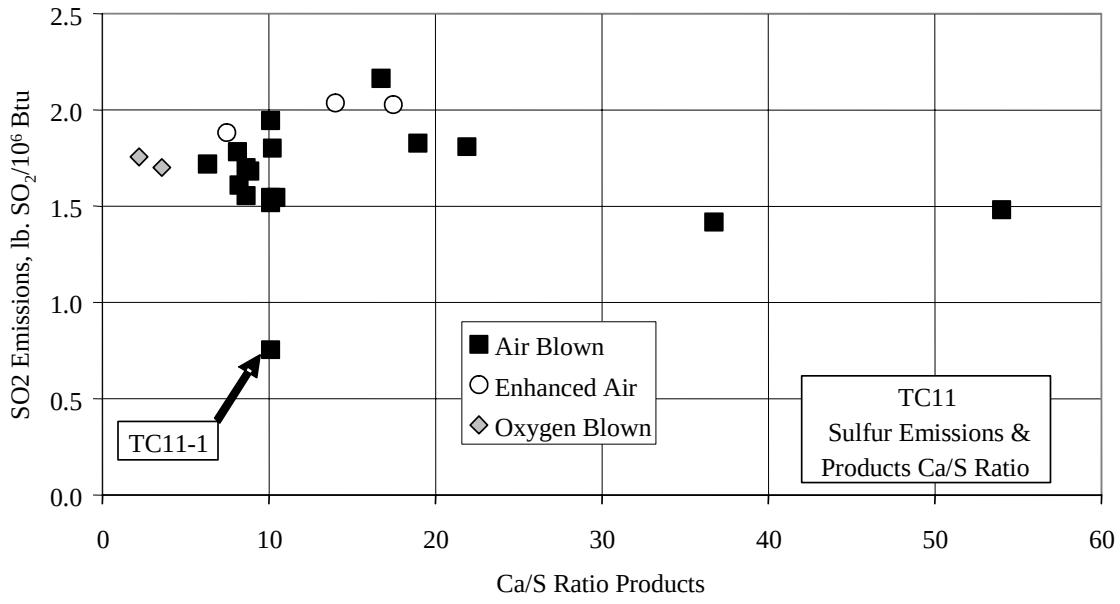

Figure 3.5-22 Sulfur Emissions and PCD Solids Ca/S Ratio

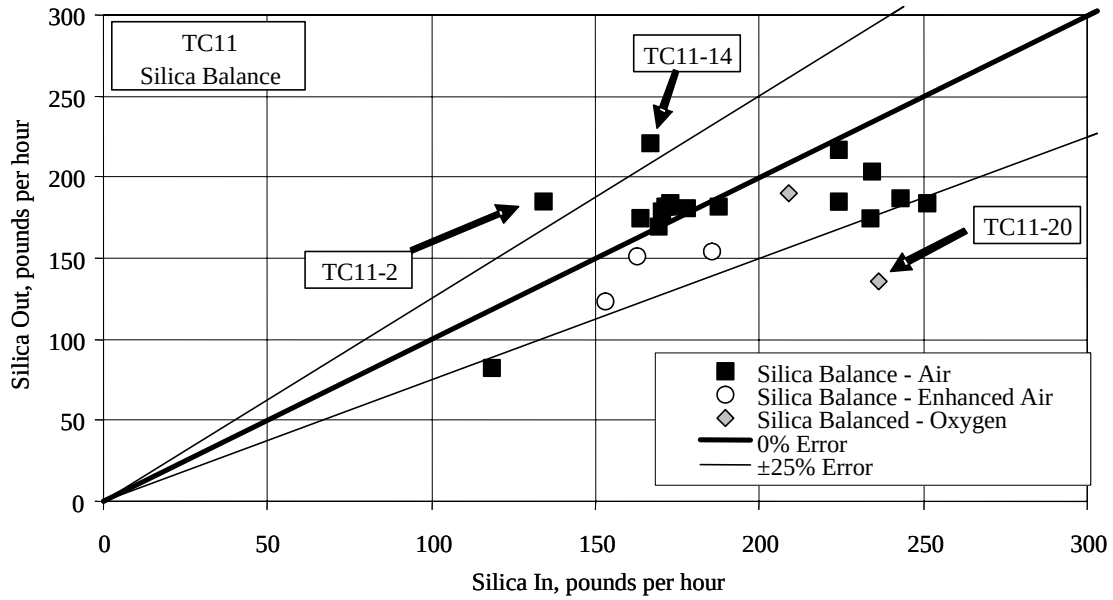

Figure 3.5-23 Silica Balance

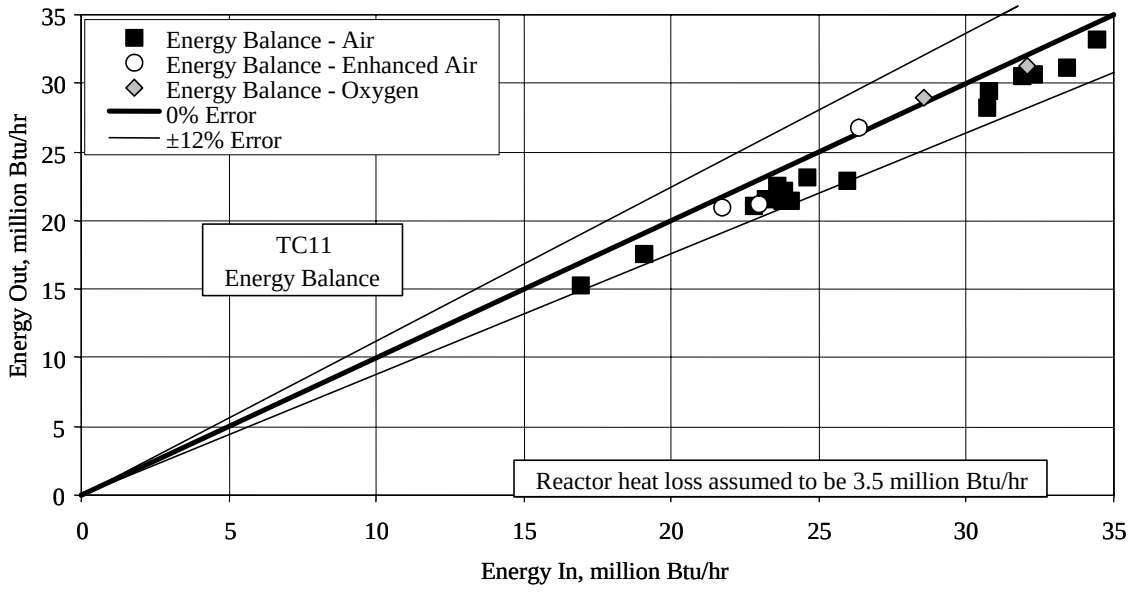

Figure 3.5-24 Energy Balance

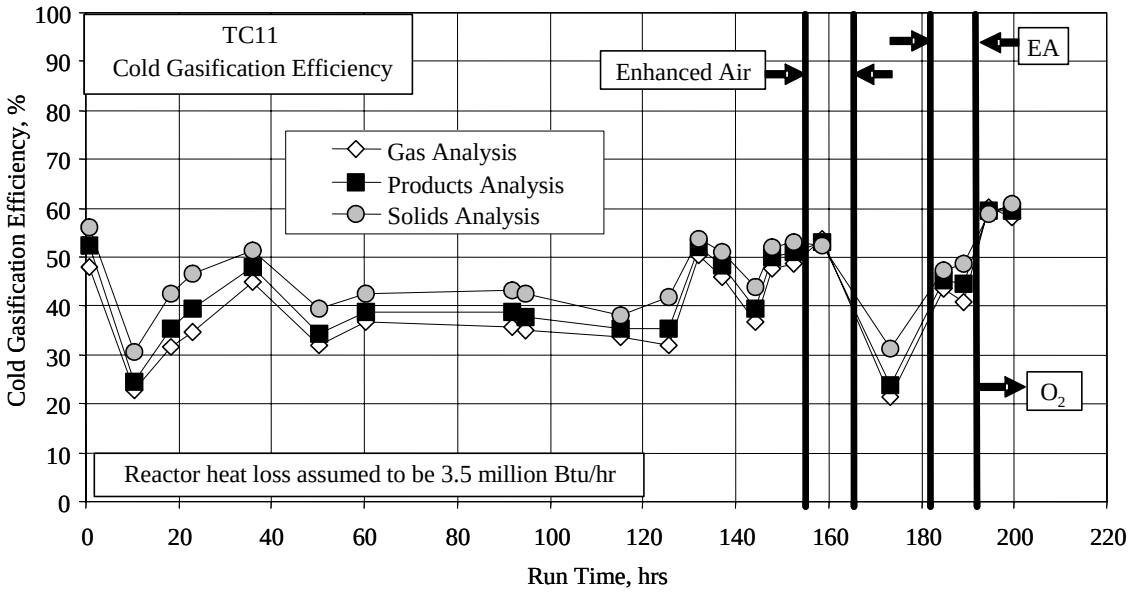

Figure 3.5-25 Cold Gasification Efficiency

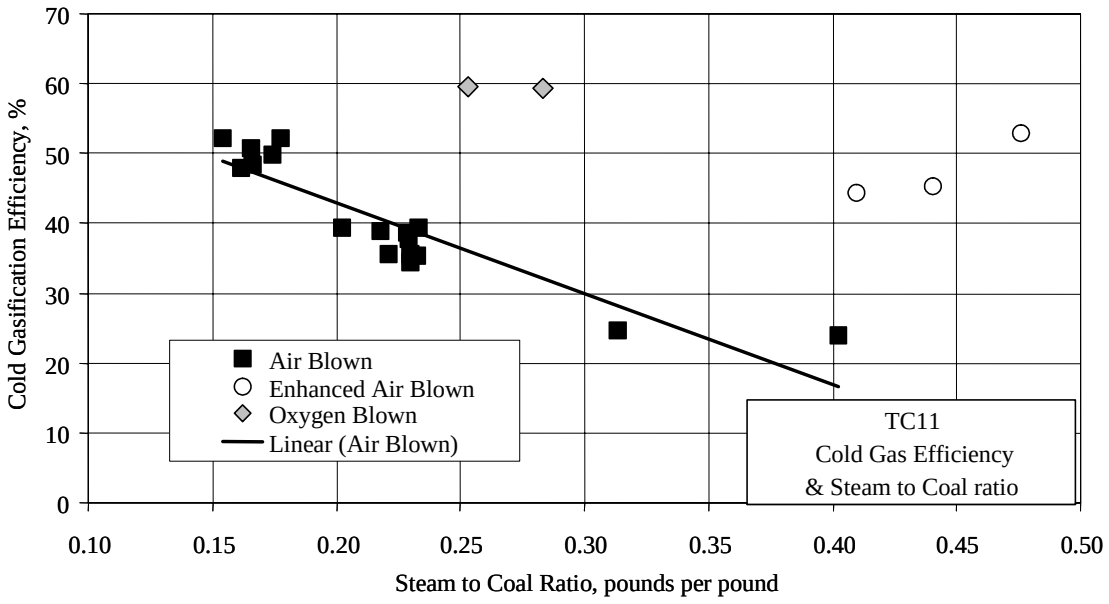

Figure 3.5-26 Cold Gasification Efficiency and Steam-to-Coal Ratio

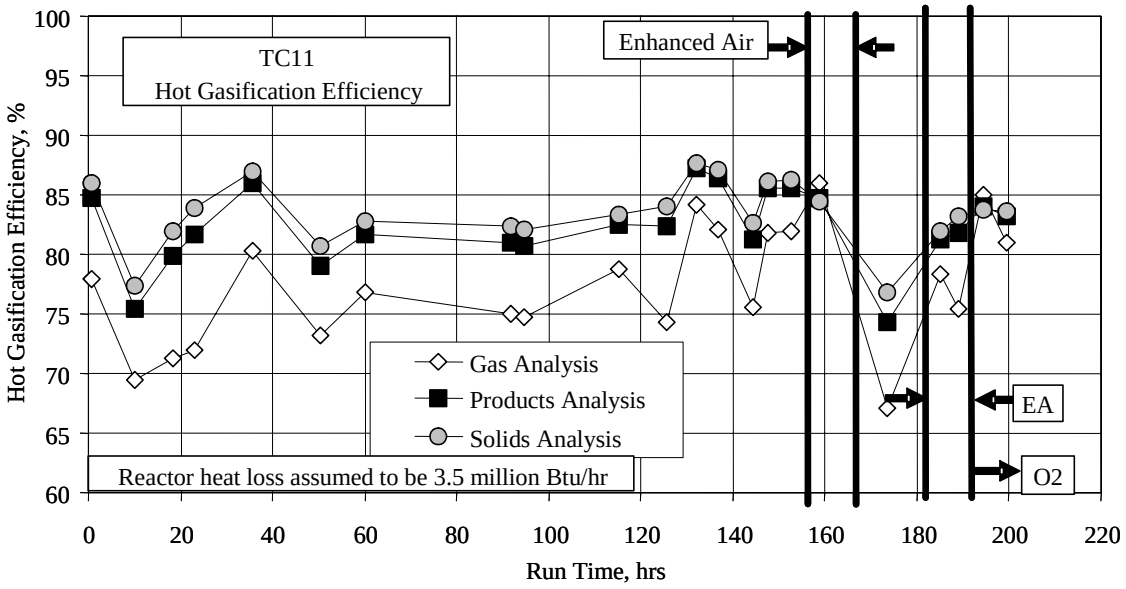

Figure 3.5-27 Hot Gasification Efficiency

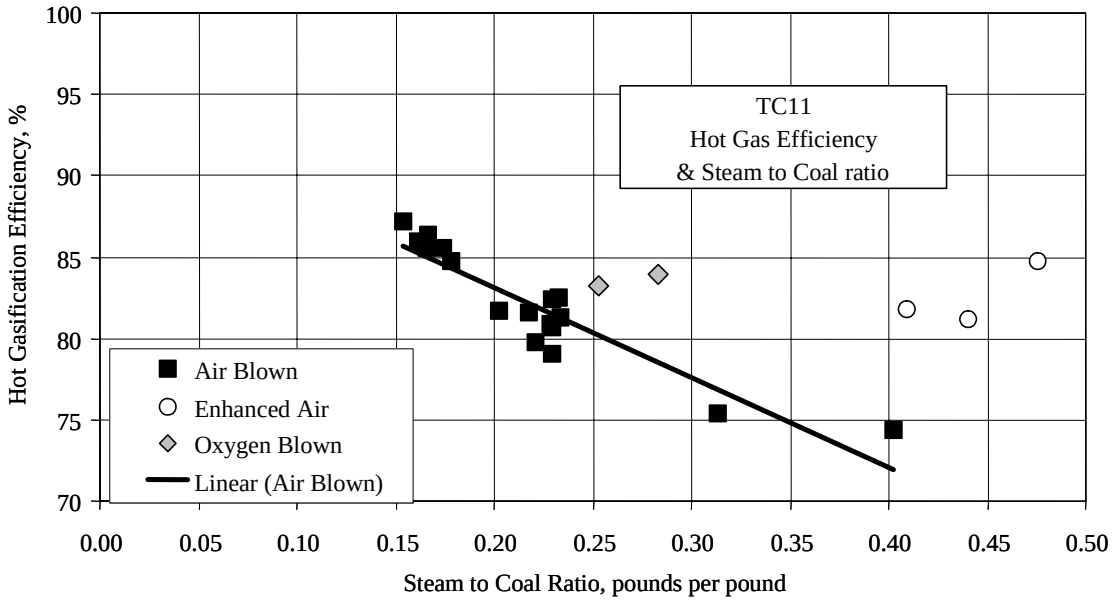

Figure 3.5-28 Hot Gasification Efficiency and Steam-to-Coal Ratio

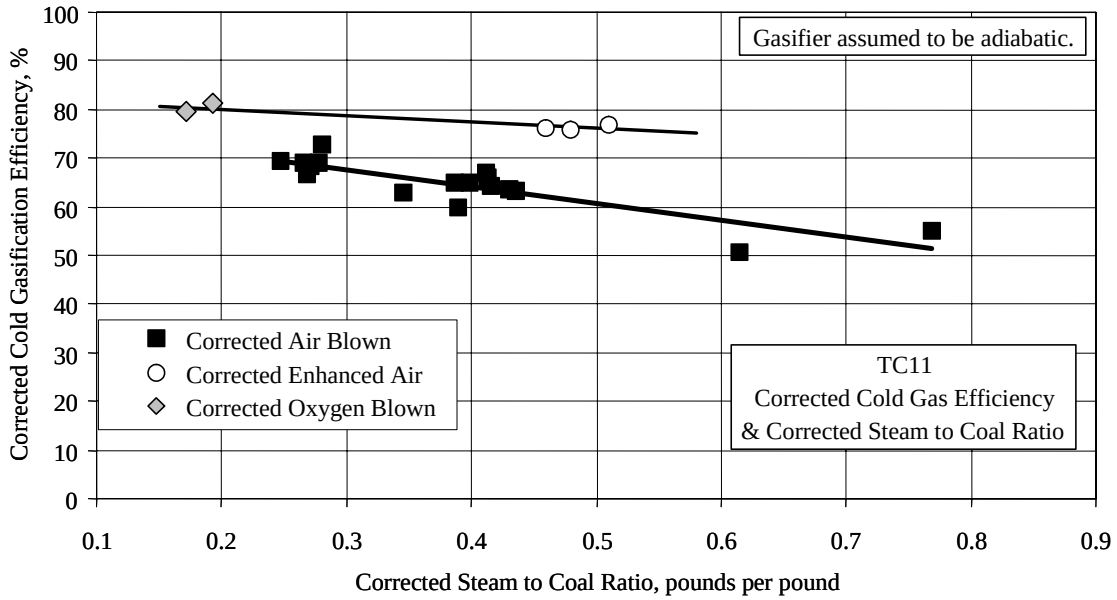

Figure 3.5-29 Nitrogen-Corrected Cold Gasification Efficiency

3.6 ATMOSPHERIC FLUIDIZED-BED COMBUSTOR (AFBC) OPERATIONS

FD0530, used to feed gasification ash (g-ash, formerly known as char) to the atmospheric fluidized-bed combustor (AFBC), was damaged at the end of TC10. Because the g-ash made from low sulfur fuels in past runs has been shown to be nonhazardous with regard to reactive sulfides, the decision was made not to repair FD0530 until a more reliable feed system could be implemented. In the interim, the g-ash will be fed directly to the ash silo. The AFBC operates on fuel oil during these times to provide high quality superheated steam to the gasifier.

The AFBC system was started on April 3 with the startup of the air compressor and lighting of the start-up heater main burner. On April 7 the fuel oil system was brought online to bring the AFBC up to a suitable temperature for producing superheated steam. During the course of TC11, the fuel oil system operated for 270 hours.

In past test runs, the variation in g-ash feed rate led to unstable temperatures in the AFBC. In TC11 burning fuel oil for the entire run smoothed the temperatures considerably as shown in Figure 3.6-1. Without g-ash combustion, the bed velocities were lower reducing the rate at which fine material was elutriated from the bed. Figure 3.6-2 shows the pressure drop across the bed during TC11. After the initial fill, sand was only added to the bed once, on April 7, nearly two weeks before shutting down.

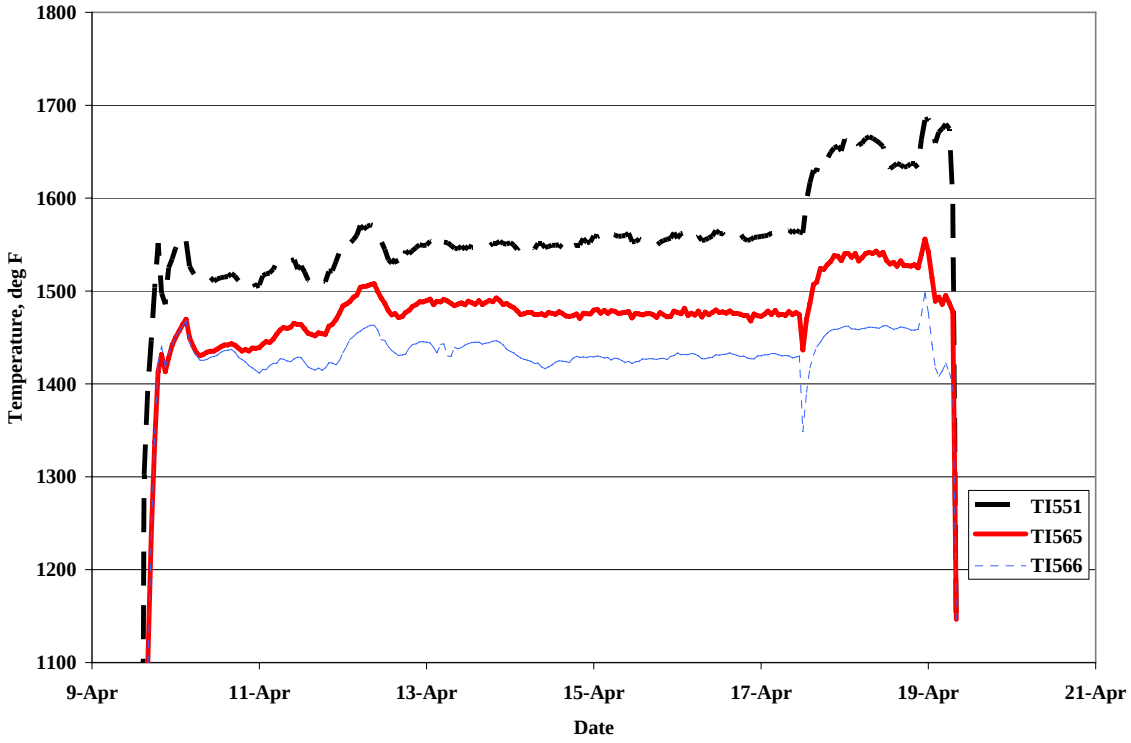

Figure 3.6-1 Temperature Profile of Bed

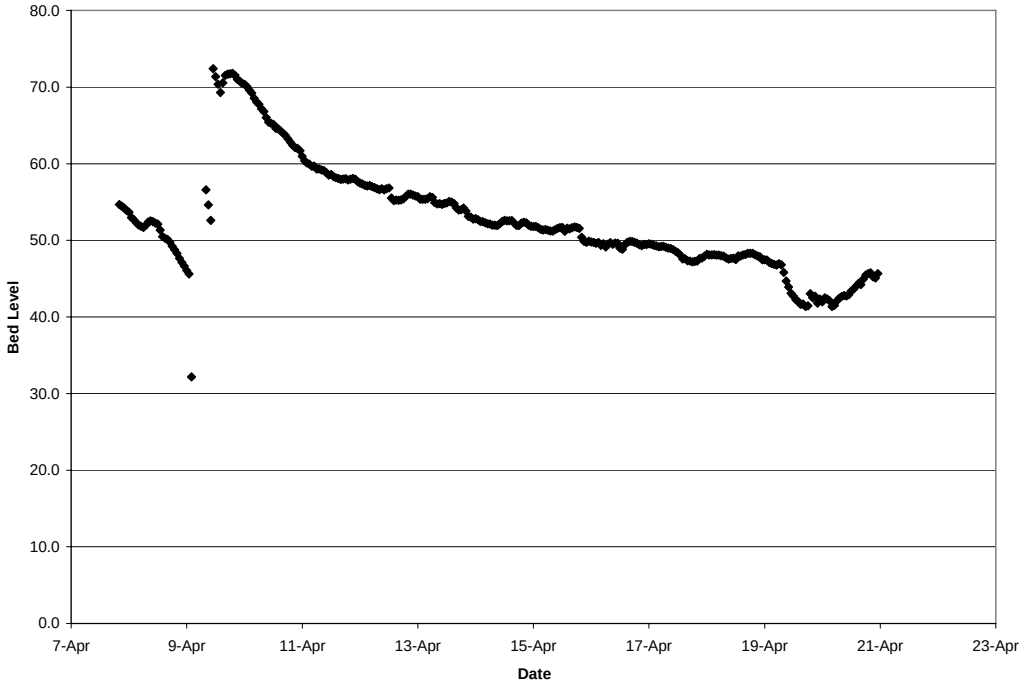

Figure 3.6-2 Pressure Drop Across Bed

3.7 PROCESS GAS COOLERS

Heat transfer calculations were done on the primary gas cooler, HX0202, and the secondary gas cooler, HX0402, to determine if the performance had deteriorated during TC11 due to tar or other compounds depositing on the tubes.

The primary gas cooler, HX0202, is between the transport gasifier cyclone, CY0201, and the Siemens Westinghouse PCD, FL0301. During TC11, HX0202 was not bypassed and took the full gas flow from the Transport Gasifier. The primary gas cooler is a single-flow heat exchanger with hot gas from the gasifier flowing through the tubes and the shell side operating with the plant steam system. The pertinent equations are:

$$Q = UA\Delta T_{LM} \tag{1}$$

$$Q = c_p M(T_1 - T_2) \tag{2}$$

$$\Delta T_{LM} = \frac{(T_1 - t_2) - (T_2 - t_1)}{\ln \frac{(T_1 - t_2)}{(T_2 - t_1)}} \tag{3}$$

Q = Heat transferred, Btu/hour
U = Heat transfer coefficient, Btu/hr/ft^2/°F
A = Heat exchanger area, ft^2
ΔT_{LM} = Log mean temperature difference, °F
c_p = Gas heat capacity, Btu/lb/°F
M = Mass flow of gas through heat exchanger, lb/hr
T_1 = Gas inlet temperature, °F
T_2 = Gas outlet temperature, °F
$t_1 = t_2$ = Steam temperature, °F

Using equations (1) through (3) and the process data, the product of the heat transfer coefficient and the heat exchanger area (UA) can be calculated. The TC11 HX0202 UA is shown on Figure 3.7-1 as 4-hour averages, along with the design UA of 5,200 Btu/hr/°F and the pressure drop across HX0202. If HX0202 is plugging, the UA should decrease and the pressure drop should increase. The UA deterioration is a better indication of heat exchanger plugging because the pressure drop is affected by changes in flow, pressure, and temperature.

The UA was above the design UA of 5,200 Btu/hr/°F for essentially all of TC11. The UA started at about 6,000 Btu/hr/°F. The UA was unsteady but rising during the first 40 hours, finally reaching 7,600 Btu/hr/°F. The UA stayed at this high value for about the next 150 hours ranging from about 7,000 to about 8,400 Btu/hr/°F for most of the period. For the

last 40 hours, the UA averaged about 6,400 Btu/hr/°F, higher than design but lower than the rest of TC11.

The pressure drop across HX0202 was fairly steady during TC11, averaging 0.7 psi and ranging generally between 0.5 and 1.1 psi. The changes in pressure drop were tied to changes in process gas flow. The last 40 hours of TC11 had the lowest pressure of TC11, averaging 0.5 psi, and was also the period of lowest syngas flow.

The average UA during TC11 was considerably higher than the UA during TC10. During TC10, the UA was below design UA of 5,200 Btu/hr/°F for most of the run, while during TC11, it was above 6,000 Btu/hr/°F for almost the entire run. The pressure drop in the two runs was similar, though it was slightly higher in TC10.

The secondary gas cooler, HX0402, is a single-flow heat exchanger with hot gas from the PCD flowing through the tubes and the shell side operating with plant steam system. Some heat transfer and pressure drop calculations were done around HX0402 to determine if there was any plugging or heat exchanger performance deterioration during TC11.

Using equations (1) through (3) and the process data, the product of the heat transfer coefficient and the heat exchanger area (UA) can be calculated. The UA for TC11 testing is shown on Figure 3.7-2 as 2-hour averages, along with the design UA of 13,100 Btu/hr/°F and the pressure drop across HX0402. If HX0402 is plugging, the UA should decrease and the pressure drop should increase.

For most of TC11, the UA of HX0402 was very close to the design UA of 13,100 Btu/hr/°F varying from 12,000 to 14,000 Btu/hr/°F. After about 180 hours of operation, the UA dropped to around 12,300 Btu/hr/°F for the rest of the run.

For most of TC11, the HX0402 pressure drop varied considerably. During the first 180 hours, it ranged from 1.6 to 3.0 psi. During the last 40 hours of TC11, the pressure drop steadied somewhat and declined to about 1.3 psi. Both the UA and the pressure drop accompanied a decrease in syngas flow during that time.

During the first 3 days of TC11, the pressure drop across HX0402 dropped from 2.4 to 0.8 psi. The pressure drop held at 0.8 psi for the next 300 hours. During the last few days of TC11, the pressure drop varied from 0.7 to 1.8 psi.

The UA of HX0402, averaging very close to the design UA, was higher than the UA found in TC10 when it averaged about 1,500 Btu/hr/°F below design. The pressure drop for HX0402 was more similar to the results from TC09 than TC10. In TC10, the pressure drop was down in the 1.0 to 1.5 psi range for most of the run.

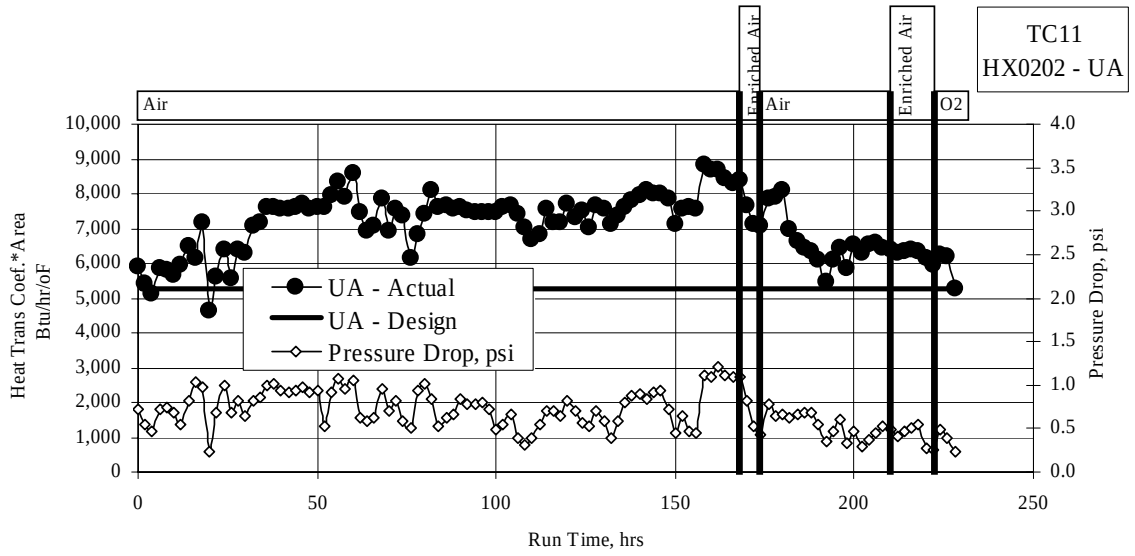

Figure 3.7-1 HX0202 Heat Transfer Coefficient and Pressure Drop

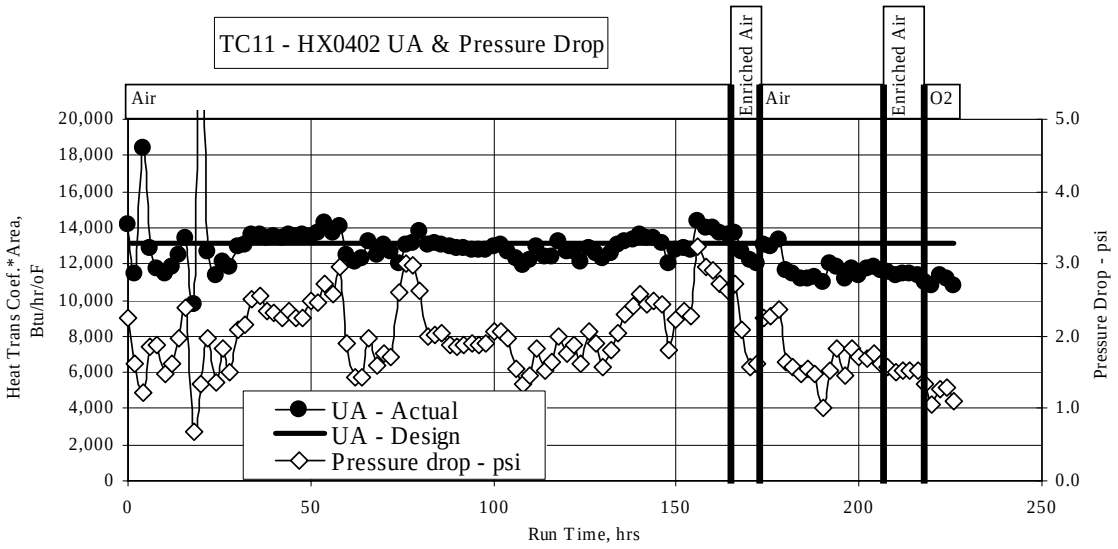

Figure 3.7-2 HX0402 Heat Transfer Coefficient and Pressure Drop

4.0 PARTICLE FILTER SYSTEM

4.1 TC11 RUN OVERVIEW

TC11 (the first test run using lignite coal) was completed in April 2003. During this run both air- and oxygen-blown gasifier operation were achieved. As in other recent test runs, this run was a demonstration of reliable particulate control device (PCD) performance. Since the addition of the lower mixing zone, particulate properties have continued to be favorable for PCD performance, resulting in a relatively low pressure drop and reduced tendency to bridge. The trend of a lower pressure drop and absence of bridging continued in TC11. A new trend was observed with the lignite coal that related gasifier operation to changes in particle properties (LOI, surface area, and dustcake drag). Despite sometimes unstable system conditions, the PCD proved to be robust and reliable. The run provided the opportunity to assess various instrumentation and system responses, to continue improved failsafe testing, and to check newly implemented logic.

TC11 consisted of 192 on-coal hours and was marked by numerous coal feeder trips. The frequent coal stoppages caused sometimes unstable system operation and several thermal excursions in the PCD due to oxygen breakthrough. Despite these conditions, there were no major problems encountered with PCD operation. No filter element failures occurred and excellent sealing of the filter vessel was demonstrated by outlet loading concentrations generally below the sampling system lower limit of resolution (<0.1 ppmw).

This report contains the following sections:

- PCD Operation Report, Section 4.2 – This section describes the main events and operating parameters affecting PCD operation. Operation of the fines removal system is also included in this section.
- Inspection Report, Section 4.3 – The complete inspection performed following TC11 is discussed in this section including details of the post-run conditions of various PCD components and of the fines removal system.
- Gasification Ash Characteristics and PCD Performance, Section 4.4 – This section includes a detailed discussion of gasification ash (g-ash) physical and chemical properties, as well as the effects of these characteristics on PCD performance. The results of PCD inlet and outlet solids sampling and dustcake sampling are presented in this section.
- Failsafe Testing, Section 4.5 – Results of failsafe testing completed to date are included in this section. Failsafe testing completed in TC11 included solids injection and gas exposure.

4.2 TC11 PCD OPERATION REPORT

4.2.1 Introduction

Despite unstable system conditions during TC11, PCD operation was successful. There were no filter element failures and no g-ash bridging. In addition, outlet loading samples showed that the PCD was leak-tight. The numerous coal feeder trips often caused oxygen breakthrough and subsequent thermal excursions. However, there was no apparent damage caused by these thermal excursions.

Ranging from approximately 40 to 60 inH_2O, the baseline pressure drop was slightly lower than that of recent runs. In general, the lower pressure drop corresponded to a lower particle drag of the lignite g-ash compared to the PRB and bituminous g-ashes recently produced in the Transport Gasifier. However, as discussed in Section 4.4, during periods of high LOI (lower carbon conversion), particle drag was comparable to PRB particle drag and higher than bituminous g-ash particle drag. Overall, the baseline pressure drop was stable, although the recurrent coal stoppages caused frequent jumps in pressure drop. Typically, the inlet temperature was 700 to 750°F, and the face velocity was 3 to 4 ft/min.

The fines removal system operated without major problems. Prior to TC11, new control logic was implemented which automatically reduces the FD0502 screw cooler speed and increases the FD0520 cycle frequency when a gasifier upset is indicated. The trigger mechanisms for the new logic to be enabled are rapid increases (at least 2°F/sec) in PCD inlet, filter element, and FD0502 screw cooler outlet temperatures. The frequent thermal excursions on the filter element surfaces caused the gasifier upset compensation logic to be enabled many times during the run.

Run statistics for TC11 are shown in Table 4.2-1. Layout 27, the filter element layout implemented for the run, is shown in Figure 4.2-1.

4.2.2 Test Objectives

For TC11, the primary objectives for the filter system were the following:

Failsafe Device Testing – After outlet loading samples consistently showed concentrations lower than the detection limit of 0.1 ppmw, online tests of the PSDF-designed failsafe and the Pall fuse were conducted, which included hot g-ash injection. In previous failsafe tests, a fluidized-bed feeder was used to inject g-ash into the interior of a filter element ahead of the failsafe to be tested. In TC11, a bypass line was used to feed g-ash from the dirty side of the PCD into the inside of the element upstream of the failsafe that was tested. Penetration through the failsafe was quantified by in situ particulate sampling at the PCD outlet. At the same time, plugging of the failsafe was monitored by recording the pressure drop across the failsafe during the testing. These tests were conducted to confirm the testing previously completed on these two types of failsafe devices. In addition to the injection tests, several Ceramem ceramic failsafes were installed for gas exposure during TC11.

Filter Element Testing – During TC11, iron aluminide filters were tested. In addition, seven of the Westinghouse inverted filter assemblies were tested again.

Additional Instrumentation – Several types of instrumentation were added to further characterize PCD performance. For example, gas flow through each plenum venturi was evaluated using pressure measurements and thermocouple readings. Also, a new metal structure was added to the PCD cone which supports resistance probes and thermocouples, and these instruments were used to monitor solids levels. To record the pressure changes caused by backpulsing, a high-speed pressure transmitter was used at various locations both upstream and downstream of the PCD.

Back-pulse Pressure Measurements – Both during heat-up on coke breeze and during coal feed, the effects of backpulse pressure and the pressure drops across an instrumented filter element were recorded. This testing was performed in an effort to optimize back-pulse parameters. Results of the testing can be found in Section 4.2.4. In addition, near the end of the run, back-pulse pressures were varied for several hours at a time so that the effect of back-pulse pressure on baseline pressure drop could be determined.

Inlet Particulate Sampling and Characterization – Since TC11 was the first test with the Falkirk North Dakota lignite, it was important to document the characteristics of the g-ash produced with this type of coal and to understand how the g-ash characteristics affected PCD performance. In situ particulate samples were collected at the PCD inlet to determine how the g-ash properties, chemistry, and flow resistance were affected by changes in coal-feed rate, sorbent addition, and air- versus oxygen-blown operation. The measured inlet particulate loadings were used in combination with PCD pressure drop data to determine the drag of the transient dustcake under various conditions. The transient dustcake drag values were compared to drag values measured in the laboratory to determine whether the pressure drop was influenced by any outside factors other than the dustcake. The physical properties and flow resistance of the TC11 g-ash were compared to the properties and drag of other g-ashes from previous runs to better understand the influence of coal type on g-ash characteristics and dustcake flow resistance. The results of the inlet sampling and characterization are discussed in Section 4.4.

Outlet Particulate Sampling and Monitoring – Recent testing in the plastic PCD cold flow model has shown that certain types of filter elements allow some particle penetration through the element. To minimize particulate emissions and, hopefully, demonstrate compliance with turbine criteria, these types of elements were removed from the PCD prior to TC11. The elements that were removed were replaced with iron aluminide elements, which were the only type of filter element installed in the PCD in TC11. Outlet sampling is reported in Section 4.4.

4.2.3 Observations/Events – April 6, 2003 Through April 18, 2003

Refer to Figures 4.2-2 through 4.2-6 for operating trends corresponding to the following list of events:

A. System Start-up. At 13:07 on April 6, 2003, back-pulsing for the PCD began. The TC11 run began on April 7, 2003, at 16:30, with the main air compressor and the gasifier start-up burner. At 08:30 on April 8, 2003, the back-pulse pressure was increased to 320 psid (i.e., 320 psi above gasifier pressure) on the top plenum and 600 psid on the bottom plenum.

B. Coal Feed Started. At 16:00 on April 8, 2003, coal feed was started, and over the next few hours several coal feeder trips occurred. Coke breeze feed was continued throughout this period of coal feed.

C. System Shutdown. At 02:07 on April 9, 2003, the cooling water system tripped which caused the instrument air and nitrogen compressors to trip. The system was therefore shut down until the problem could be resolved.

D. System Restart. At 12:50 on April 9, 2003, the start-up burner was lit, and coke breeze feed started at 18:20. Coal feed was started at 21:28 on April 9, 2003, but due to a plugged line on the FD0520 lock hopper system outlet, coal feed was discontinued at 00:23 on April 10, 2003. After clearing the FD0520 outlet line, coal feed was restarted.

E. Restarted Coal Feed. At 04:48 on April 10, 2003, after the fines removal system was cleared of solids, coal feed was reestablished. Coal feeding was very unsteady.

F. Start-up Burner Lit. At 07:30 on April 12, 2003, the coal feeder tripped. Coke breeze did not ignite, and because of loss of gasifier temperature, the start-up burner was lit. Coal feed was reestablished at 13:01 on April 12, 2003.

G. Oxygen-blown Operation Began. On April 16, 2003, system pressure was lowered so that oxygen-blown gasifier operation could begin. Due to problems with coal feeding, at 02:00 oxygen-blown operation stopped on April 17, 2003. Oxygen-blown operation was resumed at 21:00 on April 17, 2003, and continued until shutdown.

H. System Shutdown. At 17:30 on April 18, 2003, a gasifier upset occurred and the system was shut down.

4.2.4 Back-Pulse Pressure Testing

On two occasions during the run, pressure measurements were taken with a high-speed transmitter used at various places along the gasifier train. The data were taken at 100 Hz using a local data acquisition device so that the full and rapid response to back-pulsing could be recorded. The pressure taps used for these recordings were located at the PCD outlet, the PCD inlet, the primary gas cooler inlet, and the crossover, riser, loop seal, and the lower mixing zone (LMZ) sections of the gasifier. Measurements were taken during a top plenum back-pulse and during a bottom plenum back-pulse.

Data was first recorded during system heat-up with coke breeze feed on April 8, 2003, and was later recorded while on coal feed on April 16, 2003. The results of this testing are summarized in Figure 4.2-7. As expected, the highest pressure rise resulting from back-pulsing was at the PCD inlet, with the values ranging from 3.1 to 5.3 psi corresponding to pulse pressures of 430 and 794 psig, respectively. According to the measurements, the loss of pressure across the primary gas cooler (HX202) was small, from 0.2 to 0.4 psi. The effect of the back-pulse could be seen as far upstream as the lower mixing zone.

4.2.5 Run Summary and Analysis

The system was pressurized and the back-pulsing sequence was first started on April 6, 2003. The TC11 run began on April 7, 2003. Coal feed was started on April 8, 2003, and during this period of coal feed, both the FD0210 feeder and the new FD0200 feeder were used. FD0210 was used as the primary coal feeder, and the FD0200 system was operated for only a few short periods of time during the run. Soon after coal feed started, coal feeding difficulty began, possibly due to the high moisture content of the coal, and unsteady coal feeding was a constant concern throughout the run.

On April 9, 2003, due to a trip of the cooling water system that caused a loss of instrument air and nitrogen, the system was shut down for a few hours until the problem could be resolved. Later that day, coal feed was reestablished. During this period of coal feeding, only the FD0200 feeder was operated, and system operation was very erratic due to the lack of control of the coal-feed rate. Later, the FD0210 coal feeder system was used exclusively, but coal feeding continued to be problematic. On April 10, 2003, the system was shut down due to a plugged line on the fines removal system. Coal feed was restarted later that day. Following one particular coal feeder trip on April 12, 2003, gasifier temperatures dropped too low for coal or coke breeze feed, and the burner had to be lit to reheat the gasifier. Coal feed was reestablished later that day.

Oxygen-blown operation was the primary mode of gasifier operation used during the remainder of the run. The change from air- to oxygen-blown operation did not affect PCD operation significantly. Although system pressure was reduced for oxygen-blown operation, the potential increase in face velocity was offset by a reduction in the coal-feed rate and total gas flow. Because of difficulty in feeding coal and because of poor circulation in the gasifier, the run was ended on April 18, 2003.

Many of the operational problems that occurred during the run were related to the frequent coal stoppages. For the PCD, the primary problems associated with these stoppages were the resultant thermal transients on the filter elements. Often, these temperature rises were rapid enough (at least 2°F/sec) to trigger rate-of-change alarms, which in turn triggered automatic back-pulsing and nitrogen dilution as well as the fines removal system runback. Despite the thermal transients and upset conditions, PCD performance was robust. There were no filter element failures and no evidence of a leak. (The Falkirk lignite g-ash had a relatively low drag during periods of high carbon conversion, and that property was evidenced by pressure drop generally lower than that seen when gasifying other types of coals.) Throughout the run no indication of bridging was seen. Overall, PCD operation was successful with this coal, and the

run provided the opportunity to test various instrumentation, failsafes, and the newly implemented runback logic.

Table 4.2-1

TC11 Run Statistics and Steady-State Operating Parameters, April 6, 2003, Through April 18, 2003

Start Time:	4/6/03 13:07 (for back-pulse system)
End Time:	4/18/03 17:30
Coal Type:	Falkirk Lignite
Hours on Coal:	Approx. 192 hrs
Number of Filter Elements:	85
Filter Element Layout No.:	27 (Figure 4.2-1)
Filtration Area:	241.4 ft^2 (22.4 m^2)
Pulse Valve Open Time:	0.2 sec
Pulse Time Trigger:	5 min
Pulse Pressure, Top Plenum	320 psi above System Pressure
Pulse Pressure, Bottom Plenum:	600 psi above System Pressure
Pulse dP Trigger:	275 inH_2O
Inlet Gas Temperature:	Approx. 700 to 750°F (370 to 400°C)
Face Velocity:	Approx. 3 to 4 ft/min (1.5 to 2.0 cm/sec)
Inlet Loading Concentration:	Approx. 11,300 to 25,100 ppmw
Outlet Loading Concentration:	Below detection limit of 0.1 ppmw to 0.27 ppmw
Baseline Pressure Drop:	Approx. 40 to 60 inH_2O (100 to 150 mbar)

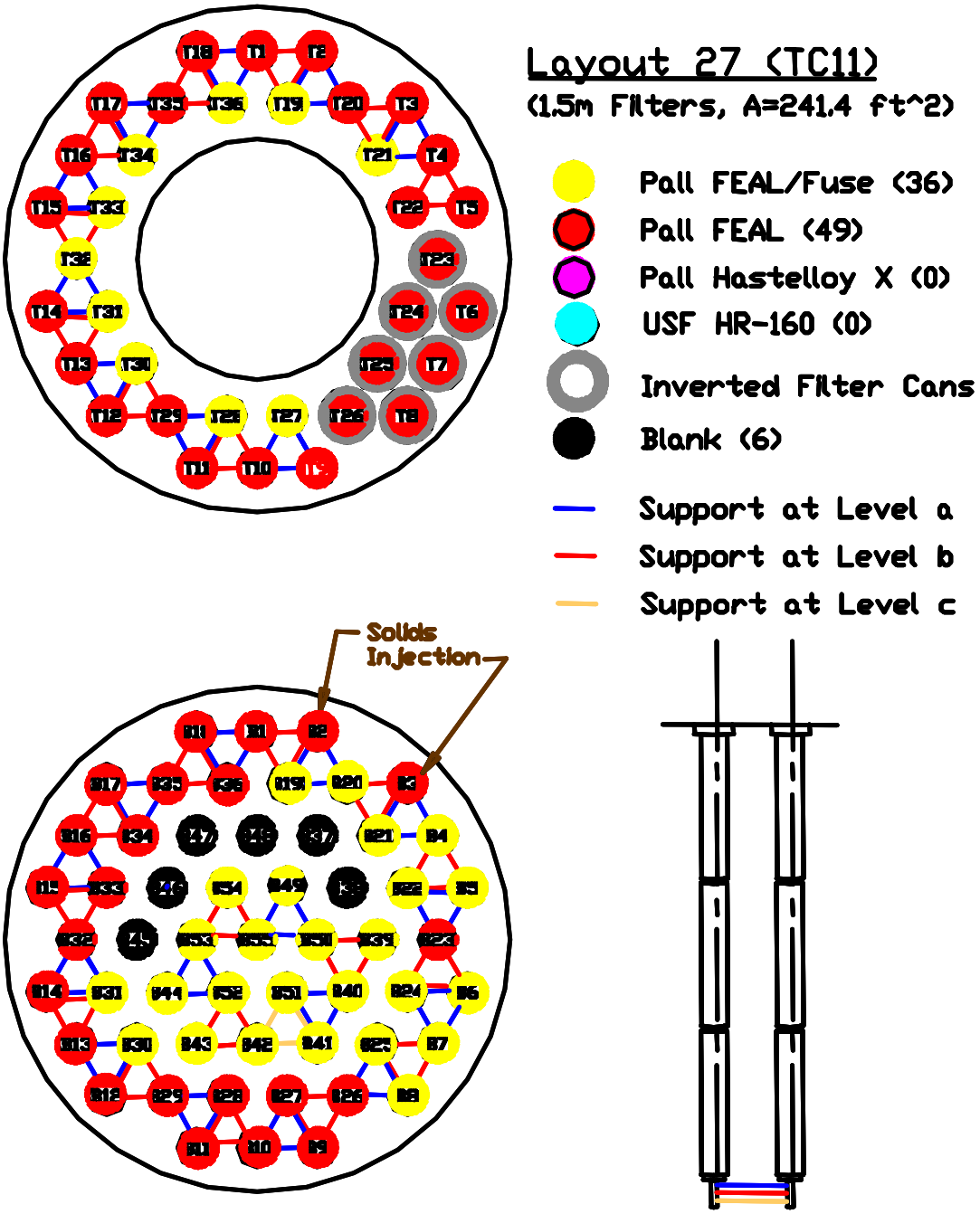

Figure 4.2-1 Filter Element Layout 27

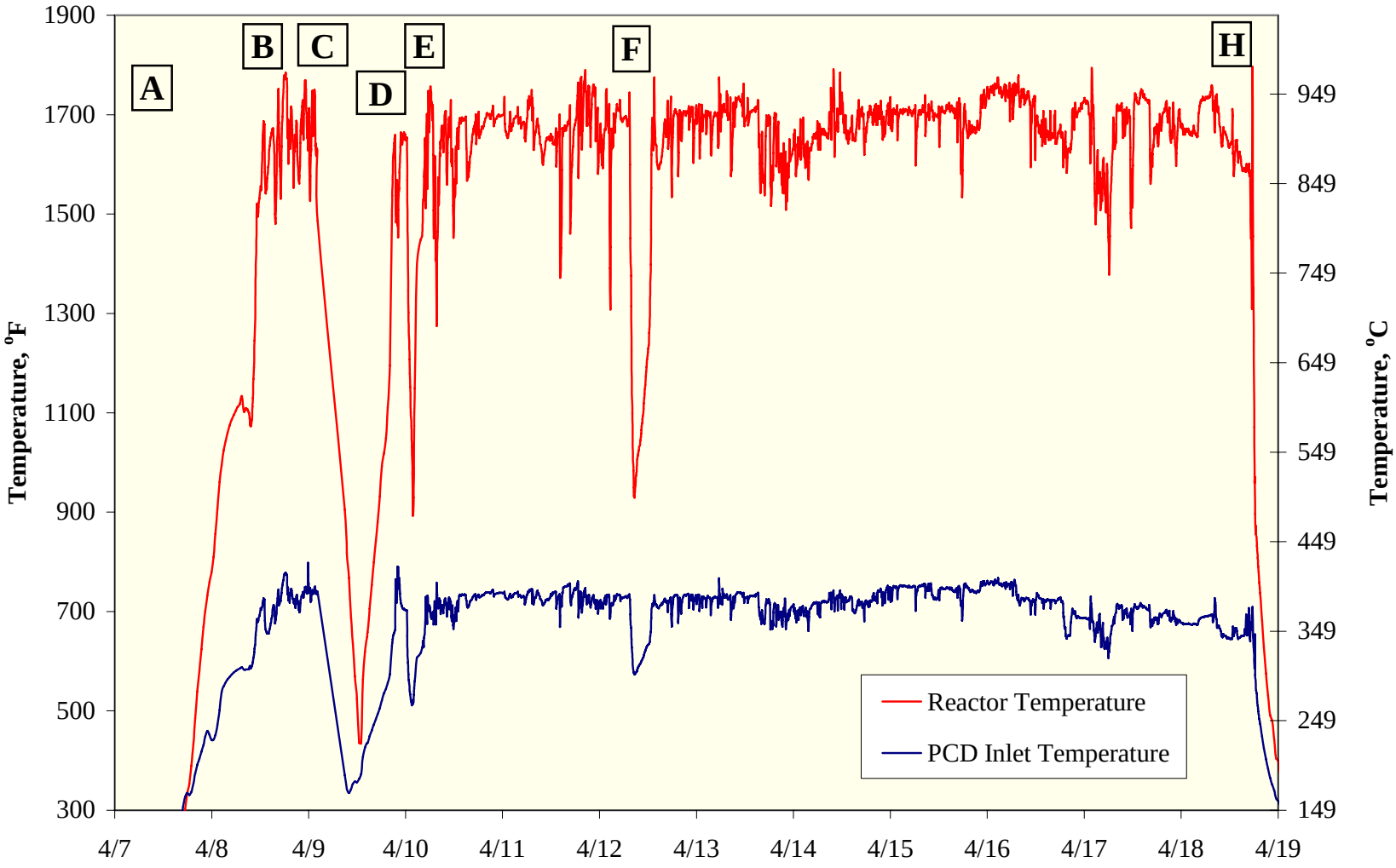

Figure 4.2-2 Reactor and PCD Temperatures, TC11

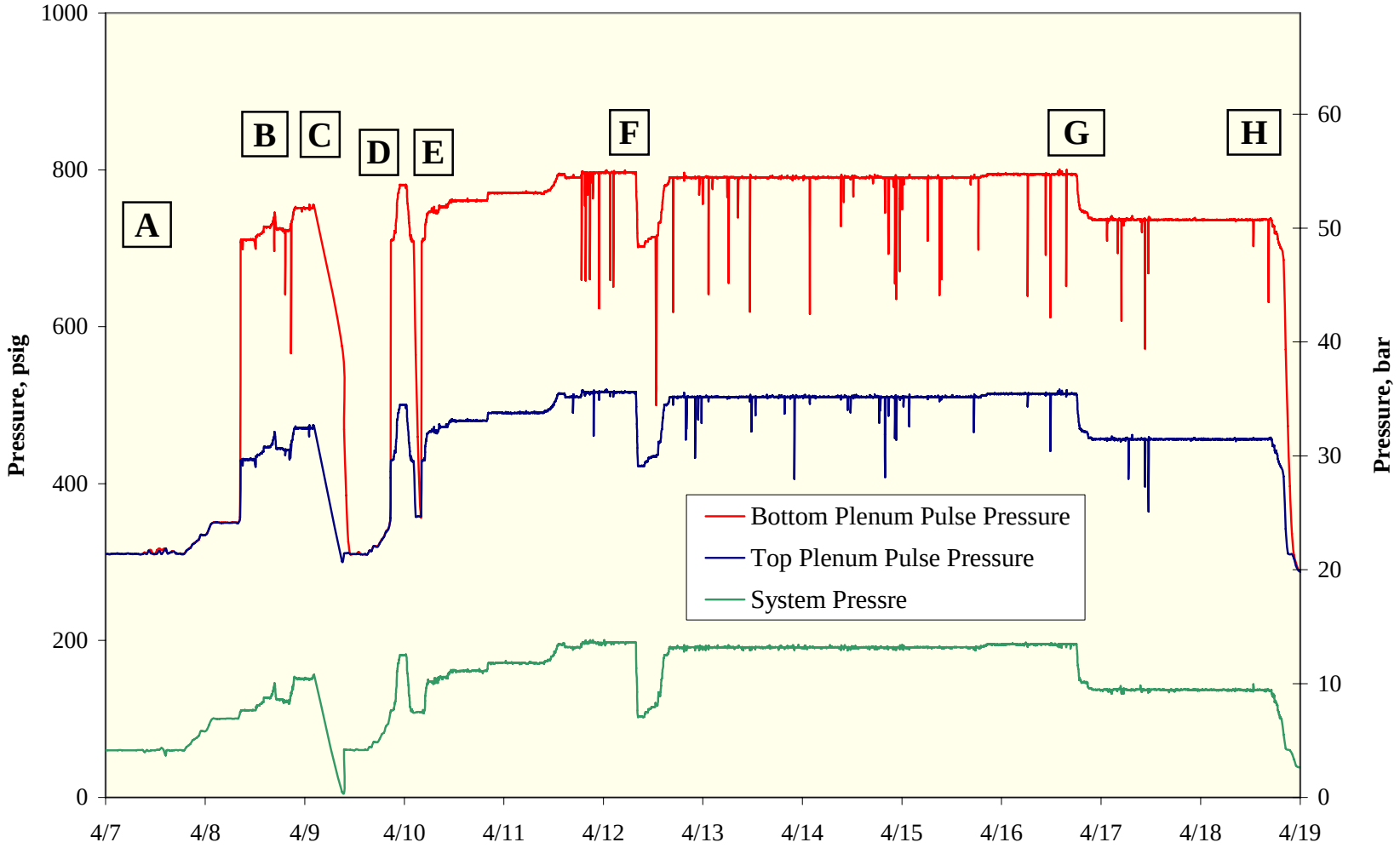

Figure 4.2-3 System and Pulse Pressures, TC11

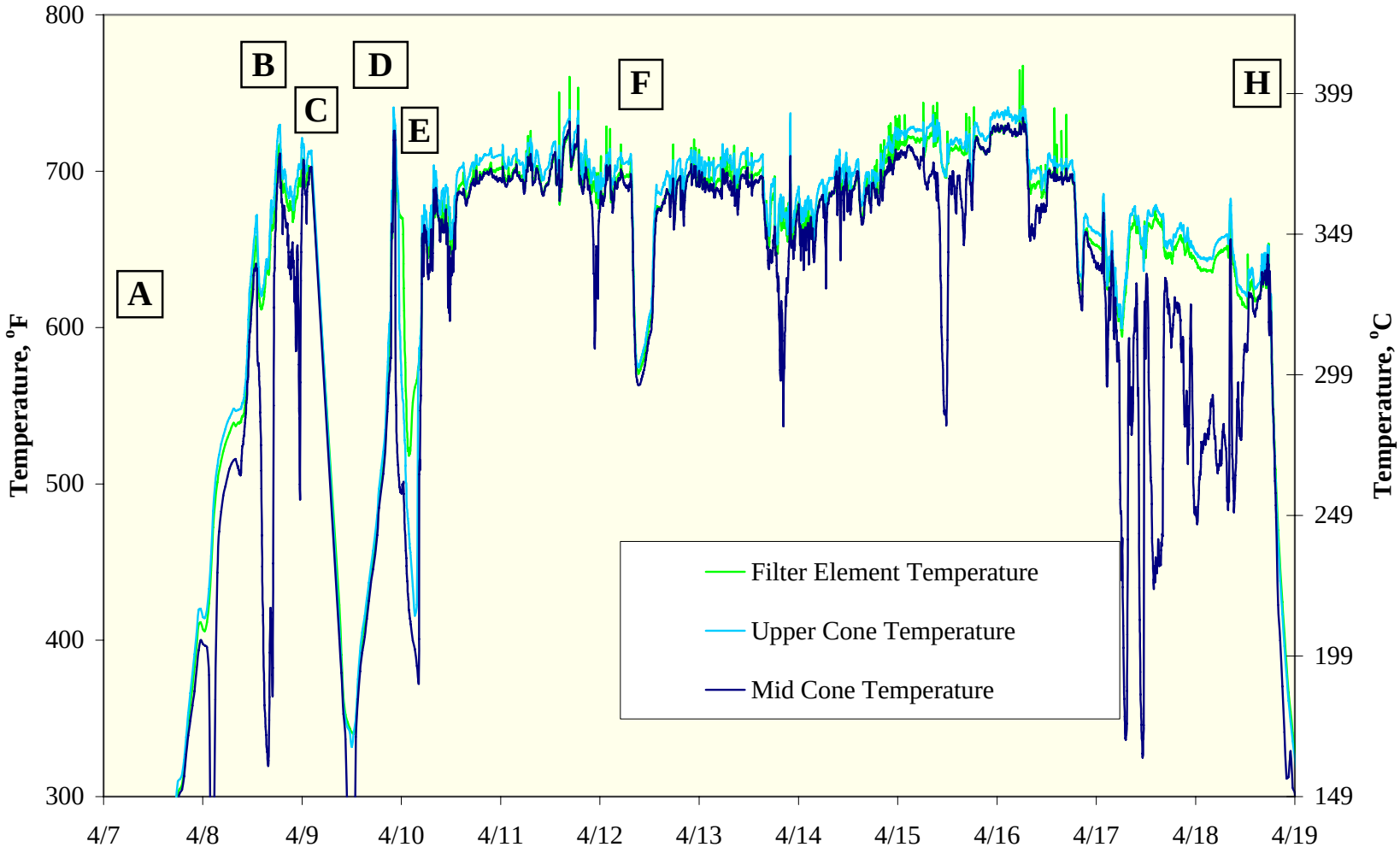

Figure 4.2-4 Filter Element and Cone Temperatures, TC11

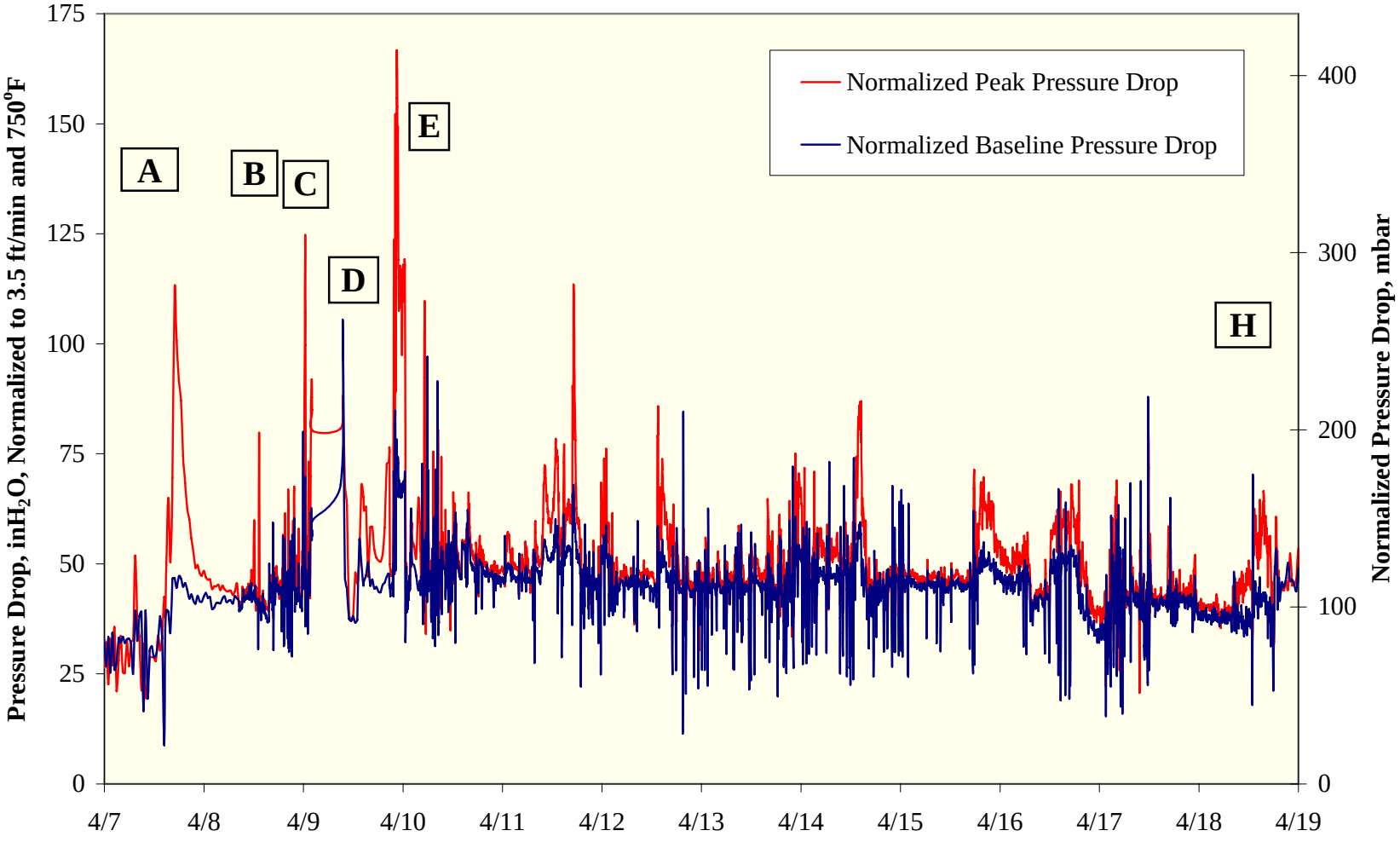

Figure 4.2-5 Normalized PCD Pressure Drop, TC11

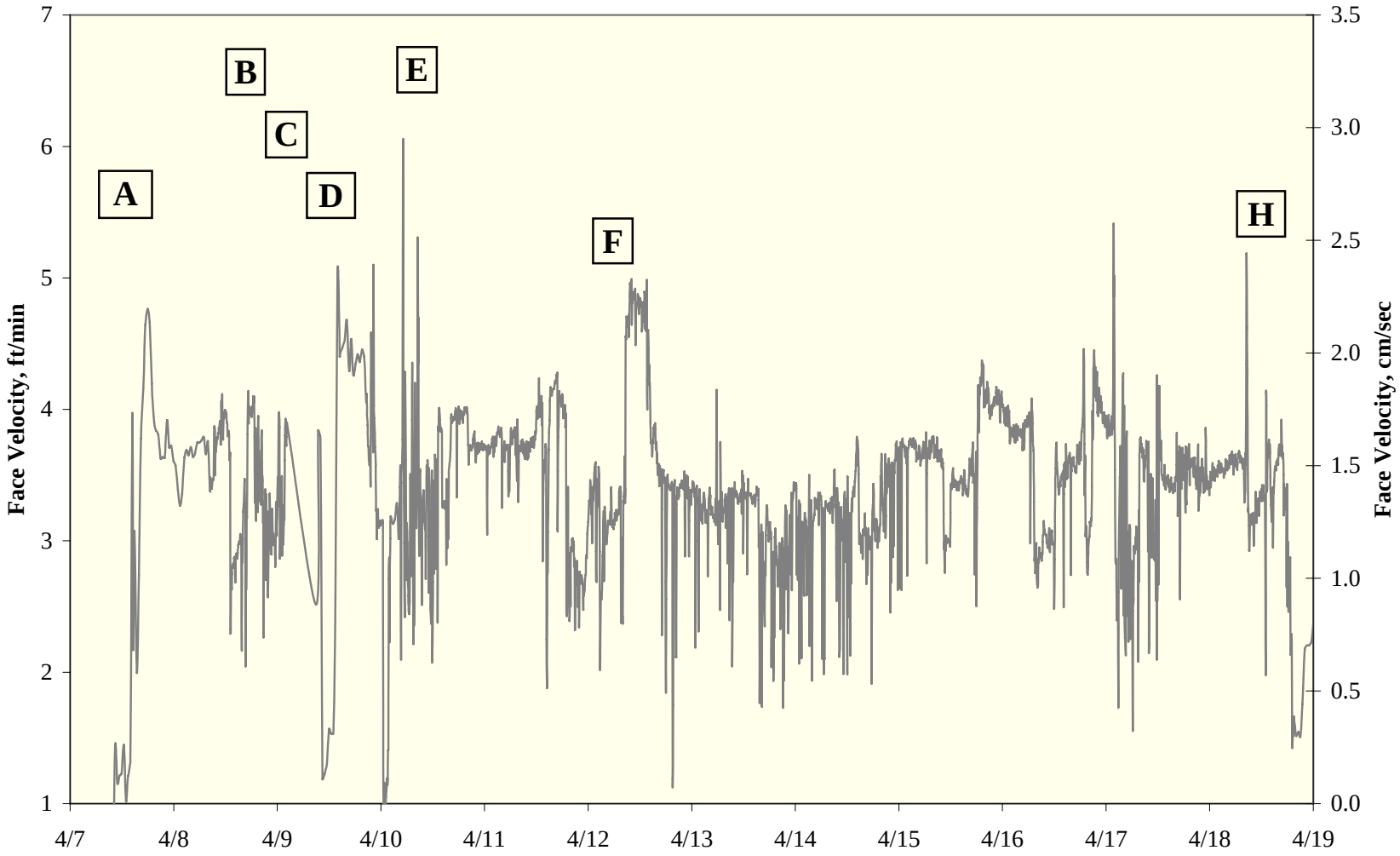

Figure 4.2-6 PCD Face Velocity, TC11

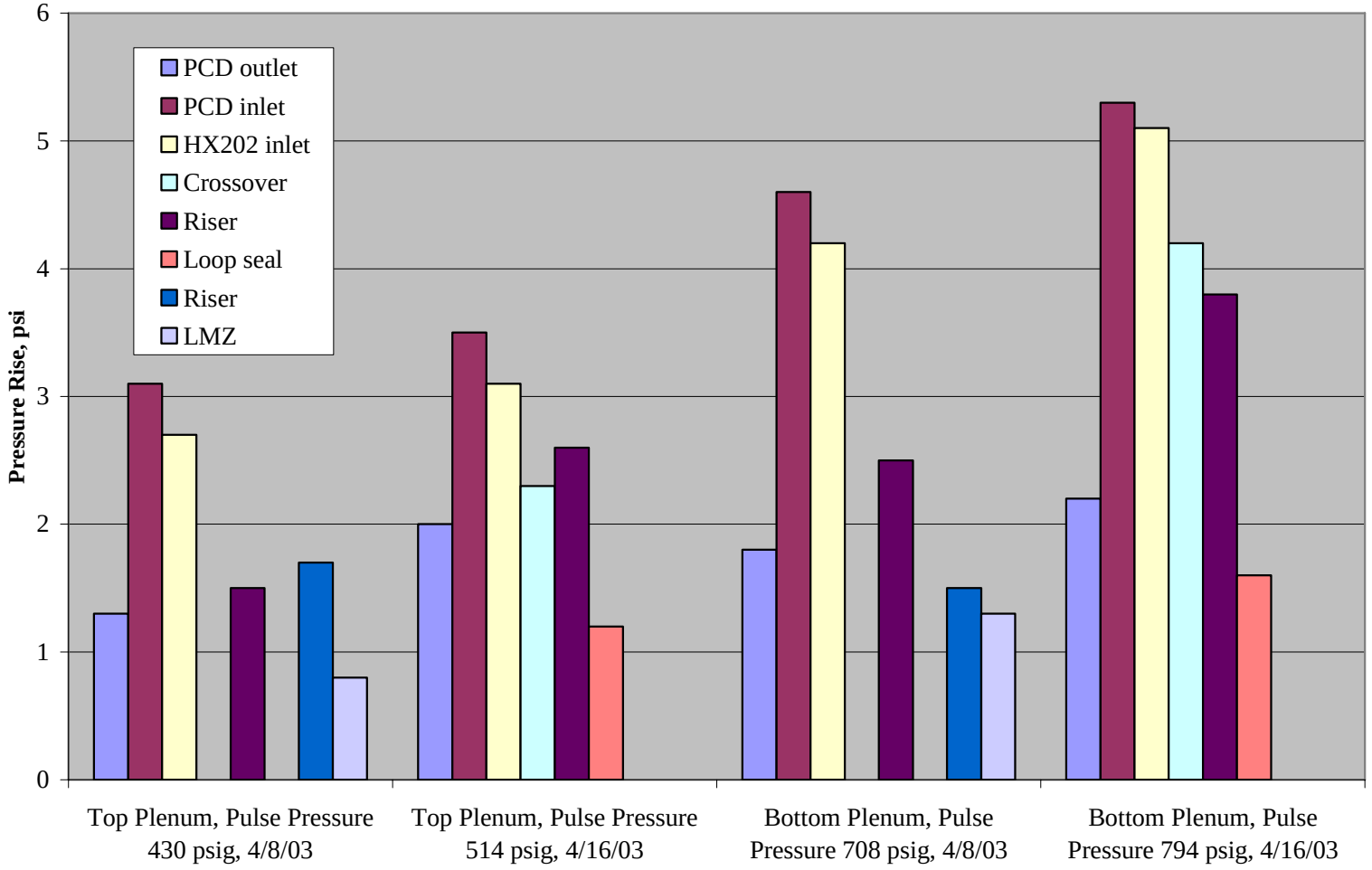

Figure 4.2-7 Pressure Responses to Back-Pulse During TC11

4.3 TC11 INSPECTION REPORT

4.3.1 Introduction

During the TC11 outage, the PCD internals were removed from the filter vessel and inspected. The outage inspection included examinations of the filter elements, their fixtures to the plenums, solids deposition, filter element gaskets, and auxiliary equipment. The subsequent sections will deal with the findings of the inspection.

4.3.2 Filter Elements

During TC11, only Pall FEAL filter elements were installed (See Figure 4.2-1). During the outage between TC10 and TC11, all the Hastelloy X and HR-160 filter elements were removed from the PCD. A cold-flow PCD model was commissioned between TC10 and TC11. The cold-flow model was designed to test filter elements and failsafe devices as a screening tool. HR-160 filter elements were used during the commissioning of the cold-flow model. It was noted that the HR-160 filter elements allowed particle penetration through the media during the back-pulse. In addition to the HR-160 filter elements, several Hastelloy X filter elements were tested, and it was found that the particle penetration occurred as well. Finally, several FEAL filter elements were tested with no solids penetration through the filter media. Based on these findings, it was decided to remove all the Hastelloy X and HR-160 filter elements from the PCD before TC11.

Shutdown after TC11 was clean, which means the top and bottom plenums were back-pulsed after coal-feed was shutdown. A total of nine Pall FEAL filter elements were removed from the lower plenum after TC11. Each element was closely inspected, and no obvious damage was noted. The welds were examined and appeared to be in good condition. The Pall FEAL filter elements have accumulated many gasification hours. The following table outlines the exposure hours of the Pall FEAL filter elements that were installed for TC11.

Exposure Hours after TC11	Number of FEAL Filters Exposed
3,089	5
2,619	3
1,676	24
2,573	2
1,306	1
608	8
192	42

Each filter that was removed was flow tested. The hours on these filter elements ranged from 192 to 2,573. Three of the FEAL filter elements had a fuse installed in them, while the other six did not. All flow tests were conducted using air at ambient temperature. Loose g-ash was blown off the outside of the filter elements with compressed air before the flow test. The filter elements were not water-washed or chemically cleaned. The results of the flow tests are shown in Figure 4.3-1 as a plot of pressure drops versus face velocities. At a face velocity of 3 ft/min, the pressure drop measured on filter elements B-6, B-7, B-8 with no fuse ranged from 18.5 to

22.4 inH_2O. These values are similar to those measured after previous gasification runs. The pressure drop was lower for the filter element with 1,306 hours than the other two; however, the difference was small and does not appear to show a change in flow resistance with operational hours. The remaining six filter elements had 192 exposure hours. None of these remaining filter elements had a fuse installed within them. At a face velocity of 3 ft/min, the pressure drop measured on the filter elements with no fuse ranged from 4 to 6 inH_2O. The pressure drop for each of the filter elements was acceptable for reinstallation for TC12.

4.3.3 G-ash Deposition

The plenum was pulled out of the PCD vessel on April 24, 2003. Figure 4.3-2 shows the internals after they were lifted out of the PCD. The initial inspection revealed that there was no bridging material present after TC11.

The average dustcake thickness was ~0.013 inches. The dustcake was not sticky or adherent as seen in earlier gasification runs. The dustcake consisted of a very thin dark outer layer and a much lighter colored inner layer. The dustcake appeared to be evenly distributed on the surfaces of the filter elements. The thin dustcake on the filter elements indicated that tar condensation was not an issue in the PCD during TC11.

On several filter elements, there were solid deposits around the filter holder on top of the filter element. Like the dustcake, the deposits appeared to be dark on the outside and lighter in color on the inside. Figure 4.3-3 shows a solid deposit and the color contrast. Samples of the deposits were collected by SRI. The samples were easily removed and broke into powder when transferred into the sample jar.

The inspection revealed that the g-ash buildup on the filter element holders, upper and lower ash shed, and filter element support brackets was not very significant. Therefore, it appears that all the changes that have been incorporated over the last several gasification runs have promoted a more stable and reliable operation within the PCD.

4.3.4 Filter Element Gasket

The current filter gasket arrangement used in past gasification runs has continued to be very reliable; therefore, it was used during TC11. The gasket types have been outlined in past run reports (see TC06 Inspection Report). During this outage all the gaskets of the filter elements and failsafe devices that were removed were inspected. The following observations were made:

- There were no apparent leak paths in the area of the failsafe holder flanges that would indicate a leak past the primary gasket.
- Some of the gaskets were cut to inspect the extent of the g-ash penetration. The inside of the primary gaskets was relatively clean.
- The gaskets between the failsafe and plenum were clean, indicating a tight seal.

Based on these findings, the gasket material performed well through the 192-hour test run.

4.3.5 Failsafes

During TC11, the following failsafe devices were tested: 3 Westinghouse Ceramic failsafes, 35 Pall fuses, and 47 PSDF-designed failsafe devices. Also, six metal fiber failsafe devices designed by Siemens Westinghouse were installed above blanks to expose different alloys to the syngas environment. Figure 4.3-4 shows the layout of the different failsafe devices during TC11. During TC11, a Pall fuse and PSDF-designed failsafe were tested by injecting dust while online. The results of this test are presented in Section 4.5.

After TC11, one Pall FEAL fuse was removed, inspected, and flow-tested. The Pall fuse appeared to be in good condition. The welds were intact, with no evidence of cracking. This failsafe device was tested by injecting solids into it; therefore, the flow resistance had increased, as expected. Future plans are to continue testing the Pall fuses by exposing them to the syngas environment and solids injection tests.

During the outage, three Ceramem failsafe devices were removed. Each failsafe was visually inspected, weighed and flow-tested. The inspection did not reveal any damage to the ceramic porous media. The post-test weights were 0.5 to 0.7 grams more than the pretest weights. Finally, the flow coefficients were 97.7 to 98.5 percent of the pretest values. Since there was no damage, no weight loss or gain, and no significant loss of flow coefficient, it was decided to reinstall these failsafe devices for TC12.

After TC11, five PSDF-designed failsafe devices were removed for inspection. Each failsafe device appeared to be in good condition with no damage noted. One of the test objectives for the PSDF-designed failsafe is to determine whether or not the porous material blinds over time. Therefore, each failsafe that was removed was flow tested during the outage.

Figures 4.3-5 through -8 show the flow test results of four of the five failsafe devices. One of the failsafes that was removed was tested with solids injection. The flow resistance of that failsafe increased as expected. Each figure is a plot of pressure drop versus flow. Each figure contains the failsafe's original flow curve (denoted virgin), flow curve before TC11, and flow curve after TC11. The graphs show that there was not any significant change in the flow curves during TC11 except for PSDF #40. This failsafe lost 25 percent of its original flow coefficient. It is important to note that this failsafe was installed before TC10 with zero exposure hours. This failsafe has not been flow tested since that time. Keep in mind that during TC10, there were many HR-160 and Hastelloy X filter elements installed in the PCD. Therefore, it is believed that the poor collection efficiency of the HR-160 and Hastelloy X filter elements caused the loss in flow coefficient. This finding is consistent with the other failsafe devices tested during this outage. Each failsafe lost ~25 percent of its original flow coefficient, and each of them were tested during a run where these filter elements were installed. Each of these failsafe devices was inspected under the microscope, and particles were found within the pores of the failsafes, but no signs of corrosion was noted. It appears that the flow coefficient of the failsafe decreases until all the available pores, smaller than the particles penetrating through the filter media, plug. Therefore, this phenomenon of pore plugging should disappear once some virgin

PSDF-designed failsafes can be tested with filter elements with higher collection efficiencies (i.e., FEAL).

4.3.6 Auxiliary Equipment

During TC11, seven prototype inverted filter element assemblies supplied by SWPC were installed in the PCD and tested. The inspection of the inverted filter assemblies did not reveal any signs of a leak. Figure 4.3-9 shows that there were no solids plugging the filter element. Therefore, further testing will continue during TC12.

Six g-ash resistance probes were tested during TC11. These probes have been described in past run reports (see TC08 Run Report). The resistance probes were located on B42 and B43 (see Figure 4.2-1 for these locations), three on each filter elements. The probes were located on the lower, middle, and upper sections of the filter elements.

During the run, all six of the resistance probes shorted. The first probe to short (< 100 ohms resistance) was on April 9, 2003. By April 14, 2003, all six probes had shorted. During the post-test inspection, all the probes were still shorted. There was no g-ash buildup to explain why the probe registered the low resistance during the run. Therefore, one of the probes was removed and disassembled for further inspection.

After the ceramic insulator was removed, it was found that one of the thermocouple wires had corroded. A black corrosion product had permeated the MgO insulation and shorted the thermocouple wire to the sheath (see Figures 4.3-10 and 4.3-11). The ceramic cement used to pot the area between the thermocouple wires and the ceramic insulator apparently did not provide a gas-tight seal over the wires. It is interesting to note that the probes started to fail less than 24 hours after coal feed. These same probes were exposed to syngas for over 400 hours during TC10, which used PRB coal as its fuel source, without any adverse reactions. Therefore, it appears that the syngas produced by gasifying lignite contained some corrosive compounds that were not present (or in much lower quantities) during the previous tests.

In the original resistance probe design, shown in Figure 4.3-12, the bare thermocouple wires extended from the insulated area to form the electrode for the probe. However, it was found that after exposure to the syngas, the thermocouple wires became brittle; therefore, the design was modified by changing the portion of the electrode that was exposed to syngas to stainless steel (see Figure 4.3-13). It was thought that the ceramic cement used to pot the area between the thermocouple wires and the alumina insulator would protect the wires from corrosion, but TC11 experience proved otherwise.

Therefore, it was decided to coat the thermocouple wires with Vishay Micro-Measurements H-Cement before the alumina insulator was installed. The H-Cement is a ceramic strain gauge cement that adheres tightly to metal and is used by SWPC Lab to protect exposed junction thermocouples on engine parts. These modifications will be tested during the TC12 test run to determine whether or not they increase the lifetime of the probe

The back-pulse pipes were removed and inspected during this outage with no significant damage noted. However, there were some tar deposits on the back-pulse pipes. The deposits were spongy in nature and had been noted and reported in the past. It does not appear that these tar deposits are causing significant corrosion. Finally, the inner liner of each back-pulse pipe was inspected. The liners appeared to be in good condition with no damage noted.

4.3.7 Fine Solids Removal System

The screw cooler (FD0502) performed well during TC11. Other than minor packing adjustments, FD0502 did not require any attention from the maintenance or operation personnel during the run. Once again, this was encouraging in light of the modifications made to FD0502. Before TC07D, several modifications were made to the drive-end stuffing box in an attempt to increase reliability (see TC07 Run Report for modification details). Since the modifications improved performance during TC07, it was decided to implement the same changes to the nondrive-end before TC08. The same set of seals has been tested on the drive-end since TC07D for a total of 1,590 on-coal hours. Also, the same set of seals has been tested on the nondrive-end since TC08 for a total of 1,289 on-coal hours. Since the new modifications continued to perform well during TC11, it was decided not to disassemble the stuffing box during this outage.

One of the methods used to determine the success of the new stuffing box modifications is tracking the packing follower gap. Figure 4.3-14 shows the packing follower gaps that were measured. The packing follower is used to compress the shaft seal rings to prevent process gas from leaking. Once there is no room to compress the follower, it is time to replace the seals. The packing follower gap has been monitored since TC08. The following table summarizes the packing follower measurements:

Run	Drive-End Gap, Inches	Nondrive-End Gap, Inches
Before TC08	1.8	1.8
After TC08/Before TC09	1.4	1.6
After TC09/Before TC10	1.1	1.4
After TC10	1.1	1.3
After TC11	0.9	1.3

The table above shows that both the drive-end and nondrive-end packing follower gaps still have room for compression. Therefore, it was decided not to disassemble FC0502 during this outage in order to accumulate operating experience with the new modifications.

The fine solids depressurization system (FD0520) required a large amount of attention by operations and process engineers during TC11. Many of the problems associated with FD0520 were related to periodic increases of solids loading to the PCD. Since FD0520 does not have a reliable level detector, increased solids loading plugged the solids removal system on a couple of occasions. As mentioned in previous run reports, a reliable solids level detector needs to be identified and installed in FD0520 in order to increase the cycle efficiency and reduce problems associated with fluctuations in solids loading.

Before TC11, an Everlasting valve was installed above the current upper spheri valve on FD0520 (see Figure 4.3-15) in order to determine whether or not it was more reliable than the spheri valve. During the outage between TC10 and TC11, the manual isolation ball valves above FD0520 were removed and replaced with an 8-inch Everlasting valve. In the past, different types of seal material have been tested such as Nomex-filled Silicone and Nomex-filled Viton. Both of these seal materials have proven to be unreliable. It was believed that the Everlasting valve was a more robust valve that would increase the reliability of the fine solids removal system. This setup allowed us to utilize the current spheri valve as a backup in case the Everlasting valve did not perform as expected.

However, we were unable to test the Everlasting valve during TC11 because of problems associated with control logic. The new setup was supposed to provide the capability to swap back-and-forth between the spheri valve and Everlasting valve. During the startup, it was learned that a solenoid valve to provide pilot gas to the control cabinet whenever the Everlasting valve was selected was not installed. Therefore, the FD0520 system was operated using the spheri valve. The valve performed well without failure. Since the run was relatively short, it was decided not to disassemble the FD0520 system during the outage. The spheri valve seal was pressure tested. The seal held pressure and was determined to be in good condition for TC12.

During the outage, a solenoid valve was installed to allow pilot gas into the control cabinet when the Everlasting valve was selected. The Everlasting valve was tested with the new modifications and operated as expected. Therefore, operating experience with the Everlasting valve should be accumulated in TC12.

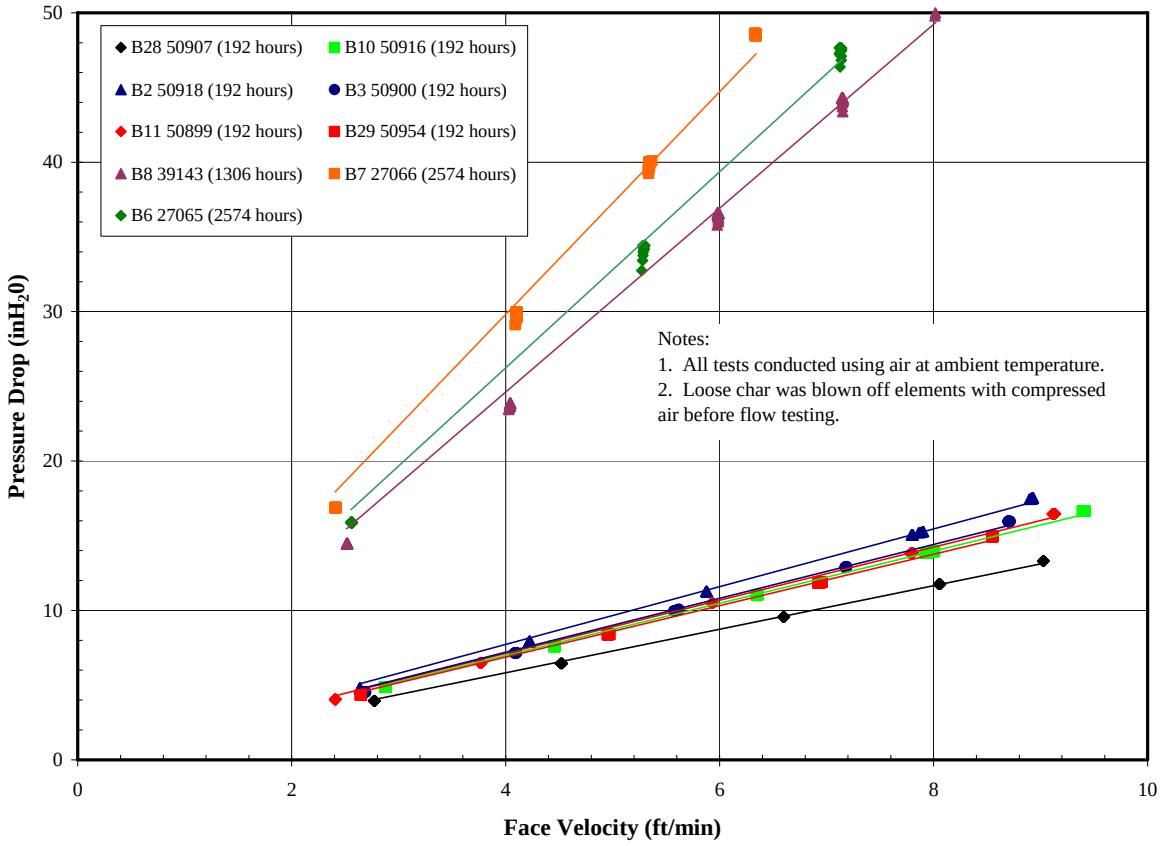

Figure 4.3-1 Pressure Drop Versus Face Velocity for Pall FEAL Filter Elements After TC11

Figure 4.3-2 PCD Plenum Removal After TC11

Figure 4.3-3 Solid Deposit on Filter Holder

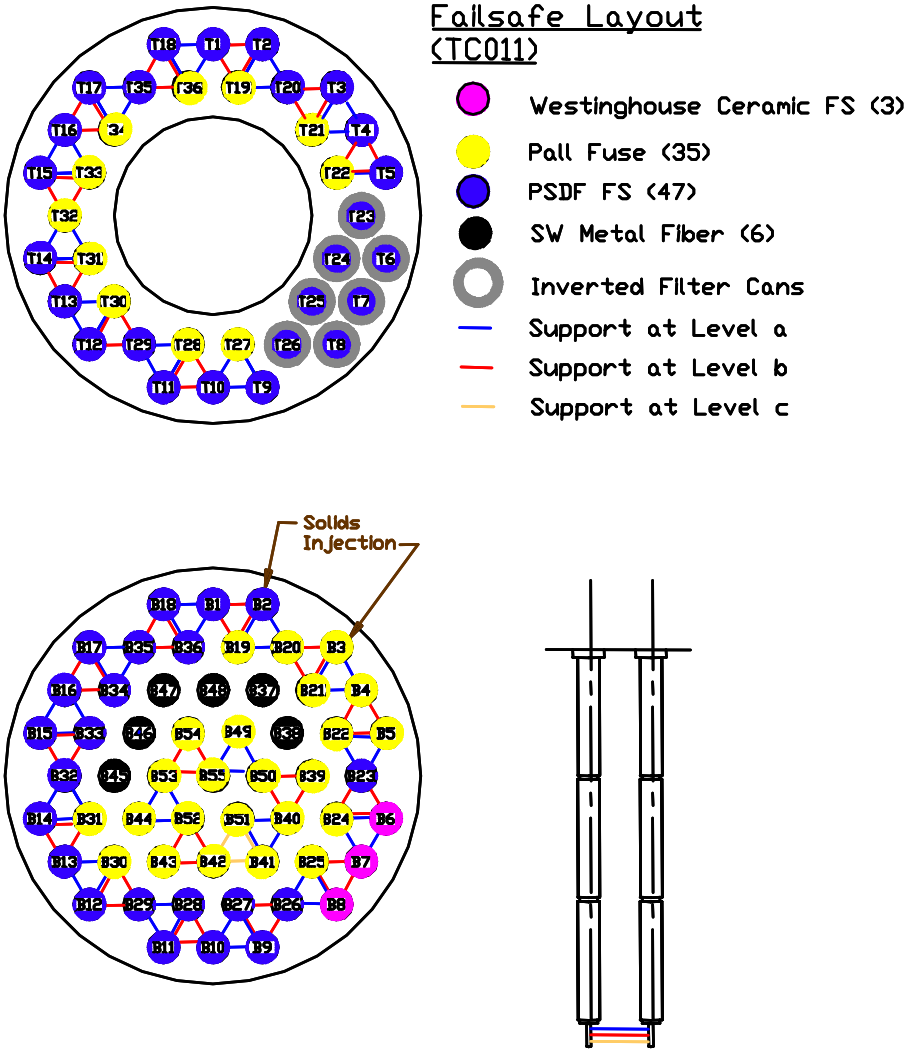

Figure 4.3-4 Failsafe Layout for TC11

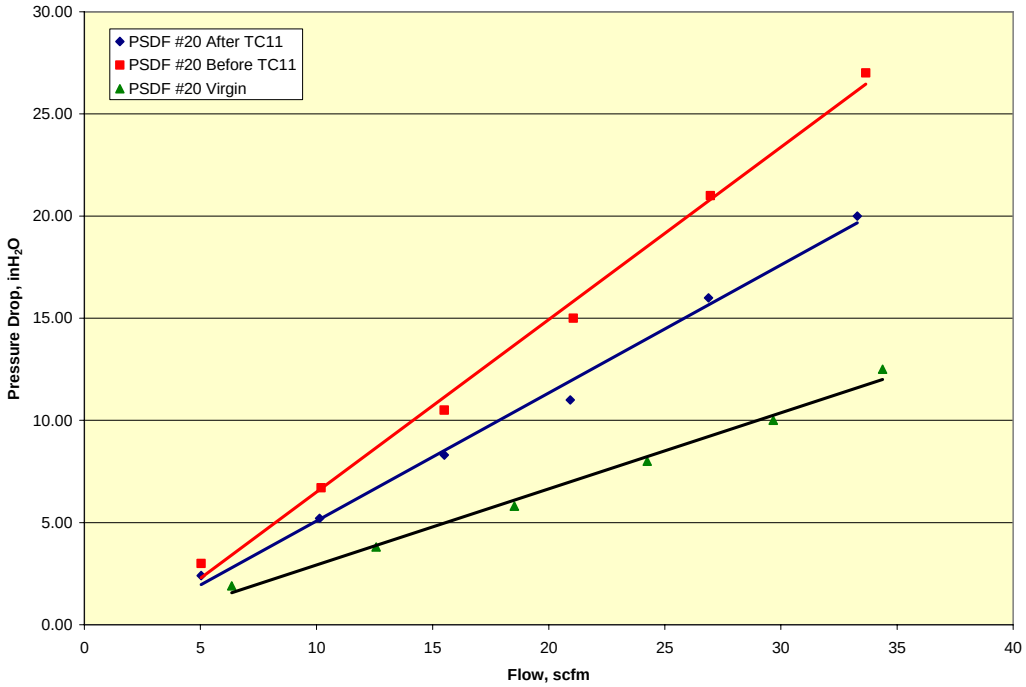

Figure 4.3-5 PSDF-Designed Failsafe #20 Before and After TC11

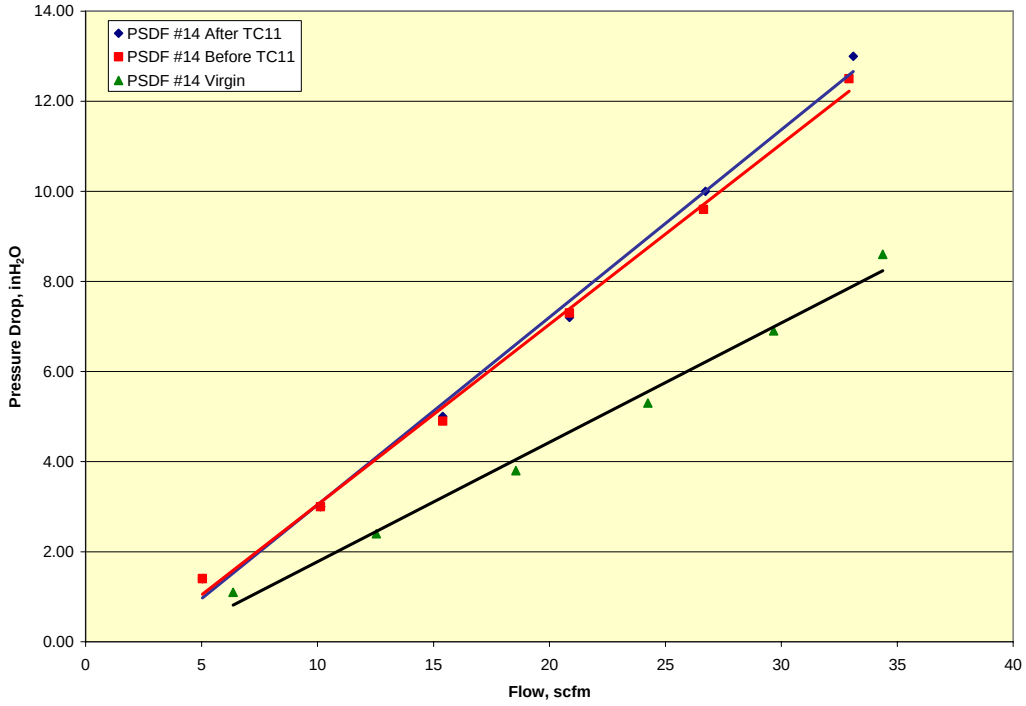

Figure 4.3-6 PSDF-Designed Failsafe #14 Before and After TC11

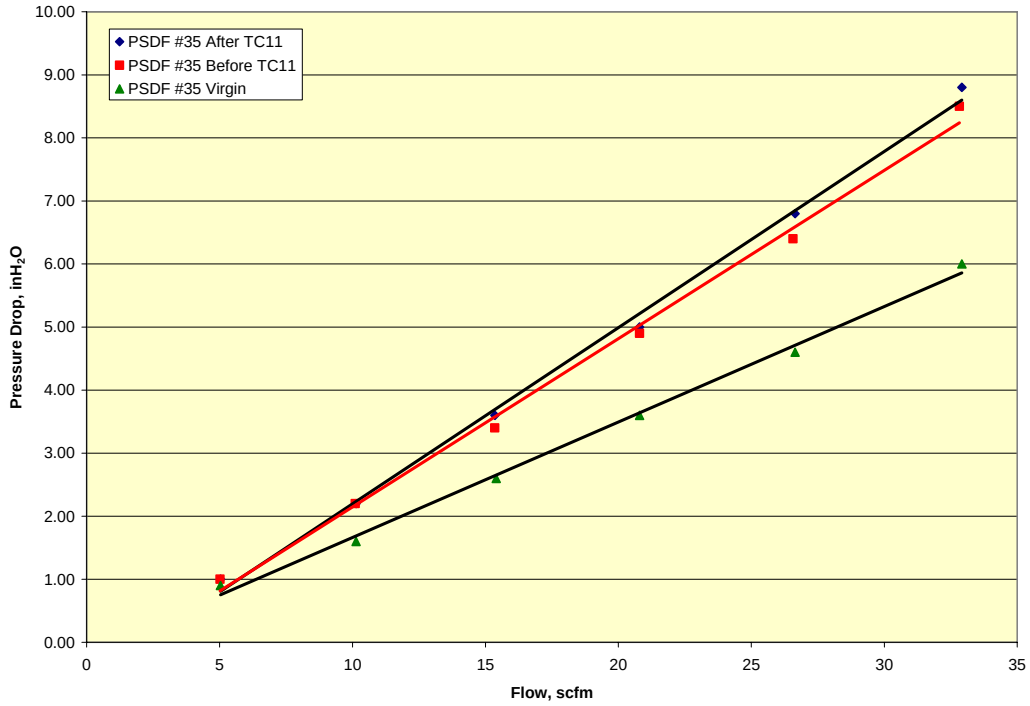

Figure 4.3-7 PSDF-Designed Failsafe #35 Before and After TC11

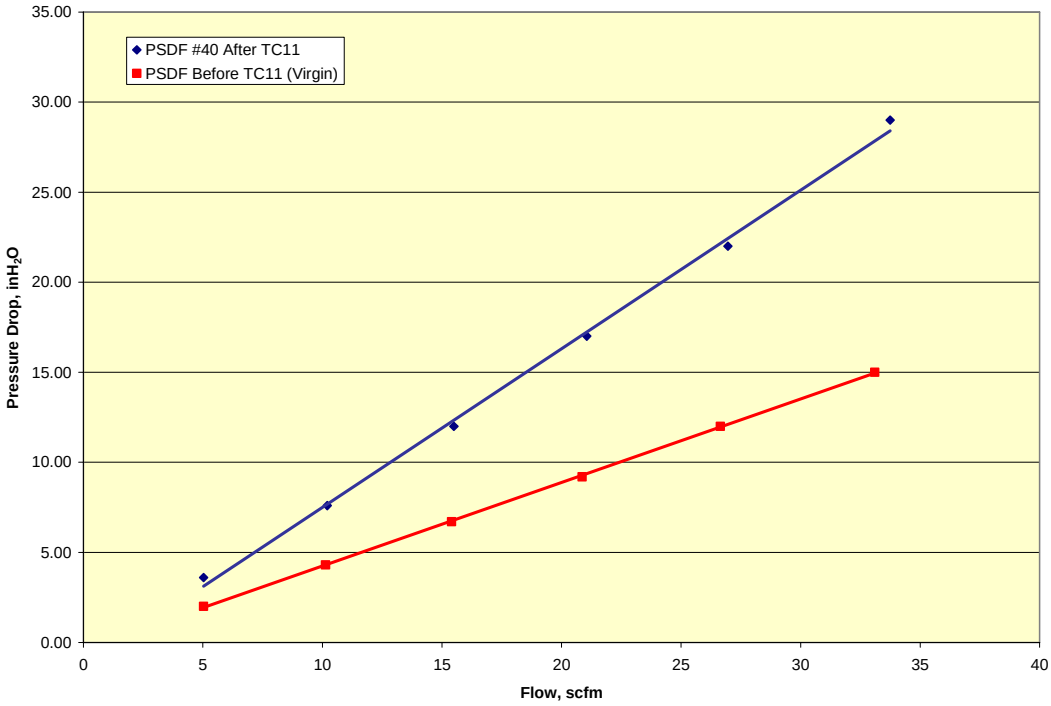

Figure 4.3-8 PSDF-Designed Failsafe #40 Before and After TC11

Figure 4.3-9 Inverted Filter Assembly After TC11

Figure 4.3-10 Side View of Probe Showing Corroded Thermocouple Wire

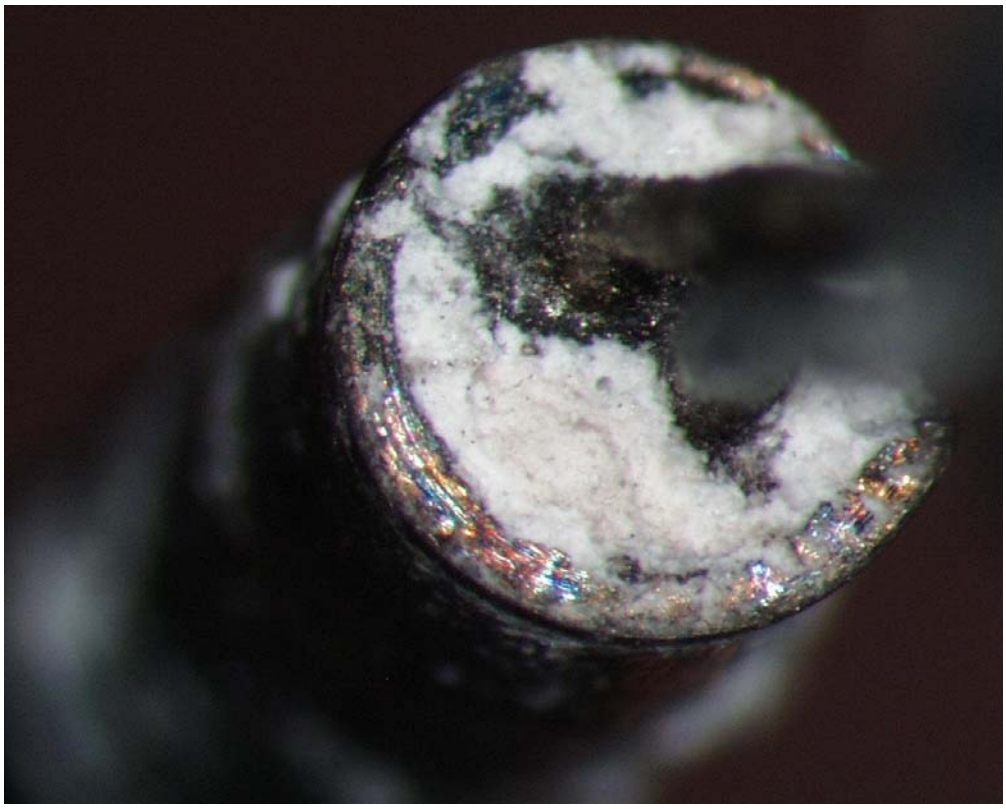

Figure 4.3-11 End View of Probe Showing Corrosion Product Permeating MgO Insulation

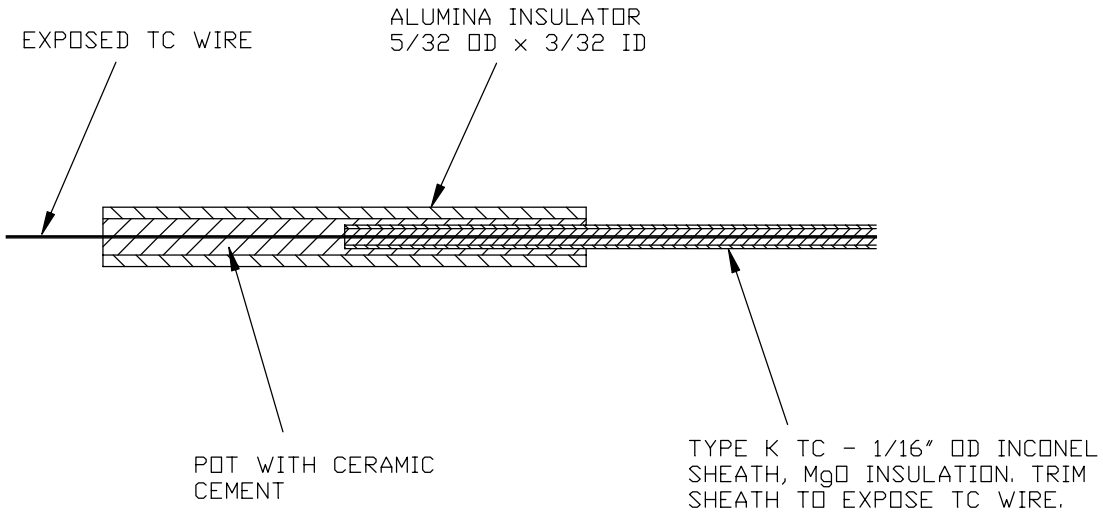

Figure 4.3-12 Original Resistance Probe Design With TC Wire Electrode

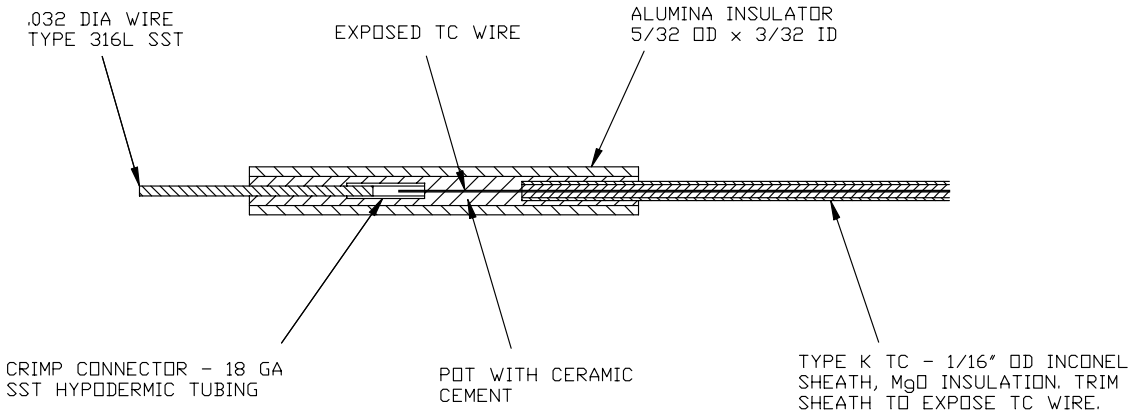

Figure 4.3-13 Modified Resistance Probe Design With Stainless Steel Electrode

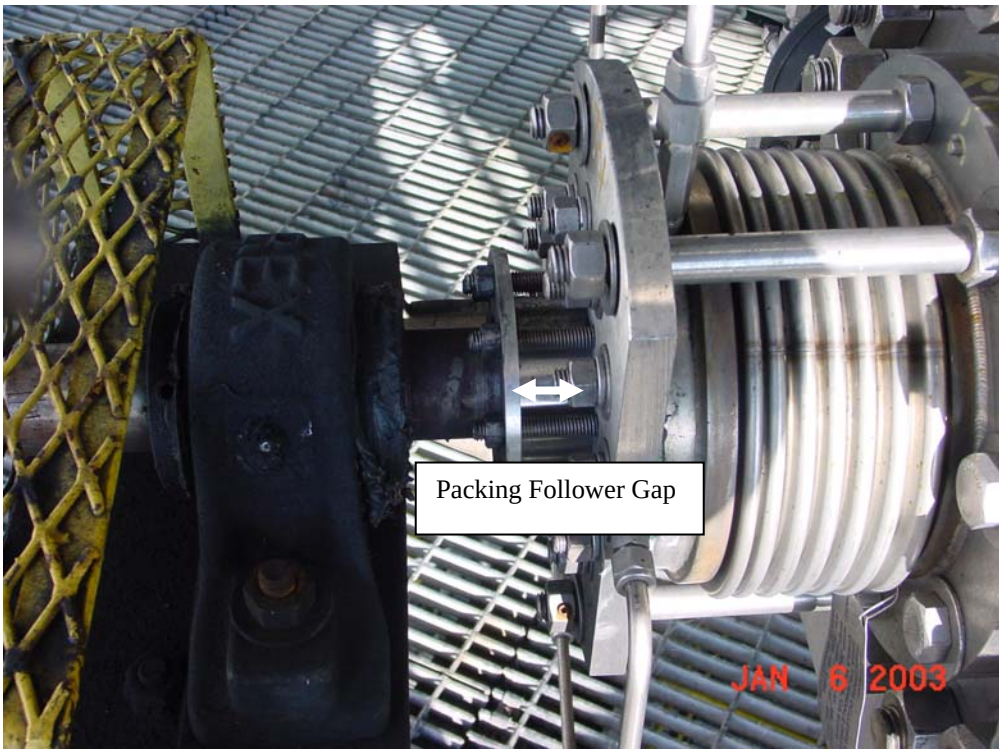

Figure 4.3-14 Packing Follower Gap on Nondrive End of FD0502 After TC10

Figure 4.3-15 Everlasting Valve Installed Before TC11

4.4 TC11 GASIFICATION ASH CHARACTERISTICS AND PCD PERFORMANCE

In the previous section on PCD operations, it was noted that the transient ΔP across the PCD varied considerably during TC11. During some periods of operation, the ΔP rise during a filtration cycle was so low that it was practically negligible. At other times, the ΔP rise was comparable to that seen in other recent gasification runs. The observed changes in transient ΔP were so large that it was difficult to imagine that they were caused solely by variations in the solids carryover to the PCD. We suspected that something was causing substantial variations in the flow resistance, or normalized drag, of the g-ash. To investigate this possibility, transient PCD drag was calculated for all of the in situ particulate sampling runs, and various correlations were tested to examine the relationship between the transient drag and the physical and chemical characteristics of the in situ samples. As discussed below, these correlations showed that a major factor affecting the transient drag was the loss on ignition (LOI) or carbon content of the g-ash.

As discussed in the section on Transport Gasifier operations, the LOI/carbon content of the TC11 g-ash during periods of low, stable coal feed was much lower than in previous gasification tests. (This difference was expected since the higher reactivity of the low-rank lignite should result in better carbon conversion.) Analysis of in situ samples collected at the PCD inlet confirmed that the LOI/carbon content was as low as 1 wt percent or less during the periods of low coal feed, and the corresponding PCD ΔP rise was very low. However, much higher rates of PCD ΔP rise were observed during periods of high coal feed, and subsequent analysis of the PCD inlet solids collected during these time periods showed that the LOI/carbon content was much higher (>10 wt percent) when the coal-feed rate was high. It is very significant that the operation of the Transport Gasifier can affect one of the fundamental properties of the particles exiting the gasifier in a way that affects the operation of the PCD. Therefore, it is important to understand this effect of LOI/carbon content on PCD performance.

Since the transient drag calculations suggested a relationship between drag and LOI/carbon content, laboratory drag measurements were made using PCD hopper samples with a wide range of LOI/carbon content. Although the range of LOI/carbon content in the hopper samples did not match that in the in situ samples exactly, the laboratory drag measurements definitely showed the same trend toward decreasing drag with decreasing LOI/carbon. These observations were very interesting because they showed that the reduction in drag was relatively small at high values of LOI/carbon (e.g., 30 to 11 wt percent). As the LOI decreased, however, the effect became more pronounced. There was a substantial reduction in drag from 11 to 7 wt percent LOI/carbon and an even more substantial reduction from 7 to 1.7 wt percent LOI/carbon. Physical characterization of the corresponding samples showed that the changes in drag were accompanied by very similar changes in specific-surface area. The samples with 30 and 11 wt percent LOI/carbon had almost identical values of specific-surface area, while, for the other samples, surface area decreased appreciably with decreasing LOI/carbon.

The remainder of this section discusses in more detail the physical characteristics and chemical composition of the TC11 g-ash and the relationships between these characteristics and the transient drag. The properties and drag of the TC11 g-ash are also compared to those of other

g-ash from previous runs to determine how the Falkirk lignite compares to PRB and bituminous coal in terms of the effects on PCD operations.

4.4.1 In situ Sampling

During the air-blown portion of TC11, SRI performed five in situ particulate sampling runs at the PCD inlet and six runs at the PCD outlet. Because of the short duration of the oxygen-blown portion, only one inlet run and two outlet runs were conducted during that portion of TC11. The results are discussed in the following sections.

4.4.1.1 PCD Inlet Particle Mass Concentrations

As shown in Table 4.4-1, the particle mass concentrations measured at the PCD inlet varied from 11,300 to 22,500 ppmw during air-blown operation. The corresponding particle mass rates ranged from about 190 to 490 lb/hr depending on coal-feed rate, which varied from about 2,400 to 3,500 lb/hr during the air-blown measurements. The single measurement that was made during oxygen-blown operation indicated a particulate loading of 25,100 ppmw, corresponding to a particle mass rate of about 350 lb/hr. At about the same particle mass rate, the corresponding particle concentration with air-blown operation was much lower (~16,000 ppmw) due to the dilution effect of the nitrogen in the syngas.

Inlet particle mass concentration was found to be directly correlated with loss on ignition (LOI). This was true for all of the air-blown samples as well as the single oxygen-blown sample. For the air-blown runs, the variation in particle concentration from 11,300 to 22,500 ppmw corresponded to a change in LOI from about 0.7 to 11.4 wt percent. The single oxygen-blown run had the highest particle loading and the highest LOI (25,100 ppmw and 16.0 wt percent). These results make sense, because an increase in LOI generally reflects a reduction in carbon conversion or more carryover of unconverted carbon from the gasifier. Subsequent sections will address the relationship between LOI and carbon content and the effect of LOI/carbon content on particulate properties.

Previous tests have shown that, at a given coal-feed rate, the same particle mass rate is obtained with air- and oxygen-blown gasification. In TC11, the single particle mass rate that was measured in oxygen-blown gasification was lower than that measured in air-blown operation at about the same coal-feed rate. This difference suggests that there were other factors that caused a lower particle carryover during the oxygen-blown gasification. The factors affecting the solids carryover are discussed in more detail in the section on Transport Gasifier operation.

4.4.1.2 PCD Outlet Particle Mass Concentrations

Particle concentrations measured at the PCD outlet are included in Table 4.4-1 and compared to other test programs in Figure 4.4-1. As shown in the table, the initial measurement that was made during startup on propane showed an elevated particle concentration (0.27 ppmw). Since there was no coal feed during this period, it may be inferred that the elevated loading was probably caused by reentrainment of dust from the outlet piping. All of the subsequent measurements were made during operation on coal, and all of these measurements were below

the lower limit of resolution (< 0.1 ppmw), with the exception of two measurements that were made during failsafe testing. This result suggests that all of the PCD seals remained intact throughout TC11, and there was no significant penetration of particles through the filter elements and failsafes during normal operation. Particulate measurements made during the failsafe testing showed that both the PSDF-designed failsafe and the Pall fuse leaked slightly, but the outlet particle loading was still very low (0.16 ppmw with the PSDF-designed failsafe and 0.15 ppmw with the Pall fuse). Details of the failsafe testing are discussed in Section 4.5.

4.4.1.3 Syngas Moisture Content

Also included in Table 4.4-1 are the syngas moisture measurements made in conjunction with the particulate sampling runs at the PCD outlet. The first sampling run, which was done during startup on propane, was too short for an accurate determination of the moisture. The subsequent runs yielded moisture measurements in the range of 9.8 to 15.2 percent by volume during air-blown operation and 18.1 to 18.4 percent by volume during oxygen-blown operation. The syngas moisture content is normally higher during oxygen-blown operation, because higher rates of steam addition are required to cool the lower mixing zone.

4.4.1.4 Real-Time Particle Monitoring

The Pollution Control and Management (PCME) DustAlert-90 particulate monitor was operational and apparently functioning properly throughout TC11. The monitor never gave any positive response that would indicate the presence of particles at the PCD outlet. This was true even during startup and during the failsafe tests when the measured particle loadings were about 0.3 and 0.2 ppmw, respectively. This result is not surprising since previous testing has shown that the DustAlert-90 is not sensitive to particle concentrations below about 0.5 to 1.0 ppmw.

The original TC11 test plan called for testing the DustAlert-90 with injected g-ash. Before the injection testing could be done, the TC11 test run was terminated due to problems with solids circulation in the Transport Gasifier. Although it was not possible to do the injection testing, the DustAlert-90 seemed to produce a reasonable signal throughout TC11. The amount of noise in the signal was consistent with previous runs, and the lack of positive response was consistent with the very low particle loadings measured at the PCD outlet.

4.4.2 Particle-Size Analysis of In situ Particulate Samples and PCD Hopper Samples

As in previous tests, a Microtrac X-100 particle-size analyzer was used to measure the particle-size distributions of the in situ particulate samples collected at the PCD inlet and the PCD hopper samples used for the laboratory drag measurements. The results for these two types of samples is discussed separately in the following sections.

4.4.2.1 In situ Particulate Samples

Figure 4.4-2 shows the measured particle-size distributions on the basis of mass concentration in individual size bands. As for the particulate loadings, the particle size results show clear differences for different levels of LOI. The three runs with the highest LOI values (run No. 2 with 10.1-percent LOI, run No. 4 with 11.4-percent LOI, and run No. 6 with 16.0-percent LOI) had size distributions that were very similar to one another. Compared to these high-LOI runs, the two samples with the lowest LOI values (run No. 5 with 0.7-percent LOI and run No. 3 with 1.3-percent LOI) had lower mass concentrations in the size range of about 1 to 30 μm. This difference between the high- and low-LOI groups of runs is obvious in the comparison of the average particle-size distributions for the two groups of runs, which are indicated by the solid line and the dashed line in Figure 4.4-2. Above 30 μm, there is overlap between the size distributions for the individual high- and low-LOI runs, and the difference between the two average-size distributions decreases as they merge together. These results suggest that most of the carbon particles, which account for the differences in LOI, are smaller than 30 μm. (The relationship between LOI and carbon content will be discussed in more detail in the section on chemical analysis.)

In Figure 4.4-3, the size distribution for the oxygen-blown run is plotted separately and compared to the average-size distribution of the other high-LOI runs and the average-size distribution of the low-LOI runs. This comparison shows that there is very little difference between the oxygen- and the air-blown size distributions that have high LOIs (> 10 wt percent). As suggested by the previous comparison, however, there is a significant difference in the size distributions of the high (> 10 wt percent) LOI group and the low (< 2 wt percent) LOI group. Again, the difference is in the particles smaller than about 30 μm, suggesting that the unconverted carbon is primarily contained in these smaller particles.

To examine the differences in particle-size distribution without the influence of any differences in the total particulate loading, the size distributions must be compared on the basis of percentage mass rather than mass concentration. Figure 4.4-4 shows a comparison of the average particle-size distributions on the basis of percentage mass for the three groups identified previously: (1) air-blown, high-LOI; (2) oxygen-blown, high-LOI; and (3) air-blown, low-LOI. This comparison shows that the size distributions are essentially identical for the air-blown, high-LOI case and the oxygen-blown, high-LOI case. This result confirms the findings of previous tests that have shown that the choice of oxidant has no effect on the particle-size distribution.

The comparison in Figure 4.4-4 also clearly shows the significant effect of LOI. Compared to the high-LOI size distributions (air- and oxygen-blown), the low-LOI, air-blown distribution contains a lower mass percentage of 1 to 10 μm particles and a higher mass percentage of particles larger than 30 μm. This difference would be consistent with an increased conversion of carbon particles, if most of the unconverted carbon in the high-LOI samples is in particles smaller than 10 μm. The reduction in the relatively fine carbon fraction should produce a concomitant increase in the fraction of larger particles, and this is confirmed by the comparison of the high- and low-LOI cases.

4.4.2.2 PCD Hopper Samples

The wide variation in LOI/carbon content that was seen in the in situ particulate samples was also evident in the PCD hopper samples. Since it was not known how the flow resistance of the g-ash would be affected by the differences in LOI/carbon content, the hopper samples used in the laboratory drag measurements were selected to cover a wide range of LOI values (1.7 to 30 wt percent). This range was roughly comparable to that found in the in situ particulate samples (0.7 to 16 wt percent). While the two ranges of LOI values do not match exactly, the degree of variation in the hopper samples should be sufficient to reveal any effects of LOI on flow resistance (drag).

Figure 4.4-5 shows the size distributions of the four hopper samples as a function of their LOI values. The measurements show a progression toward higher mass concentrations as the LOI increases, except for the decrease in mass concentration between 11 and 30 wt percent LOI. The hopper sample with the 30 wt percent LOI was obtained during oxygen-blown operation, while all of the other hopper samples were obtained during air-blown gasification. However, previous tests have shown that the choice of oxidant has no effect on the drag (see reports for test programs TC08, TC09, and TC10).

4.4.3 Measurement and Sampling of PCD Dustcakes

The original test plan for TC11 called for a semidirty shutdown of the PCD at the end of the run. Unfortunately, it was necessary to end TC11 prematurely due to problems with solids circulation in the Transport Gasifier. Because of the circulation problems, coal feed could not be reestablished after the last gasifier trip, so it was not possible to do a semidirty shutdown of the PCD as planned. By default, the PCD was shut down in a clean condition. In fact, the PCD was back-pulsed for about 24 hours after the final loss of coal feed. Because of the extensive back-pulsing after shutdown, the remaining dustcake may not accurately represent the residual cake that was present during the run.

Despite the extensive back-pulsing after shutdown, the inspection of the PCD after TC11 revealed that there was still a thin dustcake uniformly covering all of the filter elements. The cake comprised a very thin, dark gray outer layer and a very thin, much lighter colored inner layer. The lighter inner layer resembled combustion ash, while the outer darker layer seemed to be more like a typical carbonaceous g-ash. The two layers could possibly represent different materials or different degrees of carbon conversion. The individual layers were too thin to obtain separate samples for chemical analysis.

Table 4.4-2 gives dustcake thickness and areal loading measurements that were made on various filter elements in the top and bottom plenums as noted. The thickness measurements were obtained by the laser transit method described in previous reports. It was necessary to use a modified procedure for the areal loading measurements to allow the sampling of a larger area of the filter element surface to obtain enough material to accurately determine the areal loading. Because of the large area required for the areal loading measurements, it was not possible to make the thickness and areal loading measurements in the same locations or even on the same filter elements. It is preferable to make the thickness and areal loading measurements in the

same location, if possible, to allow accurate calculation of the dustcake porosity. In this case, however, the porosity values would be questionable even if they were based on collocated measurements, because of the extensive back-pulsing that occurred after TC11. Of course, the extensive back-pulsing may have also resulted in some reduction in the dustcake thickness and areal loading.

Table 4.4-3 compares the average TC11 dustcake thickness with the residual cake thicknesses measured after other gasification tests. Data from GCT4, TC06, and TC07 are not included, because the measured thicknesses were biased by tar deposition, bridging, and coke feed. Despite the extensive back-pulsing after TC11, the average residual cake thickness is not dramatically different from the other residual cake thicknesses that have been measured since the new lower mixing zone was placed in service in TC07. In the cases of the TC08, TC09, and TC10 dustcakes, we can be confident that the residual cake thickness was not altered by subsequent back-pulsing, because these tests were concluded with a semidirty shutdown. Since these cakes were all comparable to or thinner than the TC11 cake, it might be inferred that the effect of the extensive back-pulsing on the TC11 cake may not be as significant as first thought.

Based on the average values of the measured dustcake thickness and areal loading (0.013 in. and 0.023 lb/ft^2), the average dustcake porosity may be estimated to be about 85 percent. This figure is at the high end of the range of residual cake porosities determined for the PRB residual dustcakes, which have varied from 80 to 85 percent. The relatively high porosity of the TC11 cake could be blamed on the extensive back-pulsing after shutdown, but we also know that coal type has a strong influence on cake porosity. For example, the TC09 residual cake, which was produced from the Hiawatha bituminous coal, had an average porosity of 94 percent, much higher than any of the cakes made from PRB coal.

For the measurement of dustcake physical properties and chemistry, it was not possible to obtain sufficient samples from individual filter elements. To provide enough material for all of the required tests, it was necessary to combine the dustcake samples that were scraped off all of the elements in each plenum. This process resulted in a single bulk dustcake sample from the top plenum and a single bulk dustcake sample from the bottom plenum. The characterization of these samples is discussed in Sections 4.4.4 and 4.4.5.

4.4.4 Physical Properties of In situ Samples, Hopper Samples, and Residual Dustcake

This section describes the physical properties of the in situ samples collected during TC11, the TC11 hopper samples used for the laboratory drag measurements, and the residual dustcake samples collected after TC11.

4.4.4.1 In situ Particulate Samples

As shown in Table 4.4-4, there was a wide range of variation in the physical properties of the TC11 in situ samples. The largest variation was in the specific-surface area, which ranged from 3 to 105 m^2/g. No previous test program has shown such a large degree of variation in the specific-surface area of the g-ash. The variation in surface area seems to be related to changes in the loss on ignition (LOI) or carbon content of the g-ash as illustrated in Figure 4.4-6. The LOI

and carbon content also showed a wider range of variation than in any previous test program, with LOI varying from 0.7 to 16 percent and carbon content ranging from 1.2 to 16 percent. The low-LOI, low-surface-area samples were gray in color and had the appearance of combustion ash. The high-LOI, high-surface-area samples were black in color and more closely resembled the g-ash that has been produced in previous runs.

As indicated in Figure 4.4-6, the specific-surface area of the gasification ash increased as the LOI/carbon content increased. This trend is not surprising, since increasing LOI indicates decreasing carbon conversion or increasing amounts of carbonaceous solid, which generally has a relatively high surface area. Conversely, as the LOI/carbon content is reduced, the g-ash becomes more like combustion ash, which has a relatively low specific-surface area. As shown in Figure 4.4-6, the plot of surface area versus LOI is very similar in appearance to the plot of surface area versus carbon content. The reason for this similarity can be seen in Figure 4.4-7, which plots LOI versus carbon content. As the plot shows, the LOI and noncarbonate carbon are virtually equivalent. This result suggests that essentially all of the LOI is attributable to the oxidation of the noncarbonate carbon. The decomposition of $CaCO_3$ and CaS contribute very little to the LOI, because the concentrations of these components in the g-ash are very low as discussed in the section on chemical composition.

The table below compares the properties of the TC11 in situ samples with those from other PSDF gasification tests and from the TC05 combustion tests with PRB coal.

	TC11	TC10	TC09	TC08	TC07-D	TC06	TC05
Operating Mode	Gasification	Gasification	Gasification	Gasification	Gasification	Gasification	Combustion
Coal Type	Falkirk Lignite	PRB	Hiawatha Bituminous	PRB	PRB	PRB	PRB
Bulk density, g/cc	0.39-0.68	0.27	0.24	0.25	0.32	0.29	0.68
Skeletal particle density, g/cc	2.51-2.73	2.25	2.23	2.37	2.47	2.45	2.78
Uncompacted bulk porosity, %	75.1-84.6	88.0	89.2	89.5	87.0	88.2	75.5
Specific surface area, m^2/g	3-105	146	96	222	170	222	0.7
Mass-median diameter, μm	12.8-25.0	12.3	19.1	18.7	16.9	15.3	23.0
Loss on ignition, wt %	0.7-16.0	39.6	54.7	43.8	33.5	37.2	2.1

Compared to the other g-ash, the TC11 g-ash generally had higher bulk and true densities, lower bulk porosity, lower surface area, and lower LOI. In most respects the TC11 g-ash more closely resembles the combustion ash from TC05. Some of the TC11 samples actually had LOI values that were lower than the average LOI value for the TC05 combustion ash. Even the low-LOI samples, however, still had surface areas that were higher than the average surface area of the combustion ash.

4.4.4.2 PCD Hopper Samples Used for Drag Measurements

Because of the large variations in surface area and LOI/carbon content that were seen in the in situ samples, it was suspected that there may also be substantial variations in the drag of the g-ash. Therefore, the PCD hopper samples selected for the laboratory drag measurements were chosen to represent a wide range of surface area and LOI/carbon content. The properties of the hopper samples are included in Table 4.4-4 and in Figure 4.4-6. As shown in the figure, the data for the hopper samples fall on the same trend line as the data for the in situ samples. Although the selected hopper samples do not cover exactly the same range of values as the in situ samples, the degree of variation in the selected hopper samples is certainly sufficient to ascertain any effects of LOI/surface area on drag. These effects will be discussed in more detail in the section on laboratory drag measurements.

4.4.4.3 Residual Dustcake Samples

After TC11, separate samples of the residual dustcake were taken from the top and bottom plenums to look for any differences in the physical properties. This comparison was of interest because recent tests have been concluded with semidirty shutdowns, which did not allow comparison of the top and bottom residual cakes. In previous gasification runs where a clean shutdown has been performed, the properties of the residual cake have been altered or obscured by bridging, partial oxidation, or coke feed. Because of these effects, TC11 was actually the first run where we could make an unambiguous comparison of the residual cakes on the top and bottom plenums. As shown in Table 4.4-5, the differences between the top and bottom cakes appear to be relatively minor. This result suggests that there is no significant segregation of particles between the top and bottom plenums.

The table below compares the TC11 dustcake properties to the properties of the TC11 in situ samples.

	Residual Dustcake	In situ Samples
Bulk density, g/cc	0.32-0.36	0.39-0.68
Skeletal particle density, g/cc	2.29-2.34	2.51-2.73
Uncompacted bulk porosity, %	84.6-86.0	75.1-84.6
Specific-surface area, m^2/g	18-23	3-105

Mass-median diameter, μm	4.2-4.8	12.8-25.0
Loss on Ignition, wt %	19.1-24.7	0.7-16.0

Compared to the incoming g-ash, the dustcake has lower bulk and true densities, higher uncompacted bulk porosity, lower mass-median diameter (MMD), and higher LOI. The largest difference is in the MMD. Some of this difference may be caused by the dropout of large particles before they reach the filter elements, but this mechanism probably cannot fully explain the very large difference in MMD. As discussed in previous reports, there may be another mechanism by which fine particles are gradually enriched in the residual cake over time. In this mechanism, fine particles that are liberated during back-pulsing may be reentrained in the gas and recollected onto the filter elements, while larger particles drop into the hopper. Over time, this effect could result in the gradual enrichment of fine particles in the residual cake.

In previous runs, the residual dustcake has always had a lower surface area than the in situ samples, and this difference has been attributed to pore closure by sulfidation and/or consolidation. With the TC11 samples, it is not possible to say that this difference is definitely the case because the in situ samples cover such a wide range of surface area. However, the dustcake surface area (18 to 23 m^2/g) is less than the average value of surface area for the in situ samples (57 m^2/g).

The table below compares the properties of the residual dustcakes from TC11 and from previous test campaigns. The dustcake from TC08 is not included because the physical properties were altered by partial oxidation of the cake. The TC07 dustcake is omitted because the properties were biased by coke feed.

	TC11	TC10	TC09	TC06	TC05
Operating Mode	Gasification	Gasification	Gasification	Gasification	Combustion
Coal Type	Falkirk Lignite	PRB	Hiawatha Bituminous	PRB	PRB
Bulk density, g/cc	0.32-0.36	0.23	0.24	0.25	0.55
Skeletal particle density, g/cc	2.29-2.34	2.07	2.12	2.28	2.80
Uncompacted bulk porosity, %	84.6-86.0	88.9	88.7	89.0	80.4
Specific-surface area, m^2/g	18-23	91	114	257	3.9
Mass-median diameter, μm	4.2-4.8	4.6	12.4	9.3	6.7
Loss on ignition, wt %	19.1-24.7	51.8	54.7	46.2	9.3

This comparison shows that most of the properties of the TC11 residual cake fall between those of the residual cakes from the other gasification runs and the residual cake from the TC05 combustion run. This is true of all properties except the MMD. The MMD of the TC11 cake is actually about the same as the MMD of the TC10 residual dustcake, which was generated from PRB coal. The TC06 residual cake, which was also produced from the PRB coal, had a much larger MMD, but that was before the new lower mixing zone was placed in service. The surface area of the TC11 residual cake is much lower than the surface areas of the residual cakes from the other gasification runs but still significantly higher than the surface area of the TC05 combustion ash. The same trend is evident in the LOI values of the various residual dustcakes.

4.4.5 Chemical Composition of In situ Samples, Hopper Samples, and Residual Dustcake

This section discusses the chemical composition of the in situ samples collected during TC11, the TC11 hopper samples used for the laboratory drag measurements, and the residual dustcake samples collected after TC11.

4.4.5.1 In situ Particulate Samples

The chemical compositions of the TC11 in situ samples are detailed in Table 4.4-6. These compositions were calculated from the elemental analyses using the same procedures that have been described in previous reports. The calculated compositions show that the TC11 g-ash contains relatively low amounts of $CaCO_3$ (1.1 to 4.8 wt percent) and CaS (0.27 to 2.2 wt percent). This result is not surprising since no limestone was added to the transport reactor in TC11. The in situ samples contain an appreciable amount of CaO (11.2 to 15.4 wt percent), which presumably comes from calcium in the coal mineral matter. As already mentioned, the calculated noncarbonate carbon content is sufficient to account for all of the LOI. In fact, all of the calculated values of noncarbonate carbon are just slightly higher than the corresponding LOI values. The absolute differences between noncarbonate carbon and LOI are quite small for all of the samples and vary from only 0.35 to 0.81 wt percent. This slight difference is well within the uncertainties of the analytical data. Therefore, for practical purposes, it may be said that the LOI and noncarbonate carbon content are equivalent.

The table below compares the composition of the TC11 in situ samples with the average compositions of the g-ash from previous gasification test campaigns and with the average composition of the PRB combustion ash from TC05.

	TC11	TC10	TC09	TC08	TC07-D	TC06	TC05
Operating Mode	Gasification	Gasification	Gasification	Gasification	Gasification	Gasification	Combustion
Coal Type	Falkirk Lignite	PRB	Hiawatha Bituminous	PRB	PRB	PRB	PRB
Limestone Added	No	No	No	No	Yes	Yes	Yes
$CaCO_3$, Wt %	1.1-4.8	3.7	1.2	4.2	9.1	8.7	25.5
CaS, Wt %	0.7-2.2	0.4	0.6	0.7	0.1	1.3	0
$CaSO_4$, Wt %	0	0	0	0	0	0	19.6
Free Lime (CaO), Wt %	10.5-15.4	7.3	4.6	8.1	20.3	19.0	0
Noncarbonate Carbon, Wt %	1.2-16.4	39.4	53.8	43.7	24.2	33.0	3.2
Inerts (Ash/Sand), Wt %	63.7-82.0	49.2	39.9	43.3	46.3	38.0	51.7
Loss on Ignition, Wt %	0.7-16.0	39.6	54.7	43.8	33.5	33.7	3.2

This comparison shows that the most significant differences between TC11 and the other runs are in the noncarbonate carbon content, the inerts (ash/sand), and the LOI. As noted earlier, the LOI is essentially equivalent to the noncarbonate carbon content (see Figure 4.4-7). The variations in LOI/carbon content show that the carbon conversion was higher in TC11 than in any of the other gasification tests. In fact, some of the TC11 samples had a higher degree of carbon conversion than did the TC05 combustion ash. The relative concentrations of carbon and inerts (ash/sand) are undoubtedly important factors in the observed variations in surface area, because the porous carbon has much more surface area than the nonporous ash and sand.

4.4.5.2 PCD Hopper Samples Used for Drag Measurements

Table 4.4-6 also includes the chemical compositions of the PCD hopper samples used for the laboratory drag measurements. With the exception of the last hopper composite (AB12693/ AB12701), the hopper samples generally cover the same range of compositions as do the in situ samples. The last hopper composite differs from all of the other hopper and in situ samples in that it has a much higher LOI/carbon content. Despite this difference, it falls on the same trend of surface area versus LOI/carbon content (see Figure 4.4-6). The trend illustrated in Figure 4.4-6 suggests that the surface area reaches a plateau at about 100 m^2/g when the LOI/carbon content exceeds about 12 wt percent. As discussed in Section 4.4-6, the existence of this plateau is confirmed by the behavior of drag with increasing LOI/carbon, because samples with 12 and 30 wt percent LOI have essentially the same surface area and drag values.

4.4.5.3 Residual Dustcake Samples

As shown in Table 4.4-7, the residual dustcake from the top plenum was chemically very similar to the residual dustcake from the bottom plenum. This result is not too surprising given the similarity in the physical properties discussed earlier.

The table below compares the TC11 dustcake composition to the composition of the TC11 in situ samples.

	Residual Dustcake	In situ Samples
$CaCO_3$, Wt %	2.1	1.1-4.8
CaS, Wt %	4.8-5.3	0.7-2.2
Free Lime (CaO), Wt %	7.6-8.1	10.5-15.4
Noncarbonate Carbon, Wt %	17.0-21.9	1.2-16.4
Inerts (Ash/Sand), Wt %	63.7-67.6	63.7-82.0
Loss on Ignition, Wt %	19.1-24.7	0.7-16.0

Compared to the incoming g-ash, the dustcake has a higher LOI/carbon content, higher CaS, and lower CaO. The higher CaS and lower CaO may reflect the effects of additional sulfidation that occurs during prolonged exposure of the residual cake to syngas containing H_2S.
As mentioned previously, the additional sulfidation could result in pore closure, which might explain the lower surface area of the dustcake samples. In previous runs, the residual dustcake has always had a lower surface area than the in situ samples, and pore closure by sulfidation has been one factor that has been cited to explain this difference.

The table below compares the composition of the residual dustcakes from TC11 and from previous test campaigns. Again, the dustcake from TC08 is not included because the physical properties were altered by partial oxidation of the cake, and the TC07 dustcake is omitted because the properties were biased by coke feed.

	TC11	TC10	TC09	TC06	TC05
Operating Mode	Gasification	Gasification	Gasification	Gasification	Combustion
Coal Type	Falkirk Lignite	PRB	Hiawatha Bituminous	PRB	PRB
Limestone Added	No	No	No	Yes	Yes
$CaCO_3$, Wt %	2.1	3.1	3.1	13.3	21.1
CaS, Wt %	4.8-5.3	1.5	1.6	1.8	0
$CaSO_4$, Wt %	0	0	0	0	44.3
Free Lime (CaO), Wt %	7.6-8.1	5.4	2.7	10.6	0
Noncarbonate Carbon, Wt %	17.0-21.9	49.6	52.3	40.2	9.3
Inerts (Ash/Sand), Wt %	63.7-67.6	40.4	40.3	34.2	25.3
Loss on Ignition, Wt %	19.1-24.7	51.8	54.7	46.2	9.3

This comparison shows that the TC11 residual cake contains more CaS, less carbon, and more inerts than do the residual cakes from the other gasification runs. As with the in situ samples, the low carbon (and high inert) content is attributable to the high degree of carbon conversion achieved in TC11. The LOI/carbon content of the TC11 residual cake is still higher than the LOI/carbon content of the TC05 combustion cake. As discussed earlier in conjunction with the in situ samples, the surface area of the dustcake samples appears to increase with increasing amounts of LOI/carbon (or with decreasing amounts of ash/sand). However, the surface area-versus-LOI/carbon data for the TC11 residual cake fall below the trend line obtained for the in situ samples shown in Figure 4.4-6. Again, this difference is probably attributable to the pore closure associated with additional sulfidation of the residual cake.

4.4.6 Laboratory Measurements of G-Ash Drag

The RAPTOR apparatus described in previous reports was used to measure the normalized drag of the g-ash as a function of particle size. The four hopper samples used for these measurements have been described in previous sections. They were originally selected to cover a wide range of LOI. As discussed in Section 4.4.4, subsequent characterization of the samples showed that they also varied widely in their specific-surface area in accordance with their LOI values. The table below gives both properties of these samples in order of increasing LOI.

Sample Number	LOI, Wt %	Specific-Surface Area, m^2/g
AB12610	1.71	19
AB12680	7.05	24
AB12711, AB12712, AB12713	11.30	91
AB12693, AB12701	30.30	99

As indicated previously, the surface area of the samples increases with increasing LOI (or carbon content).

As shown in Figure 4.4-8, the hopper sample with the lowest LOI and lowest surface area (1.7 wt percent and 19 m^2/g) exhibited the least drag. The drag of this particular sample was at the lower end of all the drag measurements made on g-ash from the PSDF but still higher than the drag of any combustion ash samples, which are typically below 20 inWc/(ft/min)/(lb/ft^2). The sample with the highest LOI and highest surface area (30 wt percent and 99 m^2/g) exhibited the highest drag, but the sample with the next highest LOI and surface area (11 wt percent and 91 m^2/g) exhibited almost the same drag as the sample with the highest LOI. The similar drag characteristics of these two samples may be related to their similar surface area (99 vs 91 m^2/g). In any case, the results suggest that the drag increases with increasing LOI (and surface area) up to a LOI of about 10 wt percent or a surface area of about 90 m^2/g.

To put the TC11 drag measurements into perspective, Figure 4.4-8 also includes typical drag measurements made with PRB coal with the original Transport Gasifier configuration (GCT2); with the modified recycle loop (GCT3, GCT4, TC06); and with the new LMZ in service (TC07-D, TC08, TC10). The graph also includes measurements made on the TC09 g-ash from the Hiawatha bituminous coal. If the measurements are compared at a typical mean particle size of about 18 μm, the regression fits for the samples with 7, 11, and 30 wt percent LOI seem to converge to a value of about 40 inWc/(ft/min)/(lb/ft^2). At the same particle size, the regression fit for the 1.7 wt percent LOI indicates a drag of less than 30 inWc/(ft/min)/(lb/ft^2). For comparison, a drag of about 45 inWc/(ft/min)/(lb/ft^2) is indicated for the PRB g-ash generated with the same equipment configuration (new LMZ in service). These comparisons suggest that the drag of the Falkirk lignite g-ash can be nearly comparable to the drag of the PRB g-ash, or it can be significantly lower than that of the PRB g-ash, depending on the degree of carbon conversion.

In addition to the comparison with the PRB g-ash, it is also of interest to know how the Falkirk g-ash compares to a bituminous g-ash. Again making the comparison at a typical mean particle size of 18 μm, the regression fits suggest that the drag of the Hiawatha bituminous g-ash is lower than the drag of all the Falkirk lignite samples, except for the sample with the lowest LOI. The lowest (1.7 wt percent) LOI sample apparently has a drag that is comparable to that of the Hiawatha bituminous g-ash.

Based on the comparisons discussed above, the various types of g-ash may be ranked in order of decreasing drag on the basis of the samples generated with the same equipment configuration (new LMZ in service) and at the typical mean particle size of 18 μm. On this basis, the relative ranking may be summarized as follows:

PRB ≅ High-LOI Falkirk Lignite > Low-LOI Falkirk Lignite ≥ Hiawatha Bituminous

If the various g-ash is arranged in order of decreasing surface area, the order is the same, except that the surface area of the low-LOI Falkirk g-ash is actually lower than that of the Hiawatha bituminous g-ash (19 to 24 m^2/g for Falkirk versus 55 to 77 m^2/g for Hiawatha).

4.4.7 Analysis of PCD Pressure Drop

As in previous tests, the buildup of transient pressure drop across the PCD was analyzed by calculating a corresponding value of transient drag and comparing it to the drag measured by RAPTOR. The calculation procedure, which has been described in previous reports, was applied to all of the in situ sampling runs, except for run no. 1, which had a sample system leak, and run no. 5, during which the PCD ΔP rise was too small to determine accurately. The calculations of transient drag for the other runs are summarized in Table 4.4-8. The calculated transient drag at PCD conditions is listed under the column heading PCD. The corresponding normalized value of transient drag at room temperature is listed under the heading PCD@RT. This value can be compared directly with the RAPTOR drag values. The corresponding RAPTOR drag value for a given in situ run was determined by applying the appropriate regression fit of the laboratory data at the mean particle size of the in situ sample. Figure 4.4-9 compares the individual values of RAPTOR drag with their corresponding values of normalized PCD transient drag at room temperature (PCD@RT).

As shown in Table 4.4-8 and Figure 4.4-9, the lab-measured values of dustcake drag determined from RAPTOR are considerably higher than the calculated values of PCD transient drag at room temperature. However, the values do appear to vary in similar directions, and it is probably good that the lab technique remains somewhat conservative for very low drag values. Although we attempted to match LOI values between the RAPTOR and in situ samples, they were not from identical time periods, which may contribute to some disagreement.

The table below compares the average drag values (RAPTOR and PCD@RT) for the high-LOI portion of TC11 with the tests performed prior to TC11. Only the high-LOI data are used for this comparison, because these values of LOI more closely match the LOI values obtained in the tests prior to TC11. The data for both air- and oxygen-blown runs have also been averaged together, since it was previously determined that the type of oxidant has no effect on drag.

	Normalized Drag @ RT, inWc/(lb/ft^2)/(ft/min)				
	TC11 High LOI	TC10	TC09	TC08	TC07-D
Average from PCD ΔP/Δt	19	45	26	46	42
Average from RAPTOR Data	38	58	23	48	48

The above comparison suggests that the ranking of the various g-ash that was done previously on the basis of RAPTOR measurements may be changed if the ranking is instead based on the PCD transient drag determined from ΔP rise. On the latter basis, the ranking would be as follows:

PRB > Hiawatha Bituminous > High-LOI Falkirk Lignite ≥ Low-LOI Falkirk Lignite

Whereas, on the basis of the average RAPTOR drag values, the ranking would be:

PRB > High-LOI Falkirk Lignite > Low-LOI Falkirk Lignite ≥ Hiawatha Bituminous

The first ranking, based on the PCD transient drag, probably gives the most accurate depiction of the relative flow resistances of the g-ash. The ranking, based on the RAPTOR measurements, is probably not dependable because of the aforementioned problem with the LOI values of the Falkirk lignite hopper samples. From the ranking of PCD transient drag, it is clear why the ΔP was relatively low during TC11.

4.4.8 Conclusions

During TC11, there was considerable variation in the PCD ΔP rise rate during a filtration cycle. The highest rate of ΔP rise observed during TC11 (~4 inWc/min) was within the range of ΔP rise rates obtained in other gasification tests performed since the new LMZ was placed in service (~3 to 9 inWc/min). The lowest rate of ΔP rise during TC11 was so low that it was impossible to accurately determine the ΔP rise rate. Characterization of in situ particulate samples showed that the ΔP rise rate was related to the LOI/carbon content of the g-ash. When the LOI of the g-ash was very low (< 1-wt percent), the ΔP rise rate was too low to measure. The highest rates of ΔP rise occurred when the LOI of the g-ash exceeded 10-wt percent.

Laboratory drag measurements and calculation of PCD transient drag showed that the normalized drag of the g-ash increased with increasing LOI/carbon content, and this increase partly accounted for the observed effects on ΔP rise rate. The changes in ΔP rise rate were also influenced by changes in the areal loading of g-ash on the filter elements. The areal loading increased as the LOI/carbon content increased due to the carryover of increasing amounts of unconverted carbon to the PCD and because the higher LOIs typically occurred at high coal-

feed rates. This effect was evident in the particulate concentrations measured at the PCD inlet, which were strongly correlated with the LOI/carbon content of the in situ particulate samples.

The TC11 hopper sample with the lowest LOI/carbon content (~1.7 wt percent) had the lowest drag, which was at the low end of all our previous drag measurements but still higher than the drag of combustion ash. The hopper sample with the next highest LOI (~7 wt percent) had a much higher drag. The sample with 11-wt percent LOI had a still higher drag, but the increase in drag from 7- to 11-wt percent LOI was not as great as the increase in drag from 1.7- to 7-wt percent. The sample with 30-wt percent LOI had almost the same drag as the sample with 11-wt percent LOI. In other words, the effect of LOI/carbon content on the drag becomes greater as the LOI is reduced. The rate of change appears to become very large as the LOI approaches zero or as the g-ash becomes more like combustion ash.

In addition to the profound effect on drag, LOI/carbon was also found to have a strong influence on the specific-surface area of the g-ash. As the LOI of the hopper samples increased from 1.7- to 30-wt percent, the specific-surface area increased from 19 to 99 m^2/g. Interestingly, the hopper samples with 11- and 30-wt percent LOI, which had very similar drag characteristics, also had very similar surface areas (91 and 99 m^2/g).

The ash content of the Falkirk lignite coal is much higher than that of the PRB or the Hiawatha bituminous coal, but the solids carryover to the filter elements during TC11 was comparable to the solids carryover rates obtained with the other coals in previous tests. The higher ash content of the Falkirk lignite apparently does not produce a higher carryover of solids, possibly because there is much less carryover of unconverted carbon with the lignite. (The LOI of the TC11 in situ samples varied from 1.3- to 16-wt percent, while g-ash from previous tests have had LOI values in the range of 20- to 60-wt percent.) The lower LOI/carbon values of the TC11 g-ash suggests that better carbon conversion was achieved with the lignite. This result makes sense, because lower rank coals that contain more volatiles are generally gasified more easily than higher rank coals.

Table 4.4-1

PCD Inlet and Outlet Particulate Measurements for TC11

	PCD Inlet					PCD Outlet				
Date	Run No.	Start Time	End Time	Particle Loading ppmw	Particle Mass Rate lb/hr	Run No.	Start Time	End Time	Water Vapor Vol %	Particle Loading ppmw
Air Blown										
04/09/03	--	--	--	--	--	1	14:00	15:00	(1)	0.27 [2]
04/11/03	1	(3)	(3)	(3)	(3)	2	8:45	12:45	9.8	< 0.1
04/14/03	2	10:40	10:53	20200	418	3	9:45	14:09	9.3	< 0.1
04/15/03	3	9:50	10:05	16300	366	4	9:35	13:35	11.9	< 0.1
04/16/03	4	13:10	13:25	22500	491	5	13:00	15:14	11.7	0.16 [4]
04/17/03	5	13:40	13:55	11300	188	6	13:30	15:30	15.2	NA [5]
Oxygen-Blown										
04/18/03	6	9:30	9:45	25100	352	7	9:15	11:15	18.1	< 0.1
04/18/03	--	--	--	--	--	8	13:15	15:16	18.4	0.15 [6]

Notes:

1. Test too short for accurate moisture measurement.
2. Startup test on propane. Loading may be reentrained dust.
3. Sample system leak - no data on actual concentration.
4. Failsafe injection test - PSDF failsafe
5. Excessive substrate weight gain. Result invalid.
6. Failsafe injection test - Pall fuse

Table 4.4-2

TC11 Dustcake Thicknesses and Areal Loadings

Plenum	Element Type	Element No.	Dustcake Thickness, in.	Sample Wt, g	Area, $in.^2$	Areal Loading, lb/ft^2
Bottom	FEAL w Fuse	B-4	0.0126	----	----	----
Bottom	FEAL w PSDF Failsafe	B-12	0.0175	----	----	----
Bottom	FEAL w PSDF Failsafe	B-14	----	0.8576	13.125	0.021
Bottom	FEAL w PSDF Failsafe	B-15	----	0.8794	12.938	0.022
Top	FEAL w PSDF Failsafe	T-2	0.0146	----	----	----
Top	FEAL w PSDF Failsafe	T-15	0.0081	----	----	----
Top	FEAL w PSDF Failsafe	T-1	----	0.9933	13.031	0.024
Top	FEAL w PSDF Failsafe	T-3	----	0.9718	12.562	0.025
Average			0.0132	0.9255	12.914	0.023

Table 4.4-3

Comparison of Residual Dustcake Thicknesses

Run No.	Dustcake Thickness, in.
GCT1	0.065
GCT2	0.050
GCT3	0.016
TC08	0.010
TC09	0.008
TC10 -- FEAL	0.007
TC10 -- HR-160	0.012
TC10 -- Hastelloy X	0.010
TC11 -- FEAL Average	0.013

Table 4.4-4

Physical Properties of TC11 In situ Samples and Hopper Samples Used for RAPTOR

Sample ID	Run Number	Sample Date	Bulk Density g/cc	True Density g/cc	Uncompacted Bulk Porosity %	BET Specific Surface Area m^2/g	Mass-Median Diameter μm	Loss on Ignition Wt %
In-Situ Samples								
AB12705	1	04/11/03	0.45	2.63	82.9	75	14.1	10.08
AB12706	2	04/14/03	0.50	2.62	80.9	43	12.8	10.45
AB12707	3	04/15/03	0.61	2.72	77.6	14	16.7	1.27
AB12708	4	04/16/03	0.47	2.51	81.3	105	20.5	11.35
AB12709	5	04/17/03	0.68	2.73	75.1	3	25.0	0.74
AB12710	6	04/18/03	0.39	2.53	84.6	100	16.5	16.01
Average for TC11			0.52	2.62	80.4	57	17.6	8.32
Average for TC10			0.27	2.25	88.0	146	12.3	39.64
Average for TC09			0.24	2.23	89.2	96	19.1	54.67
Average for TC08			0.25	2.37	89.5	222	18.7	43.81
Average for TC07-D			0.32	2.47	87.0	170	16.9	33.46
Average for TC06			0.29	2.45	88.2	222	15.3	37.20
Hopper Samples Used for RAPTOR Measurements								
AB12610	Hopper	04/15/03	0.61	2.68	77.2	19	26.0	1.71
AB12711 712 713	Hopper Composite	04/16/03	0.50	2.47	79.6	91	17.0	11.30
AB12680	Hopper	04/18/03	0.59	2.54	76.8	24	20.2	7.05
AB12693 AB12701	Hopper Composite	04/18/03	0.50	2.17	76.9	99	19.6	30.30

Table 4.4-5

Physical Properties of TC11 Dustcake Samples

Sample Date	Sample Description	Plenum	Bulk Density g/cc	True Density g/cc	Uncom-pacted Bulk Porosity %	BET Specific Surface Area m^2/g	Mass-Median Diameter μm	Loss on Ignition Wt %
4/24/03	Residual Cake	Top	0.32	2.29	86.0	23	4.2	24.70
4/24/03	Residual Cake	Bottom	0.36	2.34	84.6	18	4.8	19.11
Average for TC11 Residual Cake			0.34	2.32	85.3	20	4.5	21.91
Average for TC10 Residual Cake			0.23	2.07	88.9	91	4.6	51.81
Average for TC09 Residual Cake			0.24	2.12	88.7	114	12.4	54.72
Average for TC06 Residual Cake[1]			0.25	2.28	89.0	257	9.3	46.23

1. TC07 dustcake not included because it was biased by coke feed; and TC08 dustcake not included because it was damaged by partial oxidation.

Table 4.4-6

Chemical Composition of TC11 In situ Samples and Hopper Samples Used for RAPTOR

Sample ID	Run Number	Sample Date	$CaCO_3$ Wt %	CaS Wt %	CaO Wt %	Non-Carbonate Carbon Wt %	Inerts (Ash/Sand) Wt %	Loss on Ignition Wt %
In-Situ Samples								
AB12705	1	04/11/03	2.48	1.35	13.42	10.76	71.99	10.08
AB12706	2	04/14/03	1.86	1.17	10.49	10.80	75.68	10.45
AB12707	3	04/15/03	1.59	0.68	14.64	1.80	81.29	1.27
AB12708	4	04/16/03	3.64	1.69	11.21	12.16	71.30	11.35
AB12709	5	04/17/03	1.14	0.27	15.43	1.17	81.99	0.74
AB12710	6	04/18/03	4.80	2.17	12.89	16.40	63.74	16.01
Average for TC11			2.58	1.22	13.01	8.85	74.33	8.32
Average for TC10			3.65	0.44	7.27	39.40	49.23	39.64
Average for TC09			1.19	0.56	4.63	53.78	39.85	54.67
Average for TC08			4.24	0.71	8.11	43.65	43.29	43.81
Average for TC07-D			9.05	0.10	20.33	24.19	46.33	33.46
Average for TC06			8.74	1.27	18.97	33.01	38.01	33.69
Hopper Samples Used for RAPTOR Measurements								
AB12610	Hopper	04/15/03	0.77	0.79	15.16	2.57	80.72	1.71
AB12711 712 713	Hopper Composite	04/16/03	1.28	2.92	2.52	11.20	82.08	11.30
AB12680	Hopper	04/18/03	1.16	0.88	13.28	7.68	77.00	7.05
AB12693 AB12701	Hopper Composite	04/18/03	4.52	2.74	1.98	33.70	57.06	30.30

Table 4.4-7

Chemical Composition of TC11 Dustcake Samples

Sample Date	Sample Description	Plenum	$CaCO_3$ Wt %	CaS Wt %	CaO Wt %	Non-Carbonate Carbon Wt %	Inerts (Ash/Sand) Wt %	Loss on Ignition Wt %
4/24/03	Residual Cake	Top	2.07	4.82	7.57	21.88	63.66	24.70
4/24/03	Residual Cake	Bottom	2.07	5.26	8.07	17.02	67.58	19.11
Average for TC11 Residual Cake			2.07	5.04	7.82	19.45	65.62	21.91
Average for TC10 Residual Cake			3.10	1.49	5.39	49.64	40.37	51.81
Average for TC09 Residual Cake			3.11	1.56	2.70	52.29	40.34	54.72
Average for TC06 Residual Cake[1]			13.27	1.78	10.59	40.19	34.17	46.23

1. TC07 dustcake not included because it was biased by coke feed; and TC08 dustcake not included because it was damaged by partial oxidation.

Table 4.4-8

TC11 Transient Drag Determined From PCD ΔP and From RAPTOR

Run No.	ΔP/Δt, inwc/min	Δ(AL)/Δt, lb/min/ft^2	FV, ft/min	MMD, μm	Drag, inwc/(lb/ft^2)/(ft/min)		
					PCD	PCD@RT	RAPTOR
Air-Blown							
2	1.95	0.0272	3.00	12.8	24	14.4	46.1
3	0.90	0.0235	3.33	16.7	12	6.9	28.7
4	3.60	0.0324	3.10	20.5	36	21.8	32.6
5	(1)	0.0123	3.23	25.0	(1)	(1)	23.4
Oxygen-Blown							
6	1.94	0.0230	2.59	16.5	33	21.2	36.3

Nomenclature:
ΔP/Δt = rate of pressure drop rise during particulate sampling run, inwc/min
Δ(AL)/Δt = rate of increase in areal loading during sampling run, lb/min/ft^2
FV = average PCD face velocity during particulate sampling run, ft/min
MMD = mass-median diameter of in situ particulate sample, μm
RT = room temperature, 77°F (25°C)
RAPTOR = resuspended ash permeability tester

Note:
1. PCD dP rise was too low to measure..

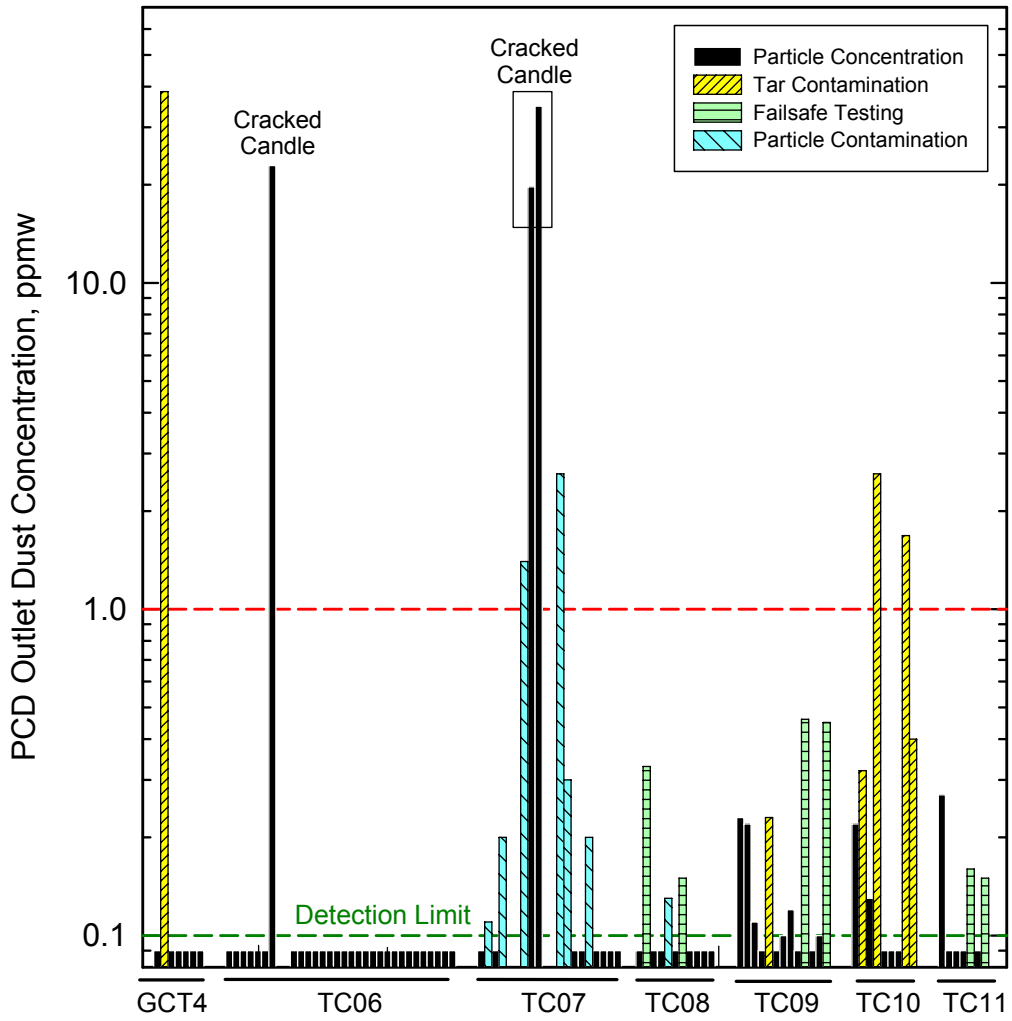

Figure 4.4-1 PCD Particle Emissions for Several Gasification Tests

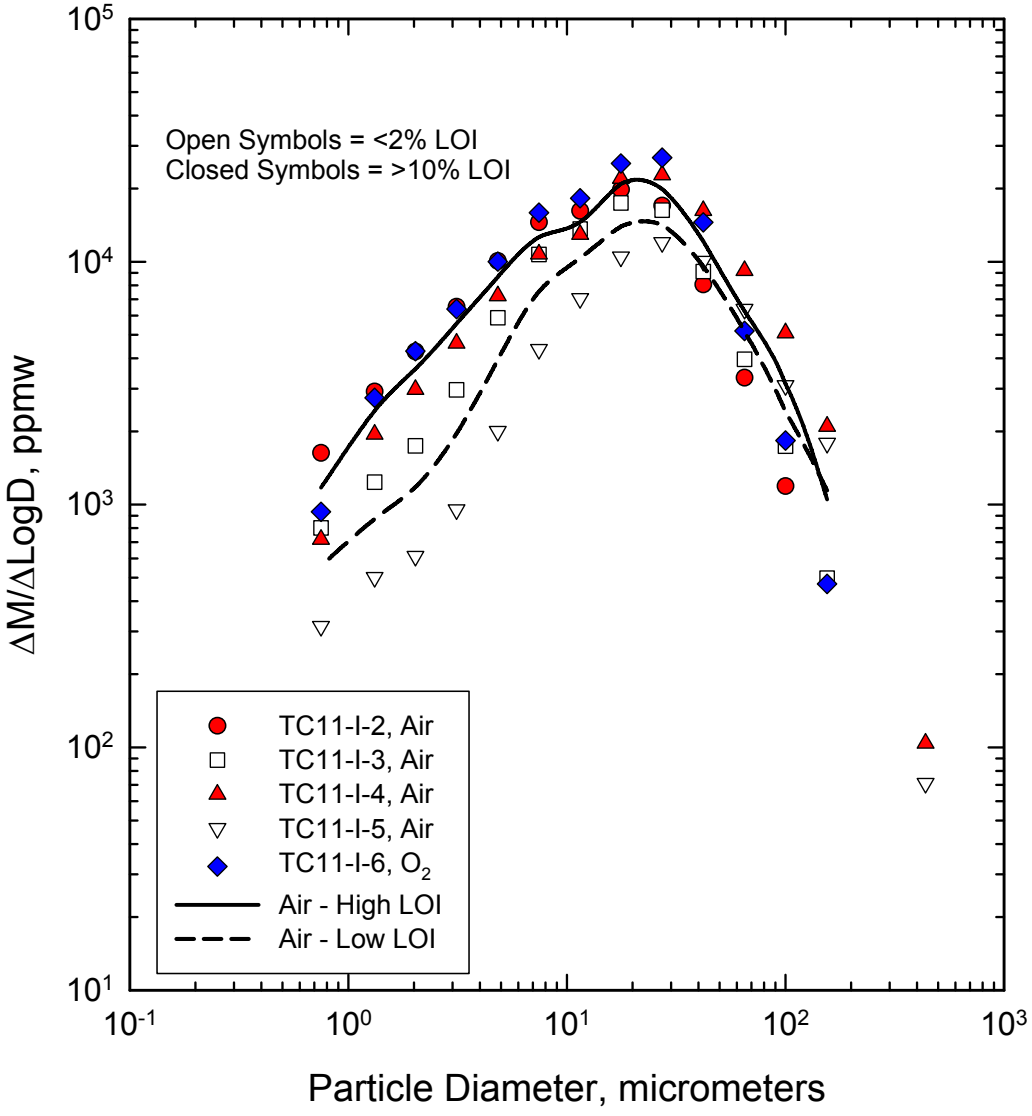

Figure 4.4-2 PCD Inlet Particle-Size Distributions for Individual In situ Samples

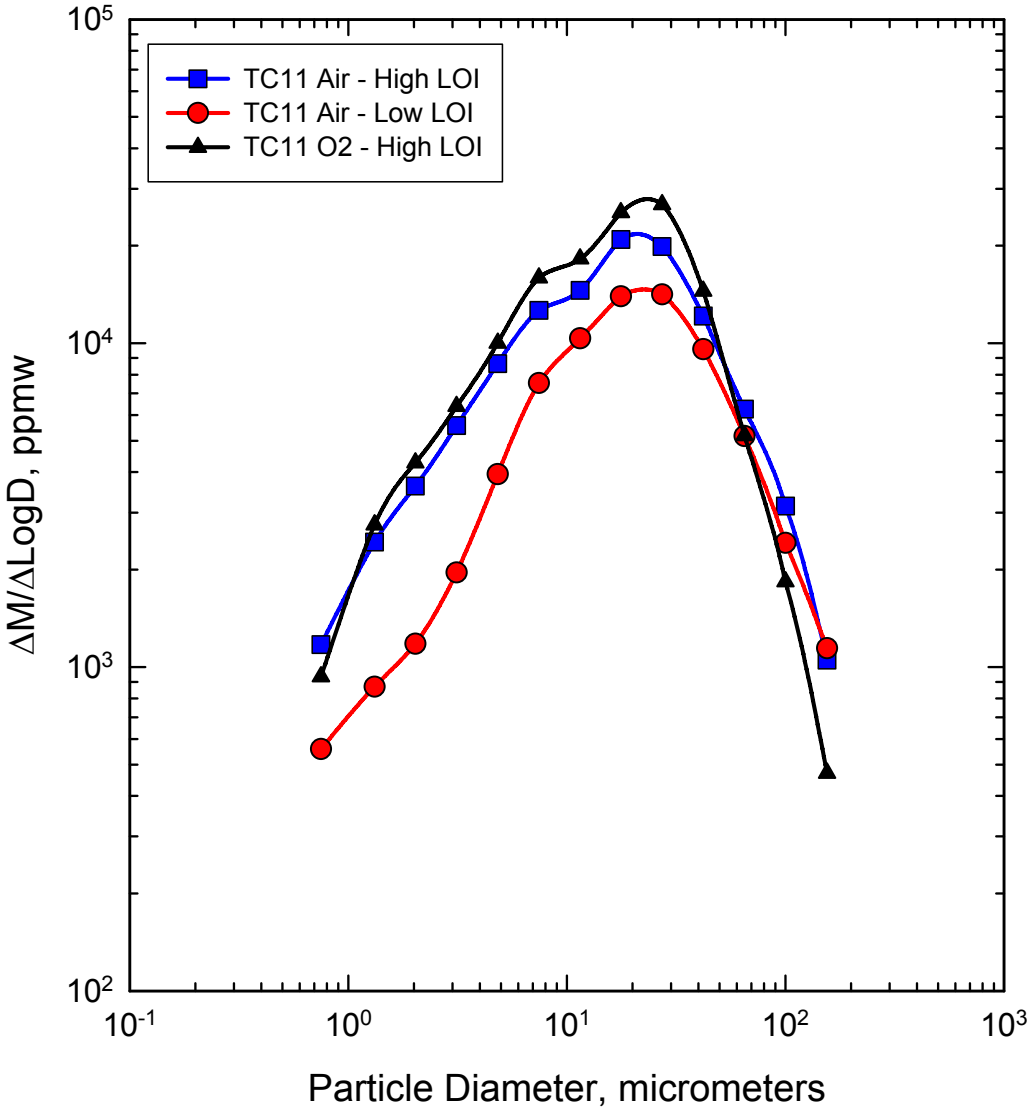

Figure 4.4-3 Comparison of Average PCD Inlet Particle-Size Distributions

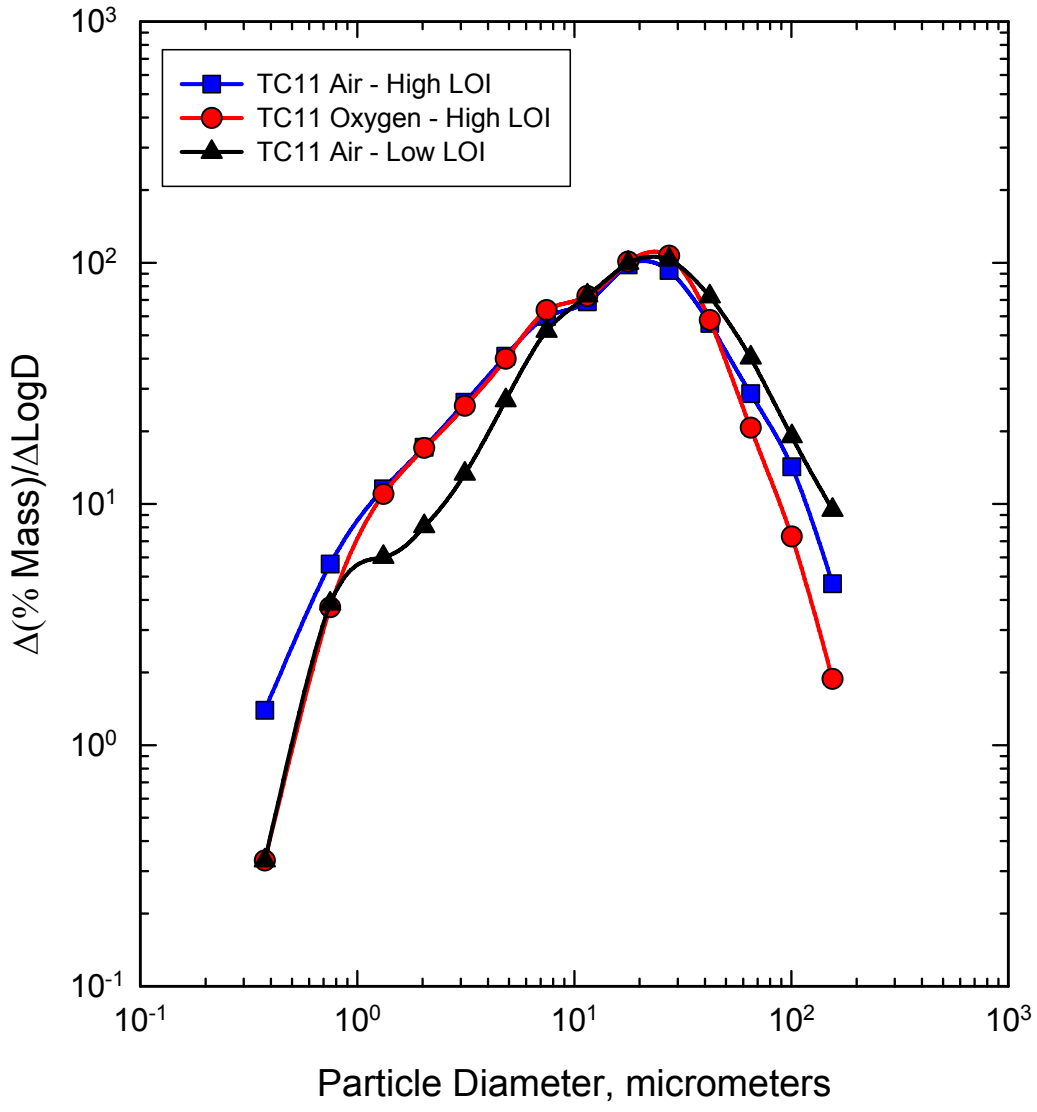

Figure 4.4-4 Comparison of Air- and Oxygen-Blown PCD Inlet Particle-Size Distributions

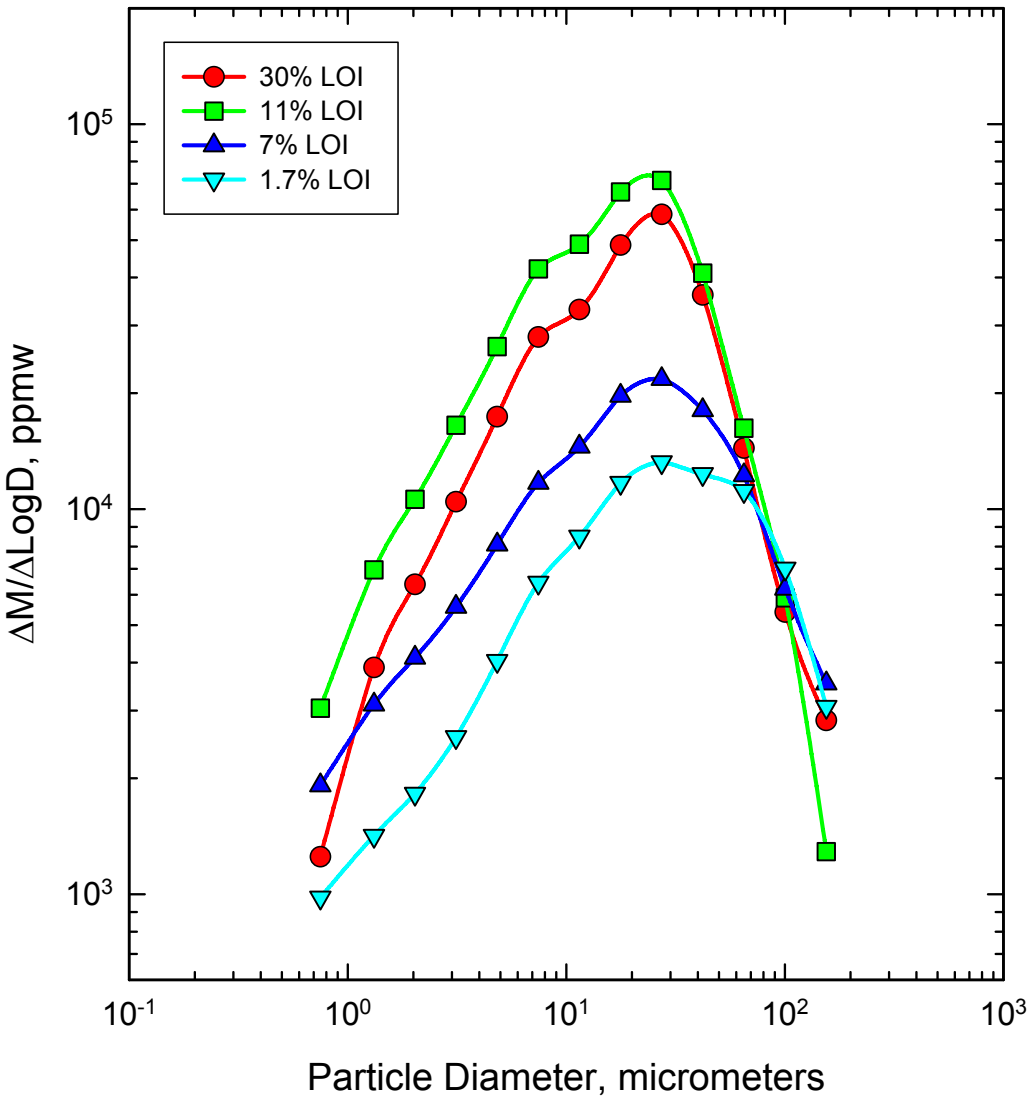

Figure 4.4-5 Particle-Size Distributions of PCD Hopper Samples With Different LOIs

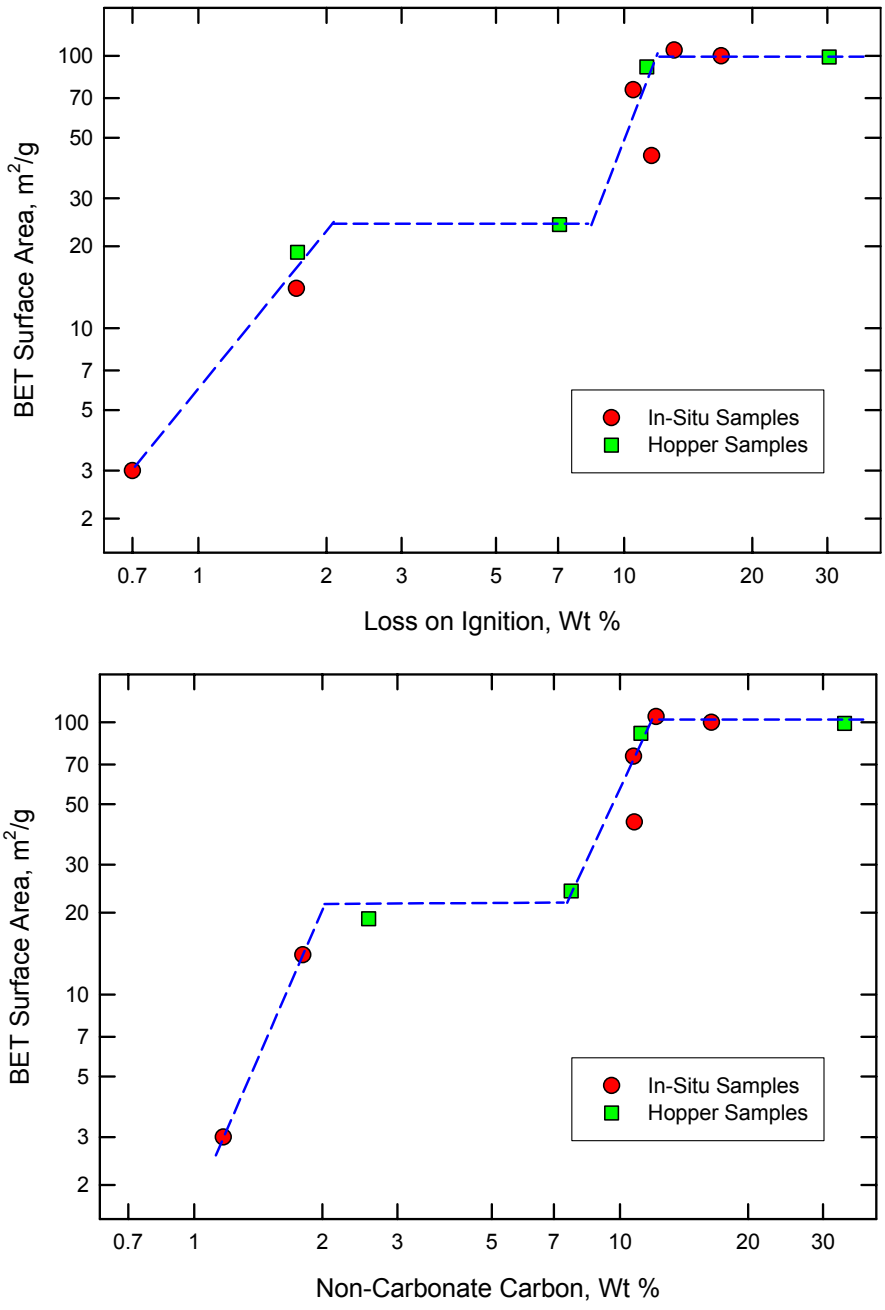

Figure 4.4-6 Attempts to Correlate BET Surface Area With Loss on Igntion and With Noncarbonate Carbon Content

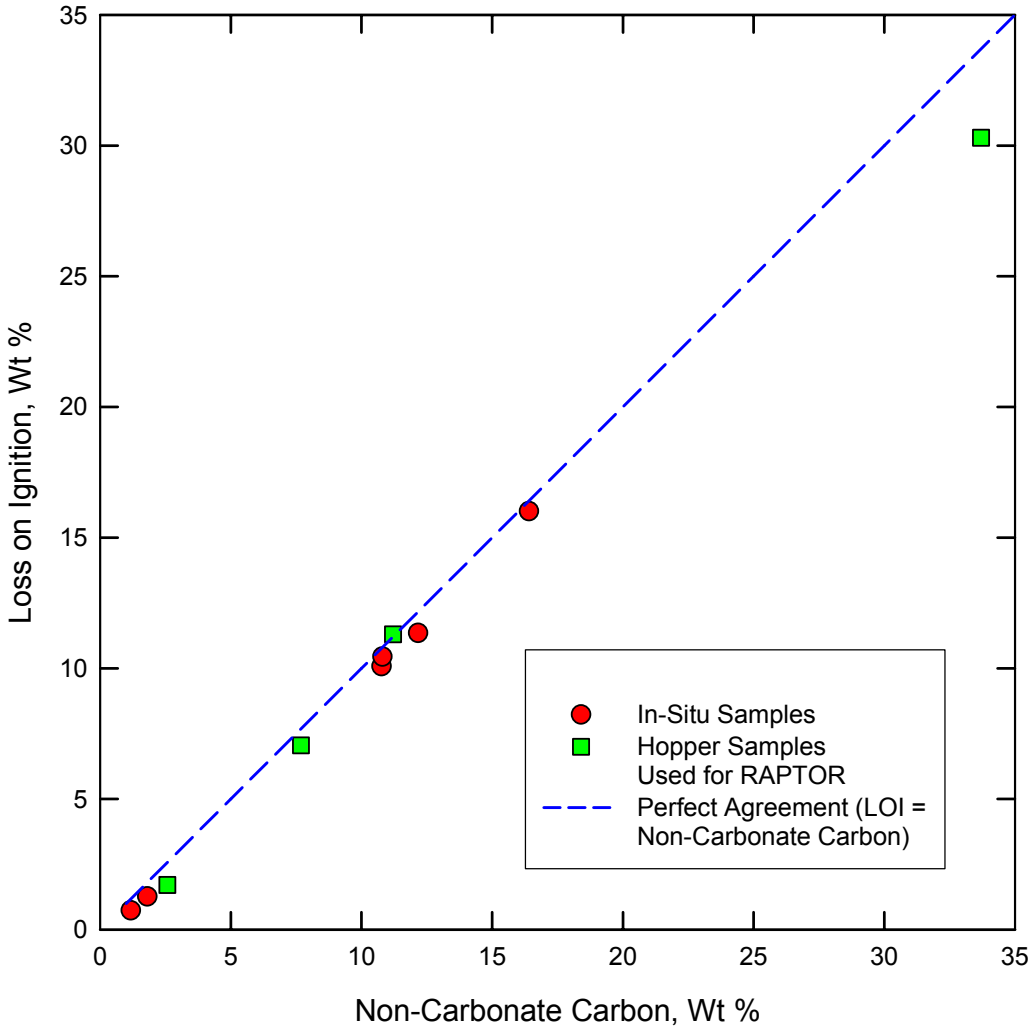

Figure 4.4-7 Agreement Between Loss on Ignition and Noncarbonate Carbon Content

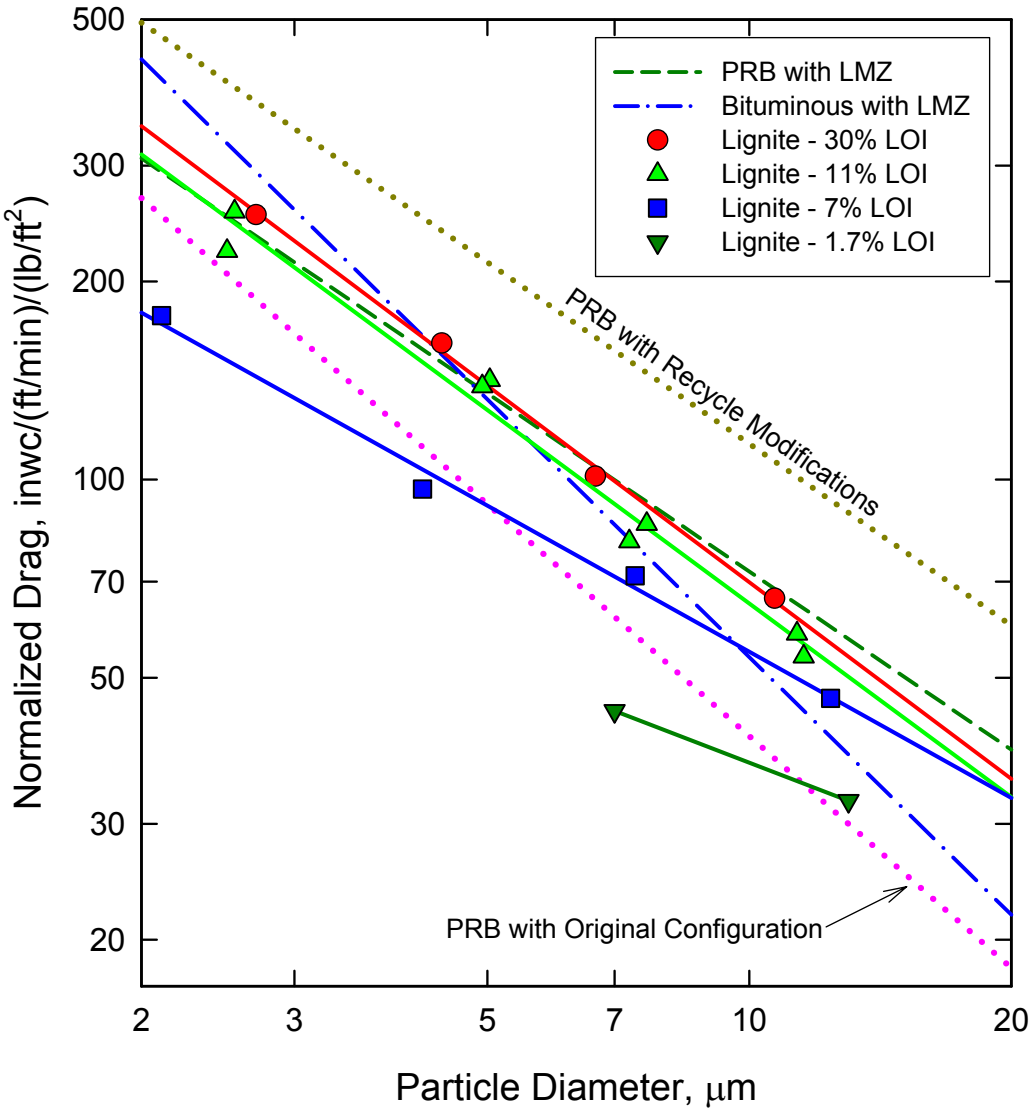

Figure 4.4-8 RAPTOR Measurements of Drag Versus Particle Size

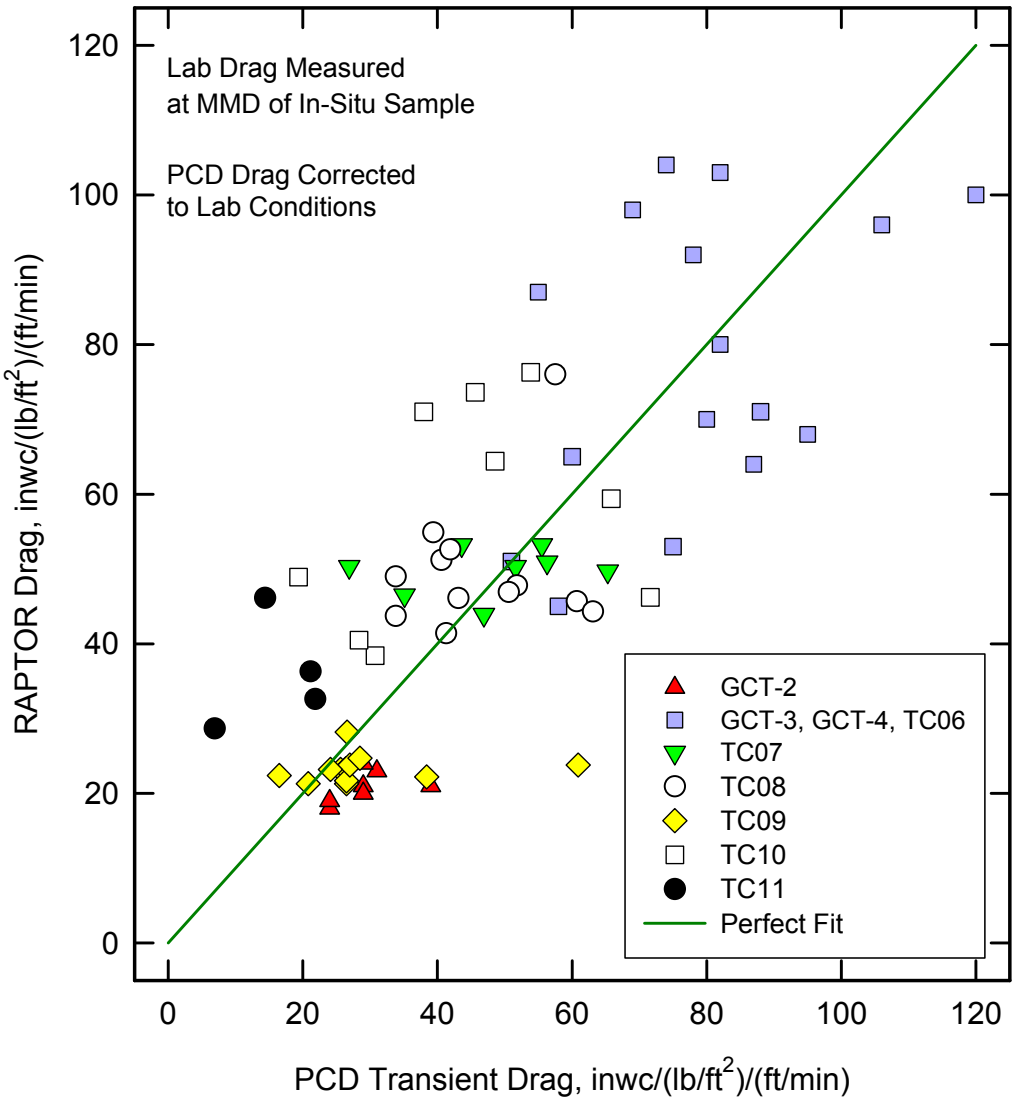

Figure 4.4-9 Comparison of PCD Transient Drag With RAPTOR Measurements

4.5 TC11 FAILSAFE REPORT

4.5.1 Introduction

One of the main objectives of the PSDF is to improve the commercial readiness of high temperature, high pressure (HTHP) gas filtration technology. HTHP gas filtration systems have established that they can achieve high collection efficiencies during stable operations; however, process upsets can cause filter element failure resulting in an outlet loading that exceeds turbine requirements. In order to reduce the risk of an unscheduled shutdown due to filter failure, a reliable failsafe device is required. The failsafe device acts as a safeguard by mechanically closing or plugging in the event of a filter element failure. Currently, a successful failsafe has not been identified; therefore, the PSDF has established a failsafe testing program to identify failsafe devices that will protect the downstream turbine while screening out poor performing failsafes. This program was developed to allow testing and performance comparison of different failsafe devices under comparable testing conditions (Refer to TC08 Run Report Section 3.5 for PSDF Failsafe Test Criteria, Plan, and Setup).

4.5.2 TC11 Solids Injection Test Setup

During TC11, g-ash was injected into two filter elements to simulate a leak in order to evaluate the effectiveness of two different failsafe designs. During previous tests, a fluidized bed feeder was used to inject solids into the filter elements. During TC11, a new system was designed that routes dirty gas out of the PCD, through an external valve and flowmeter, and then back into the PCD and into the filter element. The new test setup is shown schematically in Figure 4.5-1. Two Pall FEAL filter elements were modified and installed into the PCD. Each filter element has two ½-in.-od tubes installed through the bottom plate. One tube is used to inject solids, while the other tube is used for pressure measurements. Dirty gas is extracted from the PCD, routed through a heat-traced external piping system, and then injected into one of the filter elements. Pressure drop measurements are made between the PCD dirty side gas volume and the inside of the filter element (filter element ΔP) and between the inside of the filter element and the clean-side plenum (failsafe ΔP). The dirty-gas flow rate is measured using a venturi flowmeter. The dust leakage rate is determined by SRI's extractive outlet loading measurement. Based on the gas flow versus ΔP characteristic, the test setup (piping, valves, flowmeter, etc.,) is equivalent to a hole in the filter element approximately ¼-in. in diameter.

The two failsafe devices tested during TC11 were a PSDF-designed failsafe, which was installed at location B2, and a Pall fuse, which was installed at location B3. The Pall fuse was mounted in a separate holder and installed in the tube sheet. Rather than installing the Pall fuse down into the filter element as in the standard factory installation, the fuse was inverted and installed upward into the PCD tube sheet. Thus the gas flow direction was from inside to out, rather than outside to inside as in the factory installation.

4.5.3 TC11 Solids Injection Test (PSDF-Designed Failsafe)

The PSDF-designed failsafe injection test was performed on April 16, 2003. The outlet loading measurement was started at 13:13. The g-ash injection test started at 13:14. Both the g-ash injection and outlet loading tests were stopped at 15:14. The measured outlet loading was 0.16 ppmw. The outlet loading measurements during TC11 before the injection test were below the detection limit (< 0.1 ppmw) of SRI's extractive sampling system. Therefore, there was a measurable leak through the failsafe.

The pressure drop measurements recorded at the start of the PSDF-designed failsafe test are plotted in Figure 4.5-2. The plot shows the pressure drop as a function of time for the test. The initial plugging event was extremely rapid with the failsafe being substantially plugged, at least in terms of gas flow, within 15 seconds of the time when the injection started.

Also, plotted in Figure 4.5-2 is the ratio of the venturi flowmeter ΔP to the filter element ΔP. During the initial period, the ratio was relatively constant at around 0.20 (or 1/5). The relationship did not continue to be constant once the filter element ΔP was lower than 2 inH_2O. This was probably due to a poor zero on the filter element ΔP transducer. The venturi ΔP is expected to be a constant fraction of the filter element ΔP, since the filter element ΔP is the total differential across the injection system plumbing and the venturi ΔP. Using the known characteristics of the venturi flowmeter (throat diameter = 0.300 in., CD = 0.995), assuming that the equivalent hole in the filter element acts as a sharp-edged orifice (CD = 0.620), and assuming the following relationship, $\Delta P_{\text{FILTER ELEMENT}} \sim 5 * \Delta P_{\text{VENTURI}}$, an equivalent hole diameter of 0.255 in. was calculated. This value is close to the one that was estimated when the injection system was being designed.

Pressure drop measurements recorded at the end of the PSDF-designed failsafe test are plotted in Figure 4.5-3. Figure 4.5-3 shows that there was still a measurable amount of gas flow through the failsafe after 2 hours of g-ash injection. Note that the venturi pressure drop decreased by about 0.2 inH_2O when the valve on the injection line was closed.

4.5.4 TC11 Solids Injection Test (Pall Fuse)

The Pall fuse injection test was performed on April 18, 2003. The outlet loading measurement was started at 13:15 and the g-ash injection was started at 13:16. The outlet loading continued for two hours and was stopped at 15:16. The measured outlet loading was 0.15 ppmw, which was very similar to the loading measured during the PSDF-designed failsafe test. The solids injection line was left open after the loading test concluded. The initial intent was to continue injecting solids until the following day and perform another outlet loading test after 24 hours of continuous solids injection. However, the coal feed to the reactor was lost around 17:30 and was never reestablished.

Pressure drop measurements recorded at the start of the Pall fuse test are plotted in Figure 4.5-4. There was a rapid initial plugging event; however, the filter element ΔP did not decrease as rapidly as observed during the PSDF-designed failsafe test. The filter element and failsafe ΔP data for a 4-hour period following the start of the Pall fuse injection test are plotted in Figure 4.5-5. Two hours after the solids injection was started, the filter element ΔP was still more than

3 inH_2O, while after a similar period of time during the PSDF-designed failsafe injection test, the filter element ΔP was less than 1 inH_2O. Also, after 2 hours of injecting solids into the Pall fuse, the venturi ΔP was about 0.9 inH_2O, while the venturi ΔP during the PSDF-designed failsafe test was about 0.2 inH_2O. Therefore, it appears that there is a significantly higher gas flow rate through the plugged Pall fuse, even though both failsafe devices had approximately the same dust leakage rates.

4.5.5 Conclusions/Plans for Future Testing

The newly designed failsafe test apparatus was successful in testing the collection efficiency of two different failsafe devices. Both the PSDF-designed failsafe and Pall fuse were able to maintain the PCD outlet loading below 1 ppmw with only 1/85 filters leaking. Future testing includes repeated testing of the PSDF-designed failsafe and Pall fuse. Longer test periods are needed in order to determine whether or not the leakage rate decreases with time. Therefore, plans are to test the PSDF-designed failsafe and Pall fuse during TC12 by injecting solids continuously for 24 hours. Outlet loading tests will be collected for the first 2 hours and again on the next day. Hopefully, this test will provide information about the sealing mechanism of each failsafe.

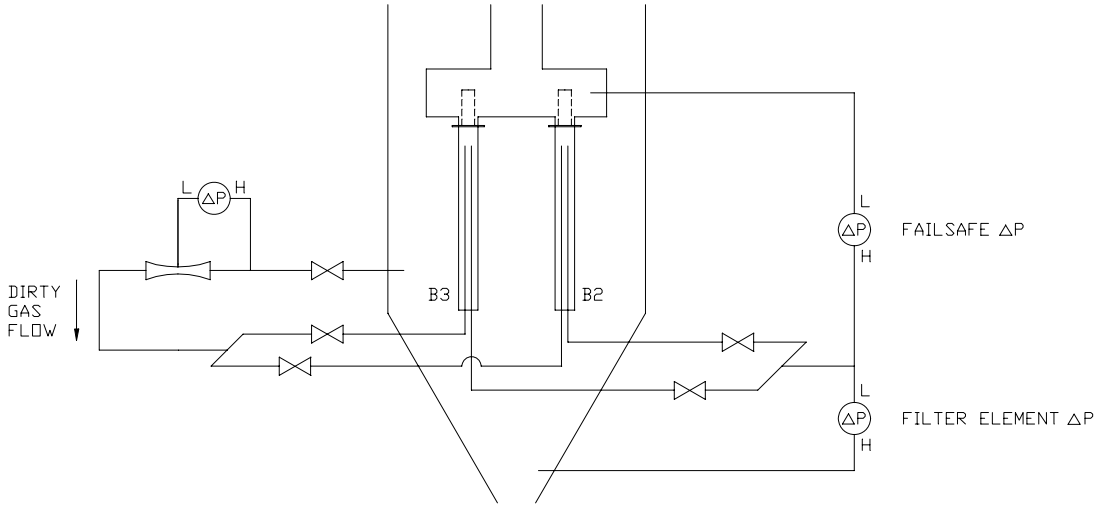

Figure 4.5-1 Setup for Failsafe Injection Test

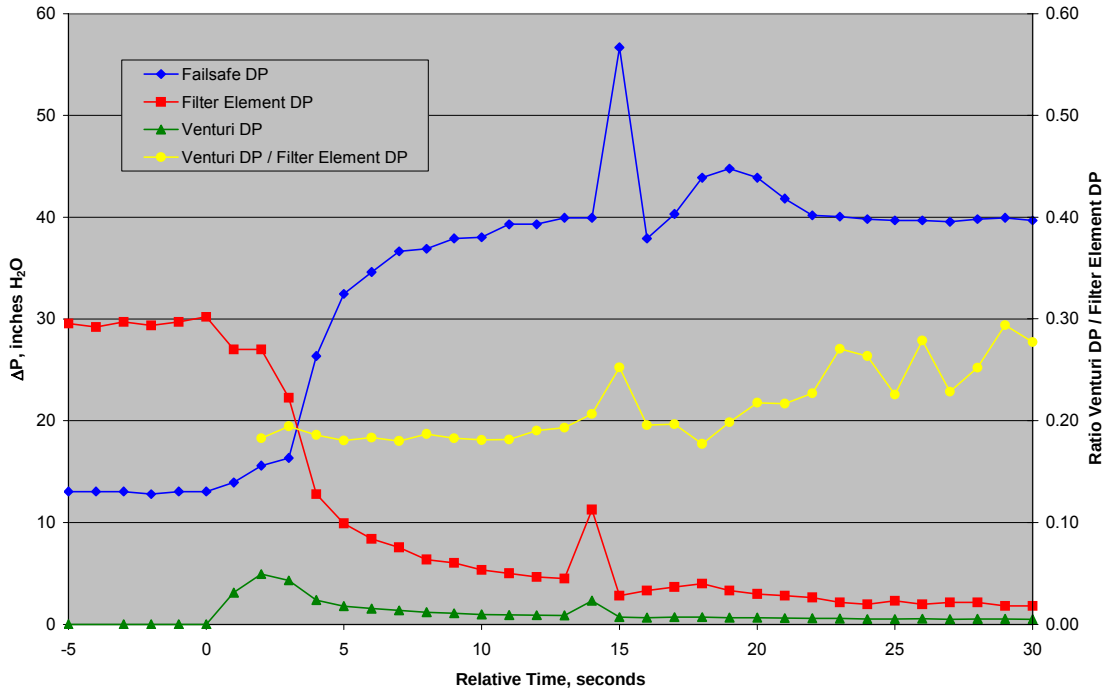

Figure 4.5-2 Start of PSDF-Designed Failsafe Injection Test on April 16, 2003

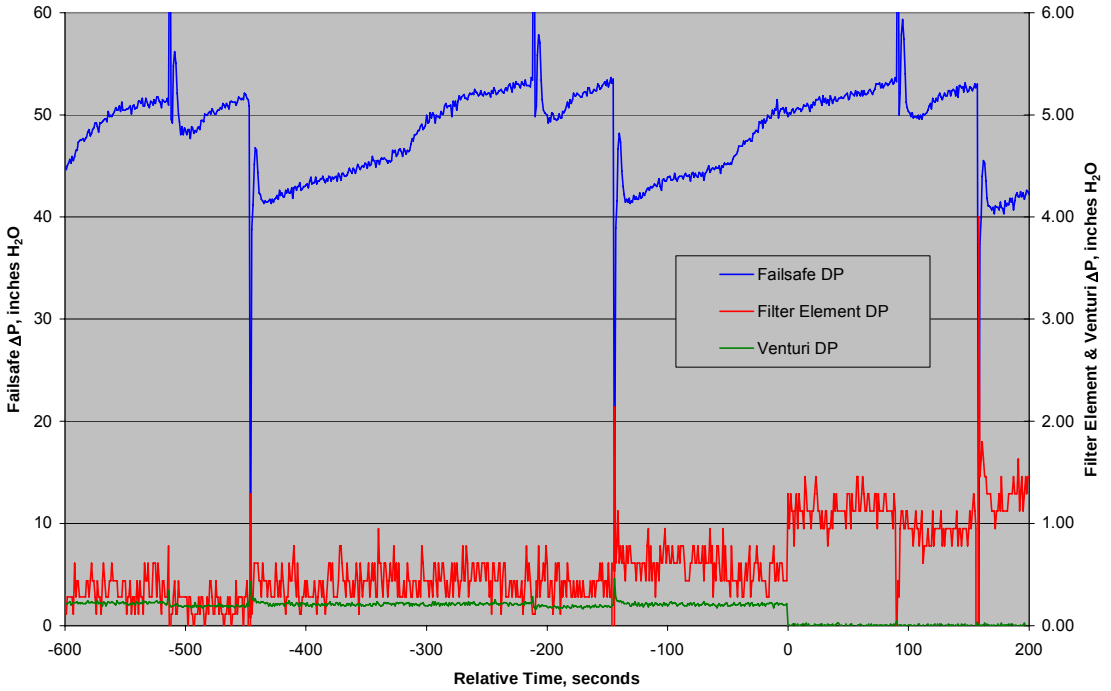

Figure 4.5-3 End of PSDF-Designed Failsafe Injection Test on April 16, 2003

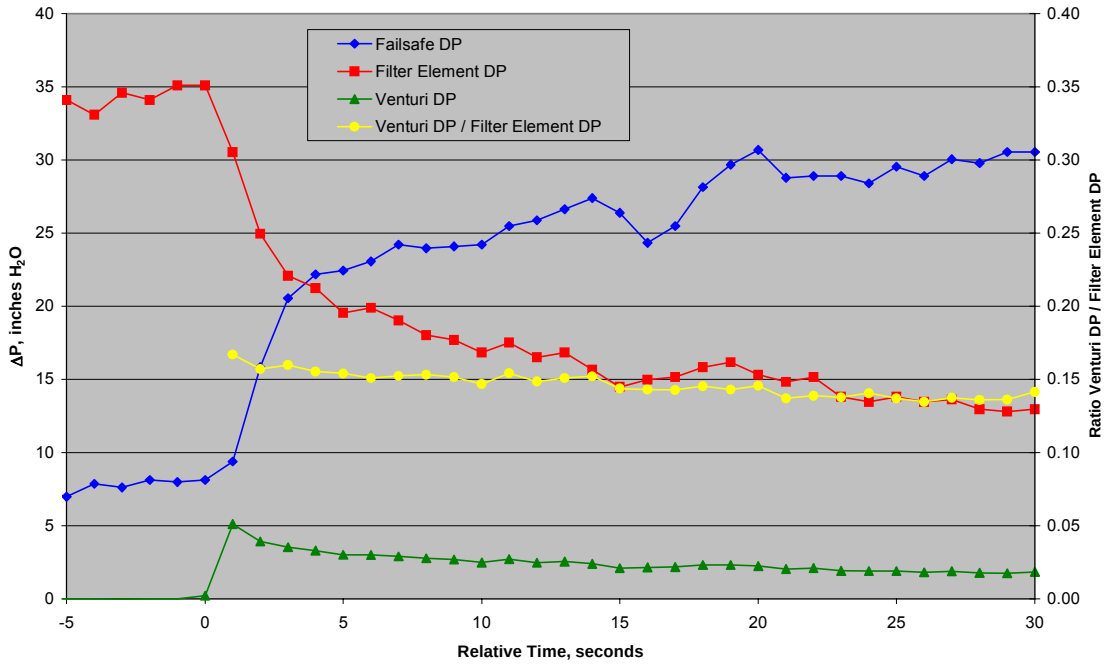

Figure 4.5-4 Start of Pall Fuse Injection Test on April 18, 2003

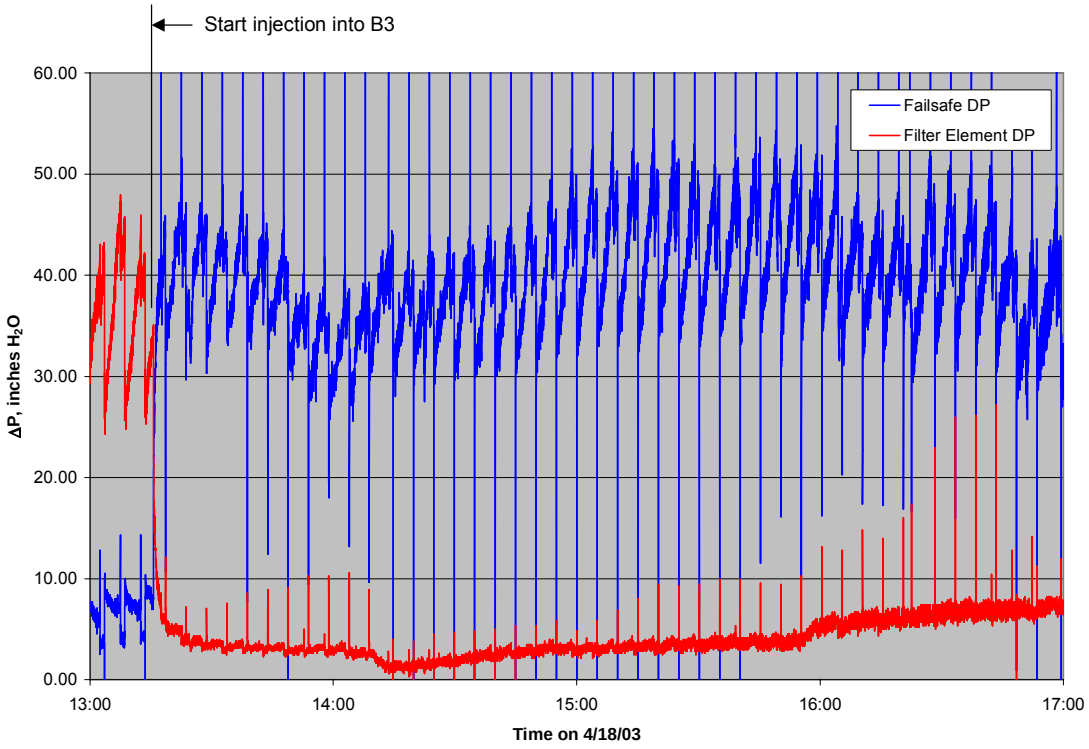

Figure 4.5-5 Pall Fuse ΔP and Filter Element ΔP for 4 Hours

TERMS

Listing of Abbreviations

AAS	Automated Analytical Solutions
ADEM	Alabama Department of Environmental Management
AFBC	Atmospheric Fluidized-Bed Combustor
APC	Alabama Power Company
APFBC	Advance Pressurized Fluidized-Bed Combustion
ASME	American Society of Mechanical Engineers
AW	Application Workstation
BET	Brunauer-Emmett-Teller (nitrogen-adsorption specific surface technique)
BFI	Browning-Ferris Industries
BFW	Boiler Feed Water
BMS	Burner Management System
BOC	BOC Gases
BOP	Balance-of-Plant
BPIR	Ball Pass Inner Race, Frequencies
BPOR	Ball Pass Outer Race, Frequencies
BSF	Ball Spin Frequency
CAD	Computer-Aided Design
CAPTOR	Compressed Ash Permeability Tester
CEM	Continuous Emissions Monitor
CFB	Circulating Fluidized Bed
CFR	Code of Federal Regulations
CHE	Combustor Heat Exchanger
COV	Coefficient of Variation (Standard Deviation/Average)
CPC	Combustion Power Company
CPR	Cardiopulmonary Resuscitation
CTE	Coefficient of Thermal Expansion
DC	Direct Current
DCS	Distributed Control System
DHL	DHL Analytical Laboratory, Inc.
DOE	U.S. Department of Energy
DSRP	Direct Sulfur Recovery Process
E & I	Electrical and Instrumentation
EDS or EDX	Energy-Dispersive X-Ray Spectroscopy
EERC	Energy and Environmental Research Center
EPRI	Electric Power Research Institute
ESCA	Electron Spectroscopy for Chemical Analysis
FCC	Fluidized Catalytic Cracker
FCP	Flow-Compacted Porosity
FFG	Flame Front Generator
FI	Flow Indicator
FIC	Flow Indicator Controller
FOAK	First-of-a-Kind
FTF	Fundamental Train Frequency

FW	Foster Wheeler
GBF	Granular Bed Filter
GC	Gas Chromatograph
GEESI	General Electric Environmental Services, Inc.
HHV	Higher Heating Valve
HP	High Pressure
HRSG	Heat Recovery Steam Generator
HTF	Heat Transfer Fluid
HTHP	High-Temperature, High-Pressure
I/O	Inputs/Outputs
ID	Inside Diameter
IF&P	Industrial Filter & Pump
IGV	Inlet Guide Vanes
IR	Infrared
KBR	Kellogg Brown & Root, Inc.
LAN	Local Area Network
LHV	Lower Heating Valve
LIMS	Laboratory Information Management System
LMZ	Lower Mixing Zone
LOC	Limiting Oxygen Concentration
LOI	Loss on Ignition
LPG	Liquefied Propane Gas
LSLL	Level Switch, Low Level
MAC	Main Air Compressor
MCC	Motor Control Center
MMD	Mass Median Diameter
MS	Microsoft Corporation
NDIR	Nondestructive Infrared
NETL	National Energy Technology Laboratory
NFPA	National Fire Protection Association
NO_X	Nitrogen Oxides
NPDES	National Pollutant Discharge Elimination System
NPS	Nominal Pipe Size
OD	Outside Diameter
ORNL	Oak Ridge National Laboratory
OSHA	Occupational Safety and Health Administration
OSI	OSI Software, Inc.
P&IDs	Piping and Instrumentation Diagrams
PC	Pulverized Coal
PCD	Particulate Control Device
PCME	Pollution Control & Measurement (Europe)
PDI	Pressure Differential Indicator
PDT	Pressure Differential Transmitter
PFBC	Pressurized Fluidized-Bed Combustion
PI	Plant Information
PLC	Programmable Logic Controller
PPE	Personal Protection Equipment

PRB	Powder River Basin
PSD	Particle-Size Distribution
PSDF	Power Systems Development Facility
ΔP or DP or dP	Pressure Drop or Differential Pressure
PT	Pressure Transmitter
RAPTOR	Resuspended Ash Permeability Tester
RFQ	Request for Quotation
RO	Restriction Orifice
RPM	Revolutions Per Minute
RSSE	Reactor Solid Separation Efficiency
RT	Room Temperature
RTI	Research Triangle Institute
SCS	Southern Company Services, Inc.
SEM	Scanning Electron Microscopy
SGC	Synthesis Gas Combustor
SGD	Safe Guard Device
SMD	Sauter Mean Diameter
SRI	Southern Research Institute
SUB	Start-up Burner
SWPC	Siemens Westinghouse Power Corporation
TCLP	Toxicity Characteristic Leaching Procedure
TR	Transport Reactor
TRDU	Transport Reactor Demonstration Unit
TRS	Total Reduced Sulfur
TSS	Total Suspended Solids
UBP	Uncompacted Bulk Porosity
UMZ	Upper Mixing Zone
UND	University of North Dakota
UPS	Uninterruptible Power Supply
UV	Ultraviolet
VFD	Variable Frequency Drive
VOCs	Volatile Organic Compounds
WGS	Water-Gas Shift
WPC	William's Patent Crusher
XRD	X-Ray Diffraction
XXS	Extra, Extra Strong

Listing of Units

acfm	actual cubic feet per minute
Btu	British thermal units
°C	degrees Celsius or centigrade
°F	degrees Fahrenheit
ft	feet
FPS	feet per second
gpm	gallons per minute
g/cm^3 or g/cc	grams per cubic centimeter
g	grams
GPa	gigapascals
hp	horsepower
hr	hour
in.	inches
inH_2O	inches water
inWg (or inWc)	inches, water gauge (inches, water column)
in.-lb	inch pounds
°K	degrees Kelvin
kg	kilograms
kJ	kilojoules
kPa	kilopascals
ksi	thousand pounds per square inch
m	meters
MB	megabytes
min	minute
mm	millimeters
MPa	megapascals
msi	million pounds per square inch
MW	megawatts
m/s	meters per second
MBtu	Million British thermal units
m^2/g	square meters per gram
μ or μm	microns or micrometers
dp_{50}	particle-size distribution at 50 percentile
ppm	parts per million
ppm (v)	parts per million (volume)
ppm (w)	parts per million (weight)
lb	pounds
pph	pounds per hour
psi	pounds per square inch
psia	pounds per square inch absolute
psid	pounds per square inch differential
psig	pounds per square inch gauge
ΔP	pressure drop
rpm	revolutions per minute
s or sec	seconds

scf	standard cubic feet
scfh	standard cubic feet per hour
scfm	standard cubic feet per minute
V	volts
W	watts